Spring 1-1-2017

# Prediction of Urban-Scale Building Energy Performance with a Stochastic-Deterministic-Coupled Approach

Hyunwoo Lim
*University of Colorado at Boulder*, Hyunwoo.Lim@colorado.edu

# PREDICTION OF URBAN-SCALE BUILDING ENERGY PERFORMANCE WITH A STOCHASTIC-DETERMINISTIC-COUPLED APPROACH

by

HYUNWOO LIM

B.A., Architectural Engineering, Sungkyunkwan University, KOREA, 2008

M.S., Architectural Engineering, Sungkyunkwan University, KOREA, 2010

A thesis submitted to the

Faculty of the Graduate School of the

University of Colorado in partial fulfillment

of the requirement for the degree of

Doctor of Philosophy

Department of Civil, Environmental and Architectural Engineering

2017

This thesis entitled:
Prediction of Urban-Scale Building Energy Performance
with a Stochastic-Deterministic-Coupled Approach
written by Hyunwoo Lim
has been approved for the Department of Civil, Environmental, and Architectural Engineering

Prof. John Zhai (Advisor)

Prof. Moncef Krarti

Prof. Wil V. Srubar

Prof. Rajagopalan Balaji

Prof. Kevin J. Krizek

Date_____

The final copy of this thesis has been examined by the signatories, and we
find that both the content and the form meet acceptable presentation standards
of scholarly work in the above mentioned discipline.

Lim, Hyunwoo (Ph.D., Architectural Engineering)

Prediction of Urban-Scale Building Energy Performance with a Stochastic-Deterministic-Coupled Approach

Thesis directed by Professor John Zhai

Urban areas consume two-thirds of the world's energy and account for 71% of global greenhouse gas emissions. In the U.S., residential and commercial buildings consume 22% and 19% of the total energy use, respectively. In response to current energy and environmental issues, policymakers have been actively engaged in the establishment of regulations and incentives to promote strategies for energy and greenhouse gas reduction in urban areas. To assist such decision makings requires an accurate and dynamic prediction and analysis of urban energy needs and developing trends, especially for building stocks.

Five primary challenges exist in modeling urban level building energy uses: (a) lack of building details for massive infrastructures (e.g., building envelope, floor area, age); (b) lack of knowledge of occupant related parameters (e.g., human behaviors, equipment power density, heating and cooling temperature set points); (c) uncertainties in building energy models; (d) unavailability of energy use data for validation; (e) computational effort. To address such challenges, a stochastic-deterministic-coupled modeling approach was developed. In this method, the energy uses of probability-based representative buildings were calculated with a deterministic engineering-based tool (e.g., EnergyPlus) with probabilistic inputs (e.g., building materials, human behaviors).

Detailed analyses were performed considering the accuracy of estimation and computational time for each step of the process. The analysis of building stock information and the impact of its uncertainty were also examined. The proposed stochastic-deterministic-coupled approach was demonstrated on the campus scale. The proposed model has the following advantages over the existing building stock models: (a) Applicable to various building types; (b) Fast computational time; (c) predictability by energy end-use type; (d) Availability of various temporal and spatial; (e) Availability for retrofit analysis of building stock. The proposed model enables cost-effective energy estimation at large scale considering uncertainties.

**ACKNOWLEDGEMENT**

I would like to thank all those who helped and supported me throughout my study in the University of Colorado Boulder. First and foremost, I would like to express my deepest appreciation to my parents (Youngtaek Lim, Jaesuk Lee), who have always loved me, encouraged me, and supported me throughout the ups and downs of my life. I am proud of being their son. I could not have accomplished the Ph.D. work without the full support of my wife, Jimin and my lovely two daughters, Yule and Terri. I dedicate this dissertation to my wife, Jimin Park.

I would like to express my sincere gratitude to my advisor, Dr. John Zhai, for his enthusiastic guidance and support from the initial to the final level of this work. I sincerely appreciate his time and effort during my Ph.D. training. I look forward to working with him again in the future. I would like to extend my sincere thanks to my committee members for their invaluable advice and suggestions: Dr. Moncef Krarti, Dr. Wil Srubar, Dr. Balaji Rajagopalan, and Dr. Kevin Krizek.

Thanks also to all friends in the University of Colorado Boulder who have always been there for me: Joowook, MJ, Sojin, Benjamin, Dareum, Byung, Alaa, Baqer, Justin, JP, Shane, Sam, Beomseok, and Hyeokjin.

I am also grateful for the funding provided by the Department of Civil, Environmental & Architectural Engineering Doctoral Assistantship for Completion of Dissertation at University of Colorado Boulder (Spring 2016).

CONTENTS

# FIGURES

# TABLES

# CHAPTER 1: INTRODUCTION

## 1.1 Background

More than 50% of the world's population lives in the urban area in 2015 (WHO & UN Habitat, 2016), and the world urban population is expected to rise to 72% by 2050 (Department of Economic and Social Affairs, 2012). Urban areas consume two-thirds of the world's energy and account for 71% of global greenhouse gas emissions (Birol, 2008). In the U.S., residential and commercial buildings consume 22% and 19% of the total energy use, respectively (EIA, 2016). Policymakers have been actively engaged in the establishment of regulations and incentives in an effort to promote strategies for energy and greenhouse gas reduction in urban areas. To assist such decision makings requires an accurate and dynamic prediction and analysis of urban energy needs and developing trends, especially for building stocks. However, extensive survey and auditing of urban building energy use are not only costly but also inadequate for predicting the dynamic characteristics of the energy demands. Simulation tools, based on reasonable inputs from public databases, are thus necessary for this purpose. Validated modeling tools can also be used to predict and analyze the implications of new technologies, products, and policies on the current and future energy use of a city.

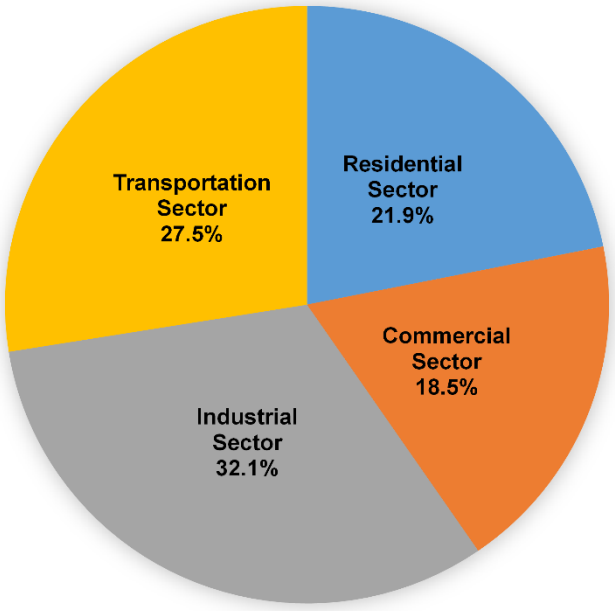


Figure 1-1 Total energy consumption by end-use sector (EIA, 2016)

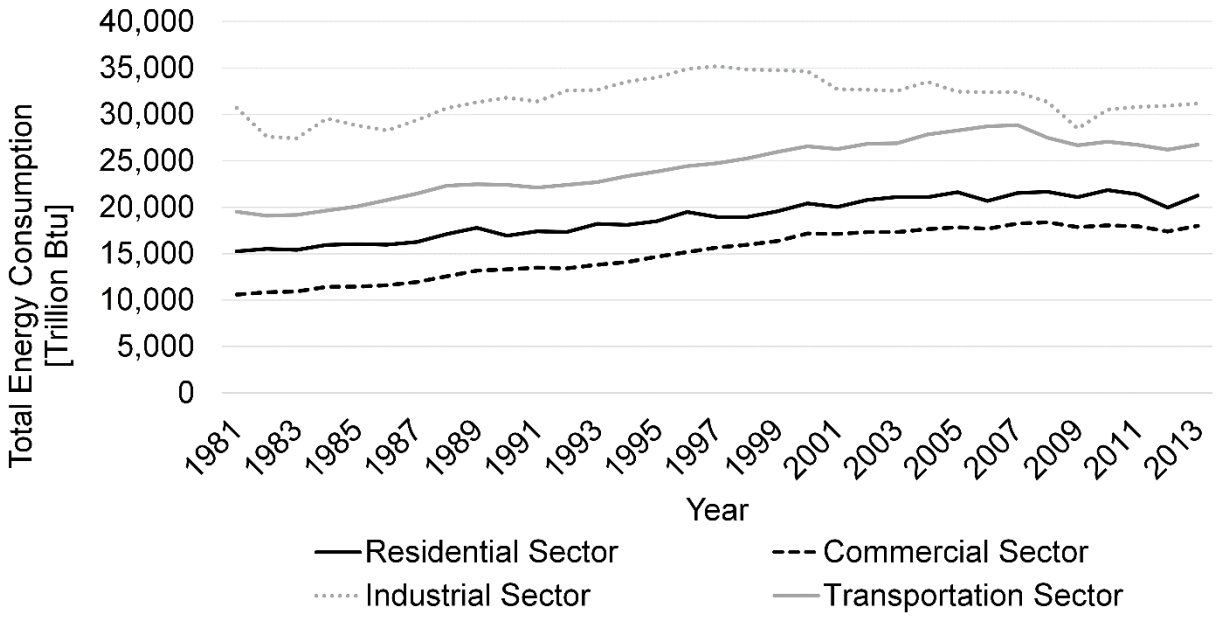


Figure 1-2 Total energy consumption by end-use sector, 1981–2013 (EIA, 2016)

## 1.2 Definition of Challenges and Objectives

The overall methodology of the research consists of two parts: developing a methodology and evaluating the methodology through a field test. Most of the existing building energy simulation tools such as EnergyPlus, eQUEST and TRNSYS can only predict energy load and thermal performance of individual buildings. To estimate the building energy use at large scale with many buildings of different sizes, types, ages, functions, and operating conditions, simply adding up all energy usages of individual buildings is not accurate as buildings operate on different schedules and intensities. One straight example is that commercial buildings operate mostly in the daytime, residential ones run in nighttime while industrial facilities may operate on a 24-7 schedule.

Five primary challenges exist in modeling urban level building energy uses: (a) lack of building details for massive infrastructures (e.g., building envelope, floor area, age); (b) lack of knowledge of occupant related parameters (e.g., human behaviors, equipment power density, heating and cooling temperature set points); (c) uncertainties in building energy models.; (d) unavailability of energy use data for validation; (e) computational effort.

Whole building simulation tool requires a large number of input variables. It is hard to know all input variables to represent the building exactly. This lack of building details could yield a different outcome according to the assumption and judgment of simulation user. In terms of large-scale, energy modeling for all buildings in the city is inefficient. To address this problem, some models utilize the archetype models that represent the building stock classified by properties such as building function and age. The single archetype model, however, cannot reasonably represent the distribution of actual buildings.

Furthermore, it is challenging to gather necessary building stock information such as total floor area, floor numbers, built year, building function, contractions, and HVAC systems. Such information is often inaccessible in the city-level. The building energy usage data also occasionally is not available because of privacy issue or legal concerns.

To address such challenges, a stochastic-deterministic-coupled modeling approach is developed. In this method, the energy uses of probability-based representative buildings are calculated with a deterministic engineering-based tool (e.g., EnergyPlus) with probabilistic inputs (e.g., building materials, human behaviors). One important criterion to judge the value of this model is that how closely the simulated results can match actual building stock energy use. Stochastic methods are employed to calibrate the model using collected field energy data. The energy consumption of the target district can be obtained by aggregating the energy distribution of such representative building.

## 1.3 Organization of the thesis

The thesis is outlined as follows;

Chapter 1 presented an overview and motivations for a stochastic building stock energy model.

Chapter 2 introduces the pros and cons of existing building stock energy model via a literature review. The limitations and issues of current stochastic building energy models are discussed.

Chapter 3 proposes a framework that can estimate building stock energy considering uncertainties and compares the stochastic methods to calibrate building stock energy consumption. The computational benefits of the meta-models are also examined.

Chapter 4 performs detailed analyses to enhance the proposed framework at an individual building. The accuracy of the meta-model and the effect of informative energy use data on the calibration are examined.

Chapter 5 determines the proposed framework along with detailed step-by-step methodologies. The possibility of ECM analysis of the proposed stochastic building stock energy model in a virtual building stock is investigated.

Chapter 6 deals with the uncertainty of building stock information. In the proposed model, the necessary information is classified according to the accessibility and the accuracy of the model is analyzed regarding uncertainty.

Chapter 7 describes the application of the proposed stochastic-deterministic-coupled model at campus-scale. Total building energy consumption is estimated through a detailed process. The proposed method is validated against the measured energy consumption data. Energy conservation measures are examined to the campus.

Chapter 8 summarized the thesis with conclusions and suggestions for future research.

# CHAPTER 2: LITERATURE REVIEW

## 2.1 Overview of Methods

Building energy model has been utilized to predict building energy demands such as electricity, gas use since the 1970s. All current building energy models including physical models (e.g., eQUEST, EnergyPlus and TRNSYS) and data-driven models (Black-box models such as Regression models, Artificial Neural Networks - ANN, and Support Vector Machine - SVM) can only predict energy and thermal performance of individual buildings. To predict the energy consumption of building stocks over time, researchers have developed a number of modeling methodologies. Swan and Ugursal (L. G. Swan & Ugursal, 2009) and Kavgic et al. (Kavgic et al., 2010) provided reviews on existing building stock models for residential sectors.

According to the principles and techniques for modeling energy consumption, building stock energy modeling methods can be broadly divided into two categories: the top-down method and the bottom-up method. The top-down methods start with the aggregated energy consumption for a given region and time. These methods typically factor into the interrelationships between the energy sector and other variables such as econometric and technological factors. The aggregated energy use can then be divided into sections according to building function or spatial proximity. The bottom-up methods work at an individual level. It calculates the energy consumption of individual end-uses or buildings and then sums them up to represent the required region. The bottom-up methods can be further divided into two categories: the statistical and engineering approaches as shown in Figure 2-1. In this review, we suggest two sub-groups of the bottom-up engineering method: namely the deterministic and stochastic approaches.

The following sections will detail the definitions and comparisons of all these methods and models, as well as discuss the opportunities and challenges for improving these methods. Section 2.2 to 2.4 review remarkable and recent top-down and bottom-up building stock models, respectively. Section 2.5.1 discusses the uncertainty issue in the deterministic bottom-up engineering methods. The stochastic approaches to

overcoming the uncertainty issue are then introduced and reviewed (Section 0 and 2.5.3) and challenges on the stochastic bottom-up engineering building stock models are discussed in Section 2.6.

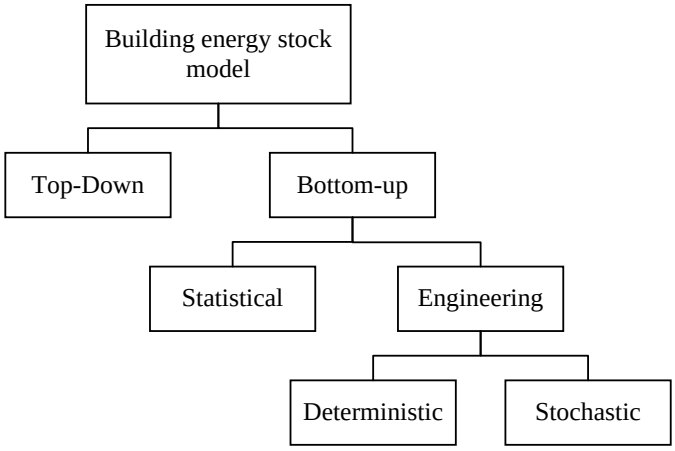


Figure 2-1 Top-down and bottom-up methodologies for building stock energy model

## 2.2 Top-down Methods

Top-down methods are primarily based on the statistical relationships between historical aggregated energy use and socio-economic factors such as population, fuel prices, climate conditions, and gross domestic product to show the connections between the energy sector and economic output. Most of these top-down models can predict the macroeconomic performance of building stock and the impacts of various "what-if" scenarios over time.

The demand module of the National Energy Modeling System (NEMS) (Energy Information Administration, 2009) is the most well-known top-down prediction tool. The purpose of NEMS is to forecast the energy, economic, environmental, and security impacts of the alternative energy policies and different assumptions in the United States. Examples of top-down models include demand modules for residential and commercial sectors in other integrated energy system models: MARKAL(Fishbone & Abilock, 1981), TIMES(Loulou et al., 2005), AIM(Matsuoka et al., 1995) and GCAM(Edmonds et al., 1994; Kyle et al., 2010). The resolution of such energy demands in the integrated energy system models roughly accounts for temporal (e.g. annual), spatial (e.g. region or national) and end-use level (e.g. total commercial, total heating energy) rather than individual buildings. Sartori et al. (Sartori et al., 2009) developed an energy

demand model for Norwegian residential and service sectors. The model utilized the activity levels of the building stock (new construction, renovation, and demolition) and energy intensities for archetypes. Norwegian dwelling stock model was further refined by Sandberg et al. (Sandberg et al., 2011; Sandberg & Brattebø, 2012) regarding historical development in energy flows since 1960 and future trends towards 2050. Vasquez et al. (Vásquez et al., 2016) proposed a dynamic Type-Cohort-Time (TCT) stock-driven modelling approach that considers demographic aspects, lifestyle-related issues, and building-specific characteristics to evaluate policies. Summerfield et al. (Summerfield et al., 2010) employed a top-down approach, based on multiple regressions, to model the annual delivered energy, price, and temperature (ADEPT) and the seasonal temperature, energy and price (STEP) for the UK households domestic sector. These models allow policymakers and the public to interpret trends in delivered energy and provide benchmarks for comparison. Since the ADEPT and STEP rely only on the energy price and the average external temperature to predict the energy use, the ability of models to identify the effectiveness of specific policy measures is limited. Like other top-down models, in these studies, there is no disaggregation for energy consumption into finer regions or individual building levels.

As an example of an effort to obtain finer scales in a top-down approach, Sailor and Lu (Sailor & Lu, 2004) disaggregated U.S. monthly state-level energy use data into hourly city-level based on the diurnal variability of the urban population. Furthermore, representative diurnal energy use profiles for summer and winter are constructed using fractional hourly load profiles. The weakness of the method includes large uncertainties and limited capabilities of predicting the application of new technologies since it is based on a population density and diurnal profiles from historical data.

These top-down methods utilize an interaction between energy sectors and other economic indicators so that it can reflect the impact of social-economic policies. Since the top-down models are dependent on historical data, it is unable to examine the consequences of specific technological advances and policies. Furthermore, they give a coarse analysis on individual end-uses and do not explicitly consider individual physical factors specific to each type of building. Therefore, top-down building stock models are not suitable to analyze the relationships among the building energy use, and the building design and

operational specifications. Most of top-down models performed a scenario analysis based on assumptions about socio-economic factors to predict future energy (Comodi et al., 2012; Kainuma et al., 1998; Sartori et al., 2009). However, top-down approach is deterministic and does not take into account the uncertainty of the energy model.

## 2.3 Bottom-up Statistical Methods

Bottom-up methods calculate the energy consumption of individual end-uses, individual buildings, or groups of buildings and then use these representative models to predict the regional or national energy consumption by different weighting approaches (L. G. Swan & Ugursal, 2009). Bottom-up methods can be further divided into two sub-categories based on its modeling mechanisms: statistical and engineering-based (physical) methods.

Statistical methods use historical data and analyze the relationships between available building information and energy use data. These methods rely on energy utility billing data (e.g., electricity, gas) from energy providers and survey data that includes human behaviors and building characteristics. Researchers have studied diverse approaches to analyzing the building stock energy consumption utilizing this information.

The Princeton scorekeeping method (PRISM) (Fels, 1986) is one of the early regression models. PRISM correlates the building energy use per billing period with the local heating or cooling degree-days. PRISM has been used broadly in the U.S. by governments, utilities, and research organizations to analyze energy conservation measures in large aggregates of houses due to its simplicity in calculation (Kavgic et al., 2010). Like other statistical modeling methods, however, it does not provide the details and flexibility for energy conservation measures. Ruch and Claridge (Ruch & Claridge, 1992) indicated that PRISM model does not estimate the energy savings for most commercial buildings, although the simple linear regression model is suitable for estimating energy use for residential buildings. The conditional demand analysis (CDA) method is another statistical technique. Turiel et al. (Turiel et al., 1987) adopted the CDA method to estimate the energy intensities of end-uses in commercial buildings in northern California, USA.

The CDA utilizes the regressions based on the presence of building characteristics and end-use appliances. One of the advantages of CDA is the convenience in the identification of the required input data using a survey of the occupant and energy billing data from the energy provider. CDA requires extensive and diverse information about appliances and building characteristics, increasing the likelihood of significant uncertainties from incorrect input data from surveys.

Recent bottom-up statistical models have used geographic information system (GIS) for data acquisition to build a model and visualize results. Girardin et al. (Girardin et al., 2010) developed EnerGIS based on GIS to model the energy requirement for Geneva, Switzerland. The linear regression model was utilized to obtain the annual consumption for heating, cooling, electricity, and hot water production and then these predictions were used to compute the required temperatures for the district heating system. The visualization of the energy consumption on the map facilitates a better understanding of energy planning and for analyzing the large-scale integration of renewable energy. Kolter and Ferreira (Kolter & Ferreira, 2011) presented a statistical approach to model energy consumption in residential and commercial buildings in Cambridge, MA, USA. They used utility data with some features from publicly available tax assessors and GIS data such as building value, square footage, building type. To develop a model, two statistic techniques were examined: linear regression and Gaussian process (GP) regression. While the GP method showed the best overall performance, the linear regression model was chosen due to its better succinctness and computational efficiency. Using the linear models, the authors developed a tool, EnergyView, which provides a visual map and compares energy use to similar buildings. Howard et al. (Howard et al., 2012) also used linear regressions to derive an annual energy use intensity (EUI) for several building functions in New Your City. The estimated EUIs were apportioned into several of end uses by ratios derived from the Residential Energy Consumption Survey (RECS) (Energy Information Administration, 2005) and the Commercial Building Energy Consumption Survey (CBECS) (Energy Information Administration, 2003) for end-use estimation. The interactive map for spatial distribution of building energy use was produced based on GIS data (http://sel.columbia.edu). The model is unable to consider the construction type and

building vintage for the energy conservation measures, although they play a major role in energy saving potential identification.

Most of the bottom-up statistical models are based on the regression techniques. The advantage of the statistical models is relatively easy to build a model once it has enough information to attribute building energy consumption to relevant building characteristic and data. Another benefit is that the statistical models are capable of considering demographics and the behaviors of occupants that have a significant influence on the energy consumption. On the other hand, the statistical methods have limitations when exploring the combined impact of several energy efficiency measures. Moreover, statistical models are unable to model hourly energy use. Some information needed for statistical models is not always possible to access because of the privacy and insufficient data.

## 2.4 Bottom-up Deterministic Engineering Methods

Bottom-up engineering models (also called physics models) explicitly account for the energy consumption of individual end-uses based on the equipment use, heat transfer and thermodynamic relationships. It predicts the energy consumption according to building properties such as geometry, envelope, climate, occupancy schedule, and equipment.

The conventional engineering building energy simulations are deterministic. The deterministic approach does not take into account the inherent uncertainties in the building and its subsystems. It always produces the same single output from given inputs. Bottom-up engineering building stock models using the deterministic approach are discussed in this section. The uncertainty issues in the deterministic methods, and the stochastic methods will be examined in the next section.

The most commonly used deterministic engineering approach is the bottom-up archetype (also called representative building or prototypical building) engineering model. This approach uses the following typical procedure:

(1) Classify building stock into several categories based on building geometry and non-geometry (e.g., function) properties, and microclimate conditions;

(2) Develop archetype buildings that present specific building stocks of each type;

(3) Predict the unit energy consumptions (energy use of one building or energy use intensity) for each archetype by using a building energy simulation tool;

(4) Obtain the total energy consumption by aggregating the calculated unit energy consumptions with proper weighting factors (e.g., number of units or floor area in each type of building sector).

Most research efforts for the bottom-up engineering methods have focused on the residential buildings. In the UK, several residential building stock models used BREDEM (building research establishment domestic energy model) (Anderson et al., 1985) as a core calculation engine for single houses to calculate energy use for each archetype (B Boardman et al., 2005; Brenda Boardman, 2007; Firth et al., 2010; Johnston, 2003; Jones et al., 2007, 2000, Natarajan & Levermore, 2007a, 2007b; Shorrock & Dunster, 1997). More detailed comparisons of UK models were discussed in Kavgic's review (Kavgic et al., 2010) and Oladokun's review (Oladokun & Odesola, 2015). In Canada, Canadian Residential Energy End-use Model (CREEM), developed by Farahbakhsh et al. (Farahbakhsh et al., 1998), based on 16 house archetypes that were derived from 8,767 actual houses' data. In Japan, the residential energy model developed by Shimoda et al. (Shimoda et al., 2003) used 20 archetypes and 23 household types for Osaka City's residential sector. The occupants' schedule determined by the national time use survey was utilized to obtain hourly energy use for hot water supply and dynamic cooling and heating load. Total energy consumption for the residential stock is estimated by multiplying the simulated energy use and the number of households and then summing them up. This concept of modeling has been developed and utilized in a series of researches (Shimoda, Okamura, et al., 2010; Shimoda et al., 2007, 2004; Shimoda, Yamaguchi, et al., 2010; Yukio Yamaguchi et al., 2008). These residential building stock models have core calculation engines tailored for residential buildings and specific regions.

The bottom-up engineering building stock models have been expanded to the commercial sector and integrated with GIS platform for acquisition and expression of data thanks to the advances in the mapping technologies. Yamaguchi et al. (Y. Yamaguchi et al., 2007a) developed 612 archetypes for the commercial sector in Osaka city and proposed a district clustering approach that develops several

representative districts based on dominant building types. The district level energy system simulation model was used applied to estimate the annual energy use intensity of each representative district (Hashimoto et al., 2007; Y. Yamaguchi et al., 2007b; Y Yamaguchi et al., 2005, 2003; Yohei Yamaguchi & Shimoda, 2010). The model can quantify the energy use intensity for each representative district, not for specific individual building. Heiple and Sailor (Shem Heiple & Sailor, 2008) created 30 archetypes in the commercial and residential sectors of Houston, U.S using the national survey data (RECS, CBECS). The energy intensities calculated by eQuest (Hirsch, 2006) were aggregated into the city scale, providing hourly and seasonal energy uses, which were visualized and compared with the top-down approach results in a GIS platform. The method has a time-intensive process of creating a set of representative building simulations. Caputo et al. (Caputo et al., 2013) developed 56 detailed archetypes considering form factor of buildings for the city of Milan, Italy. The potential energy consumption reduction derived from EnergyPlus was visualized in the GIS framework at the urban scale.

As the energy policy decisions require more detailed information to address future planning interventions, recent building stock models were developed for a finer temporal and spatial resolution. CitySim (J. J. H. Kämpf, 2009; Darren Robinson et al., 2009) is a software developed at EPFL to predict the energy demands from small neighborhoods to an entire city. It can calculate the on-site energy use for heating, cooling and lighting based on multiple physical models such as RC (resistor-capacitor network) models, Radiation models, Plant and Equipment models, and Behavioral models. One interesting feature of CitySim is that it can take into account heat gain from direct and diffuse solar radiation as well as long-wave exchanges between the walls of each building. Therefore, CitySim requires a field survey to check the glazing ratio and façade state for a 3D modeling information. CitiSim model has been used for optimization(J. Kämpf & Robinson, 2009; Vermeulen et al., 2013), analysis of the impact of occupants' stochastic behaviors (Haldi & Robinson, 2011), and combination with other platforms (Dorer et al., 2013; Perez et al., 2012). The model developed by Fonseca and Schlueter (Fonseca & Schlueter, 2015) can provide spatial (building location) and temporal (hourly) dimensions of analysis using GIS framework. The statistical and analytical methods were integrated to calculate the hourly energy use and temperature

requirements of energy services in 172 building archetypes. Statistical clustering algorithms were also integrated to classify buildings in the area. The model result was validated against measured and simulated data. However, calibration was not considered for more accurate prediction. Davila et al. (Davila et al., 2016) developed an urban building energy model that can estimate hourly demand load at individual building level for Boston, U.S.A. In the process, all 92,000 buildings in Boston were assigned into 76 archetypes that were simulated using multicore computer clusters for three days. The bottom-up engineering methods need an immense effort of processing data, creating archetypes and running simulations. However, it provides an hourly energy use resolution from a specific location to city-wide with detailed energy classifications such as building general use type and fuel type.

Since bottom-up engineering models are built on the details of individual buildings, it is possible to consider the energy variables to the physical and behavior characteristics of these buildings. In these models, the building stock is divided into several types based on the physical and functional characteristics. Energy use for each type is quantified using the archetype buildings that are representing the same building stock type. As a result, the most outstanding advantage of the bottom-up engineering models is the capability of examining new technologies and no need for historical energy use data. The use of fundamental thermodynamics and heat transfer models enables the assessment of various energy conservation measures and new technologies in the absence of historical energy data (L. Swan, 2010). However, the bottom-up engineering models require more detailed building information to calculate the energy consumption. Various model assumptions due to lack of accurate data can cause significant uncertainties on the building energy models. Furthermore, no single archetype model can reasonably represent the entire building sector of the same type. More detailed classification of archetype models is often needed to avoid this shortcoming, but this can be a massive computational burden in the simulation process. Another shortcoming of the engineering models is the assumption of occupant behaviors that can significantly alter energy consumptions. Moreover, these models do not include market interactions and tend to neglect the correlations between energy use and macroeconomic activity. To address some of these shortcomings of the engineering models, Kavgic (Kavgic et al., 2010) suggested the use of survey

data that represents the building stock including energy consumption data. Statistical survey data allows for the incorporating the effects of occupant behaviors, technological and social trends. However, the deterministic approach of engineering models has inherent constraints to accommodate various buildings' profile distributions. Table 2-1 summaries the advantages and disadvantages of each method based on (Kavgic et al., 2010; L. G. Swan & Ugursal, 2009).

Table 2-1 Pros and cons of various methods

| | Top-down | Bottom-up statistical | Bottom-up deterministic engineering |
|---|---|---|---|
| Pros. | • Capable of modeling the relationships between economic variables and energy demand<br>• Enable to model the impact of different social cost-benefit energy and emission policies and scenarios<br>• Use aggregated data<br>• Avoid detailed technology descriptions | • Enable to determine a typical end-use energy consumption<br>• Encompass occupant behaviors<br>• Include macroeconomic and socioeconomic effects<br>• Not require detailed data (only billing data and simple survey information)<br>• Easy to develop and use | • Enable to model current and prospective technologies in detail<br>• Assess and quantify the impacts of different combinations of technologies<br>• Enable to determine each end-use energy consumption<br>• Use physically measurable data |
| Cons. | • Depend on past energy economy interactions to project future trends<br>• Lack the level of technological details<br>• Coarse results<br>• No explicit representation of end-uses<br>• Lack of disaggregation into individual levels<br>• Unable to consider uncertainties | • Rely on historical consumption data<br>• Limited capacity to assess the impact of retrofit or new technologies<br>• Provide fewer data and flexibility<br>• Require large survey sample<br>• Multicollinearity<br>• Unable to consider uncertainties | • Require detailed input information<br>• Computationally intensive<br>• No economic factor<br>• Require a significant amount of technical data<br>• Behavioral assumptions for occupants<br>• Unable to consider uncertainties |

## 2.5 Bottom-up Stochastic Engineering Methods

### 2.5.1 Uncertainty issues in existing building stock models

Deterministic bottom-up engineering building stock energy models overcome some limitations of top-down and bottom-up statistical models in terms of flexibility. They can evaluate various energy conservation measures for building stock without end-use energy billing information in a region. However, they are not still able to address the uncertainty issues during the modeling.

Even for a single building, the engineering-based energy model encounters significant uncertainty challenges. Building energy simulation models are complex, requiring comprehensive inputs. Some of these inputs may be difficult to collect so that assumptions must be made to operate the models. The problem becomes more significant when expanding the simulation model from an individual building to the building stock, as only a limited number of archetype buildings are built with the aim to represent the entire building stock. Although sharing some of the main features (e.g., function, or age) within the same archetype, the representative building cannot, by all means, represent the wide actual building distributions in various building features such as building geometric properties (height, total floor area, window-wall-ratio), and materials. Finer classification is desired but under the penalty of additional computational cost.

Reinhart and Davila (Reinhart & Cerezo Davila, 2016) indicated that the building energy prediction might be largely different from measured data due to the uncertainties associated with the definition of archetypes. In the bottom-up engineering building stock model, the errors at the individual building level are higher than at the aggregate level since the inaccuracies at individual levels tend to average out at the aggregate level.

Moreover, most of the bottom-up engineering methods employ the deterministic building energy models such as EnergyPlus, eQUEST, and ESP-r. These energy models provide only one deterministic output for one building with given inputs. Hence, the deterministic bottom-up engineering methods are unable to predict the energy use of a city with many buildings of different sizes, types, ages, functions, and operating conditions.

### 2.5.2 Stochastic building energy models for Individual buildings

The stochastic approach was proposed to incorporate and handle the uncertainty factors of a building model. The concept of the stochastic approach is implemented by performing an uncertainty analysis and sensitivity analysis using the Monte Carlo method (Corrado & Mechri, 2009; Eisenhower, O'Neill, Fonoberov, et al., 2012; C. Hopfe, 2009; Lomas & Eppel, 1992; Macdonald, 2002; T. Reddy et al., 2007; Wit & Augenbroe, 2002). In this approach, the values of input parameters are sampled randomly from a given range and then feed into the energy model. The uncertainty and sensitivity are analyzed by the correlations between the variations of the input and output parameters.

Some studies attributed the building model uncertainty to occupants' behaviors and have developed the models that can explain the presence and behaviors of occupants (Haldi & Robinson, 2011; Page et al., 2007; D. Robinson et al., 2007; Darren Robinson et al., 2009, 2011). Findings from these studies suggest that building occupants' behaviors have a significant impact on the building energy performance.

Others more focused on the uncertainty emanating from the distributions of various building parameters. The Monte Carlo method has been used to represent the distribution of various buildings in a building stock (Korolija et al., 2013; Nishio & Asano, 2006; Smith, 2009). The variety of physical characteristics of buildings is considered to establish probable distributions. In these studies, however, validation and calibration with the measured data were not performed.

The calibration is to tune the inputs in a building energy model in order to match the observed data with the model outputs. A detailed review of the calibration techniques for building simulation can be found elsewhere (Coakley et al., 2014; Fabrizio & Monetti, 2015). The calibration can be done with either deterministic or probabilistic methods. The deterministic method can obtain input parameters by a manual trial-and-error method that is very time-consuming, and the result is more dependent on the user. By contrast, the probabilistic approach can deal with this problem in an efficient manner by handling the unknown inputs as random parameters with probability density functions (Tian, Wang, et al., 2014).

For the probabilistic calibration, Kennedy and O'Hagan (Kennedy & O'Hagan, 2001) proposed a generic approach for the Bayesian calibration of computer models. The authors noted the Bayesian

calibration improved traditional approaches in two ways: First, the predictions can consider all sources of uncertainties, including the remaining uncertainty over the fitted parameters. Second, the Bayesian calibration method attempts to correct any inadequacy of the model that is revealed by a discrepancy between the model predictions and the measured data from even the best-fitting parameters.

Bayesian inference is a statistical method that utilizes Bayes' theorem in Equation (1) to obtain a posterior distribution for unknown parameters (θ) given the observed data (y). The model parameters are considered to be uncertain and have a probabilistic distribution based on their plausible values. The uncertain parameters of the energy model are updated to match the model prediction with the observed data. As a result, Bayesian calibration provides the posterior distribution $p(\theta|y)$ in a form of plausible distribution of calibration parameters.

$$p(\theta|y) \propto p(\theta) \times p(y|\theta) \quad (1)$$

Where $p(\theta)$ is prior distributions assigned for uncertain parameters; $p(y|\theta)$ is a likelihood function that measures how closely model predictions match observed data.

A Markov Chain Monte Carlo (MCMC) (Gilks, 2005) method has been used to draw the posterior probability distribution in the Bayesian calibration. Bayesian calibration has been widely employed for the model predictions in other areas (e.g., ecological models (Oijen et al., 2005), hydrologic models (Liu et al., 2008; Qian et al., 2005), atmospheric model (Guillas et al., 2009), geochemistry (Tierney & Tingley, 2014), geological models (Rahn et al., 2011; W. Zhang & Arhonditsis, 2008), molecular dynamic model (Angelikopoulos et al., 2012), and biological model (Blangiardo & Richardson, 2008)).

Heo (Y. Heo, 2011; Y. Heo et al., 2012) applied a Bayesian calibration to the domain of building energy simulation. A normative energy model (base on CEN-ISO standard (ISO, 2004)) and Bayesian calibration were used to account uncertainties for retrofit analysis of existing individual buildings. Normative models approximately represent energy performance of building systems with a small number of macro-level inputs based on a simplified description of a building and its system. Therefore, it can drastically reduce the computational cost of modeling and calibration process although it has a limitation to execute fine adjustment for building's subsystems and components. Figure 2-2 illustrates the calibration

process. The first step involves the quantification of uncertain parameters in the energy model based on expert knowledge collected from surveys, standards, and technical reports. The second step is a parameter screening to select dominant parameters for calibration. In the third step, selected parameters are calibrated with given prior distributions for the parameters, utility data, and the normative building energy model. Then, the calibrated model with resulting posterior distribution is validated with the utility data. Last, the validated model propagates uncertainty to compare energy conservation measures (ECMs). From the results, the accuracy of calibrated normative model is comparable to the calibrated transient model (EnergyPlus) but requires much less computational time.

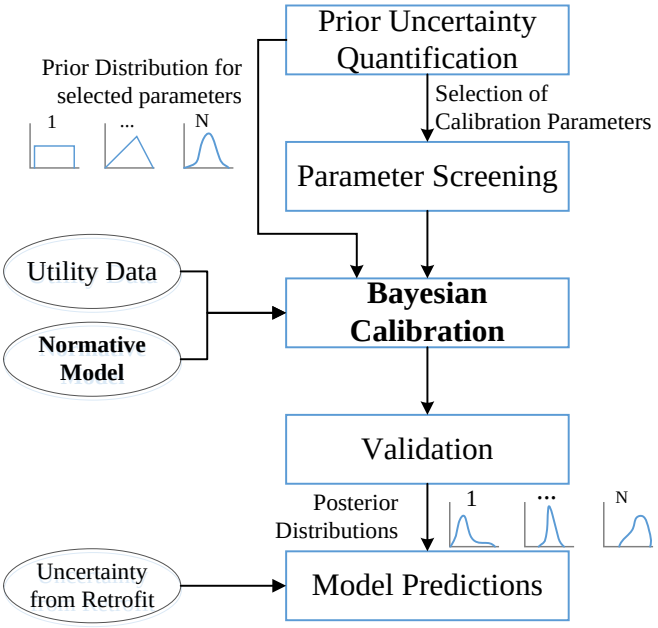


Figure 2-2 Procedure of Bayesian calibration for retrofit analysis by Heo (Y. Heo, 2011)

The Bayesian calibration procedure suggested by Heo has been used to calibrate the unknown input parameters in the individual building simulation model (Yeonsook Heo, Augenbroe, et al., 2015; Yeonsook Heo, Graziano, et al., 2015; Y.-J. Kim, Yoon, et al., 2013; Pavlak et al., 2013; Tian, Wang, et al., 2014).

### 2.5.3 Stochastic building energy models for building stock

There were a few attempts to apply the probabilistic calibration to the building stock. Booth et al. (Booth et al., 2012) discussed three sources that can cause uncertainties in building stock models: the first is uncertainty from the accuracy of the model, that is, how adequately the model represents the true process

of energy in a building. Second, it arises from different buildings characteristics within the same type of buildings. Finally, within a homogeneous building group, the uncertainty stems from two factors: differences in outcome due to random variation and a lack of knowledge on certain input parameters.

To consider the uncertainty of building stock models, Booth et al. (Booth et al., 2012) suggested the Stochastic Urban Scale Domestic Energy Model (SUSDEM). The SUSDEM is also based on Kennedy and O'Hagan (Kennedy & O'Hagan, 2001) Bayesian calibration process. It used the Energy Performance Standard Calculation Toolkit (EPSCT) developed in Georgia Institute of Technology (Lee et al., 2011) as an energy simulation tool because of the speed of the calculation and ability to assess the impact of technological interventions. The overall process is similar to Heo's method (Y. Heo, 2011; Y. Heo et al., 2012) for individual buildings. However, the calibration was performed to the average value of building stock and added the bias function into the model to reduce the difference between observed data and computer model outputs. The equation below expresses the relationship between the observed data and the computer model output:

$$z_i = \rho\eta(\mathbf{x}_i, \boldsymbol{\theta}) + \delta(\mathbf{x}_i) + e_i \quad (2)$$

$z_i$ is observed data, $\rho\eta(\mathbf{x}_i, \boldsymbol{\theta})$, represents the emulator for the computer model. $e_i$ indicates the observation error. In this model, the bias function, $\delta(\mathbf{x}_i)$, is dependent on the average daily external temperature and it is used to account for the inability of the model to fully represent the true process.

The case study of 35 flats[1] in the UK was performed to demonstrate the method. There are five steps in the Bayesian calibration. Step 1 is a selection of the calibration parameters. The Factorial Sampling Analysis (FSA, or the Morris method) was used to select dominant parameters. The authors indicated that calibrating too few parameters means that the uncertainty in other (un-calibrated) parameters is subsumed into the chosen (calibrated) parameters. Therefore, it derives distorting the physical meaning of the resultant posterior distributions. Calibrating too many parameters reduces the effectiveness and accuracy of the Bayesian inference. Step 2 is a quantification of prior uncertainty. The initial distributions for calibration

[1] An apartment on one floor forming a residence in the U.K.

parameters were estimated based on any prior knowledge or assumption. Step 3 is a formulation of calibration framework. They used a statistical model (known as an emulator or meta-model) to replace the building energy simulation model. Step 4 is a Bayesian calibration process. The posterior distribution for each unknown parameter was derived. The model calibrated to the average daily value of measured energy consumption, not for each energy consumption of 35 flats. The last step is the validation. The calibrated output is compared against the observation data. The results showed that the Bayesian calibration has almost eliminated any discrepancy between the observation data and the normative model output. However, since the calibration was performed to estimate the average energy usage for all the flats, the posterior distribution for parameters could not represent the distribution of parameters of all flats. The proposed SUSDEM was further refined and extended to large-scale by applying approximately 15,000 houses in the UK (Booth & Choudhary, 2013). Energy savings from retrofit measures were predicted considering the installation costs, the future prices of energy, the lifetime carbon savings, and increased thermal comfort.

Three primary challenges exist in the current stochastic modeling for building stock energy use:

(a) lack of building details for massive infrastructures (e.g. thermal properties such as insulations, glazing); (b) uncertainty caused from human behaviors (e.g., occupant schedule, equipment power density); and (c) lack of actual building energy use data for validation or calibration to reduce errors.

Obtaining energy usage data is one of the main challenges for the calibration. In most cases, the public data is only available at the macro-level (i.e., at the district, urban, or national level). In another research by Booth et al. (Booth et al., 2013), they suggested a method to calibrate micro-level models using macro-level data. A hierarchical framework was proposed to utilize a combination of regression analysis and Bayesian inference. The top-down stochastic method was employed to infer average energy consumption for different dwelling types using aggregated macro-level energy statistics. The top-down analysis at the macro-level provided the data for calibrating the input parameters of the bottom-up probabilistic engineering models at the micro-level (i.e., at an individual building level).

Zhao (Fei Zhao, 2012; Fei Zhao et al., 2016) proposed an approach to replicate an office building stock energy use in Chicago, U.S. from the survey data. This method used a linear inverse problem to derive

design parameters of buildings. At first, the authors set 30 unknown parameters and examined to quantify the prior uncertainty. Only 12 parameters out of 30 were chosen for calibration parameters after a sensitivity analysis. The multiple linear regression model using the selected 12 parameters was built to represent the normative building energy model for reducing computational effort. If the inverse problem is overdetermined, a set of values for the unknown parameter can be sampled by approximately satisfying the linear equation using Markov Chain Monte Carlo. In the validation, the predicted EUI distribution from the inverse problem was approximately identical with the EUI distribution of CBECS 2003 office buildings (765 samples, adjusted for Chicago's climate). The estimated parameter distributions were significantly different from the actual parameter distributions in CBECS 2003. The author indicated that the predicted building parameter distributions should not be considered as the real values, but the "best guess" of the real distributions that will produce the similar outcome of the real world. This "best guess" can be further improved using more measurement data to quantify the measurement errors between the data and the model.

Tian and Choudhary (Tian & Choudhary, 2012) applied the process to the school buildings in London, U.K. In the parameter estimation step, the authors considered two approaches for implementing the calibration: linear inverse problem and Bayesian inference. The main difference between two approaches is in the assumption of prior distributions. Linear inverse problem is represented as uniform distribution so that it is unbiased. Bayesian inference allows the user to specify the shape and spread on the prior distributions. The advantage of Bayesian calibration relative to the linear inverse problem is that one can utilize existing knowledge of building stock from previous survey, research, and reports. The distributions of input parameters were inferred to the observed energy consumption data. The inferred distributions of input parameters were used to quantify the benefits of energy conservation measures (ECMs) for the building stock. The calibration procedure for the individual building is similar to Heo (Y. Heo, 2011; Y. Heo et al., 2012)'s procedure. However, in this study, the calibration procedure was repeated to represent the building stock of secondary schools in London. They derived 2,000 sample from energy consumption data in the technical report. Then, the calibration with 5,000 of MCMC iterations was performed for every sample value of 2,000 energy data. Since the resulting total number of samples is extremely large ($5{,}000 \times$

2,000), the authors resampled 10,000 sets from the large set. This method could reduce the simulation run-time using the simple surrogate model (linear regression model) although they need to run a large number of calibrations.

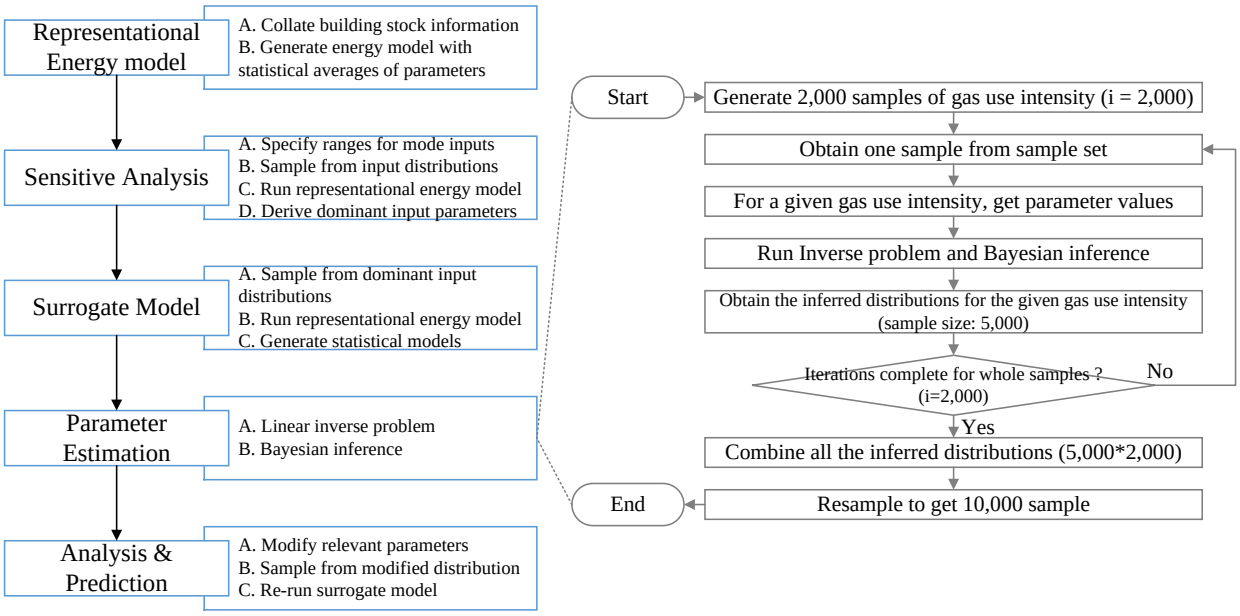


Figure 2-3 Procedure of probabilistic building stock energy model proposed by Tian et al. (Tian & Choudhary, 2012)

In the study of Yamaguchi et al. (Yohei Yamaguchi, Suzuki, et al., 2013) to quantify the energy use for supermarket at the city scale, the authors also used the Bayesian calibration framework based on Kennedy & O'Hagan (Kennedy & O'Hagan, 2001), and the process of building simulation and calibration by Heo et al. (Y. Heo et al., 2012) and Booth et al. (Booth et al., 2012). They stated that the previous application of a probabilistic approach was only limited to calibrate the model parameters to a single resolution of simulation output (e.g., monthly energy consumption). The authors also mentioned that the uncertainty of the input parameters might be changed at different time resolutions. Their studies revealed that the building insulation performance might have a considerable impact on seasonal and weekly energy consumption while its effect on annual energy use might be modest. The authors proposed a hierarchical calibration that considers annual and weekly parameter variations. In the calibration method, they selected

parameters for annual and weekly variations to calibrate the developed archetype energy model. Then, the input parameters were calibrated based on weekly energy consumptions and annual energy consumption. The proposed calibration method can consider the overall characteristics of the building stock and the influences of meteorological conditions caused by seasonal variations in energy consumption.

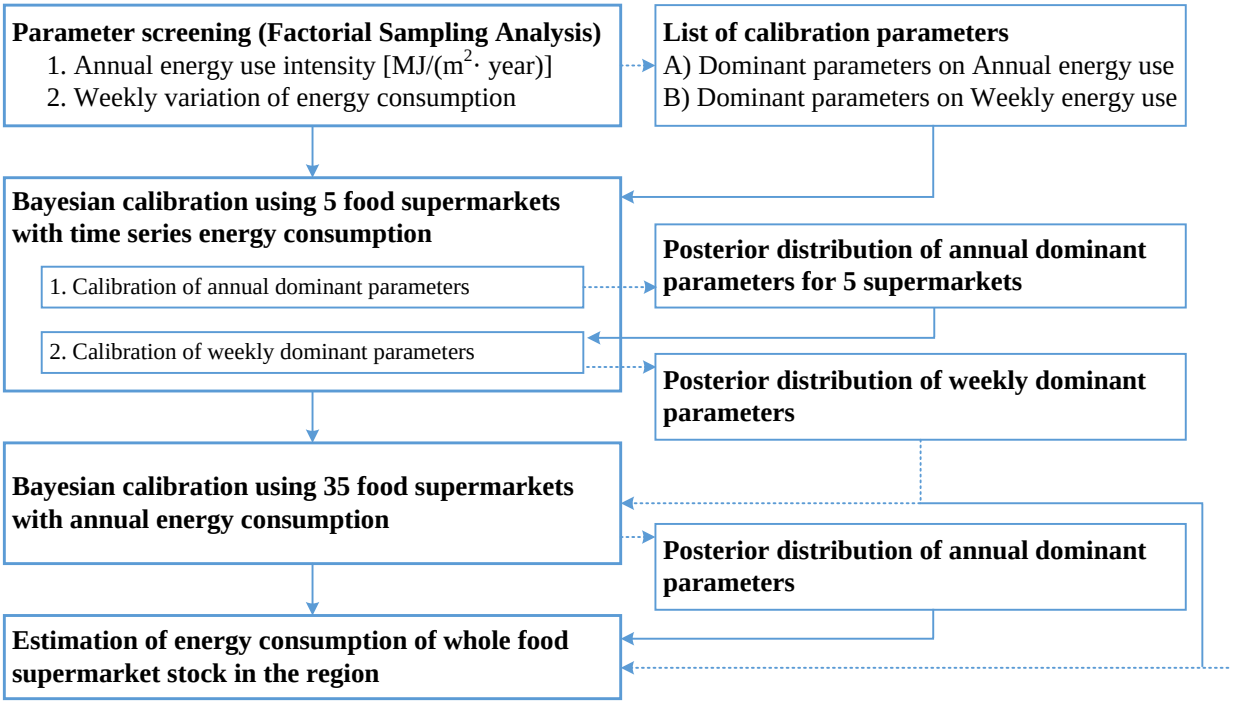


Figure 2-4 Proposed calibration process by Yamaguchi et al. (Yohei Yamaguchi, Suzuki, et al., 2013)

Kim et al. (J.-H. Kim et al., 2015) introduced "lifestyle factor" in the optimization method to consider the combined effect of occupancy variabilities such as presence, an operation of set-point temperatures, lighting schedules, and equipment use. The "lifestyle factor" is treated as a stochastic variable with four other variables: cooling coefficient of performance (COP), set-point temperature, internal gain, and infiltration. By considering the occupant factor, they reproduce more realistic EUI distribution for 2,182 apartment units in Korea than a deterministic method.

Zhao (Fei Zhao et al., 2016) proposed an approach to replicate an office building stock energy use in Chicago, U.S. from the survey data. This method used a linear inverse problem to derive design parameters of buildings. At first, the authors set 30 unknown parameters and examined to quantify the prior

uncertainty. Only 12 parameters out of 30 were chosen for calibration parameters after a sensitivity analysis. The multiple linear regression models using the selected 12 parameters was built to represent the normative building energy model for reducing computational effort. If the inverse problem is overdetermined, a set of values for the unknown parameter can be sampled by approximately satisfying the linear equation using Markov Chain Monte Carlo. In the validation, the predicted EUI distribution from the inverse problem was approximately identical with the EUI distribution of CBECS 2003 office buildings (765 samples, adjusted for Chicago's climate). The estimated parameter distributions were significantly different from the actual parameter distributions in CBECS 2003. The author indicated that the predicted building parameter distributions should not be considered as the real values, but the "best guess" of the real distributions that will produce the similar outcome of the real world. This "best guess" can be further improved using more measurement data to quantify the measurement errors between the data and the model.

Sokol et al. (Sokol et al., 2017) compared stochastic building stock energy modeling based on Bayesian calibration to deterministic simulation using literature, building data, adjusted variables using energy data. The deterministic archetype method is unable to represent the measured EUI distribution. In the Bayesian calibration, the calibration using monthly energy data is more accurate for predicting seasonal trends than the calibration using annual energy data.

Table 2-2 Stochastic building energy models

| Author | Year | Spatial Scale | Temporal resolution | Building simulation tool | Meta-model | Calibration method |
|---|---|---|---|---|---|---|
| Heo et al. (Y. Heo, 2011; Y. Heo et al., 2012) | 2011, 2012 | Individual building | Monthly | Engineering model (EnergyPlus, EPSCT) | GPE | Bayesian |
| Booth et al. (Booth et al., 2012) | 2012 | District scale (35 flats) | Daily (61 days) | Engineering model (EPSCT) | GPE | Bayesian |
| Tian et al. (Tian & Choudhary, 2012) | 2012 | Urban scale | Annual | Engineering model (EnergyPlus) | MLR | Bayesian/ Inverse problem |
| Choudhary and Tian (R. Choudhary & Tian, 2013) | 2012 | Urban scale | Annual | Statistic model | - | Bayesian |
| Booth and Choudhary (Booth & Choudhary, 2013) | 2013 | District scale (15,000 houses) | Annual | Engineering model (EPSCT) | - | Bayesian |
| Booth et al (Booth et al., 2013) | 2013 | Urban scale | Annual | Engineering model (EPSCT) | - | Bayesian |
| Kim et al. (Y.-J. Kim, Yoon, et al., 2013) | 2013 | Individual building | Monthly | Engineering model (EnergyPlus, EPSCT) | - | Bayesian |
| Yamaguchi et al. (Yohei Yamaguchi, Choudhary, et al., 2013) | 2013 | District scale (35 supermarkets) | Annual | Engineering model (In-house model ) | - | Bayesian |

| | | | | | | |
|---|---|---|---|---|---|---|
| Li et al. (Qi Li et al., 2015) | 2015 | Individual building | Monthly | Engineering model (EnergyPlus) | MLR | Bayesian |
| Kim et al. (J.-H. Kim et al., 2015) | 2015 | District scale (2,182 apartment units) | Monthly (4 months) | Engineering model (EPSCT) | - | Optimization |
| Heo et al. (Yeonsook Heo, Graziano, et al., 2015) | 2015 | Individual building | Monthly | Engineering model (EPSCT) | GPE | Bayesian |
| Tian (Tian, Wang, et al., 2014) | 2016 | Individual building | Monthly | Engineering model (EnergyPlus) | MLR | Bayesian |
| Zhao (Fei Zhao et al., 2016) | 2016 | Urban scale | Annual | Engineering model (EPSCT) | MLR | Inverse problem |
| Kang and Krarti (Kang & Krarti, 2016) | 2016 | Individual building | Monthly | Engineering model (eQUEST) | GPE | Bayesian |
| Li et al. (Qi Li et al., 2016) | 2016 | Individual building | Monthly | Engineering model (EnergyPlus) | MLR, GPE | Bayesian |
| Sokol et al. (Sokol et al., 2017) | 2017 | Urban scale | Annual, Monthly | Engineering model (EnergyPlus) | PR | Bayesian |

GPE: Gaussian Process regression Emulator, MLR: Multiple Linear Regression model, PR: polynomial regression model

## 2.6 Issues on existing stochastic building stock energy models

The probabilistic methods were used in building energy simulation to address the uncertainty challenge of deterministic building energy stock model. Monte Carlo method enables the deterministic building energy model to assess the probabilistic distribution of building energy consumption. Particularly,

the use of calibration method will improve the predictability of the building stock model. Stochastic calibration methods using engineering-based model allow users to take into account the uncertainties of unknown input information in representative building models. Moreover, it can analyze the impacts of new energy conservation measures taking advantage of the features of the engineering-based models. However, there are still remaining issues in the existing stochastic building stock energy models. Therefore, in this section, we discuss the limitations of the current stochastic building stock energy model and suggest possibilities for improvement.

### 2.6.1 Computational time

Stochastic calibration methods such as Bayesian inference and inverse problem incur a high computational cost. They use an MCMC to draw the posterior distributions for unknown parameters. The number of iterations for MCMC varies by model characteristics such as the number of unknown parameters, the range of prior distribution, etc. For one MCMC process for an individual building, it requires a number of iterations ranging from thousands to tens of thousands: 4,000 (Y.-J. Kim, Yoon, et al., 2013), 5,000 (Tian & Choudhary, 2012), 20,000 (Tian, Wang, et al., 2014), 25,000 (Fei Zhao, 2012), 30,000 (Qi Li et al., 2015), and 100,000 (Tian et al., 2016). When the MCMC process is applied to building stock, it will require additional iterations.

In an attempt to reduce computational time for dynamic building energy simulation, the following approaches have been proposed: simplified energy models, parameter screening, and meta-models.

Simplified models use the simple description of a building and its systems. It can drastically reduce simulation time as relative to the time required for the dynamic building energy simulation such as EnergyPlus, eQUEST, and TRNSYS. Normative model (e.g. EPSCT (Lee et al., 2011)) was employed in several studies (Booth et al., 2012; Y. Heo, 2011; Y. Heo et al., 2012; Y.-J. Kim, Yoon, et al., 2013; Fei Zhao, 2012). Simple hourly method" based on RC network used in CEN-ISO 13790 was employed to calibrate and optimize the unknown parameters (Henze et al., 2014; Jacob et al., 2010; Pavlak et al., 2013). However, those simplified models have limitations to forecast the impact of new technologies.

Parameter screening performs a sensitivity analysis and identifies the dominant parameters (input) affecting building energy use (output) for energy simulation models and observation study. By selecting only key variables as calibration parameters, one can reduce the number of iterations in the MCMC process. For a detailed review of sensitivity analysis, please refer to (Pianosi et al., 2016; Saltelli et al., 2000; Tian, 2013). Menberg et al. (Menberg et al., 2016) compared three sensitivity analysis methods in terms of computational costs and extractable information. However, the importance of the parameters can vary depending on the sensitivity analysis method and the target output (e.g. total, electricity, or gas energy). There is a need for a method that can determine the importance of parameters while considering various sensitivity methods and outputs. Moreover, there is insufficient research on how many parameters should be used for the calibration. Booth et al. (Booth et al., 2012) pointed out that selecting the number of calibration parameters is a "balancing act." By reducing calibration number of parameters, uncertainty in uncalibrated parameters is subsumed into the calibrated parameters. On the other hand, increasing the number of calibration parameters can lead to a reduction of accuracy and effectiveness of the Bayesian calibration (Booth et al., 2012). It is necessary to study the effects of the calculation time and the accuracy of the model depending on the number of parameters selected.

A meta-model (also called surrogate model) can be defined as a "model of model" (Eisenhower, O'Neill, Narayanan, et al., 2012), which is simpler and computationally faster than the original model. Different meta-models were applied to reduce simulation time in many studies: Multiple linear regression model (Manfren et al., 2013; Tian & Choudhary, 2012; Tian, Wang, et al., 2014; Fei Zhao, 2012), Gaussian process emulator (Booth et al., 2012; Y. Heo, 2011; Y. Heo et al., 2012; Manfren et al., 2013) and Support Vector Machines (Eisenhower, O'Neill, Narayanan, et al., 2012). Wei et al. (Wei et al., 2015) investigated the predictive performance of six meta-models (full linear, Lasso, MARS, SVM, bagging MARS, and boosting) developed based on measured data. Tian et al. (Tian et al., 2015) compared the accuracy of eight meta-models for the 114 campus buildings. Kim (Y. J. Kim, 2016) compared a prediction capability of Gaussian process emulator and polynomial chaos expansion for an uncertainty quantification. However, there are few studies on the effect of meta-model accuracy on the calibration. Further research is required

to determine which meta-models are available for the calibration. It is necessary to compare the advantages and disadvantages of each meta-model and the effect of the meta-model accuracy on the calibration results.

### 2.6.2 Building stock information for representative building

Building stock models require a wide range of information including geometric and non-geometric factors to develop representative buildings (archetypes). In practice, such building stock information is rarely available to classify and develop the representative building models. Most of existing stochastic building stock models are limited to one building type and developed with sufficient building stock information. If information is sufficient, buildings are classified into archetypes based on building properties such as building function and age. Ballarini et al. (Ballarini et al., 2014) classified residential archetypes at European level by location, age, building size, and shape. Österbring et al. (Österbring et al., 2016) integrated measured energy use and envelope area from a 2.5D GIS model to building characteristics for age-type building stock classification. Although the classification is based on such sufficient building stock information, there is a possibility of being influenced by the analyst's subjective decision. More research is required to provide appropriate and robust criteria for classifying archetypes. Classification and clustering methods using machine learning may be considered. On the other hand, if there is missing data in the building stock information, further study is required how to obtain the alternative information to substitute the required data. It is also necessary to explore how such insufficient information affects the accuracy of the building stock model.

### 2.6.3 Uncertainty in human behavior

Human behavior in building energy modeling remains the greatest uncertainty yet. Input parameters such as schedules of occupant presence, operation of appliance, equipment power density, lighting power density, and heating and cooling set point temperature are related to human behavior. In particular, an occupant schedule is the most important factors to classify building type. Such parameters related to human behavior have a significant impact on energy use in individual buildings (Clevenger et al., 2014; Hong & Lin, 2013; Silva & Ghisi, 2014). However, in building energy modeling, it has traditionally been calculated

using deterministic simplified hourly schedules and peak load. Much research is underway to identify the uncertainty of human behavior in buildings. Most of the research has been based on surveys, but in recent years, there has been an attempt to develop stochastic occupancy profiles for individual building using occupancy sensor (Diraco et al., 2015; Duarte et al., 2013; Wang et al., 2016), Bluetooth positioning (J. Zhao et al., 2014), and random process (Chen et al., 2015; O'Neill & Niu, 2017). The identification of actual occupancy schedule may contribute to accurate building energy forecasting and occupancy-based control.

For the building stock, Evins et al. (Evins et al., 2015) confirmed that physical variables such as fabric properties and geometries have a greater impact on energy use than behavioral variables such as occupancy and lighting. However, they found that stochastic schedules provide much smoother hourly energy use profile due to interactions of different occupant, appliance profiles. They also recommended using stochastic profiles rather than deterministic profiles when temporal behavior is important, such as finding peak loads. He et al. (He et al., 2015) emphasized the need for stochastic occupancy profiles for high-resolution temporal (e.g. hourly) energy analysis, showing that deterministic profiles have unrealistic peak loads. Comparing thermal demands from deterministic and stochastic schedules, there was substantial differences in hourly demand profiles but relatively small differences in total daily demands. As pointed out by He et al. (He et al., 2015), for energy analysis with low temporal resolution (e.g. annual) or large-scale regions, the effect of human behavior may not be significant due to an averaging effect. In addition to studying appropriate occupant behavior models, it is necessary to grasp more precisely the impact of human behavior on building stock energy use at various temporal and spatial resolutions.

### 2.6.4 Energy use data for calibration

The calibration process requires quality energy use data. Most building stock models perform calibration with sufficient energy use data. However, most of the modeler have difficulties in accessing the energy utility data for individual buildings due to privacy issues and absence of monitoring systems. It is necessary to study whether the model can be calibrated with insufficient energy use data. Tian et al. (Tian et al., 2016) investigated how to determine informative energy data in Bayesian calibration using correlation

analysis and a hierarchical clustering method. This method can improve understanding of the amount and quality of energy usage data required for Bayesian calibration.

### 2.6.5 Calibration process and results

Another challenge arises from the calibration process. Most of the building stock energy models include complicated Bayesian calibration process requiring specialized knowledge. The lack of transparency in existing models to date in the calibration process may pose challenges in accessing the models and interpreting results. Careful technical and systematic details in Bayesian calibration are required for policymakers and public.

There is also an issue of whether the calibrated building parameter distributions can accurately represent the real distribution. Zhao (Fei Zhao et al., 2016) argued in his research that the calibrated building parameter distributions should be considered as "best guess" of the real world. Future research should investigate the relationship between the estimated parameter distribution and the actual distribution, which will improve an understanding the energy conservation measures of building stock.

### 2.6.6 Aggregation

Aggregation is one of the most distinctive aspects of stochastic building stock modeling compare to the individual building modeling. There are two types of aggregation. One is the aggregation from the representative building to one type of building stock. Another is collecting different building stock types. The most straightforward method is that the energy use of building stocks is calculated by multiplying the EUI distribution of representative building models by total floor area. Tian (Tian & Choudhary, 2012) used the number of students per school to estimate gas consumption by all schools in London when the total floor area of schools is not available. More research is required to combine the diverse building stock types in the target district and to explore how to aggregate on different temporal and spatial scales.

## 2.7 Summary

Many researchers have made considerable efforts to advance the estimation of building energy consumption at large-scale. These models can be broadly divided into two methods: top-down and bottom-

up. The bottom-up models can be further classified into two types of approaches: statistical and engineering models. Top-down approaches are often used for supply analysis based on the energy demand by taking account of historical data and macroeconomic indicators. The top-down models lack the comprehension of building characteristics and transparency in the correlations between the indicators. Moreover, the top-down models have limitations to disaggregate the total energy consumption into the each sector or building stocks.

The bottom-up statistic models work at a disaggregated level, but it needs numerous databases of empirical data to investigate the relationships between each component and energy use. The statistical models have a limited capacity to assess the impact of energy conservation measures or new technologies. The bottom-up deterministic engineering building stock models can consider the impact of new technologies to reduce energy consumption in the building stock without historical data. However, these models have disadvantages of computational efficiency and capability of covering the uncertainties.

To overcome the uncertainty issue, some stochastic building stock models were proposed. Currently, there have been only a few studies that take into account the uncertainty associated with the large-scale building stock. However, these stochastic building stock energy models have considerable limitations, including high computational cost, low accessibility to the detailed building stock information and lack of transparency in the calibration process. Further research should be conducted to predict and evaluate the building stock energy consumption in order to cope with these challenges.

# CHAPTER 3: STOCHASTIC-DETERMINISTIC-COUPLED APPROACH FOR BUILDING ENERGY PREDICTION

## 3.1 Introduction

To address the uncertainty issues, some authors proposed probabilistic methods to represent the uncertainty of input parameter, by defining the input parameters as distributions. Moreover, the building stock energy models were calibrated based on the statistical methods. For the calibration, an linear inverse problem (Tian & Choudhary, 2012; Fei Zhao et al., 2016) and Bayesian inference (Booth et al., 2012; Tian & Choudhary, 2012) were used (See Table 3-1).

The main purpose of this chapter to compare two approaches (linear inverse problem and Bayesian inference) for model calibration. Moreover, the effect of using meta-models for calibration is examined. The accuracy and computational cost are examined to select a proper method for estimation of building stock energy. This paper is structured as follows. First, the calibration processes of each literature were reviewed and compared at each step. Base on the compared methodologies, the combination of progress are established to examine the methodologies with theoretical backgrounds. Then, the suggested combinations are applied to predict the building energy use at the campus level. Finally, the estimated energy consumption data are compared to each other to find a proper methodology for the building stock.

Table 3-1 Comparison of methodologies

| Author | Building energy model | Parameter screening | Meta-model | Calibration method | Aggregation |
|---|---|---|---|---|---|
| Tian and Choudhary (Tian & Choudhary, 2012) | EnergyPlus | Standardized Regression Coefficient | Multiple Linear Model | Linear inverse problem | EUI*pupil number*assumed pupil density*factor of school size |
| | | Multivariate Adaptive Regression Splines | | Bayesian Inference | |

| | | | | | |
|---|---|---|---|---|---|
| Booth et al. (Booth et al., 2012) | EPSCT (Energy Performance Standard Calculation Toolkit) | Morris method | Gaussian Process Emulator | Bayesian Inference | Energy consumption *Number of buildings |
| Zhao (Fei Zhao, 2012) | EPSCT | Stepwise regression analysis | Multiple Linear Model | Linear inverse problem | Weighting factor |

## 3.2 Methodology

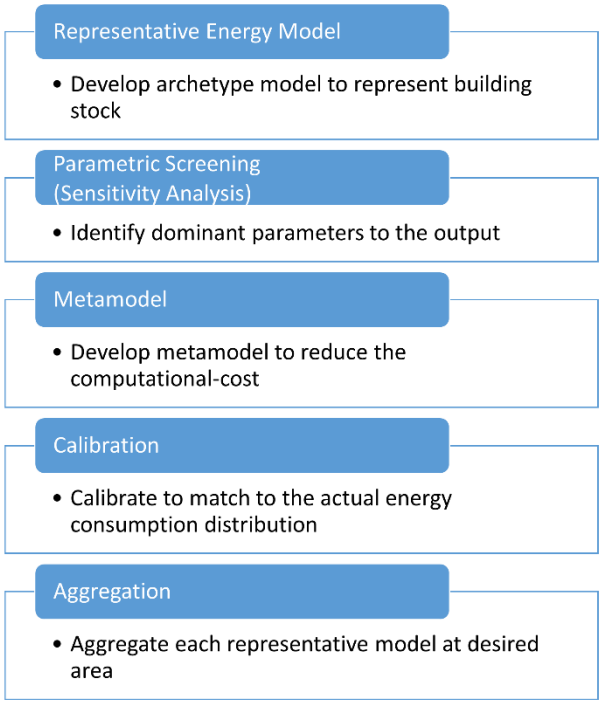


Figure 3-1 Flowchart of progress

### 3.2.1 Representative model

#### 3.2.1.1 Development of representative building

The first step is to develop representative building models. After analyzing the building stock information such as building type, number of floors, building floor area and so forth, representative building models are developed to represent one building stock. It is necessary to choose proper number of

representative building models since it affects both accuracy of result and analysis time. For example, if one selected only two representative buildings such as residential and commercial building, the computational cost will be not expensive. On the other hand, if more detailed archetypes are developed considering the building's age or functions, the computation cost will be expensive, however, more accurate building energy prediction is avaiable.

#### 3.2.1.2 Building energy simulation tools

For the building stock energy model, diverse building energy models have been adopted to estimate the building energy use of representative building. In the study of Tian and Choudhary (Tian & Choudhary, 2012), EnergyPlus was employed as an energy simulation model. Transient simulation models such as EnergyPlus, eQUEST can be used to model a building and systems at a high level of detail. The transient simulation models has an advantage when detailed design and sizing of specific systems need to be evaluated in terms of the overall energy consumption in the building (Y. Heo, 2011). However, this level of detail tends to place burden to the modeling process for large-scale simulations.

Since computational intensive energy simulation is necessary for stochastic modeling, Booth (Booth et al., 2012) and Zhao (Fei Zhao, 2012) used a quasi-steady-state model based on the Energy Performance Standard Calculation Toolkit (EPSCT) as an energy model. This model is based on a set of normative calculations outlined in the international standards set by the European Committee for Standardization (CEN) and the International Organization for Standardization (ISO). The CEN-ISO based model is possible to generate deterministic energy use estimations for thousands of houses in a few minutes. However, such simple models have limitation to apply and estimate new technologies.

#### 3.2.1.3 Selecting uncertain input parameter

In the individual building simulation model, there are numerous input variables. It is impossible to the user to know all of the input values correctly. Although the user identifies some design values, there might be differences between the design values and actual values due to other influences such as external

temperature fluctuations or occupancy's use pattern. Therefore, the building simulation has inherent uncertainty.

In the terms of building stock scale, it is also impossible to utilize one deterministic representative building model to represent the all buildings in the district. Since each building has a different function, envelope, schedule, and HVAC system, the representative building model also has many uncertainties. Therefore, the uncertain input parameters should be chosen to represent the probability of all buildings in the building stock.

#### 3.2.1.4 Input range

To make a deterministic model to a probabilistic model, they specified a range of input parameters.

Tian and Choudhary (Tian & Choudhary, 2012) adopted two categories of sufficient statistical data for the representative building model: (a) Building information such as floor area, height of buildings, construction characteristics. (b) Operational characteristics including the HVAC system, internal heat gains, detailed schedules for inputs. These data were collected from diverse sources such as published literature, the national survey (such as RECS, CBECS), and geographic information system (GIS) database. In addition, the sufficient actual energy use data are required to calibrate for the representative buildings.

#### 3.2.1.5 Monte Carlo simulation

Once input parameter ranges are chosen, it is needed to propagate the uncertainty of the representative building model. Monte Carlo method has chosen to derive the stochastic results for each representative building in many studies (Booth et al., 2012; Y. Heo et al., 2012; Y.-J. Kim, Yoon, et al., 2013; Tian & Choudhary, 2012; Yohei Yamaguchi, Suzuki, et al., 2013). Monte Carlo method is a computational method to obtain numerical results rely on repeated random sampling. It runs a number of deterministic dynamic energy simulation by sampling a set of input parameters from the input parameter ranges. The probabilistic outcomes could be obtained by Monte Carlo method.

### 3.2.2 Parameter screening (sensitivity analysis)

The parameter screening is process to select the calibration parameters. The dominant input parameters on the simulation output can be identified by sensitivity analysis. Then, we can determine the number of parameters to be calibrated.

Selection of the calibration parameter is important to the calibration progress. Booth et al. (Booth et al., 2012) viewed that selecting the number of parameters to calibrate is a "balancing act". For a given amount of the observed data, if the number of parameters is too few, the uncertainty in un-calibrated parameters could be contained within the calibrated parameters, thus the physical meaning of the estimated posterior distribution can cause a distortion. On the contrary to this, when there are too many parameters to calibrate, the accuracy and effectiveness of the calibration methodology will be reduced for a given amount of measured data. Increasing in the number of calibration parameters entails the need for numerous runs for the calibration algorithm, resulting in a more computational effort for the calibration progress. A balance must be reached, therefore, between the accuracy of the calibration and the effort put into data collection.

In Tian and Choudhary's study (Tian & Choudhary, 2012), they performed the sensitivity analysis using SRC (Standardized Regression Coefficient) and MARS (Multivariate Adaptive Regression Splines). First four significant parameters out of the 16 parameters on heating energy consumption were selected as calibration parameters: the heating setpoint temperature, ventilation, infiltration rate and U-value of the roof.

The factorial sampling method (FSA or Morris method) was utilized in Booth et al. (Booth et al., 2012). FSA assesses the interactions between different parameters and can show the mean and standard deviation of the effect of varying an individual parameter visually. A large mean and large standard deviation indicates that the parameter is dominant to the result. Four parameters were selected for calibration: internal setpoint temperature, fraction of space heated, heating system COP and air leakage at 50 Pa.

Zhao performed a stepwise regression analysis to find the best subset and obtained 24 of 30 candidate variables. Then, 24 variables were ranked by their absolute t-statistic values using multiple linear

regression. As a result, the first 12 variables were selected the calibration parameters (Fei Zhao, 2012). Tian also reviewed the sensitivity analysis methods in building energy analysis in his study (Tian, 2013).

### 3.2.3 Meta-models (Surrogate models)

As stated above, physical whole building model can be computationally expensive since it requires much computing time to process enormous parameters. The meta-model (surrogate model) can be introduced to overcome expensive computational cost. Meta-model is a statistic model that correlates the input and output of simulations. It can mimic the whole building energy model. The main reason for using meta-model is that it requires much less simulation time than running detailed building energy simulation models such as EnergyPlus, eQUEST.

Tian (Tian & Choudhary, 2012) and Zhao (Fei Zhao, 2012) used multiple linear regression model (MLR) using OLS (ordinary least squares) that is most commonly used statistical method for estimation of building energy consumption. Booth (Booth et al., 2012) accepted the Gaussian Process Emulator (GPE). It is also a well-known technique for data analysis as it allows for dealing with problems associated with multiple time and space variables such as real-time building energy simulation and model predictive control since it can work with highly multivariate input/output (Manfren et al., 2013). The selection of meta-model should be conducted based on the consideration of the accuracy of the detailed energy model and the reduction of computational effort.

### 3.2.4 Calibration method

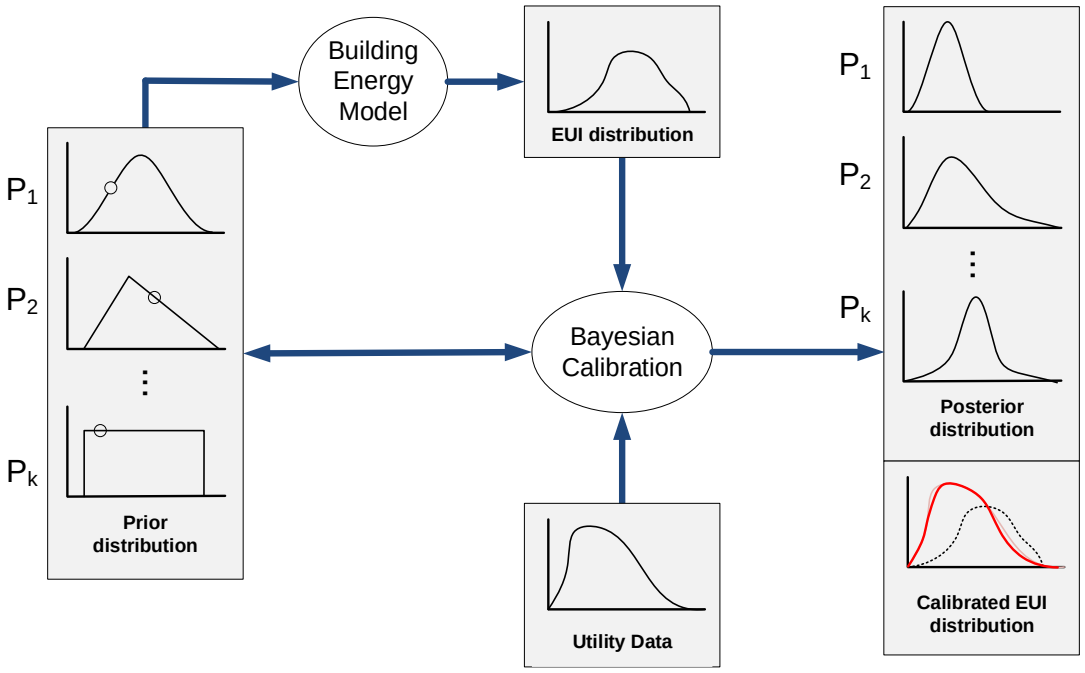


Figure 3-2 Concept of Bayesian calibration

There is a discrepancy between the simulated result and observation data due to unknown input data and the uncertainty associated with a simulation. The calibration is a process to minimize the difference. It is also a method about how we can derive the input distribution by a statistical model having the output of model. Zhao (Fei Zhao, 2012) used the linear inverse problem, and Booth (Booth et al., 2012) utilized the Bayesian inference for calibration. Tian (Tian & Choudhary, 2012) calibrated using both methods and compared the results. In the linear inverse problem, the problem is considered as a linear inverse problem constrained by linear equality and inequality conditions (upper and lower bound of input parameters). On the contrary, we can specify our prior belief about the parameters in the Bayesian inference, and the posterior value are derived based on Bayesian theorem.

The main difference between the two methods is the method of assuming the prior distribution of a parameter. Linear inverse problem can only specify uniform distribution with upper and lower bounds. In the Bayesian inference, it can define the shape of a distribution and range of input parameters. It enables to

use our existing knowledge from previous literature such as research, report, survey (Tian & Choudhary, 2012).

### 3.2.5 Combination of methodologies

Based on the detailed review of three papers, we examined each progress in detail and selected four options for the possible combination. Table 3-2 contains the combination of method at each progress. In this study, the options were performed and compared considering accuracy and computational time.

Table 3-2 Combination options of the process

| | **Representative model** | **Parameter screening** | **Meta-model** | **Calibration method** |
|---|---|---|---|---|
| **Opt.1** | EnergyPlus | Stepwise regression analysis | - | Bayesian Inference |
| **Opt.2** | EnergyPlus | Stepwise regression analysis | Multiple Linear Model | Linear inverse problem |
| **Opt.3** | EnergyPlus | Stepwise regression analysis | Multiple Linear Model | Bayesian Inference |
| **Opt.4** | EnergyPlus | Stepwise regression analysis | Gaussian Process Emulator | Bayesian Inference |

## 3.3 Demonstration of Principles

### 3.3.1 Representative model

EnergyPlus has been widely used in the individual building energy simulation filed and has been tested extensively. As mentioned above, the transient simulation models such as EnergyPlus tend to be a burden in the large-scale simulation due to its high level of detail. However, since we need to consider the expandability for application of new technologies, EnergyPlus was selected as an energy model.

The buildings in University of Michigan at Ann Arbor (from now on UM) were chosen as a subject of the case study due to the detailed building and energy information available for 75 buildings on UM

campus. Energy Management team in UM has monitored the energy consumption of all UM buildings ("Energy Management Michigan," n.d.). Other building information such as built year, renovation year, number of floors, building primary function can be gathered from another campus website (University of Michigan, n.d.). Out of 75 buildings, 30 buildings were chosen as a 'campus building' type according to building main function, energy use data. The campus building type includes office buildings, classroom buildings, halls, libraries. The campus building type in UM was utilized to compare the detail in the methodology. We will compare eight different methodologies through the campus building stock in UM.

Then, we developed a representative building energy model for campus-type in UM. The base EnergyPlus model was created by the EnergyPlus Example File Generator (EEFG) (U.S. Department of Energy, n.d.). In the EEFG, building type was specified as an 'Office'. The average number of floors and average total floor area of 30 campus type buildings in UM were used as a building geometry; average number of floor is four, and average total floor area is 10,337$m^2$. The Building internal zone were simplified by four perimeter zones and one core zone. The Schedules were also generated by EEFG. The TMY3 weather data of Ann Arbor, MI was utilized for the simulation model. This input values created by the EEGF was modified to apply the input parameter ranges.

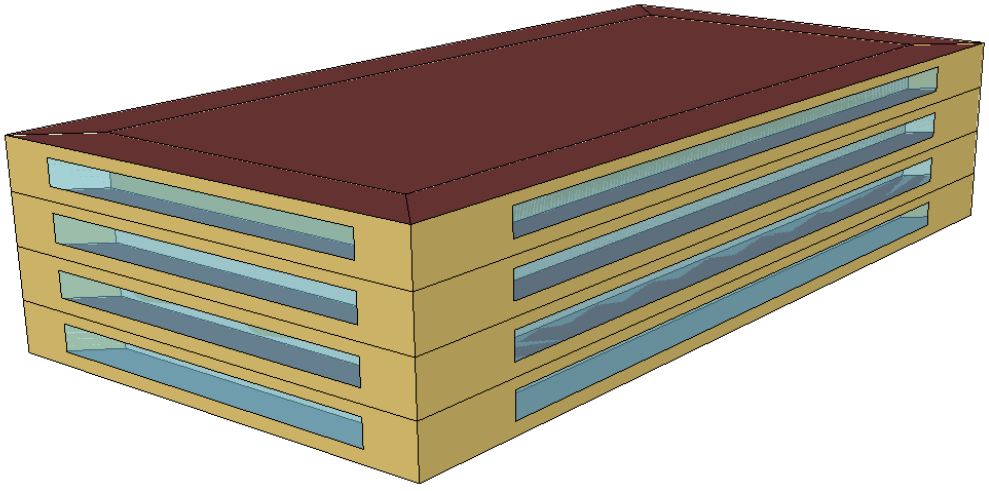

Figure 3-3 Representative building model for Campus-type

There are much input parameters for a dynamic building energy simulation model. In this study, we consider 12 parameters as input variables based on existing literature. (Booth et al., 2012; Tian &

Choudhary, 2012; Fei Zhao, 2012): Roof Insulation Thickness [m], Wall Insulation Thickness [m], Window U-Factor [W/m$^2$K], Window Solar Heat Gain Coefficient [-], Equipment power density [W/m$^2$], Lighting power density [W/m$^2$], Heating setpoint [◦C], Cooling setpoint [◦C], Occupancy [m$^2$/person], infiltration [ACH], Boiler efficiency [-], Cooling COP [-]. These input variables are listed in Table 3-3. The distribution of input parameters was assumed as a triangular distribution to consider the maximum, minimum range, as well as the most plausible value for each parameter. The values indicate a triangular distribution: Minimum - Mode - Maximum. These ranges are derived from the extant literature, standards, and report, then applied 30% of the safety factor to represent the plausible values for existing building parameters.

Table 3-3 Variable list and input range

| | Model Parameters [Unit] | Values (Campus Type)* | Source |
|---|---|---|---|
| P1 | Roof Insulation Thickness (ROOF) [m] | 0.01 - 0.116 - 0.25 | (ASHRAE, 2004; Deru et al., 2011; Griffith et al., 2008; Huang & Franconi, 1999; Tian & Choudhary, 2012; Fei Zhao, 2012) |
| P2 | Wall Insulation Thickness (WALL) [m] | 0.01 - 0.046 - 0.25 | (ASHRAE, 2004; Deru et al., 2011; Griffith et al., 2008; Huang & Franconi, 1999; Tian & Choudhary, 2012) |
| P3 | Window U-Factor (WIN) [W/m$^2$K] | 1 - 3.35 - 5 | (ASHRAE, 2004; Deru et al., 2011; Huang & Franconi, 1999; Tian & Choudhary, 2012) |
| P4 | Window SHGC (SHGC) [-] | 0.1 - 0.39 - 0.9 | (ASHRAE, 2004; Deru et al., 2011; Tian & Choudhary, 2012) |
| P5 | Equipment power density (EPD) [W/m$^2$] | 1 - 11.67 - 60 | (S Heiple, 2007; Huang & Franconi, 1999; Thornton et al., 2011; Tian & Choudhary, 2012; Fei Zhao, 2012) |
| P6 | Lighting power density (LPD) [W/m$^2$] | 1 - 12.43 -40 | (ASHRAE, 2004; S Heiple, 2007; Huang & Franconi, 1999; Tian & Choudhary, 2012; Fei Zhao, 2012) |
| P7 | Heating setpoint (HSP) [◦C] | 17 -21 - 25 | (Bonnema et al., 2013; Deru et al., 2011; Tian & Choudhary, 2012) |
| P8 | Cooling setpoint (CSP) [◦C] | 20 - 24 - 28 | (Deru et al., 2011; Tian & Choudhary, 2012) |
| P9 | Occupancy (OCC) [m$^2$/person] | 2 - 14.37 - 56.7 | (Bonnema et al., 2013; Deru et al., 2011; Huang & Franconi, 1999; Fei Zhao, 2012) |
| P10 | Infiltration rate (INF) [ACH] | 0.1 - 0.56 - 1.3 | (Griffith et al., 2008; Y. Heo, 2011; C. J. Hopfe & Hensen, 2011; Tian & Choudhary, 2012) |
| P11 | Boiler efficiency (BOILER) [-] | 0.5 - 0.72 - 0.95 | (Deru et al., 2011; Griffith et al., 2008; Huang & Franconi, 1999; Tian & Choudhary, 2012) |
| P12 | Cooling COP (COP) [-] | 2 - 2.65 - 4 | (Deru et al., 2011; Yu & Chan, 2004) |

* Values indicate a triangular distribution: Min. - Mode – Max.

#### 3.3.1.1 Propagation of uncertainty

The Monte Carlo (MC) method was used to derive the probabilistic results. The MC simulation generates a random number from the given range of the input parameter and iterates the energy simulation. Latin Hypercube Sampling (LHS) (McKay et al., 1979) is one of the most used sampling methods in the studies that deal with a stochastic building simulation. It was applied and validated in a number of previous studies. (Eisenhower, O'Neill, Fonoberov, et al., 2012; Y. Heo et al., 2012; C. J. Hopfe & Hensen, 2011; Y.-J. Kim, Yoon, et al., 2013; Tian, Wang, et al., 2014; Fei Zhao, 2012) The Monte Carlo simulation was performed using jEPlus tool (Y. Zhang & Korolija, 2010) to sample the random number and iterate EnergyPlus.

#### 3.3.1.2 Sampling size

To find proper LHS sample size, the convergence diagnostic was conducted. The number of LHS increases from 10 to 1,500, gradually. The LHS is run ten times for each sample size. The Root Mean Square Error (RMSE) is used to evaluate the accuracy of the LHS size.

$$\mathrm{RMSE} = \left(\frac{1}{\mathrm{N}}\sum_{i=1}^{N}(y_i - \hat{y}_i)^2\right)^{\frac{1}{2}} \tag{3.1}$$

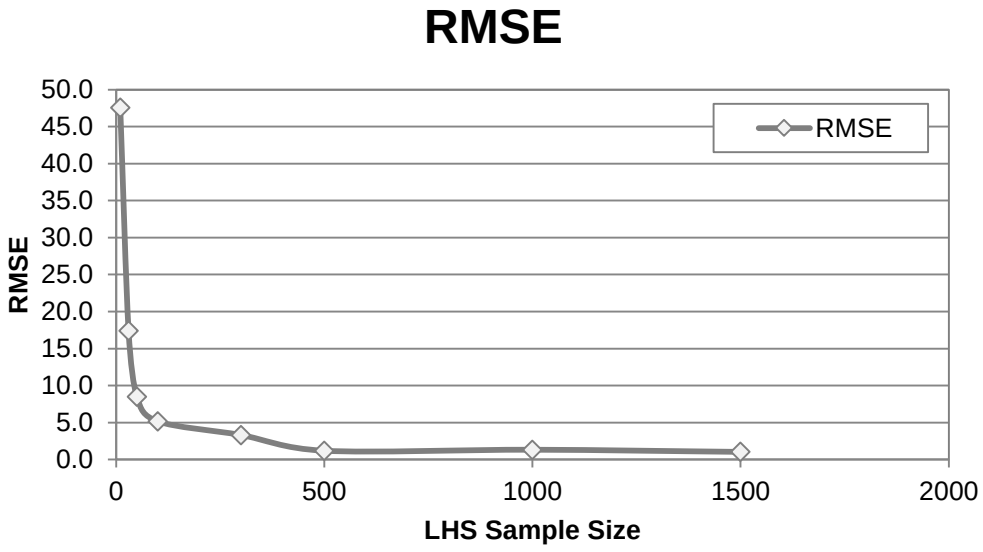


Figure 3-4 LHS sampling size

As seen in Figure 3-4, the RMSE does not change substantially where the sample sizes are greater than 500. In order to minimize the effect of uncertainty from the random sampling, therefore, a sample size of 1,000 was selected for this simulation.

3.3.1.3 Monte Carlo method result

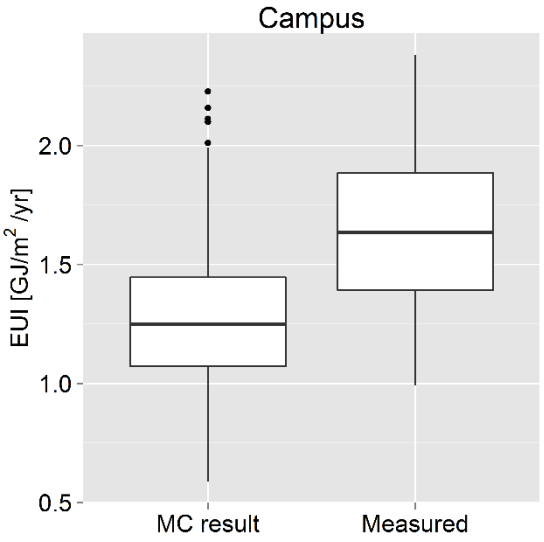


Figure 3-5 Results of MC simulation

The results of MC simulation using EnergyPlus are shown in Figure 3-5. The electricity and gas consumptions calculated in EnergyPlus were combined as a unit of GJ (Gigajoule) and then divided by the total floor area of the representative building to present the energy use intensity ($GJ/m^2$). There is a significant difference between MC simulation results and the measured data. The calibration will be conducted by modifying the input parameters to reflect the actual energy consumption distribution.

3.3.2 Parameter screening (sensitivity analysis)

Regression method is one of the most frequently used methods for sensitivity analysis in building energy analysis (Tian, 2013). It identifies the variables that have a significant impact on the simulation output to determine the number of parameters for calibration. A lower number of parameters reduces the computational cost. The 1,000 samples from MC simulation are used to perform a stepwise regression analysis. Table 3-4 presents the list of the t-values, p-values, change of $R^2$ and adjusted $R^2$ of each regression

step. 12 parameters are ranked by the descending order of t-values. The higher absolute t-values means that it is more significantly correlated to the EUI. The EPD is most dominant, and the CSP is the least dominant on the annual total EUI.

For the parameter screening, the R function "regsubsets()" in the "leaps" package (Thomas Lumley based on Fortran code by Alan Miller, 2017) can find the best subsets using Bayesian information criterion (BIC) (Schwarz, 1978). Figure 3-6 shows the best subset of a particular size and Figure 3-7 indicates the change of BIC according to variable size. The change of BIC is reduced dramatically after eight variables. Therefore, eight parameters are selected for meta-model and calibration parameters. The adjusted R-squared of selected eight parameters is 0.9229 while that of all parameters (12) is 0.9262. There are no significant differences in adjust R-squared between models with 12 variables and 8 variables. However, as results of convergence diagnostic (Gelman & Rubin, 1992), the Bayesian calibration for 12 parameters required 4,000 iterations, and the Bayesian calibration for 8 parameters required 3,000 iterations. By reducing the calibration variables, it is possible to reduce the iteration of simulation required for the Bayesian calibration. In this way, parameter screening should be performed taking into account the balance between model accuracy and computational cost.

Table 3-4 Sensitivity analysis of 12 parameters for Campus type buildings

| Ranking | Parameters | t value | p-value | $R^2$ | $R^2$(adj) |
|---|---|---|---|---|---|
| 1 | EPD | 81.52 | < 0.001 | 0.5229 | 0.5224 |
| 2 | LPD | 44.77 | < 0.001 | 0.6825 | 0.6818 |
| 3 | INF | 44.60 | < 0.001 | 0.8377 | 0.8372 |
| 4 | BOILER | -21.98 | < 0.001 | 0.8775 | 0.8770 |
| 5 | HSP | 21.28 | < 0.001 | 0.9090 | 0.9086 |
| 6 | WIN | 9.47 | < 0.001 | 0.9161 | 0.9156 |
| 7 | COP | -7.39 | < 0.001 | 0.9204 | 0.9198 |
| 8 | ROOF | -6.45 | < 0.001 | 0.9236 | 0.9229 |
| 9 | SHGC | 4.92 | < 0.001 | 0.9254 | 0.9247 |
| 10 | WALL | -4.03 | < 0.001 | 0.9266 | 0.9258 |
| 11 | OCC | 2.06 | < 0.001 | 0.9269 | 0.9260 |
| 12 | CSP | 1.60 | < 0.001 | 0.9270 | 0.9262 |

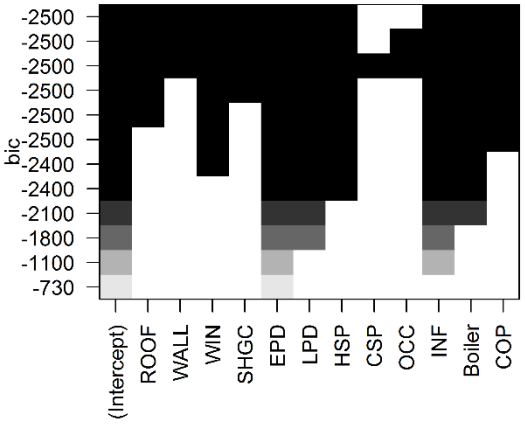


Figure 3-6 Best subset of a particular size from one to 12 variables

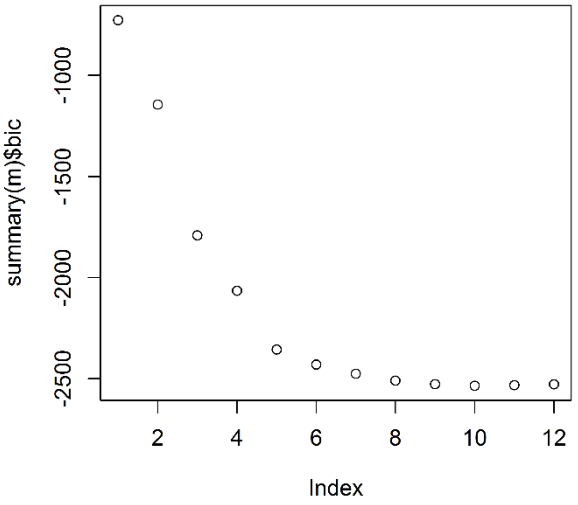


Figure 3-7 BIC tracking according to variable size

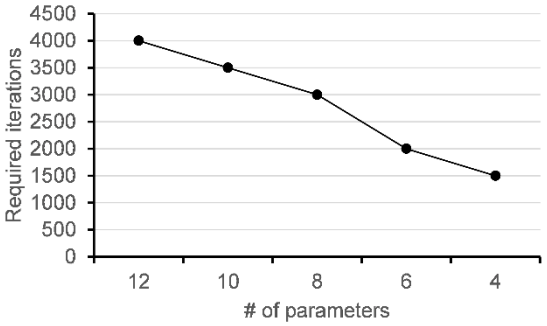


Figure 3-8 Required iterations number depending on the number of parameters

### 3.3.3 Meta-models

Monte Carlo simulation method is performed to present stochastic uncertainty in building simulation. It is a way to iterate the simulation using sampling from uncertain input parameter range. A number of samples are necessary to ensure the quality of simulation. It derives massive computation power and efforts. It demands significantly time-consuming to use the dynamic building energy model like EnergyPlus for Monte Carlo simulation. Therefore, two types of meta-models replacing the EnergyPlus were considered to reduce the computational time. 1,000 of input-output sets were obtained using

EnergyPlus. Among 1,000 of data, 700 of data are used for training data to make model and then 300 of data are used for testing. Three options could be considered in this step: None meta-model (using EnergyPlus for calibration), multiple linear regression model (MLR), and Gaussian process emulator (GPE).

#### 3.3.3.1 Multiple linear regression model

The simplest model of regression is a multiple linear regression model (MLR). This model can be formed as the following expression:

$$y_i = \beta_1 x_{i1} + \cdots + \beta_p x_{ip} + \varepsilon_i = x_i^T \beta + \varepsilon_i \ , \qquad i = 1, \ldots, n \tag{3.2}$$

Where $y_i$ is the output, x denotes inputs, β is regression coefficients and ε is error. The multiple linear regression model was developed using 'lm' function in R-package 'stats' (R Core Team, 2016).

#### 3.3.3.2 Gaussian Process Emulator

Gaussian processes (GPs) are commonly utilized as surrogate statistical models for predicting output of computer experiments (Santner et al., 2003). A Gaussian process defines a probability distribution of $f(x)$ which is composed of input $x$ and target $y$. Then distribution of $f(x)$ is used to predict the value of $y_*$. The basic idea of the GP is that the corresponding output are modeled as a multivariate Gaussian distribution. The multivariate Gaussian is defined as:

$$p(x; \mu, \Sigma) = \frac{1}{(2\pi)^{n/2}|\Sigma|^{1/2}} \exp\left(-\frac{1}{2}(x-u)^T \Sigma^{-1}(x-\mu)\right) \tag{3.3}$$

where, $x$ is a vector valued random variable; μ is the mean of the distribution; Σ is the covariance matrix; $n$ is the number of input variables; $|\Sigma|$ is the determinant of covariance matrix

There are several useful characteristics of the multivariate Gaussian: normalization, marginalization, conditioning and summation (Rasmussen, 2006). GP model is defined by a mean function $m(\cdot)$ and a covariance function $k(\cdot,\cdot)$, with $x_1, \ldots, x_n \in X$ and the corresponding value $f(x_1), \ldots, f(x_m)$ :

$$\begin{bmatrix} f(x_1) \\ \vdots \\ f(x_m) \end{bmatrix} = N\left(\begin{bmatrix} m(x_1) \\ \vdots \\ m(x_m) \end{bmatrix}, \begin{bmatrix} k(x_1,x_1) & \cdots & k(x_1,x_m) \\ \vdots & \ddots & \vdots \\ k(x_m,x_1) & \cdots & k(x_m,x_m) \end{bmatrix}\right) \tag{3.4}$$

We can denote this using notation,

$$f(\cdot) \sim GP(m(\cdot), k(\cdot,\cdot)) \tag{3.5}$$

$$m(x) = E[x] \tag{3.6}$$

$$k(x, x') = E[(x - m(x))(x' - m(x'))] \tag{3.7}$$

Now, GP can be regarded as finding the mean function and covariance function. It is hard to find the covariance so that we assume that the covariance function has some particular parameter and it is called as kernel function $k(x, x')$. Therefore, Gaussian processes are kernel based probability distributions and any valid kernel function can be used as a covariance function. Common covariance functions are discussed by Rasmussen (Rasmussen, 2006). A popular choice is the squared exponential (Ebden, 2008; Rasmussen, 2006), scaling parameter $\sigma_f$ and length scale $l$ are hyperparameters which are identified from the training data using a maximum likelihood optimization.

$$\mathrm{k(x, x')} = \sigma_f^2 \exp\left(-\frac{(x - x')^2}{2l^2}\right) \tag{3.8}$$

Once the mean and covariance functions are defined, GPs follows the basic rules of the multivariate Gaussians.

Gaussian processes provide probability distributions over functions. Gaussian Process emulator (GPE) means making Gaussian process regression model using Gaussian process based on Bayesian theorem and training data.

Consider observing a data set $D = \{(x_i, y_i)_{i=1}^n\} = (X, y)$. The GPE is developed with Gaussian noise error.

$$y_i = f(x_i) + \varepsilon_i \tag{3.9}$$

Where the $\varepsilon_i$ are i.i.d (independent identically distribute) noise variables $\varepsilon \sim N(0, \sigma^2)$. The prior distribution over function $\mathrm{f}(\cdot)$ is assumed as zero-mean Gaussian process and this simplifies the calculation without loss of generality.

$$f(\cdot) \sim GP(0, k(\cdot,\cdot)) \tag{3.10}$$

The posterior on $f$ is a GP since the prior on $f$ is a GP and likelihood is Gaussian. We can make predictions using this characteristic.

$$p(y_*|x_*, D) = \int p(y_*|x_*, f, D)p(f|D)df \tag{3.11}$$

we can use the marginal likelihood to compare and tune covariance functions

$$p(y|X) = \int p(y|f, X)p(f)df \tag{3.12}$$

Assume that we want to predict the value $y_*$ at new input point $X_*$. The marginal distribution over any set of input points belonging to X should have a joint multivariate Gaussian distribution.

$$\begin{bmatrix} f \\ f_* \end{bmatrix} |X, X_* \sim N\left(0, \begin{bmatrix} K(X,X) & K(X,X_*) \\ K(X_*,X) & K(X_*,X_*) \end{bmatrix}\right) \tag{3.13}$$

From the i.i.d. noise,

$$\begin{bmatrix} \varepsilon \\ \varepsilon_* \end{bmatrix} \sim N\left(0, \begin{bmatrix} \sigma^2 I & 0 \\ 0^T & \sigma^2 I \end{bmatrix}\right) \tag{3.14}$$

Now, we can present GPE

$$\begin{bmatrix} y \\ y_* \end{bmatrix} |X, X_* = \begin{bmatrix} f \\ f_* \end{bmatrix} + \begin{bmatrix} \varepsilon \\ \varepsilon_* \end{bmatrix} \sim N\left(0, \begin{bmatrix} K(X,X) + \sigma^2 I & K(X,X_*) \\ K(X_*,X) & K(X_*,X_*) + \sigma^2 I \end{bmatrix}\right) \tag{3.15}$$

The predictive distribution of $y_*$ given $y$ is

$$y_*|y, X, X_* \sim N(\mu^*, \Sigma^*) \tag{3.16}$$

Where

$$\text{mean function } \mu^* = K(X_*,X)(K(X,X) + \sigma^2 I)^{-1} y$$

$$\text{covariance } \Sigma^* = K(X_*,X_*) + \sigma^2 I - K(X_*,X)(K(X,X) + \sigma^2 I)^{-1} K(X,X_*)$$

The marginal likelihood which is a function of hyperparameters can be expressed as

$$p(y|X) = N(0, k(x,x') + \sigma^2 I) \tag{3.17}$$

Where its log is:

$$\ln p(y|X,\theta) = -\frac{1}{2}\ln\det(k(x,x') + \sigma^2 I) - \frac{1}{2}y^T(k(x,x') + \sigma^2 I)^{-1}y + const \tag{3.18}$$

This equation can be optimized as a function $\sigma_f$, $l$ and $\sigma$.

Above analytical method is utilized to find the maximum likelihood estimates (MLE) of all unknown parameter (hyperparameters). Other methods to estimate the conditional posterior and predictive distributions are discussed by Rassmussen (Rasmussen, 2006) and Vanhatalo (Vanhatalo & Riihimäki, 2012). In this study, GPE of given data set (the results of EnergyPlus Monte Carlo simulation) was developed using *mlegp* function in R-package '*mlegp*'. (Dancik, 2013)

Table 3-5 shows the comparison between multiple regression linear model and Gaussian process emulator. GPE takes more time to build the model using given dataset while it is more accurate. GPE can emulate the result of EnergyPlus more correctly than Multiple Linear regression model.

Table 3-5 Comparison between MLR and GPE

| | **Multiple Linear Regression** | **Gaussian Process Emulator** |
|---|---|---|
| | 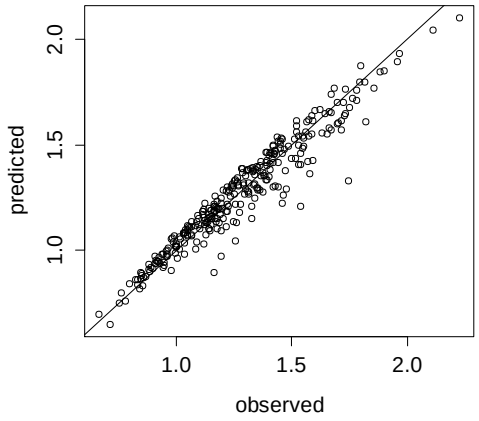 | 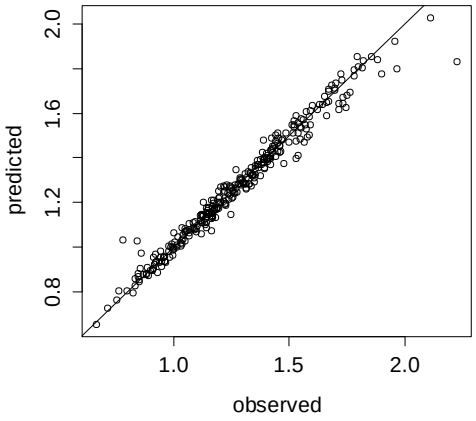 |
| **Time for making the model** | 0.1 second | 32 min |
| **RMSE** | 0.074 | 0.047 |

| | | |
|---|---|---|
| **Pearson's product-moment correlation** | 0.962 | 0.985 |

### 3.3.4 Calibration methods

#### 3.3.4.1 Linear inverse problem

The solving inverse problem can be defined as deriving the input from the given (known) output of the model. A linear inverse problem is a special inverse problem using linear function. A linear model can be written in matrix notation as $\boldsymbol{Ax} = \boldsymbol{b} + \epsilon$, where $\boldsymbol{x}$ is a vector of variables, and $\epsilon$ is an error vector. Given parameter matrix $\boldsymbol{A}$, calculating value of $\boldsymbol{b}$ for $\boldsymbol{x}$ is a forward problem. On the contrary, estimating the parameter vector $\boldsymbol{x}$ is an linear inverse problem using data of $\boldsymbol{b}$ and $\boldsymbol{A}$.

A general formulation considering equality and inequality constraints can be expressed as:

$$\begin{cases} \text{linear model: } \mathbf{Ax} = \mathbf{b} + \varepsilon \\ \text{equality constraints: } \mathbf{Ex} = \mathbf{f} \\ \text{inequality constraints: } \mathbf{Gx} \geq \mathbf{h} \end{cases} \tag{3.19}$$

There are two types of problems: over-determined and under-determined. Over-determined linear system contains more independent equation than the unknown variable. In this case, there is only on the solution in the least squares sense. An over-determined linear system can be solved by minimizing a norm of the error term, $\varepsilon = \mathbf{Ax} - \mathbf{b}$.

Under-determined linear systems contain more unknown variables than independent equations, meaning that it usually has an infinite amount of solutions. This model can be solved by sampling the feasible region of an underdetermined linear problem in a uniform way.

In this study, the R function xsample() in 'limSolve' pakage was utilized (Van den Meersche et al., 2009) to produce a sample set of vector x which corresponding the equality constraints and inequality constraints to solve the under-determined linear linear inverse problem from multiple linear regression model which is developed in 3.3.3.1. The sample set of vectors is either uniformly distributed over their feasible range. This algorithm are performed in two steps:

(1) The equality constraints $\mathbf{Ex} = \mathbf{f}$ are eliminated:

The elements $x_{(i)}$ in the exact equality $\mathbf{Ex} = \mathbf{f}$ are not first linearly transformed to a vector $\mathbf{q}$ to make all elements linearly independent. If the solutions exist for the system $\mathbf{Ex} = \mathbf{f}, \mathbf{Gx} \geq \mathbf{h}$, all solutions x can be written as:

$$x = x_0 + \boldsymbol{Zq} \tag{3.20}$$

$\mathbf{Z}$ is an orthonomal matrix that serces as a basis for the null space of $\mathbf{E}: \mathbf{Z^T Z} = \mathbf{I}$ and $\mathbf{EZ} = \mathbf{0}$. There are no equality constraints for the elements in $\mathbf{q}$. Therefore, the problem is reduced to:

$$\begin{cases} \boldsymbol{A'q} - \boldsymbol{b'} = \varepsilon \\ \boldsymbol{G'q} - \boldsymbol{h'} \geq 0 \end{cases} \tag{3.21}$$

With $\mathbf{A'} = \mathbf{AZ}, \mathbf{B'} = \mathbf{Ap} - \mathbf{b}, \mathbf{G'} = \mathbf{GZ}$ and $\mathbf{h'} = \mathbf{Gx_0} - \boldsymbol{h}$. $\mathbf{q}$ can be sampled without meeting any exact equality constraints.

(2) The distribution of $\mathbf{q}$ is sampled numerically using a random walk (based on the Metropolis algorithm (Roberts, 1996)). In the random walk step, the Markov chain Monte Carlo (MCMC) sampling method has been used. The new samples $\mathbf{q_2}$ are drawn randomly from a jump distribution with a PDF $j(\cdot|\mathbf{q_1})$ that only depends on the previous accepted point $\mathbf{q_1}$. In this study, the "mirror algorithm" is used for the random walk. The new sample point $\mathbf{q_2}$ is either accepted or rejected based on the following satisfaction criterion. (Van den Meersche et al., 2009)

$$\text{if } r \leq \frac{p(\mathbf{q_2})}{p(\mathbf{q_1})}\ acceopt\ \mathbf{q_2}, \qquad else\ keep\ \mathbf{q_1} \tag{3.22}$$

with $0 < r \leq 1$ the satisfaction ratio and $p(\cdot)$ the PDF of the target distribution. Therefore, the MCMC can derive the posterior density functions after adequate number of iterations.

The sample set of vector $\mathbf{q}$ and the acquired sample set of vector $\mathbf{x}$, has a distribution that is bounded by the inequality constraints. In this study, the range of input variables in Table 3-3 were set as inequality constraints.

3.3.4.2 Bayesian inference (Bayesian calibration)

Bayesian calibration (Kennedy & O'Hagan, 2001) is a statistic inference method that tune unknown parameters to match the model output and observation. Bayesian calibration is based on Bayes' theorem and provides a posterior distribution for unknown parameters $\theta$ given the observed data $y$.

$$p(\theta|y) = \frac{p(y|\theta) \cdot p(\theta)}{p(y)} \propto p(y|\theta) \cdot p(\theta) \tag{3.23}$$

$p(\theta)$ is the prior probability, $p(y|\theta)$ is the likelihood, $p(\theta|y)$ is posterior probability. The posterior distribution is calculated by product of a likelihood function and a prior distribution.

The observation data $y$ can be expressed by the simulation model results having known parameter $x$, unknown parameter $\theta$, and observation errors $\varepsilon$.

$$y_i = \eta(x_i, \theta) + \varepsilon_i \tag{3.24}$$

$$\varepsilon_i \sim N(0, \sigma^2) \tag{3.25}$$

For the likelihood function, the most frequently used assumption for the $\varepsilon_i$ is that they are independent and identically distributed (i.i.d.) normal distribution with 0 mean and $\sigma^2$ variance.

$$f(y|\theta) = \prod_{i=1}^{n} \frac{1}{\sqrt{2\pi\sigma^2}} \exp[-\frac{(\varepsilon_i)^2}{2\sigma^2}] \tag{3.26}$$

The $\varepsilon_i$ term can be substituted by Eq. (3.24) as the following:

$$f(y|\theta) = \prod_{i=1}^{n} \frac{1}{\sqrt{2\pi\sigma^2}} \exp[-\frac{\left(y_i - \eta(x_i, \theta)\right)^2}{2\sigma^2}] \tag{3.27}$$

Therefore, the likelihood can be regarded as the normal distribution function which has model output mean and $\sigma^2$ variance. To handle easier, the prior and posterior function can be represented as a log-function. Now, the posterior distribution function is the sum of log-prior function and log-likelihood function.

When the posterior distribution cannot be calculated analytically, it is possible to utilize sampling techniques (Bolstad, 2011). We employed Markov Chain Monte Carlo (MCMC) method. MCMC produces independent draws from the posterior distribution. It is a class of algorithms that produce a chain of simulated draws from a distribution where each draw is dependent on the previous draw. Metropolis-Hastings algorithm (HASTINGS, 1970; Metropolis et al., 1953) is one of the frequently used sampling techniques to derive a sequence of random sample set.

To use MCMC for Bayesian inference, it is important to determine the number of iterations to represent the posterior distributions of interest adequately. In this study, the number of iterations was chosen as 3,000 after performing Gelman and Rubin diagnostic (Brooks & Gelman, 1998). The initial 10% of total iterations (300 samples) were discarded as "burn-in" samples to eliminate the initial random samples since they have not stabilized.

The most different characteristic of Bayesian inference as compared with the linear inverse problem is that we can employ our previous knowledge to derive the prior distribution. However, specification of the prior distribution is significantly important since this affects the final inferred (posterior) distributions. In this study, the prior distribution is assumed as a triangular distribution as shown in Table 3-3.

To summarize, the Linear inverse problem considers all values of input parameters within specified lower and upper limits to be equally plausible. The Bayesian inference allows more informative prior distribution of the inputs that helps constrain the model better. Therefore, Bayesian inference is more appropriate when there is good and reliable information about the building stock.

#### 3.3.4.3 Observation data

Calibration is the process of using a building simulation for an existing building. The various inputs are tuned or calibrated to achieve a close match between the predictions and the observed energy use.

In the stochastic calibration for individual building, the calibration target is only one building (Y. Heo et al., 2012; Y.-J. Kim, Yoon, et al., 2013; Manfren et al., 2013; Tian, Wang, et al., 2014). However, when we consider a calibration for building stock, the calibration should perform to replicate the distribution

of building energy consumption for building stock. In several studies that execute the stochastic calibration for building stock, they sampled several target value from the actual energy consumption distribution. Then, the calibration is iterated to the different sampled target values and re-sampled from the calibrated result. (Tian & Choudhary, 2012; Yohei Yamaguchi, Suzuki, et al., 2013; Fei Zhao, 2012)

## 3.4 Results

### 3.4.1 Distribution

From Figure 3-9 to Figure 3-12 represent the prior and the posterior distributions of eight input parameters of each option. A dotted gray line represents the prior density distribution, and an orange solid line indicates the posterior density distribution. It shoud be noted that the prior density distribution does not exist in the linear inverse problem (Figure 3-10) since solving linear inverse problem cannot use our prior knowledge for the parameters.

In the all cases, there were significant changes in the posterior density distributions of EPD, LPD and INF. The posterior distributions of these three parameters shifted to the upper bound to make the higher energy use intensity. These three parameters were the most influence parameters to the energy consumption as a result of sensitivity parameters.

The posterior distributions for other parameters have only small changes, and these posterior distributions are greatly influenced by the prior distribution. This is because only annual total energy usage data was used for the calibration. If there is a small data sample, the posterior distribution tends to be affected by the prior distribution. Using different prior distribution shape and range significantly affects to the posterior distribution. It is the most distinguished feature of Bayesian inference and the reason we should consider a proper prior estimation in the case of small data sample based on expert knowledge and literature.

Comparing the posterior distribution using different energy models (Figure 3-9, Figure 3-11, and Figure 3-12), those have similar posterior distributions. It means that the performance of the original model can be expressed by using the metamodel under the given conditions. In the Heo's study (Y. Heo, 2011),

the author utilized the normative model and EnergyPlus as a tool for calibration, and demonstrated that the similar results can be derived with the normative model compared to the EnergyPlus.

One thing to be noted is that the estimated posterior distribution for building parameter should not be considered as the actual distribution of building parameter for the target area. Since a representative building covers diverse size and shape of buildings in the building stock, it is more plausible that the estimated posterior distribution is regarded as "best guess" that can produce the similar energy consumption result of the actual building stock. The "best guess" can be refined by reducing the error between the model and actual building using more measurement data. (Fei Zhao, 2012)

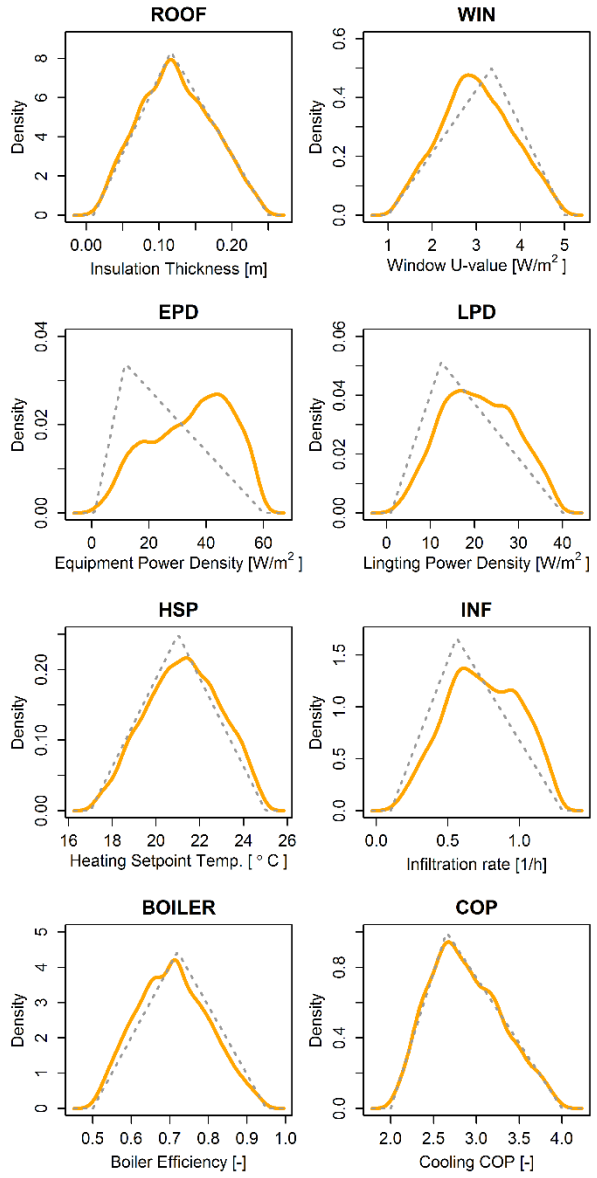


Figure 3-9 Prior and Posterior distributions of parameters: EP-Bayesian method (Opt.1)

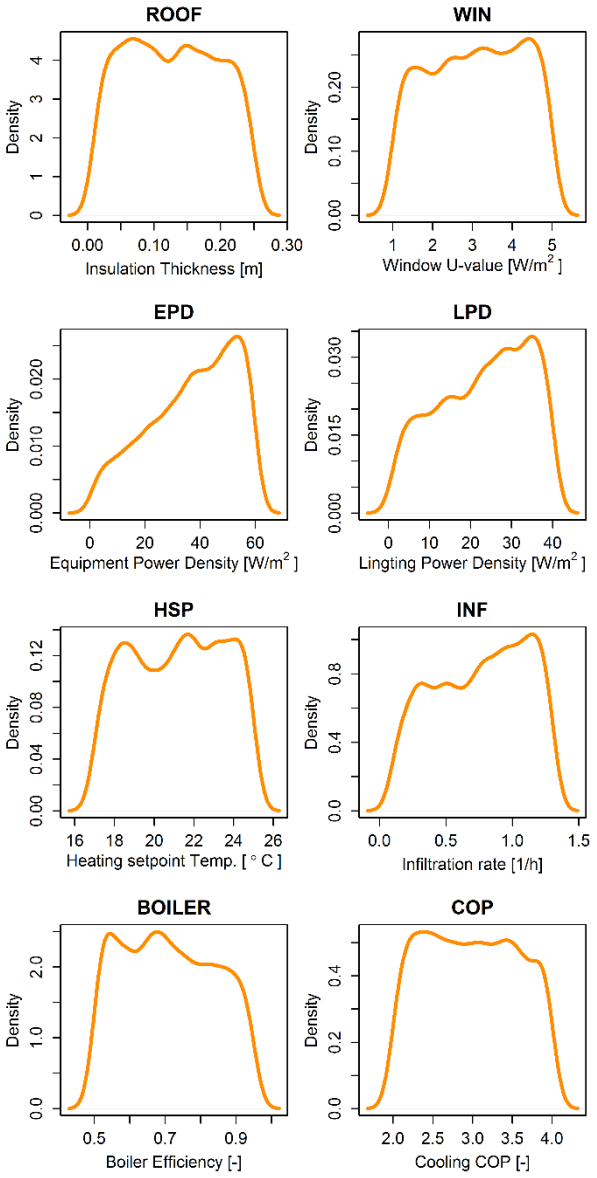


Figure 3-10 Estimated distribution of parameters: MLR-Linear inverse (Opt.2)

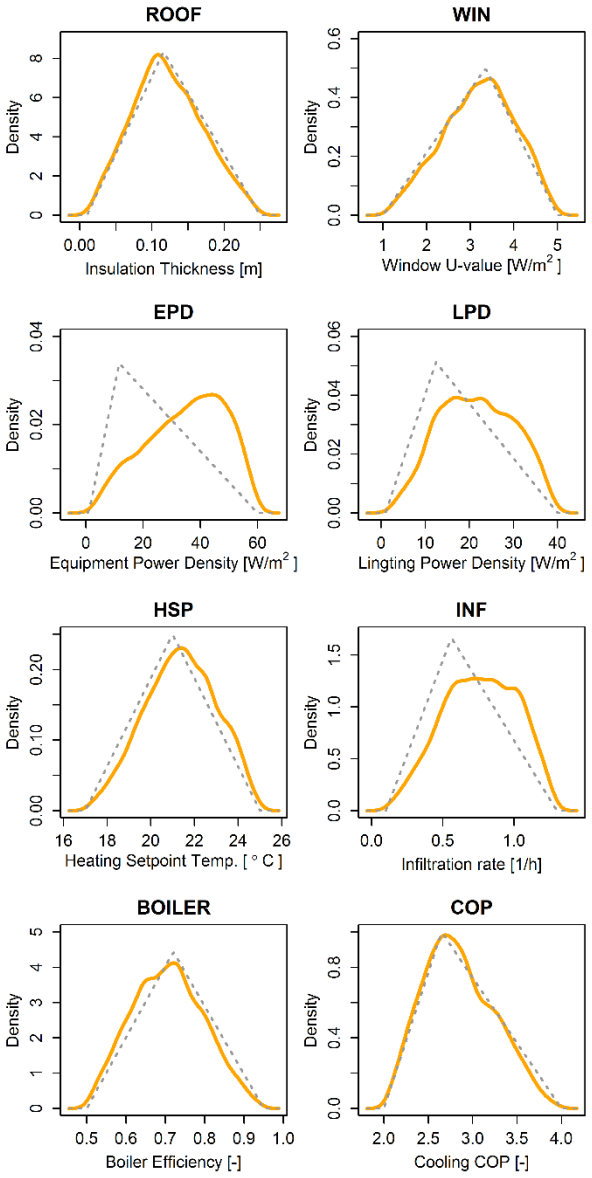


Figure 3-11 Prior and Posterior distributions of parameters: MLR-Bayesian method (Opt.3)

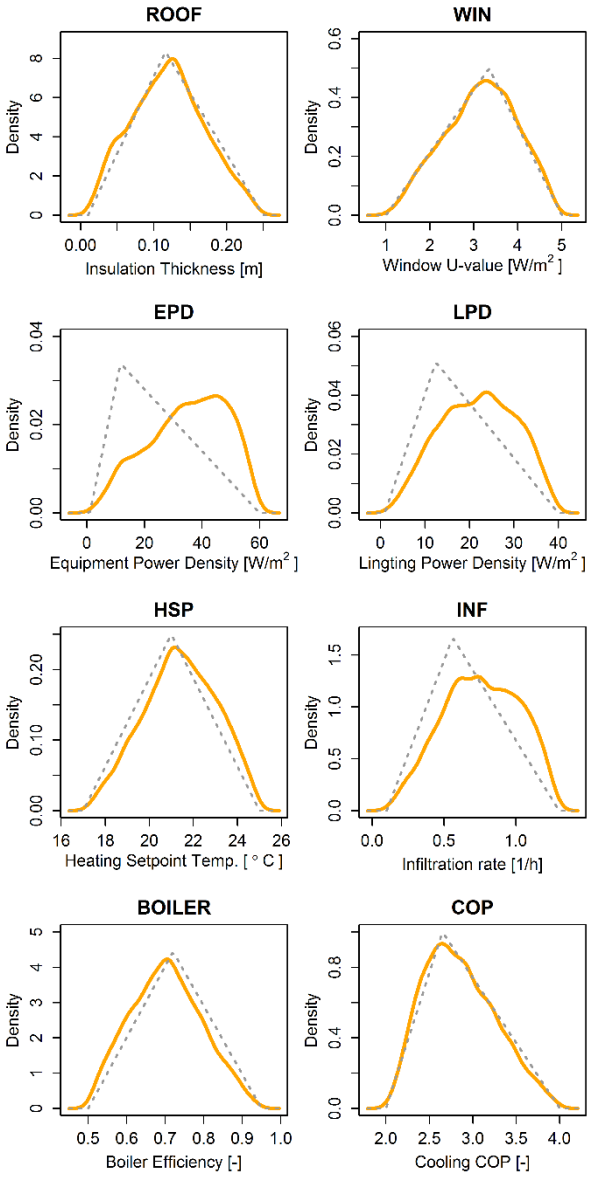


Figure 3-12 Prior and Posterior distributions of parameters: GPE-Bayesian (Opt.4)

In the results of the linear inverse problem (Figure 3-10), like the results of the Bayesian inference, the expected distribution of EPD, LPD, and INF parameters are largely biased to the upper bound to make the EUI larger. The estimated distribution of BOILER is slightly biased to the lower bound for such a reason. The predicted distribution for less dominant parameters appears to be close to a uniform distribution. This is because linear inverse problem only assumes the prior distribution as a uniform distribution. From Figure 3-13 to Figure 3-16 show the energy use intensity (EUI) distribution of prior, posterior and measured data. In the all cases, the posterior EUI distributions approximated the measured EUI distributions.

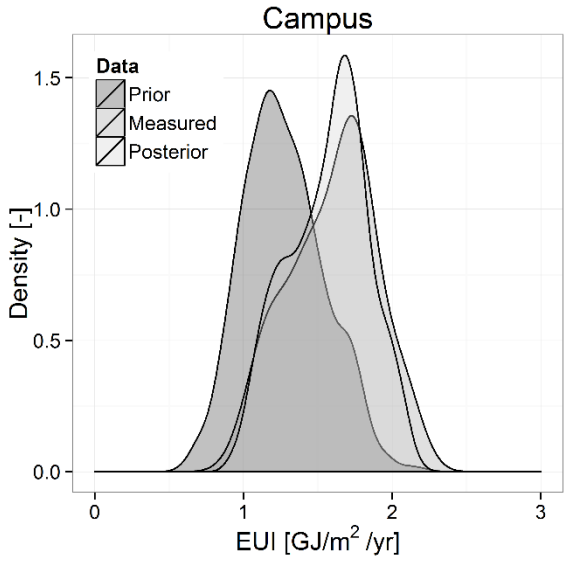


Figure 3-13 Distributions of EUI: EP-Bayesian method (Opt.1)

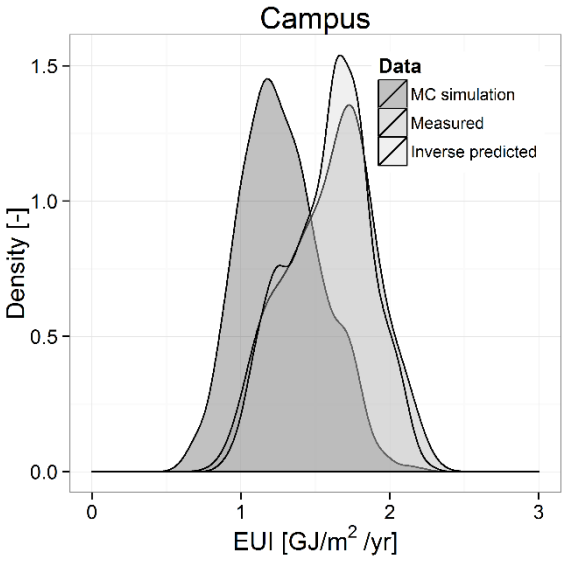


Figure 3-14 Distributions of EUI: MLR-Linear inverse method (Opt.2)

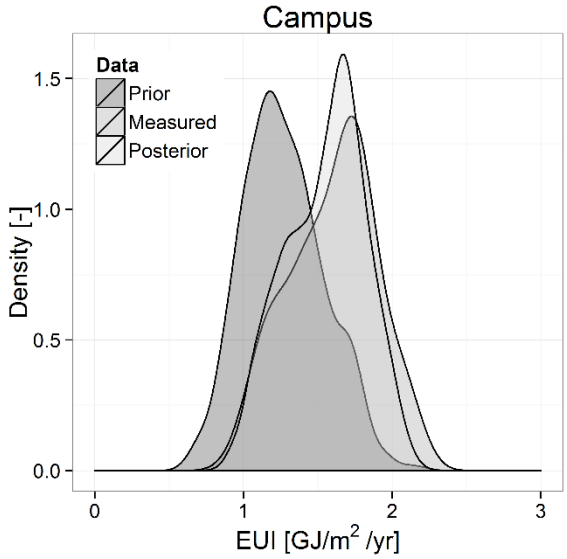


Figure 3-15 Distributions of EUI: MLR-Bayesian method (Opt.3)

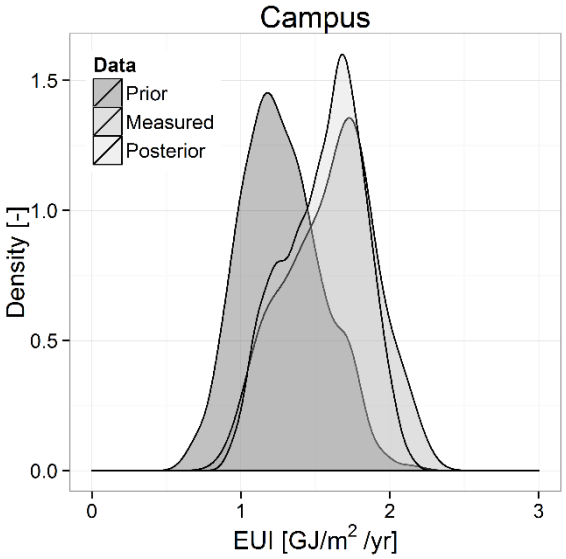


Figure 3-16 Distributions of EUI: GPE-Bayesian method (Opt.4)

### 3.4.2 Computational cost

Monte Carlo simulation and calibration using MCMC are extremely time-consuming progress. In the Table 3-6, simulation run time for each option was compared sequentially. 1,000 of Monte Carlo EnergyPlus simulations took about 5.5 hours to derive a data set for the sensitivity analysis and making meta-model. The multiple linear regression model (MLR) (Opt. 2 and Opt. 3) is fast to build, whereas the Gaussian Process Emulator (GPE) takes about 30 minutes. In the calibration step, estimation through the linear inverse problem using the MLR (Opt. 2) is the fastest. The Bayesian calibration using the MLR (Opt. 3) and the GPE (Opt. 4) took about 1 min and 10 min, respectively. The Bayesian calibration without meta-model (using the EnergyPlus, Opt 1) took a considerably long time, about 1,500 hours. These simulation run times were performed on a personal computer with an Intel Core i7-4790@ 3.6GHz and assumed that all simulations were conducted using only one processor. If multiple thread process can be used, the runtime will be reduced. Computing time will be one of the criteria to select most practical option with the accuracy of the calibration.

Table 3-6 Simulation times

| | | Opt.1 | Opt.2 | Opt.3 | Opt.4 |
|---|---|---|---|---|---|
| Time for each step (s) | Monte Carlo | 19,800 | 19,800 | 19,800 | 19,800 |
| | Making meta-model | - | 0.02 | 0.02 | 1,965 |
| | Conducting calibration | 5,512,653 | 11 | 62 | 625 |
| Total time | Hours: Minutes: Seconds | 1,536:47:33 | 5:30:11 | 5:31:02 | 6:13:10 |

### 3.4.3 Accuracy

The calibrated EUI distributions were compared with three criteria. The first and second are for evaluating accuracy of the estimated EUI distribution by root mean square error (RMSE) of the mean and standard deviation. The third one is two samples K-S (Kolmogorov–Smirnov) test. The K-S test can be used to compare two samples in statistics, the p-value as a result of the test is from 0.0 to 1.0, and the higher value means two distributions are more similar. The p-value of less than 0.05 means that the two samples were drawn from different distributions while a p-value exceeding 0.05 provides no such evidence. The K-S test compared the posterior EUI distribution and the measured EUI distribution.

Figure 3-17 and Figure 3-18 present the RMSE of the mean and standard deviation of each EUI distribution. A low value is accurate to the observed EUI distribution. The calibration using MLR-Linear inverse problem (Opt. 2) was the most accurate in terms of mean and standard deviation. It is because there are fewer restriction to sample the parameters to fit the observation in the calibration progress than Bayesian inference. The p-value of two sample K-S test result is shown in Figure 3-19. The P-values of all cases are very high (Opt. 1, 2, 3 and 4). The results suggest that all methods are reliable to estimate EUI distribution regardless of meta-model or calibration method.

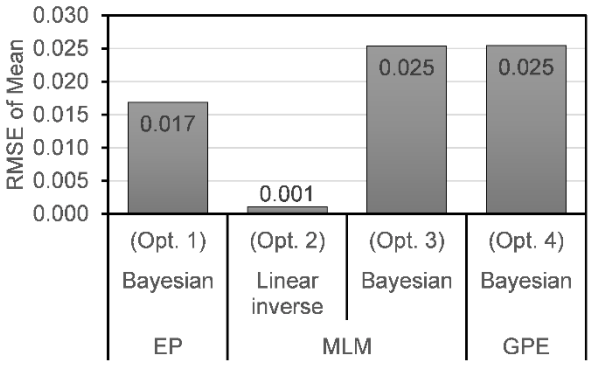


Figure 3-17 RMSE of mean

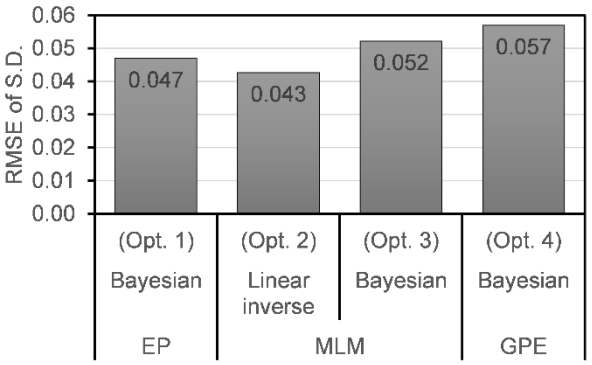


Figure 3-18 RMSE of standard deviation

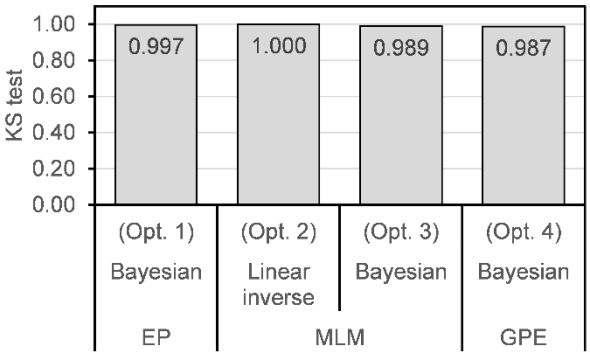


Figure 3-19 Two sample K-S test

## 3.5 Discussion and Conclusion

Calibration methods were compared to make a stochastic-deterministic-coupled building energy model, and the effects of meta-models were examined in this chapter. The detailed methodologies of literature were reviewed and compared. Then, four alternatives were suggested using a combination of different methods at each progress step. Case study was conducted for 30 buildings in the university campus. The representative building energy model was developed for campus buildings. The developed model was calibrated to the actual building energy consumption data. The accuracy and computational cost are examined to compare the four alternatives. In summary, some conclusions are drawn as follows:

- Using the meta-models to calibrate has similar performance to calibration with the original dynamic building energy model, while greatly reducing computation time.

- When calibrating for annual energy use, both calibration approached showed good agreement with measured energy use.
- Calibration using the linear inverse problem can match well with the actual distribution than Bayesian inference. However, the availability of existing knowledge on building stock information is limited in the linear inverse problem.
- Bayesian calibration can specify the shape and range on the prior distribution of input parameters. Bayesian calibration is more appropriate when there is reliable information about building stock.
- The calibration results confirm that the posterior distribution is significantly affected by the prior distribution for the less dominant parameters when using only annual total energy use. These findings suggest three points. First, when the measurement data is small, the prior distribution should be more careful. Second, when there is a large amount of measured data, further study is required to examine whether the accuracy of the calibration differs according to the type of meta-model. Third, it is necessary to analyze the effect of the amount of measurement data on the accuracy of calibration.

# CHAPTER 4: PREDICT SINGLE BUILDING ENERGY USE WITH STOCHASTIC-DETERMINISTIC-COUPLED APPROACH

In this chapter, the proposed stochastic method is analyzed in detail in individual building to solve the questions raised in previous chapter. In chapter 4.1, the effect of meta-model accuracy on Bayesian calibration is examined. In chapter 4.2, one of the most important factors in the calibration, the measured energy use data, is studied. The effect of the quality and quantity of the measured data on the calibration results are investigated with a method of determining the informative energy use data.

## 4.1 The effect of meta-model accuracy on the Bayesian calibration

### 4.1.1 Introduction

Building energy simulation tools and techniques have been widely applied to the evaluation of building performance for several decades. Simulation models emulate physical relationships that result from various internal and external actions in a building. These tools and techniques enable users to determine the appropriate size of HVAC systems and estimate energy performance at a relatively low cost. However, due to the complexity and uncertainty of building simulations, it is difficult to match predicted values with measured values. Therefore, a calibration is required to achieve more accurate prediction by manipulating variables in the simulation. The calibration is to tune the input parameters in a simulation model to minimize discrepancies between prediction and observed data. Detailed reviews of the calibration technique for building simulation can be found elsewhere (Coakley et al., 2014; Fabrizio & Monetti, 2015; Fumo, 2014; T. A. Reddy, 2006).

The approaches of building model calibration can be classified into four (Clarke et al., 1993; T. A. Reddy, 2006): (1) Calibration based on manual, iterative, and pragmatic intervention; (2) Graphical-based calibration methods; (3) Calibration based on special tests and analysis procedures; (4) Analytical and mathematical approaches.

Coakley et al. (Coakley et al., 2014) classified the approaches into two broad categories: manual and automated methods. Manual methods mainly rely on the experience of the user. The user repeatedly manipulates the model inputs to tune the simulation result in the manual methods. The automated methods have an automated process to help model calibration.

Bayesian calibration is the automated calibration using mathematical techniques. It is a statistical method that utilizes Bayes' theorem to obtain posterior distributions for unknown parameters given observed data. Kennedy and O'Hagan (Kennedy & O'Hagan, 2001) proposed a generic approach for the Bayesian calibration of computer models. The Bayesian calibration is more effective than the traditional approach in two ways: First, the prediction can consider all sources of uncertainty through the use of prior input distribution. Second, Bayesian calibration method corrects model inadequacy due to discrepancies between model predictions and observed data. The Bayesian calibration has been widely employed for model predictions in many areas (ecological models (Oijen et al., 2005), hydrologic models (Liu et al., 2008), atmospheric model (Guillas et al., 2009), geochemistry (Tierney & Tingley, 2014), geological models (Rahn et al., 2011), molecular dynamic model (Angelikopoulos et al., 2012), and biological model (Blangiardo & Richardson, 2008)).

Heo (Y. Heo et al., 2012; Yeonsook Heo et al., 2011) applied the Bayesian calibration to the building energy simulation area to account uncertainties during retrofit of existing buildings. The Bayesian calibration procedure has been used in the building analysis for calibration of unknown input (Berger et al., 2016; Yeonsook Heo et al., 2013; Yeonsook Heo, Augenbroe, et al., 2015; Kang & Krarti, 2016; Qi Li et al., 2016, 2015), retrofit analysis (Yeonsook Heo et al., 2013; Yeonsook Heo, Augenbroe, et al., 2015), comparison with traditional calibration method (Pavlak et al., 2013), use of simplified model (Y.-J. Kim, Yoon, et al., 2013; Pavlak et al., 2013), influence of uncertainties in the input data (Yeonsook Heo, Graziano, et al., 2015), determination of informative energy data (Tian et al., 2016), calibration of sensor error (Yoon & Yu, 2017), and prediction of building stock energy use (Booth & Choudhary, 2013; Booth et al., 2012, 2013; Ruchi Choudhary, 2012; Tian & Choudhary, 2012; Yohei Yamaguchi, Suzuki, et al., 2013).

Table 4-1 Bayesian calibration for building energy model

| Author | Year | Building energy model | Parameter screening | Meta-model | Calibration method |
|---|---|---|---|---|---|
| Heo et al. (Y. Heo et al., 2012; Yeonsook Heo et al., 2011) | 2011, 2012 | EPSCT (Energy Performance Standard Calculation Toolkit) | Morris method | GPE | Bayesian |
| Tian and Choudhary (Tian & Choudhary, 2012) | 2012 | EnergyPlus | SRC (Standardized Regression Coefficient) / MARS(Multivariate Adaptive Regression Splines) | MLR | Inverse problem/ Bayesian |
| Booth et al. (Booth et al., 2012) | 2012 | EPSCT | Morris method | GPE | Bayesian |
| Zhao et al. (Fei Zhao, 2012; Fei Zhao et al., 2016) | 2012, 2016 | EPSCT | Stepwise regression analysis | MLR | Inverse problem |
| Manfren et al. (Manfren et al., 2013) | 2013 | Simplified (Energy signature mode)/ Detailed (unspecified) | Pearson's coefficient/ information theoretic ranking criterion | GPE | Bayesian |
| Li et al. (Qi Li et al., 2015) | 2015 | EnergyPlus | Lasso method | MLR | Bayesian |
| Heo et al. (Yeonsook Heo, Graziano, et al., 2015) | 2015 | EPSCT | Morris method | GPE | Bayesian |

| | | | | | |
|---|---|---|---|---|---|
| Tian et al. (Tian et al., 2016) | 2016 | EnergyPlus | SRC / Random Forest | MLR | Bayesian |
| Li et al. (Qi Li et al., 2016) | 2016 | EnergyPlus | Lasso method | MLR, GPE | Bayesian |
| Kang and Krarti (Kang & Krarti, 2016) | 2016 | eQUEST | Local sensitivity analysis | GPE | Bayesian |
| Sokol et al. (Sokol et al., 2017) | 2017 | EnergyPlus | - | GPE | Bayesian |

The main advantage of the Bayesian calibration is that it naturally accounts for the uncertainty in models using a prior distribution of the input parameters. However, stochastic calibration methods such as the Bayesian inference incur a high computational cost. A Markov Chain Monte Carlo (MCMC) (Gilks, 2005) method is used to draw posterior probability distributions in Bayesian calibrations. The MCMC requires numerous iterations of the building energy simulation from thousands to tens of thousands resulting in a massive computational burden.

To reduce the MCMC computational time, the following methods have been proposed: a simplified energy model, and a meta-model. Simplified models use simple descriptions of a building and its systems. It can drastically reduce simulation time compared to dynamic building energy simulation such as EnergyPlus, eQUEST, and TRNSYS. However, the simplified models have a limitation to analyze details in the building and diverse energy conservation methods.

A meta-model (also called surrogate model) can be defined as a "model of model" (Eisenhower, O'Neill, Narayanan, et al., 2012), which is simpler and computationally faster than an original model. Table 4-1 shows diverse meta-models applied to reduce simulation time in many studies: Multiple linear regression model (Manfren et al., 2013; Tian & Choudhary, 2012; Tian, Wang, et al., 2014; Fei Zhao, 2012), Gaussian process emulator (Booth et al., 2012; Y. Heo, 2011; Y. Heo et al., 2012; Manfren et al., 2013) and Support Vector Machines (Eisenhower, O'Neill, Narayanan, et al., 2012).

Such meta-models differ in prediction accuracy and computational cost to build due to differences in algorithm and fundamentals. Therefore, the appropriate meta-model should be chosen considering the

accuracy and computational cost. Wei et al. (Wei et al., 2015) investigated the predictive performance of six meta-models developed using measured data. Tian et al. (Tian et al., 2015) compared the accuracy of eight meta-models for the 114 campus buildings. Kim (Y. J. Kim, 2016) compared the prediction capability of Gaussian process emulator and polynomial chaos expansion for an uncertainty quantification. In these studies, however, there was no consideration regarding the computational time of meta-models.

If the meta-model is used for the Bayesian calibration, the meta-model accuracy may affect the accuracy and computational time of the Bayesian calibration. Li et al. (Qi Li et al., 2016) confirmed that linear model including main and interaction effect terms has comparable results with the Bayesian calibration using Gaussian process emulator. However, further research is required to provide guidance in selecting the proper meta-model for the Bayesian calibration.

There is a need to find out if a more accurate meta-model leads to more accurate calibration. The accuracy of the Bayesian calibration can be divided into two: how accurately the true input parameter is estimated and how well the building energy usage is predicted. In addition to parameter estimation and prediction performance, the computational cost of the Bayesian calibration is used as criteria. These analyses help to select the appropriate meta-model according to the calibration goals.

The study aims to examine the effect of meta-model accuracy on the accuracy of Bayesian calibration. In the methodology section, Bayesian calibration method and selected meta-models are described in detail followed by a description of the case study. The third section compares calibration results and analyzes the accuracy of Bayesian calibration. The final section summarizes the overall findings and implications of the study.

### 4.1.2 Methodology

The calibration analysis in this study was based on the procedure shown in Figure 4-1. The first step is to establish a building energy model based on building information. In the second step, a degree of uncertainty is determined by selecting unknown parameters and those variations. The combinations of inputs are constructed using a sampling method. The combinations are fed into the building energy

simulation program to obtain an input-output set. A large number of the input-output sets are required to supply sufficient data for the next step. Next step uses a sensitivity analysis to identify dominant inputs (parameters) affecting the output (energy consumption in this study). By selecting only important variables as calibration parameters, the time and effort required during the calibration process can be reduced. However, the parameter screening was omitted in this study due to only six unknown parameters were selected as input parameters. The third step is to develop meta-models using the input-output set from the step two. The Bayesian calibration will use the meta-models rather than the original detailed energy simulation model to reduce simulation time significantly. The next step is to estimate the unknown parameters from the Bayesian calibration and compare posterior distributions to the observed values. All the statistical analyses were performed using R program, software for statistical computing and graphics (R Core Team, 2016).

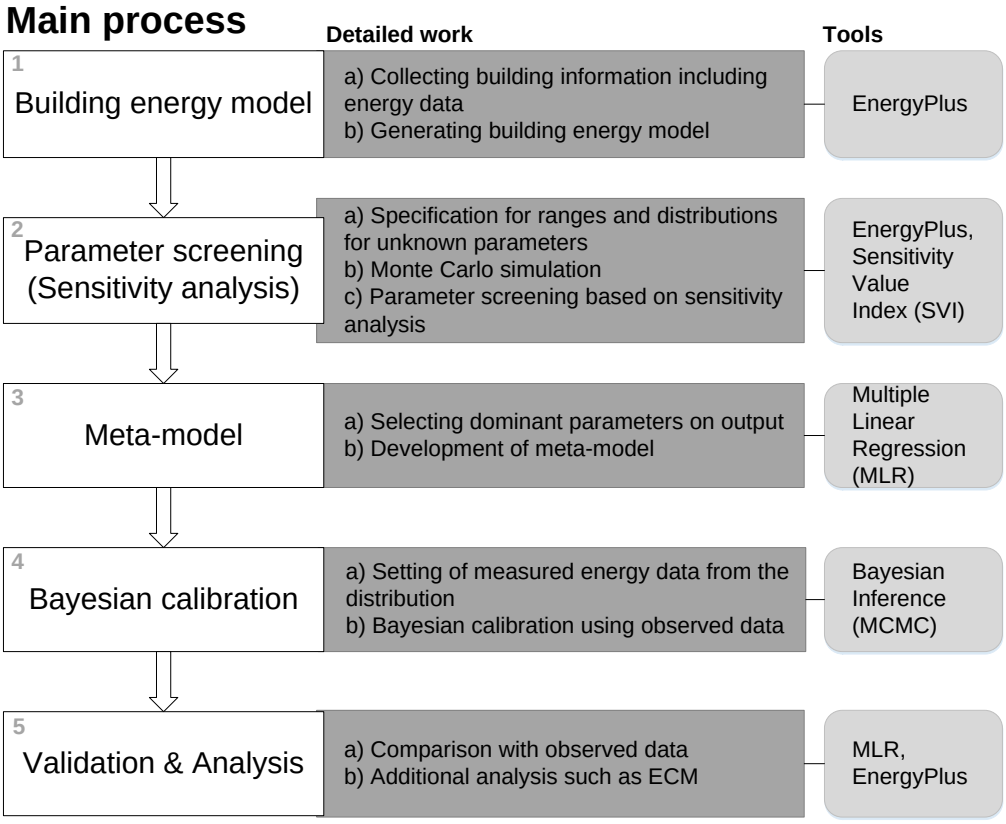


Figure 4-1 Procedure of Bayesian calibration

#### 4.1.2.1 Building energy model

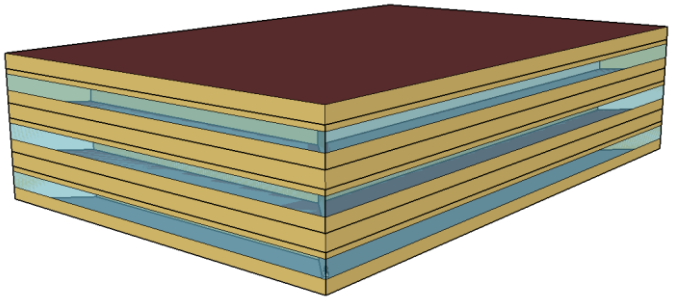

Figure 4-2 DOE reference medium office building

A medium office building from the U.S. Department of Energy (DOE) reference building, shown in Figure 4-2, was used for the case study in this analysis. The office building is a three-story rectangular building with a total floor area of 4,982 $m^2$. The key features of the office building are shown in Table 4-2.

In this study, it is assumed that all buildings in the virtual building stock have same geometry and schedule. The goal of this study is to verify the methodology. Therefore, the uncertainty of the parameters that are easy to interpret is considered first, and the difficult parameters that had large uncertainties were eliminated to minimize uncertainty in inputs. The stochastic occupancy schedule and the effect of building geometry will be considered in future work.

Table 4-2 Main features of the office building

| Component | Item | Parameters | Unit |
|---|---|---|---|
| Envelope | Floor area | 4982 | $m^2$ |
| | Floor levels | 3 | - |
| | Window-wall ratio | 0.33 | - |
| | Thermal Zoning | core zone with four perimeter zones on each floor | - |
| | Wall U-value | 0.48 | $W/m^2K$ |
| | Roof U-value | 0.35 | $W/m^2K$ |
| | Window U-value | 3.24 | $W/m^2K$ |
| | SHGC (solar heat gain coefficient) | 0.39 | - |
| | Infiltration rate (Air changes per hours) | See Table 4-3 | $W/m^2$ |
| | Lighting power density | See Table 4-3 | $W/m^2$ |

| | | | |
|---|---|---|---|
| Internal heat gains | Equipment power density | See Table 4-3 | W/m$^2$ |
| | Hourly schedules for set-point for heating and cooling, occupants, lights, and equipment | DOE Reference building | - |
| HVAC systems | System Type | MZ-VAV | - |
| | Heating Type | Gas furnace and electric reheat | - |
| | Cooling Type | PACU | - |

The building was assumed to be located in Boulder, Colorado, US and the weather data was downloaded from the EnergyPlus weather file database. Table 4-3 lists the range of unknown input parameters. Unknown parameters are six, and the range of unknown parameters could be obtained from the literature, field survey and prior knowledge of experts. However, in this analysis, the ranges of unknown parameters were determined arbitrarily based on the default value of the reference building.

The simulation was performed using EnergyPlus, developed by the United States Department of Energy (DOE) (Crawley et al., 2001). The EnergyPlus is a whole building energy simulation and widely used in the field of building energy simulation and has also been tested extensively. The advantage of using EnergyPlus is that input data file is text format. Therefore, the model definitions can be easily edited for parametric studies (Tian et al., 2016). Moreover, the EnergyPlus provides detailed energy use results and process loads by calculating heating, cooling, ventilating, and other energy flows as well as water use in buildings that define heat and mass transfer flow in the building. It also includes many advanced systems and is regularly updated. Therefore, the EnergyPlus allows users to take account of various energy conservation measures and novel systems compared with other simplified simulations.

Table 4-3 Input parameters and ranges

| Parameters | Short names | Range | | Unit |
|---|---|---|---|---|
| | | Case 1. Base | Case 2. Wide | |
| Equipment Power Density | EPD | 11-15 | 7.7-19.5 | W/m$^2$ |
| Lighting Power Density | LPD | 12.5-17.5 | 8.75-22.75 | W/m$^2$ |
| Heating Set-point | HPS | 19.5-22.5 | 15.5-26.5 | $^o$C |
| Cooling Set-point | CSP | 22.5-25.5 | 18.5-29.5 | $^o$C |
| Occupancy | OCC | 15-25 | 10.5-32.5 | m$^2$/person |
| Infiltration | INF | 0.6-0.8 | 0.42-1.04 | ACH |

Six input parameters and prior distributions are defined in Table 4-3. All prior distributions are assumed as a uniform distribution. The study varies the ranges of input parameters to explore the associated accuracy of the meta-models: base and wide range. The wide ranges were extended 30 percentage from the base range. The 100 training combinations of inputs are created by the quasi-random sampling (Sobol' sequence, (Sobol, 1998)). Sobol's sequence generates uniform sample points, resulting in fast convergence and robust results (Burhenne et al., 2011; Kucherenko et al., 2011). Additional 100 testing samples were constructed by the Latin Hypercube Sampling (Mckay et al., 2000). A total of 200 input sets were then fed into the EnergyPlus to obtain the input-output matrix. This process is called 'uncertainty propagation.' The obtained input-output matrix is utilized to build meta-models in next step. The uncertainty propagation was performed by jEPlus software (Y. Zhang, 2009).

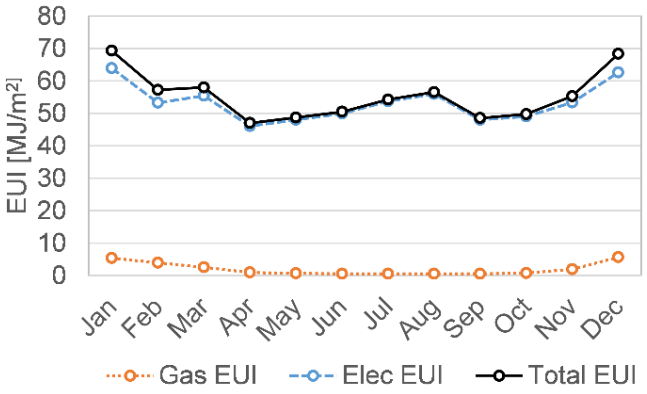


Figure 4-3 Average energy consumption

Figure 4-3 shows monthly average energy use intensity for 100 training set. The energy use intensity (EUI, MJ/m$^2$) for electricity and gas were used for energy performance indicators. In the office building used in this analysis, the electricity is dominant on the energy use because the DOE office medium reference building has a packaged air-conditioning unit for cooling and a gas furnace with electric reheat for heating. The gas usages from April to October have only base loads for domestic hot water. Therefore, the gas data for only five months (January, February, March, November, and December) were used for the calibration considering the accuracy of the meta-model. All 12-month data was used for the electricity.

4.1.2.2 Suggestion of sensitivity value index (SVI)

As stated above, the parameter screening was omitted. However, the sensitivity analysis was performed to identify which parameter is more important among six parameters to the building energy use. It helps to better understand the results of Bayesian calibration. Various sensitivity analysis methods have been applied in building energy area (Tian, 2013). In this study, we utilized three different approaches to offer robust analysis results: SRC (standardized regression coefficient), random forest variable importance and T-value. For detailed information, please refer to (Tian, 2013). In this analysis, the annual electricity and gas use data were used for the sensitivity analysis. Importance ranking of parameters may vary according to the fundamentals of sensitivity method and the target output. To consider different values from the three sensitivity analyses (SRC, Random forest variable importance,and T-value) and two target outputs (annual electricity and gas use), the sensitivity value index (SVI) was suggested as shown in the equation (4.1). The values from the sensitivity analysis were normalized and then aggregated so that the importance of parameters can be compared considering the difference of sensitivity methods and target output.

$$\sum_{l=1}^{m} \frac{\sum_{j=1}^{k}\left(\frac{V_{i,j}}{\sum_{i=1}^{n}|V_{i,j}|}\right)}{m \cdot k} \times 100 = Sensitivity\ Value\ Index\ (SVI)(\%) \qquad (4.1)$$

Where $i$ is the parameter, $n$ is the number of parameters ($n = 6$), $j$ is the sensitivity method, $k$ is the number of sensitivity methods ($k = 3$, (SRC, Random forest variable importance, and T-value)), $l$ is the target output, $m$ is the number of target output ($m = 2$ (annual electricity and gas))

#### 4.1.2.3 Meta-models

Computer modeling is a simulator that aims to replicate actual phenomenon. A meta-model (also called surrogate model) is a simplified representation or approximation of the simulator. It is built using a training set of simulator runs. The purpose of meta-model is to run faster than the original simulator itself.

The following five meta-models are investigated and compare: multiple linear regression model (MLR), neural network (NN), support vector machine (SVM), multivariate adaptive regression splines (MARS), and Gaussian process emulator (GPE). Those meta-models are used in building energy and building system analysis: MLR (Qi Li et al., 2015; Manfren et al., 2013; Tian, Song, et al., 2014; Fei Zhao et al., 2016), NN (Aydinalp et al., 2004; Kalogirou, 2000; Yang et al., 2005), SVM (Eisenhower, O'Neill, Narayanan, et al., 2012), MARS (Tian, Song, et al., 2014), and GPE (Y.-J. Kim, Ahn, et al., 2013; Manfren et al., 2013; Riddle & Muehleisen, 2014; Tian, Song, et al., 2014; Fei Zhao et al., 2016).

The brief descriptions and R packages for meta-models are listed in Table 4-4. Tian et al. (Tian et al., 2015) developed eight statistical energy models (meta-models) using observational data and compared their performance. More comprehensive descriptions and theoretical fundamentals for meta-models and machine learning methods can be found in (Foucquier et al., 2013; J. Friedman et al., 2001; Rasmussen, 2006).

##### 4.1.2.3.1 Multiple linear regression model

If more than one regression variable is known to affect the output, the multivariate model explains more of the variation and provide better predictions than single-variable models. The multiple linear regression model is;

$$y_i = \beta_1 x_{i1} + \cdots + \beta_p x_{ip} + \varepsilon_i = x_i^T \beta + \varepsilon_i \ , \qquad i = 1, \ldots, n \tag{4.2}$$

Where $y_i$ is the output, x denotes inputs, β is regression coefficients, and ε is an error or unexplained variation in $y$. The multiple linear regression model was developed using 'lm' function in R-package 'stats' (R Core Team, 2016).

Table 4-4 Descriptions of meta-models

| | Meta-models | Characteristics | R package (function) | Reference |
|---|---|---|---|---|
| **Parametric models: Linear models** | MLR | The simplest form. Model the relationship between several independent or predictor variables and a dependent or criterion variable. | stats (lm) | (Faraway, 2014) |
| **Non-parametric models** | NN | Inspired by the learning process of a human brain. ANNs are a system made up of some simple, highly interconnected processing elements | neuralnet (neuralnet) | (McCulloch & Pitts, 1943) |
| | SVM | Based on the concept of decision planes that define decision boundaries. Produce nonlinear boundaries by linear learning machine mapping into high-dimensional kernel induced feature space. | kernlab (ksvm) | (C.~Cortes et al., 1995) |
| | MARS | a generalization of stepwise linear regression by modeling non-linearities and interactions between variables | earth (earth) | (J. H. Friedman, 1991) |
| | GPE | Gaussian processes (GP) generalize multivariate Gaussian distributions over finite dimensional vectors to infinite dimensionality. Gaussian processes emulator (GPE) represents the posterior of true function as a GP using the observed data. | Gpfit(GP_fit) | (Quadrianto et al., 2010; Rasmussen , 2006) |

4.1.2.3.2 Neural network

The neural network (NN) is a model based on the human brain. In neural networks, nodes that mimic neurons can be divided into as input, hidden, and output layers. The neural network is known to have excellent prediction performance. In particular, since the input values are combined in the hidden layer, nonlinear problems can be solved.

When inputs are given to a neural network, those values are transmitted and reaches the hidden layer. The nodes of the hidden layer are activated in response to a given input. The activated hidden node calculates the output value and passes the result to the output layer. Each transmission is weighted. Let $w_{ji}$ be the weight given to the connection between node $i$ of the input layer and node $j$ of the hidden layer, and let $x_1, \cdots, x_n$ be the input to the input layer. The values given to the input layer then converge to the hidden layer node $j$ as follows.

$$\text{net}_\text{j} = \sum x_i w_{ji} + w_{j0} \tag{4.3}$$

This value, which is passed to node $j$, is called net activation, and such a formula is called a integration function.

The output of the hidden layer is calculated by carrying the net activation over the activation function. If the activation function is a sigmoid function, then the output can be calculated as follows (Ekici & Aksoy, 2009):

$$\text{f}(\text{net}_\text{j}) = \frac{1}{1 + e^{-(net_j)}} \tag{4.4}$$

The learning of the neural network model is the adjustment work of the weight $w$. The sum of squared error (SSE) between expected and predicted outputs for inputs is minimized though iteration. If there is a difference, the weights are adjusted from the output node to the connected hidden node, from the hidden node to the input node. This is called a back propagation algorithm. R package, neuralnet (Fritsch & Guenther, 2016) was used for training. The number of hidden layer was set to five for each monthly model.

4.1.2.3.3 Support Vector Machine

The Support Vector Machine (SVM) is a model that find a line (or a plane) that maximizes the difference between data belonging to different categories and classifies the data based on the line. The method of SVM can be extended to solve regression problems. This is called support vector regression (SVR). The basic idea for regression is to use kernel function, map the input space into a high-dimensional feature space via a non-linear mapping and to perform a linear regression in this feature space (Qiong Li et

al., 2009). When supposing that all normalized input parameters $X$, and $Y$ is the normalized output. The SVR approximates the relationship between the input and output as following (Qiong Li et al., 2009; Smola & Schölkopf, 2004):

$$\mathrm{Y} = f(\mathrm{X}) = \sum_{i=1}^{N} (\alpha_i - \alpha_i^*) K(X_i, X) + b \tag{4.5}$$

where $\alpha_i$, $\alpha_i^*$ are Lagrange multipliers, $K(X_i, X)$ is kernel function.

R package, kernlab (Karatzoglou et al., 2004) was used for training. The ANOVA radial basis kernel *anovadot* was selected as a kernel function due to it performs well in multidimensional regression problems.

$$\mathrm{k}(X_i, X_j) = (\sum_{k=1}^{n} \exp\left(-\sigma\left(X_i^k - X_j^k\right)^2\right)^d \tag{4.6}$$

where $\mathrm{X}^{\mathrm{k}}$ is the $k$th component of $X$.

4.1.2.3.4 Multivariate adaptive regression splines

Multivariate adaptive regression splines (MARS) was proposed by Friedman (J. H. Friedman, 1991). MARS is a nonparametric regression technique including stepwise linear regression, spline regression, and recursive partitioning (de Wilde & Tian, 2010). MARS extends the linear model to model nonlinearity, making it suitable for higher dimensional inputs.

MARS use piecewise linear basis functions to distinct independent variable intervals. In general, splines have pieces, and the interface points between pieces are called knots, denoted as $t$.

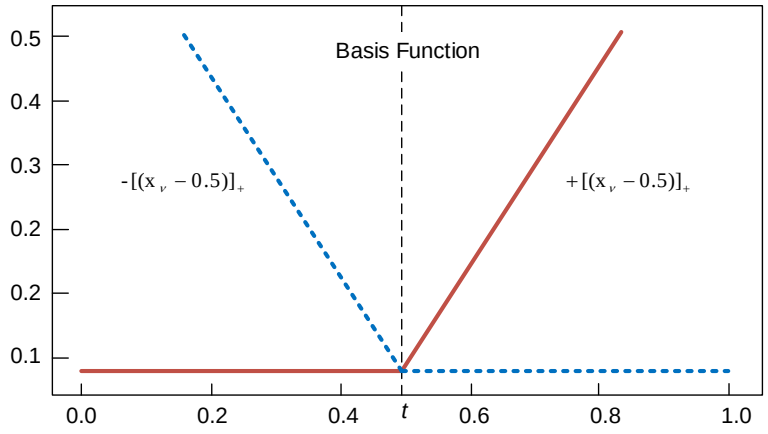


Figure 4-4 Basis function

$$[-(x_v - t)]_+^q = \begin{cases} (t - x_v)^q & if\ x_v < t \\ 0 & \text{otherwise} \end{cases} \tag{4.7}$$

$$[+(x_v - t)]_+^q = \begin{cases} (t - x_v)^q & if\ x_v \geq t \\ 0 & \text{otherwise} \end{cases} \tag{4.8}$$

Where $(q \geq 0)$ is the power to which splines are raised and determines the degree of smoothness of the resultant function estimate; $q = 1$ in Figure 4-4.

MARS uses collection of functions comprised of reflected pairs for each input $X_j$ with knots at each observed value $x_{ij}$ of input

$$B_m(X) = \prod_{j=1}^{Km} \left[ s_{m,j} \times \left( X_{v(m,j)} - t_{m,j} \right) \right]_+ \tag{4.9}$$

If all input values are distinct, then set $B_m(X)$ contains $2Np$ functions where, $N$ is a number of observations, and $p$ is a number of input variables. MARS model has the general form:

$$f(X) = c_0 + \sum_{m=1}^{M} c_m B_m(X) \tag{4.10}$$

Where $km$ is the number of truncated linear functions multiplied in the $m$th basis function. $Km$ should not be larger than the maximum interaction among variables $I_{\max}$.

$X_{v(m,j)}$ is the input variable corresponding to the $j$th truncated linear function in the $m$th term; $t_{m,j}$ is the knot value corresponding to variable the $X_{v(m,j)}$; $s_{m,j}$ is the selected sign $+1$ or $-1$;

$f(X)$ is the dependent variable predicted by the MARS model; $c_0$ is a constant; $B_m(X)$ us the $m$th basis function, which may be a single basis function; and $c_m$ is the coefficients estimated by minimizing the residual sum of squares for the $m$th basis function.

In the model building procedure, forward pass, backward pass, and generalized cross validation are required. The forward pass is a step in testing a new function products and determining which product decreases training errors. To improve model predictive ability, the backward pass deletes the redundant basis function to fix the overfitting. Generalized cross-validation (GCV) is to estimate the optimal number of terms in the model (Cheng & Cao, 2014). R package, earth (Milborrow, 2017) was used for training.

4.1.2.3.5 Gaussian process emulator

The Gaussian process is suitable for implementing a stochastic non-parametric model using mean function and covariance function. The uncertainty of the prediction error can be considered for a time series model. The Gaussian process emulator (or Gaussian process regression model) is a linear regression model with Gaussian noise. The following description is referenced in these papers: (MacDonald et al., 2015; Ranjan et al., 2011). Let the $i$-th input and the corresponding output of the model be denoted by a $d$-dimensional vector, $x_i = (x_{i1}, \dots, x_{id})^\top$ and $y_i = y(x_i)$ respectively. For the experimental design, $D_0 = \{x_1, \dots, x_n\}$ is the set of $n$ input trails stored in an $n \times d$ matrix $X$. The outputs are held in the $x \times 1$ vector $Y = y(X) = (y_1, \dots, y_n)^\top$. The model output, $y(x_i)$, is modeled as

$$y(x_i) = \mu + z(x_i); \qquad i = 1, \dots, n, \tag{4.11}$$

Where $\mu$ is the overall mean, and $z(x_i)$ is a GP (Gaussian Process) with $E(z(x_i)) = 0$, $Var(z(x_i)) = \sigma^2$, and $Cov\left(z(x_i), z(x_j)\right) = \sigma^2 R_{ij}$. In general, $y(X)$ has a multivariate normal distribution, $N_n(1_n\mu, \Sigma)$, where $\Sigma = \sigma^2 R$ is formed with correlation matrix $R$ having elements $R_{ij}$, and $1_n$ is a $n \times 1$ vector of all ones. For the correlation structure (kernel function), Gaussian correlation function was used in this process given by

$$R_{ij} = \prod_{k=1}^{d} \exp\{-\theta_k |x_{ik} - x_{jk}|^2\}, \qquad \text{for all i, j} \tag{4.12}$$

Where $\theta = (\theta_1, \dots, \theta_d) \in [0, \infty)^d$ is a vector of hyper-parameters. The closed form estimators of $\mu$ and $\sigma^2$ given by

$$\hat{\mu}(\theta) = (1_n^\top \mathrm{R}^{-1}\, 1_n)^{-1}(1_n^\top \mathrm{R}^{-1}\, Y) \tag{4.13}$$

$$\hat{\sigma}^2(\theta) = \frac{\left(Y - 1_n\hat{\mu}(\theta)\right)^\top R^{-1}(Y - 1_n\hat{\mu}(\theta))}{n}, \tag{4.14}$$

are used to obtain the negative profile log-likelihood

$$-2\log(L_\theta) \propto \log(|\mathrm{R}|) + n\log\left[\left(\mathrm{Y} - 1_\mathrm{n}\hat{\mu}(\theta)\right)^\top R^{-1}\left(Y - 1_n\hat{\mu}(\theta)\right)\right], \tag{4.15}$$

for estimating the hyper-parameters $\theta$, where $|\mathrm{R}|$ denotes the determinant of $R$.

Following the maximum likelihood approach (MAP: Maximum A Posteriori), the best linear unbiased predictor at $x^*$ is

$$\hat{y}(x^*) = \hat{\mu} + r^\top R^{-1}(Y - 1_n\hat{\mu}) = \left[\frac{(1 - r^\top R^{-1}1_n)}{1_n^\top R^{-1}1_n}1_n^\top + r^\top\right]R^{-1}Y = C^\top Y, \tag{4.16}$$

with mean squared error

$$\begin{aligned} s^2(x^*) &= \mathrm{E}\left[\left(\hat{y}(x^*) - y(x^*)\right)^2\right] = \sigma^2(1 - 2C^\top r + C^\top RC) \\ &= \sigma^2\left(1 - r^\top R^{-1}r + \frac{(1 - 1_n^\top R^{-1}r)^2}{1_n R^{-1}1_n}\right), \end{aligned} \tag{4.17}$$

where $\mathrm{r} = \left(\mathrm{r}_1(x^*), \dots, r_n(x^*)\right)^\top$, and $\mathrm{r_i}(x^*) = Cor(z(x^*), z(x_i))$. In practice, the parameters $\mu, \sigma^2$ and $\theta$ are replaced with their respective estimates.

The stability of GP estimation algorithm can be highly dependent on the design point used to build the GP model and its corresponding simulator outputs. If any pair of design points in the input space are close to each other, the spatial correlation matrix $R$ can be near-singular and hence the GP model fitting process computationally unstable. A popular approach to overcome this numerical instability is to introduce a small nugget or jitter parameter by replacing $R$ with $R_\delta = R + \delta I$. However, replacing $R$ with $R_\delta = R + \delta I$ requires additional smoothing of the simulator data that is undesirable for emulating a deterministic simulator. Ranjan et al. (Ranjan et al., 2011) proposed a lower bound on $\delta$ to minimize the unnecessary over-smoothing.

$$\delta_{lb} = \max\left\{\frac{\lambda_n(\kappa(R) - e^a)}{\kappa(R)(e^a - 1)}, 0\right\} \tag{4.18}$$

where $\lambda_n$ is the largest eigenvalue of $R$ and $e^a$ is the threshold of condition number $\kappa(R)$ that ensures a well-conditioned $R$. Ranjan et al. suggest $a = 25$ for space-filling Latin hypercube designs. R package, GPfit (MacDonald et al., 2015) was used for fitting a GPE in this study. GPfit uses the GP model with $R_\delta = R + \delta I$. The estimate of correlation hyper-parameters is obtained by minimizing the deviance using a multi-start gradient based search (L-BFGS-B) algorithm. See (MacDonald et al., 2015) for further details.

#### 4.1.2.4 Bayesian analysis

Bayesian analysis is a statistical method that utilized Bayes' theorem in Equation (4.19) to obtain a posterior distribution for unknown parameters $(\theta)$ given the observed data $(y)$. All the uncertainty in building energy models are expressed in probabilities. The input parameters are considered to be uncertain and have a probabilistic distribution based on their plausible values. The uncertain parameters of the building energy model are updated to match the model prediction and the observed data. As a result, Bayesian calibration provides the posterior distribution $p(\theta|y)$ in a form of plausible distribution of calibration parameters.

$$p(\theta|y) = \frac{p(y|\theta) \cdot p(\theta)}{p(y)} \propto p(y|\theta) \cdot p(\theta) \tag{4.19}$$

Where $p(\theta)$ is prior distributions assigned for uncertain parameters; $p(y|\theta)$ is a likelihood function that measures how closely model predictions match the observed data.

A Markov Chain Monte Carlo (MCMC) (Gilks, 2005) method is used to draw the posterior probability distribution in the Bayesian calibrations. Estimation of the probabilistic model distribution involves complex integrals. Yet, these integrals are not calculable because of high dimensionality or cannot be evaluated using calculus in most of the cases. The MCMC allows approximations using stochastic sampling routines. Metropolis-Hastings sampling (Gelman et al., 2014) methods were used to solve the MCMC. The Bayesian calibration framework was conducted in R.

In an MCMC process, a sufficient number of iterations is required to explore the entire feasible range. In the previous chapter, 3,000 iterations were sufficient because only the annual total energy data was used for the calibration, but this study calibrates for 12 monthly energy data for electricity and gas energy use, requiring a 100,000 of iterations. A preliminary study using the Gelman and Rubin diagnostic (Gelman & Rubin, 1992) showed that the potential scale reduction factor (PSRF) for each parameter was lower than 1.1 which means the Markov Chain has converged when the iteration number is larger than 100,000.

Table 4-5 lists all the ten cases used in this study to compare the accuracy of the result from the Bayesian calibration. We expressed each case as case *i-j*, where $i$ represents the range of the input parameters and $j$ represents the type of meta-models.

Table 4-5 Cases of Bayesian analysis

| **Meta-models** | **Short names** | **Range** | |
|---|---|---|---|
| | | Case 1 (Base) | Case 2 (Wide) |
| Multiple Linear Regression | MLR | Case 1-1 | Case 2-1 |
| Neural Network | NN | Case 1-2 | Case 2-2 |
| Support Vector Machines | SVM | Case 1-3 | Case 2-3 |
| Multivariate Adaptive Regression Splines | MARS | Case 1-4 | Case 2-4 |
| Gaussian Process Regression Emulator | GPE | Case 1-5 | Case 2-5 |

In this study, we randomly chose one data point from the 100 extra data set (testing set), and the selected data point was used as a target building. The accuracy of the meta-model was evaluated using two criteria: R2 (R-squared) and the coefficient of variation with root mean square error (CVRMSE).

R2 calculates the proportion of total variation explained by the fitted regression model from the equation (4.20). The accurate regression models have higher R2 value.

$$R^2 = 1 - \frac{\sum_{i=1}^{n}(y_i - \hat{y}_i)^2}{\sum_{i=1}^{n}(y_i - \bar{y}_i)^2} \quad (4.20)$$

The Root Mean Square Error (RMSE) is calculated from equation (4.21).

$$\mathrm{RMSE} = \sqrt{\frac{\sum_{i=1}^{n}(y_i - \hat{y}_i)^2}{n}} \tag{4.21}$$

CVRMSE (Coefficient of Variation of the Root Mean Square Error) is a non-dimensional form of the RMSE. It relatively measures normalization of the magnitude by the mean of observations. The model with lower CVRMSE is a more accurate model. The extra 100 simulation runs were regarded as a testing data set. Then, R2 and CVRMSE were calculated to compare the performance of the meta-models developed from the first 100 simulation runs.

$$\mathrm{CVRMSE} = \frac{\mathrm{RMSE}}{\bar{y}} \tag{4.22}$$

Where, $\hat{y}_i$ denotes a predicted variable value for period $i$, $y_i$ is an observed value for period $i$, and $\bar{y}$ is the mean of all observed variable values. The accuracy of Bayesian calibration results was evaluated by the CVRMSE to the observed data of the target building. The CVRMSE values to the input parameters and total EUI values for monthly and annul were compared at each case.

### 4.1.3 Results

#### 4.1.3.1 Results of sensitivity analysis

Table 4-6 compares the results obtained from the sensitivity analysis using the annual electricity and the gas energy use. The results are only for the base case. As described in section 2.2, the SVI considers different results from three sensitivity analysis methods (SRC, Random forest, T-value) and two energy outputs (annual electricity and annual gas EUI). A higher absolute value indicates a more important parameter affecting the energy use. The most dominant parameter in the base case is the cooling set point temperature (CSP), while the most important parameter for the wide case is the occupant density (OCC) in the given office building. As the range of input parameters changes, the importance of parameters changed.

Table 4-6 Results of sensitivity analysis (SVI)

| Case | Parameter | Annual Elec EUI | | | Annual Gas EUI | | | SVI | Rank |
|---|---|---|---|---|---|---|---|---|---|
| | | SRC | Random forest | T-value | SRC | Random forest | T-value | | |
| Base (Case 1) | EPD | 0.44 | 103.81 | 56.49 | -0.11 | 17.96 | -7.75 | 14.2% | 4 |
| | LPD | 0.38 | 72.18 | 48.22 | -0.12 | 22.04 | -8.29 | 12.3% | 5 |
| | HSP | 0.49 | 140.89 | 63.05 | -0.19 | 32.62 | -13.05 | 18.6% | 3 |
| | CSP | -0.53 | 130.97 | -68.30 | 0.55 | 155.01 | 36.98 | 30.5% | 1 |
| | OCC | -0.02 | -1.08 | -2.45 | -0.74 | 188.80 | -50.38 | 22.0% | 2 |
| | INF | 0.09 | 4.13 | 11.85 | 0.04 | 0.86 | 2.62 | 2.5% | 6 |
| Wide (Case 2) | EPD | 0.61 | 55.15 | 18.19 | -0.11 | 1.37 | -2.01 | 16.3% | 3 |
| | LPD | 0.54 | 58.17 | 16.10 | -0.06 | 0.09 | -1.10 | 14.5% | 5 |
| | HSP | 0.88 | 17.03 | 14.25 | -0.28 | 7.99 | -2.68 | 15.5% | 4 |
| | CSP | -0.83 | 13.49 | -13.41 | 0.63 | 39.00 | 5.96 | 24.0% | 2 |
| | OCC | 0.05 | -6.05 | 1.43 | -0.73 | 76.06 | -12.85 | 26.4% | 1 |
| | INF | 0.17 | -2.75 | 4.97 | -0.02 | -2.87 | -0.37 | 3.2% | 6 |

#### 4.1.3.2 Meta-models

Table 4-7 shows the time to develop each meta-model using 100 of training samples. Each meta-model has 17 monthly energy models (12 electricity and 5 gas model). The multiple linear regression model has the least time to build while the Gaussian process emulator took about 20 minutes.

Table 4-7 Meta-model making time

| Meta-models | Seconds |
|---|---|
| MLR | 0.05 |
| NN | 1.58 |
| SVM | 2.93 |
| MARS | 4.03 |
| GPE | 1223.29 |

Cross-validation is the most frequently used method of creating a model. The cross-validation is a process of modeling and evaluating data divided by training data and validation data. Repeating the process k times is called k-fold cross validation. The performance of different models can be compared with the cross-validation. The following is the phase of 10-fold cross-validation:

1. Divide the data into 10 pieces, $D_1$, $D_2$,…,$D_{10}$.

2. Initialize the value of K to 1.

3. Set $D_k$ as a validation data and create a model using other data.

4. Evaluate the model performance using the validation data, $D_k$. Let $P_k$ be the performance of the evaluated model.

5. If $K$ is lower than 9, $K = K + 1$ and go step 3. If $K = 10$, it ends.

6. This process determines the performance of the model, $P_1$,$P_2$,…,$P_{10}$, and the final performance can be determined by their average.

In this study, R package, cvTools (Alfons, 2012) was used for the cross validation. The performance of models was compared with RMSE. Figure 4-5 shows the monthly RMSE of each meta-model obtained through the cross-validation. These results show the GPE is the most accurate, and the MLR is the least accurate. As the range of input parameters increases (Case 2), the error increase of MLR is higher than other meta-models. Since the MLR is a linear model, there is a limitation to replicate non-linear complex building energy model. Non-linear meta-models (NN, SVM, MARS, and GPE) showed a better accuracy compared to the MLR. Especially, the GPE had the best accuracy in both base and wide cases.

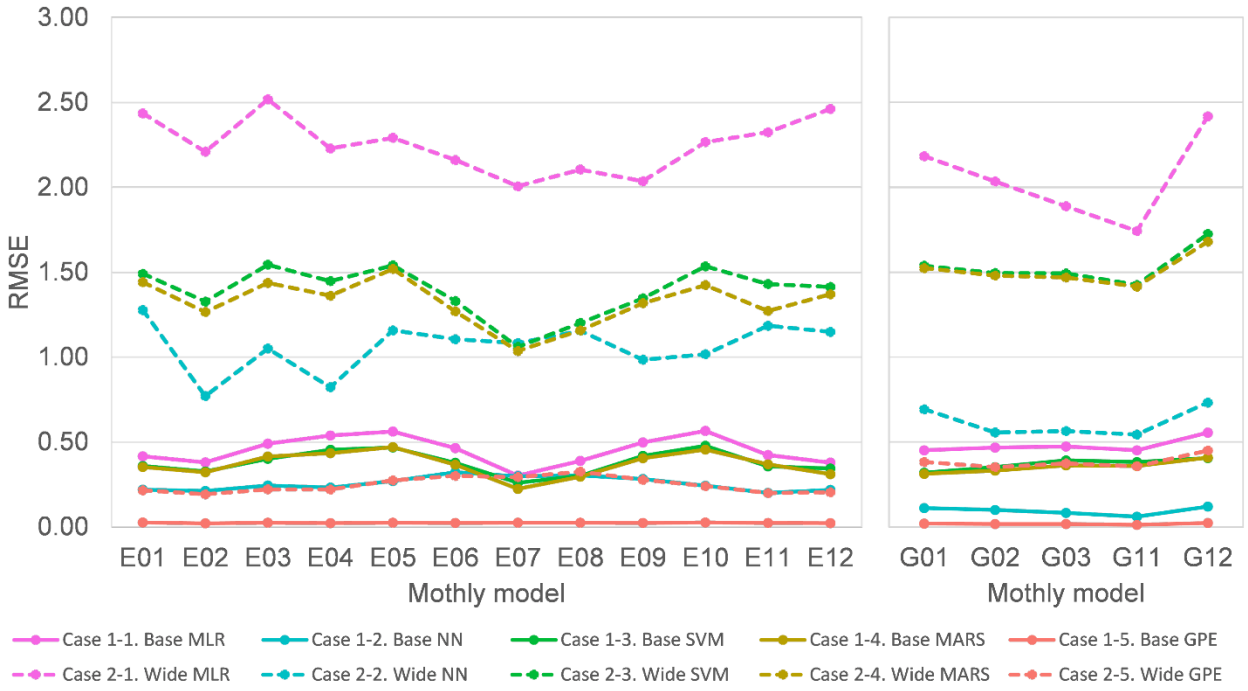


Figure 4-5 RMSE of meta-models

#### 4.1.3.3 Bayesian calibration

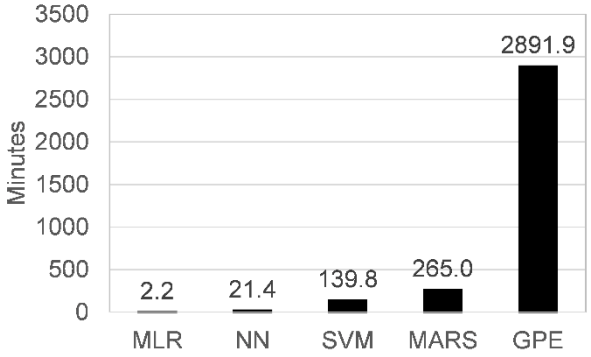


Figure 4-6 Computing time for MCMC

##### 4.1.3.3.1 Computational cost

Figure 4-6 shows the computing time of MCMC when each meta-model is used. The calibration using the MLR was the fastest (2.2 minutes) to sample 100,000 of chains, while the calibration using the GPE took about 48.2 hours. The MCMC simulation time is anticipated more than 70 days without meta-models (using EnergyPlus model). Using the meta-model reduces the simulation time in the MCMC process. However, the simulation time differs depending on the type of meta-model.

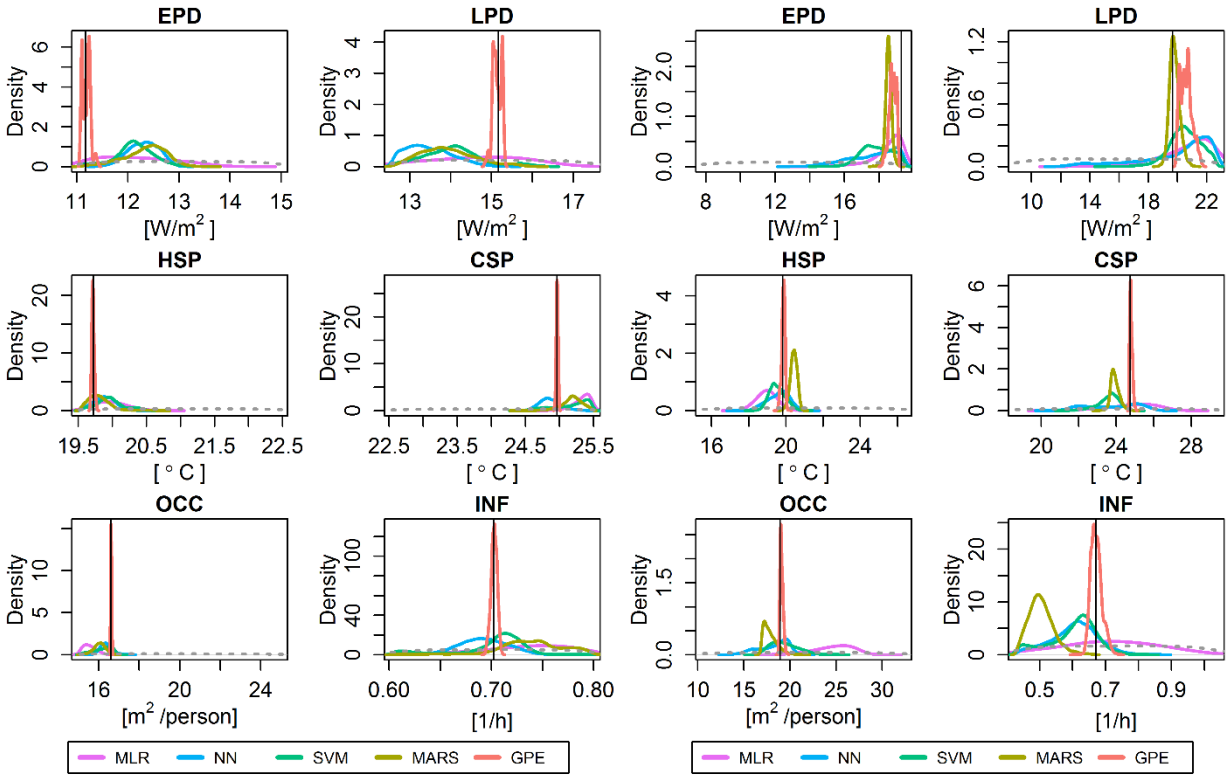


(a) Base case (b) Wide case

Figure 4-7 Posterior distributions for each parameter

4.1.3.3.2 Parameter estimation

Figure 4-7 compared posterior distributions of the calibration using each meta-model in the base case and the wide case. The vertical black lines are true input values for each parameter. The gray dotted lines are prior distributions which are uniform distributions, and the solid colored lines are posterior distributions. In all cases, the posterior distributions were calibrated to be closer to the true values as compared to the prior distributions. Despite the high computing costs, calibration using the GPE was the most accurate in the both the base case and the wide case.

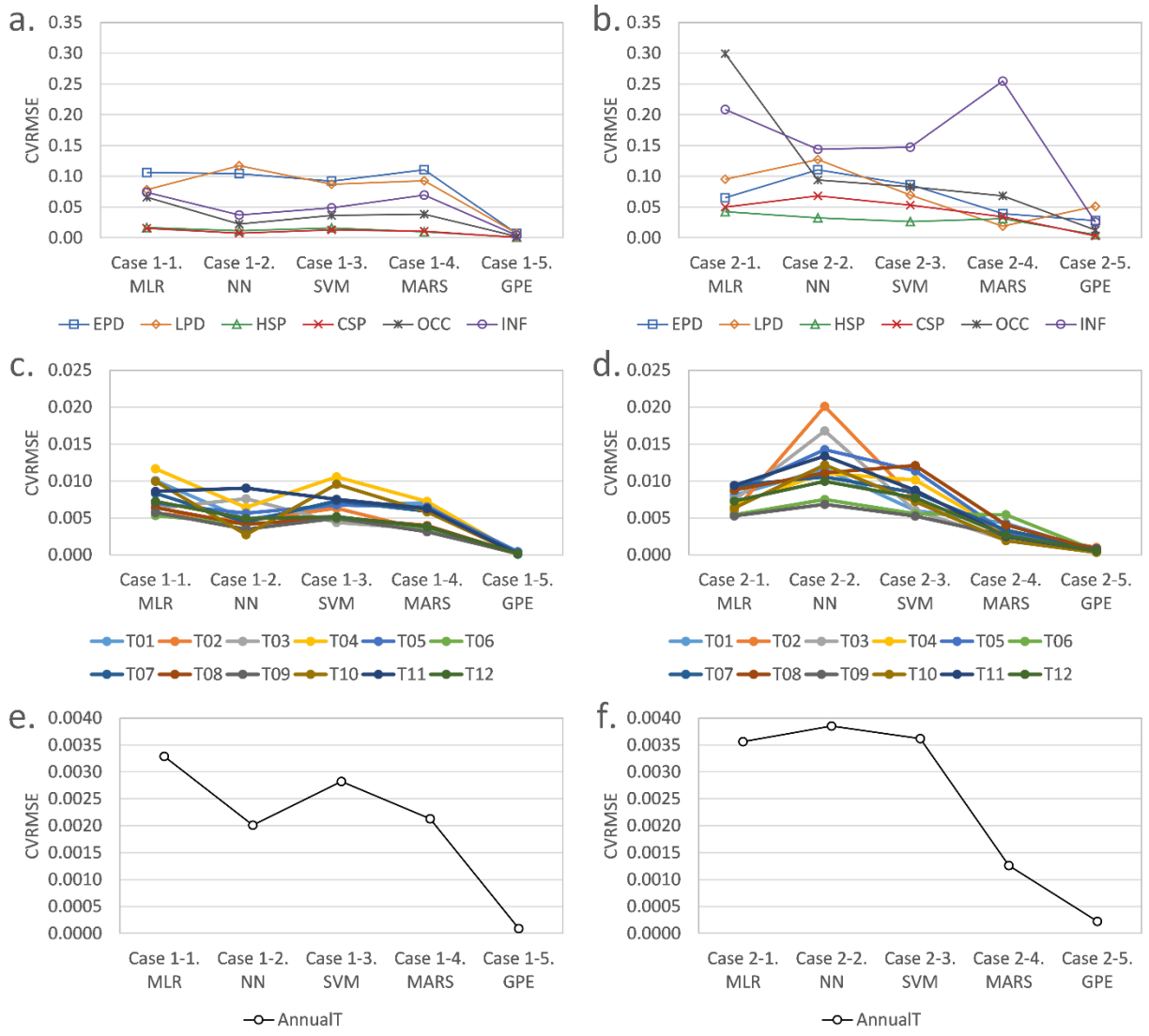


Figure 4-8 CVRMSE results to the true parameter and EUI

Figure 4-8-a and b provide the CVRMSE of posterior distributions for parameters in the case 1 (base range) and the case 2 (wide range). The more accurate meta-model has found the true value of unknown parameter accurately. Like the accuracy of the model itself, the calibration accuracy decreases as the range of input parameter increases. In particular, the CVRMSE of the linear model showed a larger increase than other models. Linear models have limitations in the wide range to express the complexity of building energy models extensively. Using non-linear meta-models such as NN, SVM, MARS, and GPE is better to estimate the true input values than using the linear regression model. Especially, the calibration results using GPE are remarkably accurate than using other meta-models, while it requires the longest

computing time (Figure 4-6). As the range of input parameter increased (From Case 1-5 to Case 2-5), the increase in CVRMSE of calibration using the GPE was relatively small compared to other results. This is because the GPE has excellent predictive accuracy as shown in Figure 4-5.

Looking at the relationship between the parameter sensitivity and the parameter estimation, the calibration of the dominant variables tends to be more accurate in general. However, in both cases, the importance ranking does not match the accuracy rankings of parameter estimation. These discrepancies are potentially caused by differences in energy data. The sensitivity analysis was conducted using annual electricity and gas energy use, and the calibration was performed with monthly energy use. Another possible reason is that the effects of electricity energy use and gas energy use are assumed the same in the calculation of the SVI. However, the electricity is dominant in the given office building. To account for energy use characteristics in the sensitivity analysis, a weighting factor may be applied to variables related to electricity use. Further research is also needed to examine the relationship between dominant parameters and parameter estimation accuracy.

4.1.3.3.3 Prediction performance

Figure 4-8 (c) to (f) show the CVRMSE for 12 monthly total EUI and annual total EUI, respectively. The average CVRMSEs of 12 monthly EUI are compared in Table 4-8. Similar trends with the parameter estimation have been confirmed in energy use prediction. The accuracy of the calibration result tends to be accurate when using more accurate meta-models. The calibration using the GPE had the lowest CVRMSE of EUI. The GPE was robust to change of input parameter range. Other non-linear meta-models showed a few better results than MLR in the base case. Interestingly, in the wide case, the prediction performance of the MLR (Case 2-1) was comparable with NN (Case 2-2) and SVM (Case 2-3) while the MLR had the worst accuracy for the parameters estimation. A possible reason is that the Bayesian calibration using the MLR can find more output combinations closer to the measured EUI data due to the simplicity of the MLR. However, in the wide range case, the accuracy of the parameter is lower because of the large model error of the MLR.

#### 4.1.3.3.4 Discussion

The calibration using the GPE can significantly reduce the simulation time compared to using the EnergyPlus, but it takes longer than calibration using other meta-models. Even though there were some discrepancies between the true input parameters and the estimated posterior distributions, all calibrated models can predict the observations well. In the base case, the CVRMSE for monthly and annual total monthly EUI were less than 1.2 % and 0.3%, respectively. In the wide case, the CVRMSE for monthly and annual total monthly EUI were less than 2 % and 0.4 %, respectively. These results improve the applicability of the MLR in cases where energy prediction is the main purpose and where the rapid calculation is required such as real-time building assessment and large-scale calibration. However, the accuracy of parameter estimation will be lower than using other more accurate meta-models. Adding an interaction and transformation can increase the predictive capability of the linear model (Faraway, 2014; Tian et al., 2016). Further research is required to improve the accuracy of the MLR with comparable computational cost.

Selecting proper meta-models is a balancing process between the computational cost and the accuracy of parameter estimation and energy prediction. The methodology and findings presented in this paper can help to select the meta-model in the Bayesian calibration.

Table 4-8 Average CVRMSE

| **Base** | **Case 1-1. MLR** | **Case 1-2. NN** | **Case 1-3. SVM** | **Case 1-4. MARS** | **Case 1-5. GPE** |
|---|---|---|---|---|---|
| **Aver. CVRMSE for 6 parameters** | 0.059 | 0.050 | 0.049 | 0.055 | 0.004 |
| **Aver. CVRMSE for 12 monthly total EUI** | 0.008 | 0.005 | 0.007 | 0.005 | 0.000 |
| **Wide** | **Case 2-1. MLR** | **Case 2-2. NN** | **Case 2-3. SVM** | **Case 2-4. MARS** | **Case 2-5. GPE** |
| **Aver. CVRMSE for 6 parameters** | 0.127 | 0.096 | 0.078 | 0.074 | 0.021 |
| **Aver. CVRMSE for 12 Monthly Total EUI** | 0.007 | 0.012 | 0.008 | 0.003 | 0.001 |

### 4.1.4 Conclusion

The analysis presented in this paper evaluates the accuracy of the Bayesian calibration for building energy models associated with the accuracy of meta-models. Due to the Bayesian calibration requires the massive interaction of building energy model, a meta-model is used to reduce the computing time. The main goal of the analysis is to assess the effect of meta-model's accuracy on the accuracy of estimated values in the Bayesian calibration.

The main findings from the analysis of the impact of meta-models' accuracy to Bayesian calibration include

(1) The SVI (Sensitivity Value Index) was suggested to consider different sensitivity analysis methods and outputs. The SVI can determine a comprehensive importance ranking of parameters taking into account the various sensitivity methods and outputs.

(2) Five meta-models (MLR, NN, SVM, MARS, and GPE) were compared to replace the EnergyPlus model in the Bayesian calibration process. The GPE had the best prediction performance, and the MLR was the least accurate. In particular, as the range of input parameter increased, the prediction performance of MLR was substantially decreased than other non-linear meta-models since the MLR has limitation to present the non-linear nature of building energy model.

(3) Using meta-models reduces computing time in the Bayesian calibration process. To sample 100,000 of chains, calibration using the MLR took 2 minutes, and calibration using the GPE took 2,892 minutes. The accurate tends to take longer simulation time. However, these are considerable reductions compared to the anticipated computing time of 70 days without the meta-models.

(4) The accuracy of Bayesian calibration was improved when using more accurate meta-model. The calibration with the GPE showed the best accuracy in both parameter estimation and EUI prediction performance. This is because the GPE can replicate relatively accurately the complicated original building energy model than other meta-models while it requires the longest computing time. In terms of parameter estimation, using the MLR showed comparable accuracy with other non-linear meta-models such as NN,

SVM, and MARS in the base input range. In the wide input range case, the accuracy of parameter estimation using the MLR was greatly reduced.

(5) Although there were some disagreements in the parameter estimation, all the calibrated models can predict well the energy use for the observations. In the base case, the CVRMSE were less than 1.2% for monthly EUI and 0.3% for annual EUI. In the wide case, the CVRMSE were within 2% for monthly EUI and 0.4% for annual EUI.

(6) Selecting proper meta-models is a balancing process between the computational cost and the accuracy of parameter estimation and energy prediction. The findings found through the proposed method and analysis will help to select the meta-model in the Bayesian calibration.

In summary, the Bayesian calibration requires considerable iterations of building energy model. To reduce the simulation time, we can substitute the complex building energy model for a meta-model. This study has confirmed that the computing time and the accuracy of calibration varied according to the type of meta-model. Therefore, it is important to select a proper meta-model regarding the degree of simulation time and the accuracy. Using the GPE showed the best accuracy while it took a long time than others. Focusing only on simulation time and energy usage prediction, the availability of Bayesian calibration using MLR has been confirmed. Adding an interaction and transformation can increase the predictive capability of the linear model (Faraway, 2014; Tian et al., 2016). More research is needed to improve the accuracy of the Bayesian calibration using the MLR.

## 4.2 Determination of informative energy data for Bayesian calibration

### 4.2.1 Introduction

Building energy simulation tools have been widely used for optimal design and control, and retrofit analysis for a building. In existing buildings, the difference between measured data and predicted output is inescapable due to uncertainty issues. The uncertainties in building models are due to insufficient building information, simplification of modeling processes, and behavior of occupants. Model calibration techniques have been used to reduce the difference between the measured and the predicted energy data. Calibration tunes the input parameters in a simulation model to minimize the discrepancy. Calibration techniques estimate the probability distributions of unknown inputs and provide posterior distributions given the observed data. Among various calibration techniques, Bayesian calibration has received increasing attention in the calibration of building energy model because of its expandability and accuracy.

Heo et al. (Yeonsook Heo et al., 2011) first applied the Bayesian calibration to account for uncertainties during the retrofitting of existing buildings. Bayesian calibration technique has been used for a variety of purposes: to estimate input parameters (Y. Heo et al., 2012; Kang & Krarti, 2016; Y.-J. Kim, Yoon, et al., 2013; Manfren et al., 2013; Tian et al., 2016), to clarify uncertainty of climate (Tian & de Wilde, 2011), and to predict building stock energy use (Booth & Choudhary, 2013; Booth et al., 2012, 2013; Ruchi Choudhary, 2012; Tian & Choudhary, 2012; Yohei Yamaguchi, Suzuki, et al., 2013).

As shown in Table 4-9, previous studies utilized as much energy use data as possible to calibrate in the given situation. However, there was a lack of discussion on the type and amount of energy data affecting the accuracy of Bayesian calibration.

Table 4-9 Building energy data used in Bayesian calibration

| Author | Year | Calibration method | Calibration target | Data type | Note |
|---|---|---|---|---|---|
| Heo (Y. Heo et al., 2012; Yeonsook Heo et al., 2011) | 2011, 2012 | Bayesian | individual building | 12 monthly gas data | heating only building |
| Tian and Choudhary (Tian & Choudhary, 2012) | 2012 | Inverse problem/ Bayesian | building stock | annual gas use data | heating only building |
| Booth et al. (Booth et al., 2012) | 2012 | Bayesian | building stock | 61 days of electricity use data | electricity only building |
| Zhao et al. (Fei Zhao, 2012; Fei Zhao et al., 2016) | 2012, 2016 | Inverse problem | building stock | annual total energy use data | - |
| Kim et al. (Y.-J. Kim, Yoon, et al., 2013) | 2013 | Bayesian | individual building | annual heating and cooling energy use data | - |
| Manfren et al. (Manfren et al., 2013) | 2013 | Bayesian | individual building | 12 monthly electricity and 12 monthly gas use data | - |
| Heo et al. (Yeonsook Heo, Graziano, et al., 2015) | 2015 | Bayesian | individual building | 12 monthly total energy use | - |
| Yoonsuk Kang and Moncef Krarti (Kang & Krarti, 2016) | 2016 | Bayesian | individual building | 12 monthly electricity and 12 monthly gas use data | - |

Tian et al. (Tian et al., 2016) indicated this issue and identified informative data in Bayesian calibration using correlation analysis and a hierarchical clustering method. This study aims to determine and choose informative energy data for accurate Bayesian calibration via correlation analysis and hierarchical clustering methods.

### 4.2.2 Methodology

The overall process is similar to the method described in Chapter 4.1. The first step is to establish the building energy model using the EnergyPlus. Then, a degree of uncertainty of the building model is determined by the selection of unknown parameters and variations of the selected parameters. The combinations of inputs are constructed using a sampling method. The combinations are fed into the building energy simulation program to obtain an input-output set. A large number of the input-output sets are required to supply sufficient data for the next step. The second step is to use a sensitivity analysis to screen parameters. This step identifies the dominant input (parameters) affecting the output (energy consumption). By selecting only important parameters as calibration parameters, we can exclusively focus on the important parameters and reduce the simulation runs in the calibration process. In this study, the parameter screening was omitted because only six unknown parameters were selected as input parameters. The third step is implementation of correlation and cluster analysis to examine the features of energy consumption data. We can classify the energy use data into several groups that have a similar trend. Based on the classification, we can determine which energy data are informative or uninformative. The fourth step is to create a meta-model using the input-output set from step one. Bayesian calibration will use the meta-model rather than the actual energy simulation programs to reduce the simulation time significantly. The last step is to obtain the unknown parameters from the Bayesian calibration and compare the accuracy of these posterior distributions to the target values.

#### 4.2.2.1 Building energy model

A medium office building from the U.S. Department of Energy (DOE) reference building, shown in Figure 4-9, was used for the case study in this analysis. The office building is a three-story rectangular building with a floor area of 4,982 $m^2$. The main features of the office building are shown in Table 4-10.

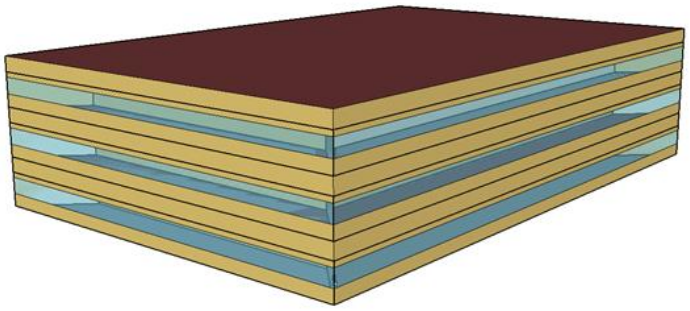

Figure 4-9 DOE reference medium office building (Medium Office Reference Building new construction 90.1-2004)

Table 4-10 Main features of the office building

| Component | Item | Parameters | Unit |
|---|---|---|---|
| Envelope | Floor area | 4982 | $m^2$ |
| | Floor levels | 3 | - |
| | Window-wall ratio | 0.33 | - |
| | Thermal Zoning | core zone with four perimeter zones on each floor | - |
| | Wall U-value | 0.48 | $W/m^2K$ |
| | Roof U-value | 0.35 | $W/m^2K$ |
| | Window U-value | 3.24 | $W/m^2K$ |
| | SHGC (solar heat gain coefficient) | 0.39 | - |
| | Infiltration rate (Air changes per hours) | See Table 4-11 | $W/m^2$ |
| Internal heat gains | Lighting power density | See Table 4-11 | $W/m^2$ |
| | Equipment power density | See Table 4-11 | $W/m^2$ |
| | Hourly schedules for set-point for heating and cooling, occupants, lights, and equipment | DOE Reference building | - |
| HVAC systems | System Type | MZ-VAV | - |
| | Heating Type | Gas furnace and electric reheat | - |
| | Cooling Type | PACU | - |

The building was assumed to be located in Boulder, Colorado, US and the weather data was obtained from the EnergyPlus weather file database ("Weather Data | EnergyPlus," n.d.). Table 4-11 lists the selected unknown input parameters and the range of them. Specifically, the chosen parameters are equipment power density, lighting power density, heating set-point, cooling set-point, occupancy, and infiltration. The ranges of unknown parameters were determined arbitrarily based on the default value of the reference building.

Table 4-11 Input parameters and ranges

| Parameters | Short names | Range | Unit |
|---|---|---|---|
| Equipment power density | EPD | 11 - 15 | $W/m^2$ |
| Lighting power density | LPD | 12.5 - 17.5 | $W/m^2$ |
| Heating set-point | HPS | 19.5 - 22.5 | $^oC$ |
| Cooling set-point | CSP | 22.5 - 25.5 | $^oC$ |
| Occupancy | OCC | 15 - 25 | $m^2$/person |
| Infiltration | INF | 0.6 - 0.8 | ACH |

The prior distributions for six input parameters were assumed as a uniform distribution. The 300 training samples and 100 testing samples of inputs were created by the Latin Hypercube Sampling (Mckay et al., 2000). Total 400 of input set were then fed into the EnergyPlus to obtain the input-output matrix. This process is called 'uncertainty propagation.' The obtained input-output matrix is utilized to build the meta-models in next step. The uncertainty propagation was performed by jEPlus software (Y. Zhang, 2009).

Figure 4-10 shows monthly average energy use intensity for 300 training set. The energy use intensity (EUI, $MJ/m^2$) for electricity and gas were used for energy performance indicators. For the office building, the electricity is dominant on the energy use because the DOE office medium reference building has a packaged air-conditioning unit for cooling and a gas furnace with electric reheat for heating. The gas usages from April to October have only base loads for domestic hot water. Therefore, the gas data for only five months (January, February, March, November, and December) were used for the calibration considering the accuracy of the meta-models. All 12-month energy data was used for the electricity.

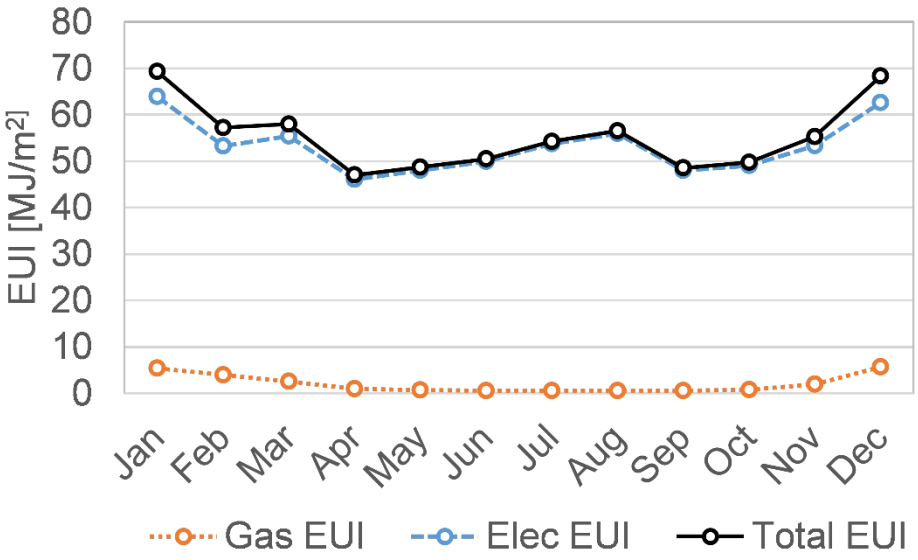


Figure 4-10 Average monthly energy use

4.2.2.2 Sensitivity analysis

As stated above, the parameter screening was omitted. However, the sensitivity analysis was performed to identify which parameter is more important among six parameters to the building energy use. It helps to explain the degree of uncertainty in the estimated parameters as results of Bayesian calibration. The sensitivity value index (SVI) was suggested in Chapter 4.1. Using the SVI, we considered different ranking from diverse sensitivity analysis methods and different outputs. In this study, we performed three sensitivity analysis methods for both electricity use and gas use: SRC (standardized regression coefficient), random forest variable importance and T-value. For detailed information about three sensitivity analysis methods, please refer to (Tian, 2013).

The SRC is the most popular method of the building energy analysis due to its availability and simplicity. It removes the original unit of measurement for variables in a regression equation by normalization. These coefficients are converted to a scale from -1 to 1. Therefore, we can more easily compare the effect sizes of parameters measured on different scales. The SRC is more suitable for linear relationships between inputs and outputs (Tian et al., 2016). The random forest method (Breiman, 2001) is an ensemble learning for classification and regression that construct a number of decision trees. The random forest can assess the relative importance of variables based on the decrease of classification accuracy when

values of a variable in a node of a tree are permuted randomly (Diaz-Uriarte & Alvarez de Andres, 2005). A larger decrease in accuracy indicates that the variable is more important than others. T-value can also be used to determine the important variable in regression analysis. The T-value is a statistic value for testing whether the corresponding regression coefficient is different from zero. The high absolute value of t means that the factor is more important than others.

The sensitivity value index (SVI) was suggested as shown in the equation (1). The values from the sensitivity analysis were normalized and then aggregated so that the importance of parameters can be compared considering the difference of sensitivity methods and target output.

$$\sum_{l=1}^{m} \frac{\frac{\sum_{j=1}^{k}\left(\frac{V_{i,j}}{\sum_{i=1}^{n}|V_{i,j}|}\right)}{k}}{m \cdot k} \times 100 = Sensitivity\ Value\ Index\ (SVI)(\%) \tag{4.23}$$

Where $i$ is the parameter, $n$ is the number of parameters ($n = 6$), $j$ is the sensitivity method, $k$ is the number of sensitivity methods ($k = 3$, (SRC, Random forest variable importance, and T-value)), $l$ is the target output, $m$ is the number of target output ($m = 1$ (total, electricity or gas))

4.2.2.3 Correlation and Cluster Analysis

The correlation and clustering analysis were used in this research to examine the features of building energy use data. The correlogram (or corrgram) is a graph of the correlation matrix. It is useful to highlight the most correlated variables in a data table. The correlation coefficients are colored according to the value. The Pearson Product-Moment Correlation measures the strength of a linear association between two variables and is denoted by $r$.

$$r = \frac{1}{n}\sum_{i=1}^{n}\left(\frac{x_i - \mu_x}{\sigma_x}\right)\left(\frac{y_i - \mu_y}{\sigma_y}\right) \tag{4.24}$$

Where $r$ is the Pearson correlation coefficient between two variables($x$ and $y$), n is the number of observations, $\mu_x$ is the mean of the variable $x$, $\mu_y$ is the mean of the variable $y$, $\sigma_x$ the standard deviation of the variable $x$, and $\sigma_y$ is the standard deviation of the variable $y$.

The Pearson correlation coefficient, $r$, ranges from -1.0 to +1.0. A value of 0 indicates that there is no association between the two variables. The closer $r$ is to +1 or -1, the more closely the two variables are related. If $r$ is positive, it means that as one variable gets larger the other gets larger. If $r$ is negative it means that as one gets larger, the other gets smaller.

The purpose of cluster analysis is to allocate a set of observation sets into groups that are similar or close to one another regarding certain characteristics. There are broadly two types of clustering methods based on distance-algorithms where objects are clustered into groups according to their relative closeness to each other (T. A. Reddy, 2011): partitional clustering and hierarchical clustering. Partitional clustering determines the optimal number of groups by performing the analysis with a different pre-selected number of clusters. Compared to the partitional clustering method, the hierarchical clustering method does not need to select the number of clusters, and it is more appropriate for example when the data set has naturally-occurring or physically-based nested relationships (Dunham, 2006). The hierarchical clustering allows one to identify closeness of diverse objects at different levels of aggregation. It starts with individual objects and then gradually merging these in a sequential method according to their relative closeness. As a result, there is only a single cluster including all objects at the highest level. In this research, each monthly end-use energy data were considered as the object. Therefore, the energy use data in different groups can be considered as having different characteristics of energy use, while the objects with similar characteristics of energy use were grouped together. The diagram from the hierarchical clustering is called tree diagram or dendrogram that allows one to identify objects which are close to each other at different levels. If two groups are significantly different, the energy data in two groups can be considered as informative energy data. After the correlation and cluster analysis, the cases were decided to determine whether the informative and uninformative energy data affect the accuracy of Bayesian calibration.

#### 4.2.2.4 Meta-models

A meta-model is a simplified representation of the building energy model. The biggest drawback of the Bayesian calibration is that it requires a massive number of simulation runs. This may result in an enormous amount of time to complete the simulation runs. To reduce the computational time, a meta-model

is used instead of EnergyPlus. In the previous chapter, we confirm that the calibration using the multiple linear regression (MLR) models could obtain reasonable calibration result in the prediction of energy consumption. Tian et al. (Tian et al., 2016) indicated the advantages of using the MLR models: robustness, intuitive relationship between input and output, and expandability using transformation such as interaction and second-order terms.

The accuracy of meta-model is evaluated by using two criteria: R2 and RMSE (root mean square error). The higher R2 value means that the model is more accurate and a lower RMSE value indicates a better model. The MLRs were developed from the training data (200 samples) and then evaluated using the test data (extra 100 samples).

#### 4.2.2.5 Bayesian analysis

In the Bayesian analysis, all the uncertainty in the building energy model can be regarded as probabilities. The six input parameters listed in Table 4-11 are estimated based on monthly energy data for electricity and gas. Bayesian inference was applied to calibrate uncertain parameters in a building energy model. The prior belief in the actual values of uncertain parameters is updated by given observed data on building in the Bayes' theorem. As a result, Bayesian calibration provides the posterior distribution $p(\theta|y)$ in a form of plausible distribution of calibration parameters.

$$p(\theta|y) = \frac{p(y|\theta) \cdot p(\theta)}{p(y)} \propto p(y|\theta) \cdot p(\theta) \tag{4.25}$$

Where, $p(\theta)$ is prior distributions assigned for uncertain parameters; $p(y|\theta)$ is a likelihood function that measures how closely model predictions match the observed data.

A Markov Chain Monte Carlo (MCMC) (Gilks, 2005) method is used to depict the posterior probability distribution in the Bayesian calibrations. Estimation of the probabilistic model distribution involves complex integrals. However, these integrals are not calculable because of high dimensionality or cannot be evaluated using calculus in most of the cases. The MCMC allows approximations using stochastic sampling routines. Metropolis-Hastings sampling (Gelman et al., 2014) methods were used to solve the MCMC. The Bayesian calibration framework was conducted in R, software for statistical analysis.

In an MCMC process, a sufficient number of iterations is required to explore the entire feasible range. 100,000 of iteration number was used in this study. A preliminary study using the Gelman and Rubin diagnostic (Gelman & Rubin, 1992) showed that the potential scale reduction factor (PSRF) for each parameter was lower than 1.1 which means the Markov Chain has converged when the iteration number is larger than 100,000.

To evaluate the accuracy of the Bayesian calibration, one data point was selected as a target building among the 100 testing data set. The input parameters and the energy use simulated from EnergyPlus model were considered as true values for the calibration.

The accuracy of the Bayesian calibration results was evaluated by the coefficient of variation with root mean square error (CVRMSE) to the true values of the target building. CVRMSE is a non-dimensional form of the RMSE. It relatively measures normalization of the magnitude by the mean of observations. The model with lower CVRMSE is a more accurate model. The CVRMSE values to the input parameters, and total EUI values for monthly and annual were compared to each case.

### 4.2.3 Results

#### 4.2.3.1 Results from sensitivity analysis

Figure 4-11 to Figure 4-13 show the sensitivity analysis results for monthly total energy, electricity, and gas. The analysis is based on the SVI considering three sensitivity analysis methods: SRC (standardized regression coefficient), random forest variable importance and T-value. As described in Chapter 4.1.2.2, each of the sensitivity methods provide sensitivity values, and a higher absolute value means a more influential parameter. Using the SVI, the values from the sensitivity analysis were normalized to identify the important parameters considering the difference of sensitivity analysis methods.

Figure 4-11 presents the ranking of importance influencing monthly total energy use in the building. The important parameters were significantly different by month. In the cold season, the heating set point temperature (HSP) is the most important factor, while the equipment power density (EPD) becomes more important in the hot season. In the ranking of importance for monthly electricity use (Figure 4-12), it shows a similar trend. It is because the electricity usage is dominant on the total energy use in the office building

section 0. The main end-use energy for electricity would change from the heating energy to the equipment since this DOE office building uses a gas furnace with electric reheat for heating. Figure 4-13 provides the important factors affecting monthly gas energy use. They are not much different by month because the gas energy use data in the summer were not included in this analysis. The occupant density is the most important parameter in the all the months. The next important factors are the cooling set point temperature (CSP) and heating set point temperature (HSP).

In the previous chapter, the sensitivity analysis was performed using the annual energy consumption data. It presented an overall trend of relative importance for input parameters. More detailed information can be obtained by conducting a sensitivity analysis with monthly energy use data. As shown in Figure 4-11, the most dominant parameter in the summer is different from that in the winter. It helps to understand the features of energy consumption in buildings. For the purpose of energy model calibration, this suggests that getting information on HSP is more important for the better match between simulation and observed data in winter, while the equipment power density data can greatly improve the accuracy of calibration in summer.

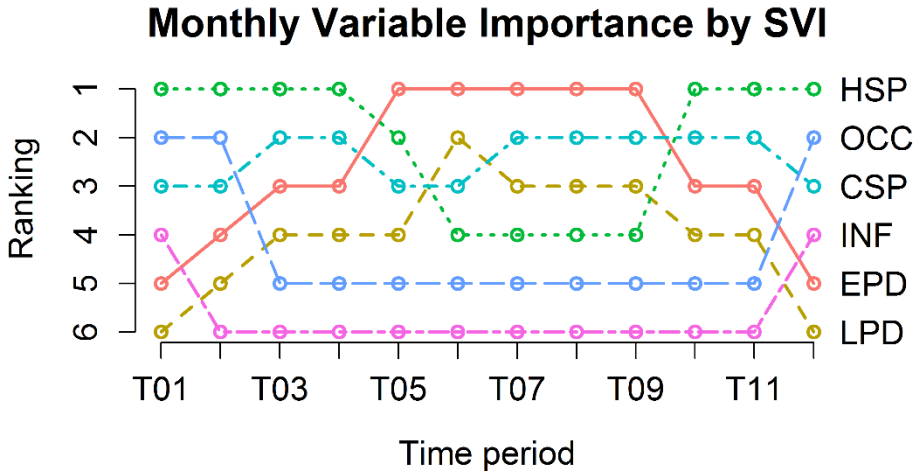


Figure 4-11 Sensitivity Value Index (SVI) using monthly total energy use

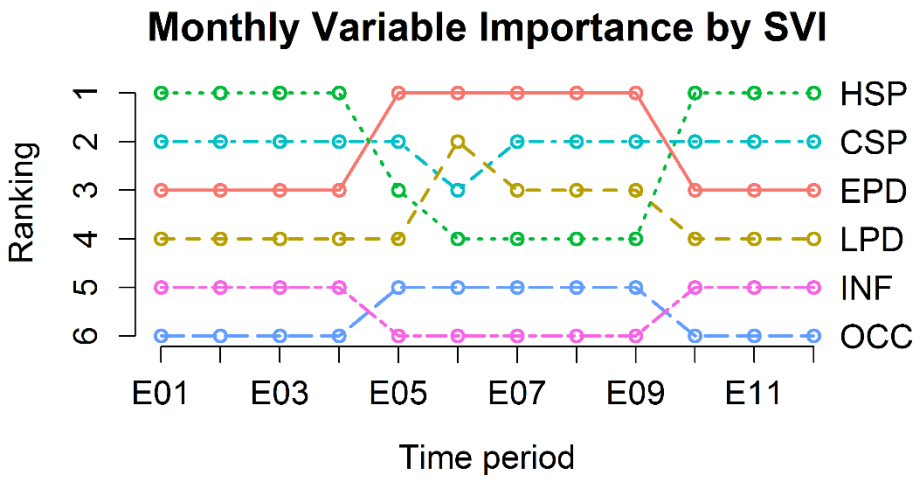


Figure 4-12 Sensitivity Value Index (SVI) using monthly electricity energy use

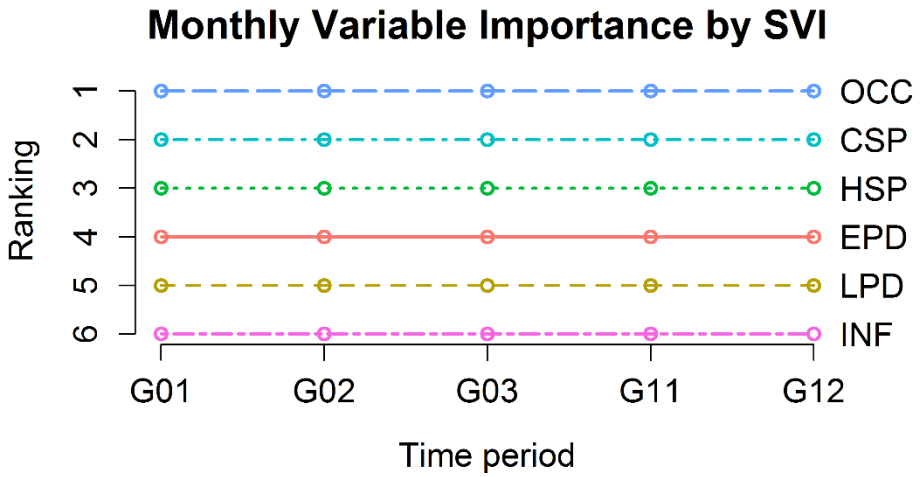


Figure 4-13 Sensitivity Value Index (SVI) using monthly gas energy use

4.2.3.2 Results from correlation and cluster analysis

Figure 4-14 to Figure 4-16 show the correlograms and dendrograms for monthly total energy use, electricity use, and gas use. The color in the correlogram shows the correlation coefficient as results from the correlation analysis. The color change from blue to red means an increase of correlation coefficient. We found an obvious seasonal pattern in the correlograms. The left side of correlogram is the dendrogram as results from the hierarchical cluster analysis. In the analysis using total energy use (Figure 4-14) and electricity (Figure 4-15), there is one cluster including all energy data at the highest level. At the second level, the total energy use and electricity use data are divided into three groups. According to the correlation and cluster analysis, monthly energy data was classified into three groups: winter, summer, and transition months. The winter season includes January, February, March, November, and December. The summer

months are June, July, August, and September. The transition months are April, May, and October. For the gas energy use (Figure 4-16), two clusters were identified from the analyses: winter and transition months. The winter months of gas data are January, February, and December. The transition months of gas data are March and November.

Regarding the findings from above analyses, the combinations of different energy consumption data can be used to determine the informative data for the Bayesian calibration. In this study, the informative data refer to the monthly energy use data from different clusters that have a large difference in the correlation and cluster analysis. The uninformative data are the monthly energy use data with high similarity (Tian et al., 2016).

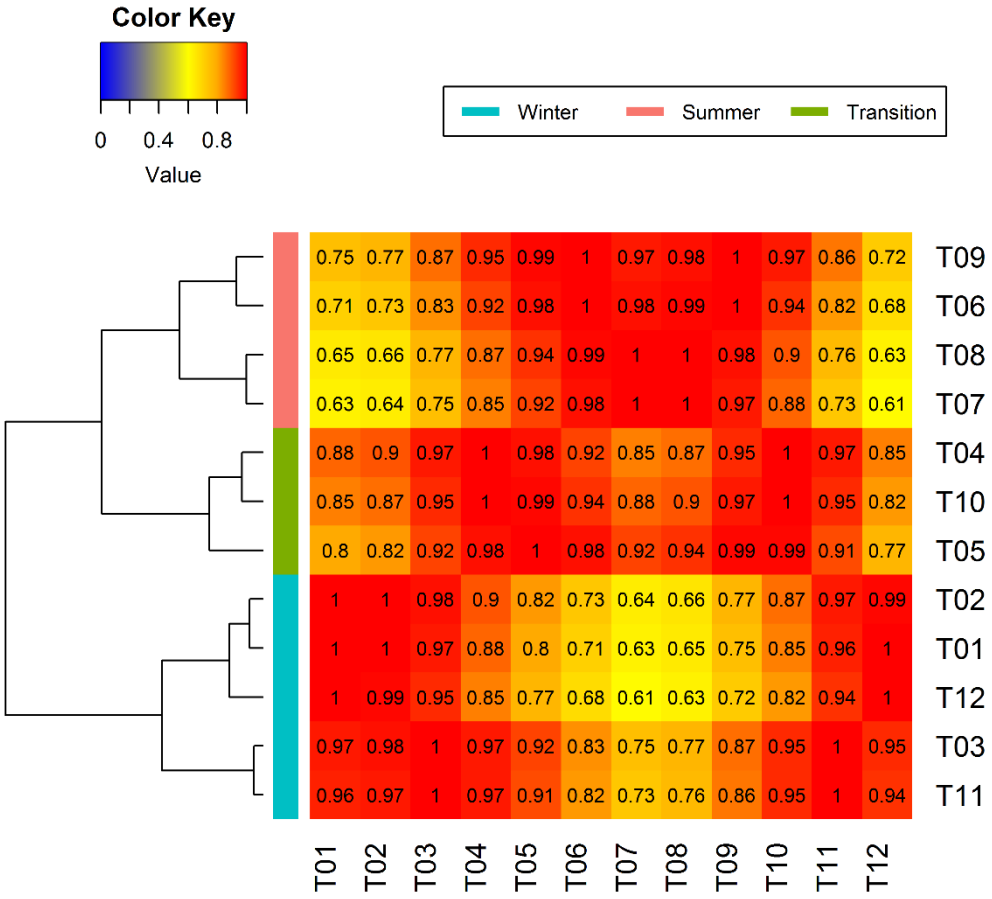


Figure 4-14 Correlogram and dendrogram for total energy use

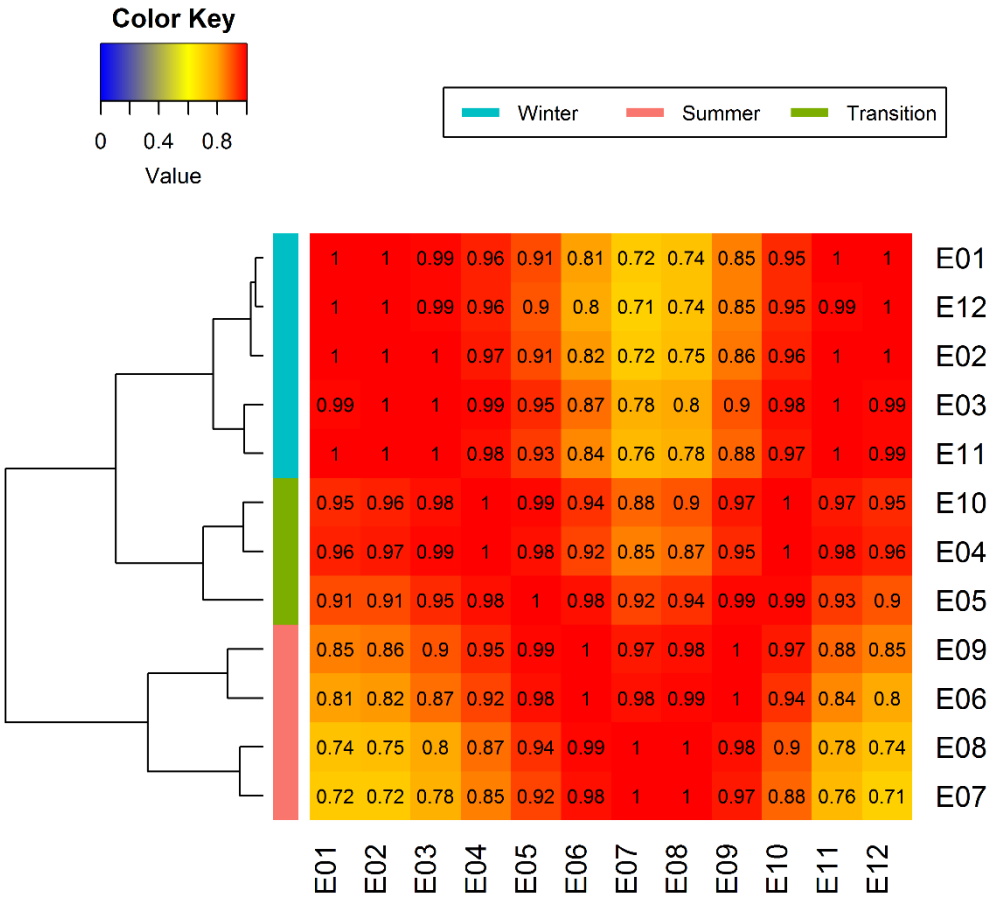


Figure 4-15 Correlogram and dendrogram for electricity energy use

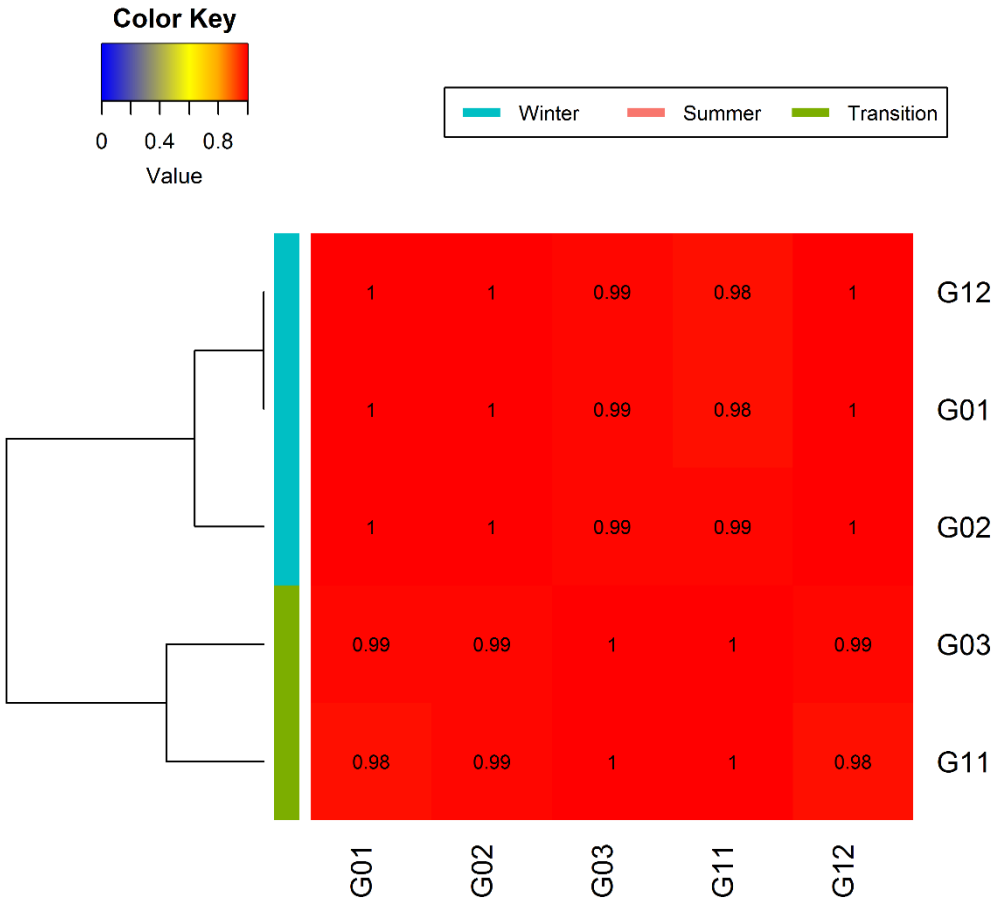


Figure 4-16 Correlogram and dendrogram for gas energy use

4.2.3.2.1 Case selection

Table 4-13 presents all the cases used in this study. Table 4-12 describe the name of the case. The first letter is the type of energy consumption data. For instance, 'T' indicates total energy use, and 'EG' indicates electricity and gas. The first number before a hyphen is the number of energy use data. The second number after a hyphen shows whether the case is informative or not. For example, case EG4-2 is informative energy data using four monthly energy use data: electricity data for January and July, and gas data for January and March.

The least number of energy use data are Case T1-1, Case E1-1, and Case G1-1 that are all uninformative data. On the other hand, the maximum number of energy data is 17 (Case EG17-2) which is

12 monthly electricity and 5 monthly gas energy data. Note that Case T8-1 and Case E8-1 are predicted to be informative enough although they are classified as uninformative. This is because those cases have eight monthly energy data from different clusters. By comparing the cases, the effect of informative and uninformative energy data on the Bayesian calibration can be analyzed.

Table 4-12 Example of case

e.g.) Case **T1-1**

| Energy use data type | # of monthly energy data | Informative |
|---|---|---|
| EG: Elec. & Gas,<br>T: Total,<br>E: Electricity,<br>G: Gas | 1, 2, 4, 8, 12, 17 | 1: Uninformative data ,<br>2: Informative data |

Table 4-13 Summary of cases

| | | | | | |
|---|---|---|---|---|---|
| Elec. & Gas | Uninformative | Case EG2-1 | Case EG4-1 | Case EG8-1 | |
| | Energy data | AE, AG | E01, E02,<br>G01, G02 | E01, E02, E03,<br>E11, E12,<br>G01, G02, G12 | |
| | Informative | | Case EG4-2 | Case EG8-2 | Case EG17-2 |
| | Energy data | | E01, E07,<br>G01, G03 | E01, E04, E07,<br>E08, E12,<br>G01, G03, G12 | E01 - E12,<br>G01, G02, G03,<br>G11, G12 |

| | | | | | |
|---|---|---|---|---|---|
| Total | Uninformative | Case T1-1 | Case T4-1 | Case T8-1 | Case T12-1 |
| | Energy data | AT | T01, T02, T11,<br>T12 | T01 - T08 | |
| | Informative | | Case T4-2 | Case T8-2 | Case T12-2 |
| | Energy data | | T01, T04, T07,<br>T08 | T01, T02, T04,<br>T07,<br>T08, T09, T10,<br>T12 | T01 - T12 |

| | | | | | |
|---|---|---|---|---|---|
| Elec. | Uninformative | Case E1-1 | Case E4-1 | Case E8-1 | |
| | Energy data | AE | E01, E02, E11, E12 | E01 - E08 | |
| | Informative | | Case E4-2 | Case E8-2 | Case E12-2 |
| | Energy data | | E01, E04, E07, E08 | E01, E02, E04, E07, E08, E09, E10, E12 | E01 - E12 |

| | | | | | |
|---|---|---|---|---|---|
| Gas | Uninformative | Case G1-1 | | | |
| | Energy data | AG | | | |
| | Informative | | Case G3-2 | Case G5-2 | |
| | Energy data | | G01, G02, G03 | G01, G02, G03, G11, G12 | |

4.2.3.3 Results from regression analysis

Figure 4-17 shows the results of regression analysis for total, electricity, and gas energy use. As a result, the accuracy of the model using training data set is higher than that using testing data set regarding R2 and RMSE. However, the results using testing data were not significantly different with the training data regarding R2 and RMSE. The results confirm that the multiple linear regression models are accurate enough for Bayesian calibration in the given case.

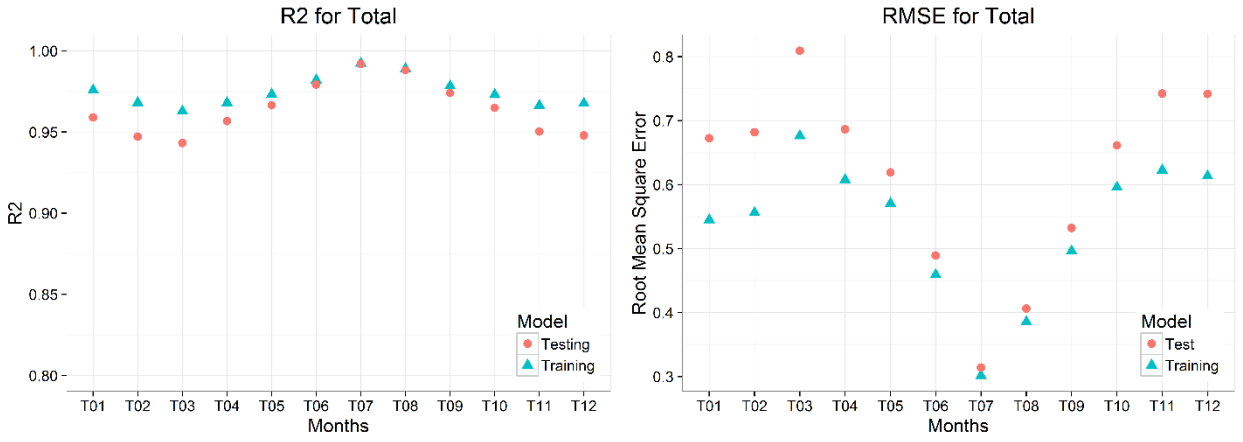

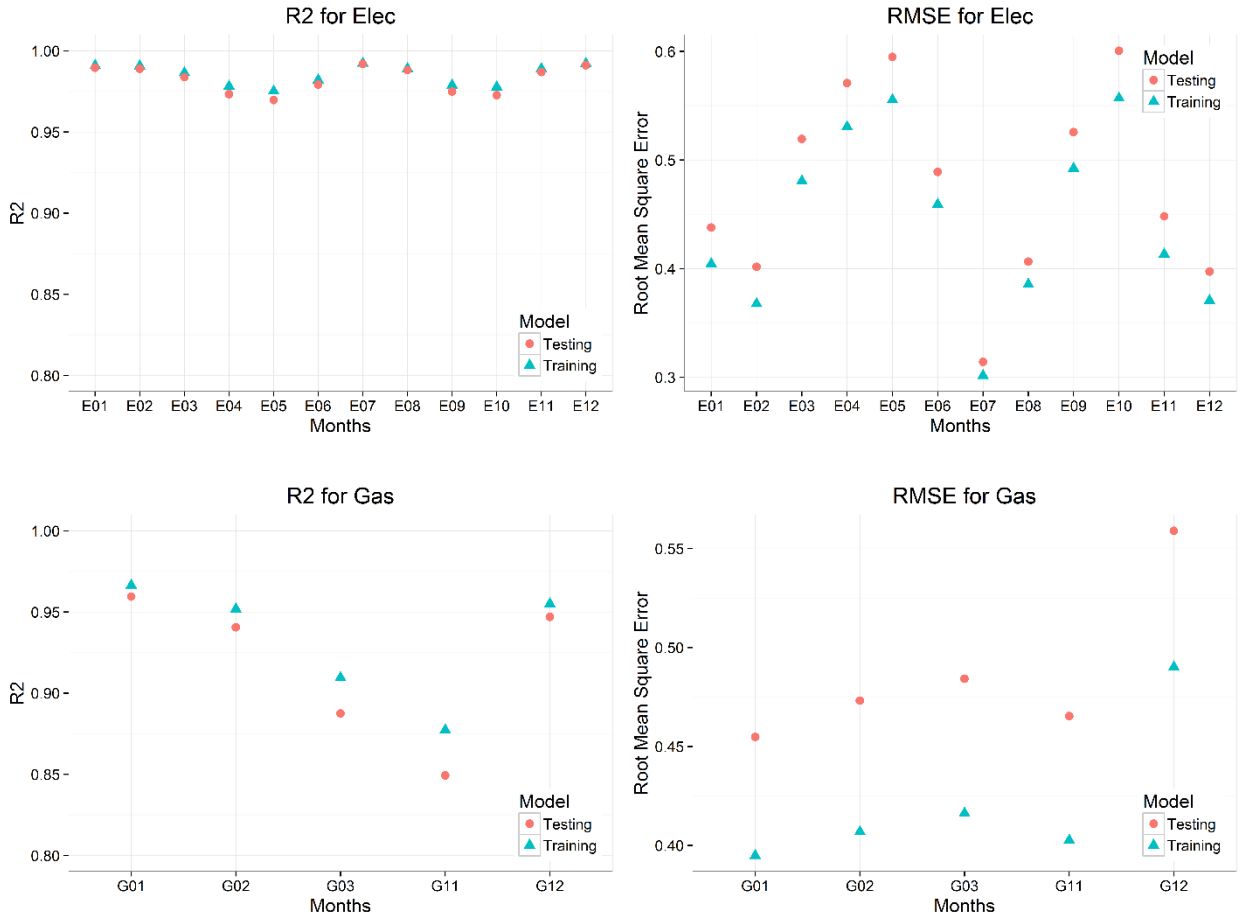


Figure 4-17 Results of regression analysis

4.2.3.4 Results from Bayesian analysis

Figure 4-18 (a) and (b) compares six parameter's distributions between case EG2-1 and case EG17-2. The dotted gray lines are the prior distribution, and the solid orange lines are the posterior distribution. The black vertical lines are the true values in the target building. If the posterior distributions are closer to the corresponding vertical lines, the results of Bayesian calibration are more accurate. The input parameters estimated from case EG2-1 have larger variations compared to case EG17-2.

Figure 4-18 (c) and (d) illustrates the distributions of EUI (energy use intensity) for case EG2-1 and case EG17-2. The red distributions are prior EUI distribution, and the green distributions are the posterior distribution. The solid black lines are the true energy consumption values. The posterior EUI distributions became closer to the true EUI value and the range of distribution narrowed. For the remaining results refer to Appendix A. CVRMSE values were compared for quantitative analysis.

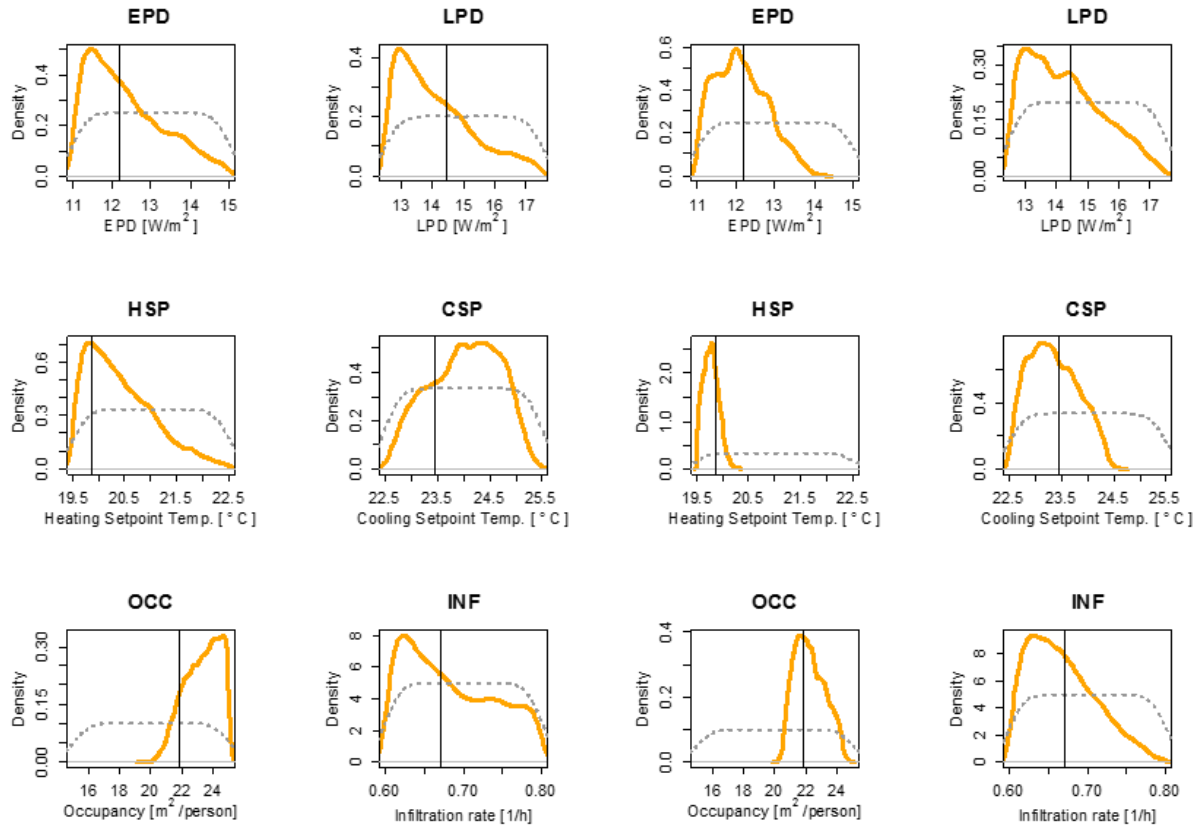


(a) Parameter distribution for Case EG2-1

(b) Parameter distribution for Case EG17-2

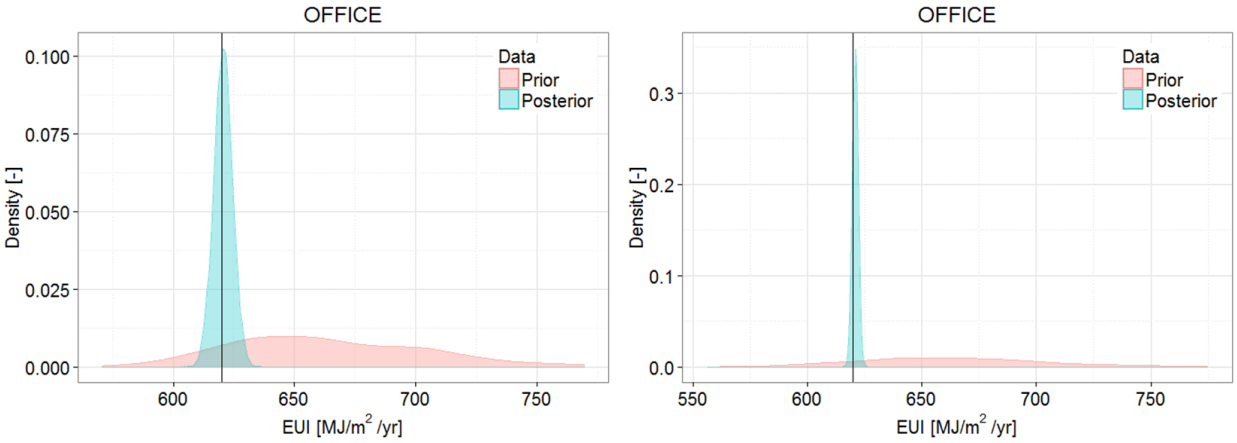


(c) EUI distribution for Case EG2-1

(d) EUI distribution for Case EG17-2

Figure 4-18 Distributions of input parameters and annual EUI

#### 4.2.3.4.1 Case EG

Case EG used both electricity and gas consumption data. Figure 4-19 shows CVRMSE results for each input parameters, monthly total EUI and annual total EUI. In the CVRMSE analysis for the parameter, the more the number of energy data, the more accurate results were obtained. Furthermore, accuracy can be improved when we use informative energy data rather than uninformative energy data. This indicates that the estimated posterior distributions are more reliable from the informative data when we use the same number of energy use data. In the CVRMSE analysis for monthly total EUI and annual EUI, as with the results for parameters, the higher the number of energy data, the more accurate results were obtained. The calibration results using four informative energy data (case EG4-2) were more accurate than results using eight uninformative energy data (case EG8-1).

In the closer inspection of CVRMSE results of monthly energy for case EG 4-1, the case EG4-1 has been correctly calibrated in all winter groups (January, February, December, November, and March), even though only energy data for January and February were used. However, the transition and summer groups were less accurate. The CVRMSE values were the largest for the summer group which is the least related to the winter group. This trend can also be seen in EG 8-1. However, because we used more energy data here, more accurate calibration results were obtained.

In particular, case EG2-1 showed poor accuracy for parameter and monthly total EUI while predicting performance for annual total EUI was comparable to the result of informative energy data. Since the calibration is made for the annual electricity and gas energy data, the accuracy for annual data is high. Meanwhile, as shown in Figure 4-20, using only two annual energy data (case EG2-1) can reduce the simulation time by about 51% compared to using 17 monthly energy data. Therefore, these results suggest that different energy data can be used depending on the purpose of calibration. For example, if detailed monthly forecasts are required, monthly energy measured data will be needed. On the other hand, if only annual energy consumption forecasts are taken into consideration, the annual energy can be selected for the calibration with low computational cost.

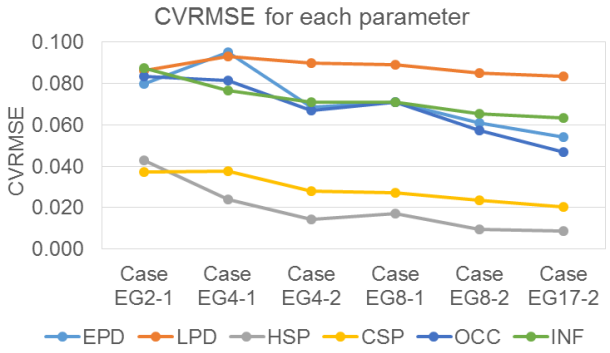


(a) CVRMSE for each parameter

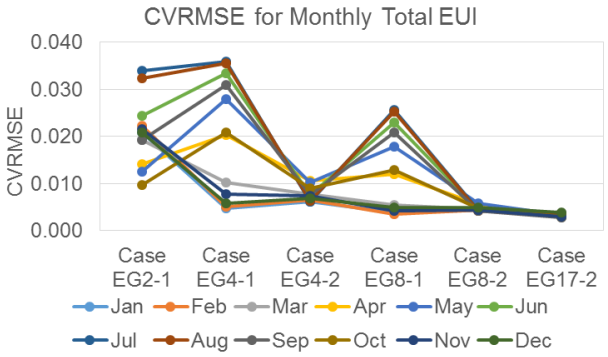


(b) CVRMSE for monthly total EUI

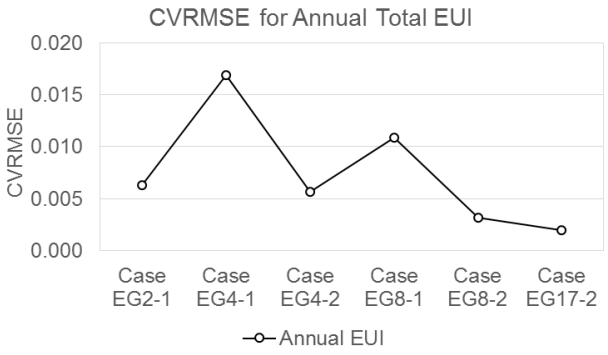


(c) CVRMSE for annual total EUI

Figure 4-19 CVRMSE for case EG

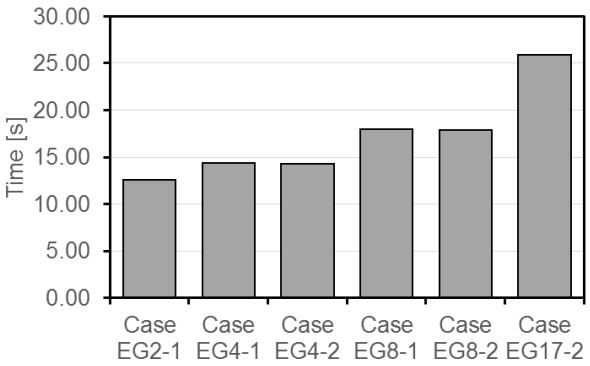


Figure 4-20 Computation time for Bayesian calibration

#### 4.2.3.4.2 Case T

Figure 4-21 shows CVRMSE results of Bayesian calibration using only total energy use data. Case EG17-2, the most accurate result, was also compared together. The difference between case T4-2 result from informative data and case T4-1 result from uninformative data is significant, while case T8-1 and case T8-2 show similar results. As expected, using eight of the monthly data from January to August is already informative enough since eight consecutive monthly total energy data covers all three different groups (winter, summer, and transition).

In case T4-1, similarly to case EG4-1, since energy data for January and February were used to calibrate, the months belonging to the winter group were corrected most accurately. Then, the transition group was the second most accurate, and the summer group was the least accurate. The difference in the accuracy of the calibration according to the cluster group was clearly shown.

CVRMSE results using 12 monthly total energy data (case T12-2) were similar to those using 17 energy data (case EG17-2) in terms of estimating energy use. This can be explained by the reason that total energy use is used as a calibration criteria. However, using a different type of energy data (case EG17-2) is more accurate than total energy usage data (case T12-2) when estimating the input parameters.

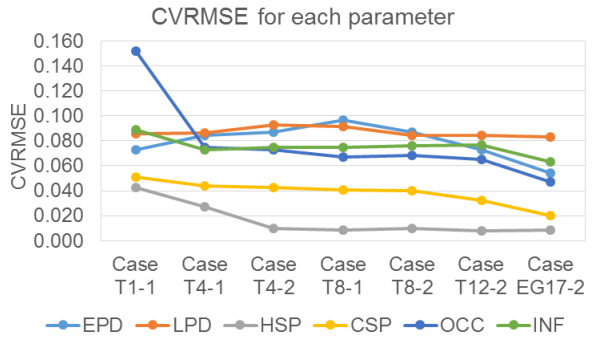


(a) CVRMSE for each parameter

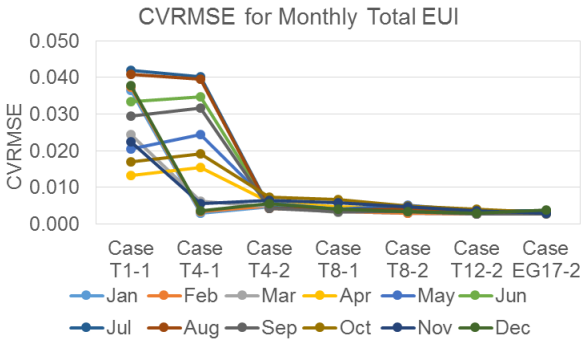


(b) CVRMSE for monthly total EUI

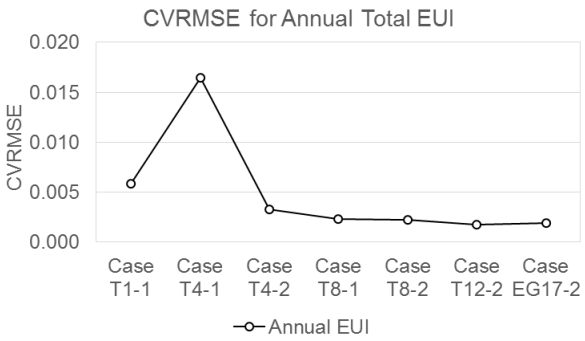


(c) CVRMSE for annual total EUI

Figure 4-21 CVRMSE for case T

#### 4.2.3.4.3 Case E

Figure 4-22 compares the calibration result using only electricity energy data. The most accurate results, case EG17-2, were compared together. Case E8-1 and case E8-2 have similar CVRMSE values since case E8-1 is already sufficiently informative data as in case T8-1. When using only electrical energy data, the accuracy of calibration is much lower than when using only total energy or when using both electric energy and gas energy together. It can be interpreted that the OCC, which is the most dominant factor in the use of gas energy (see Figure 4-13), cannot be properly calibrated when the calibration only uses electricity energy data. Indeed, in all cases, the CVRMSE values of the OCC were very large.

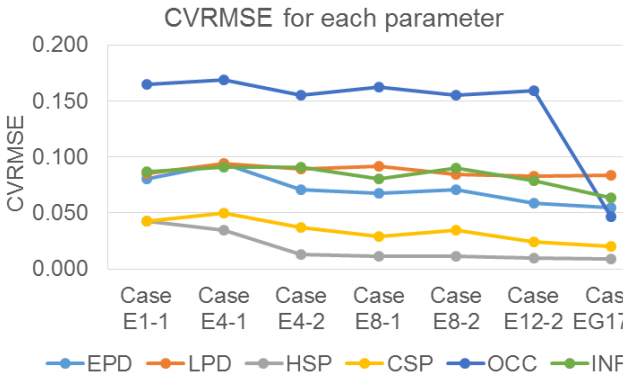


(a) CVRMSE for each parameter

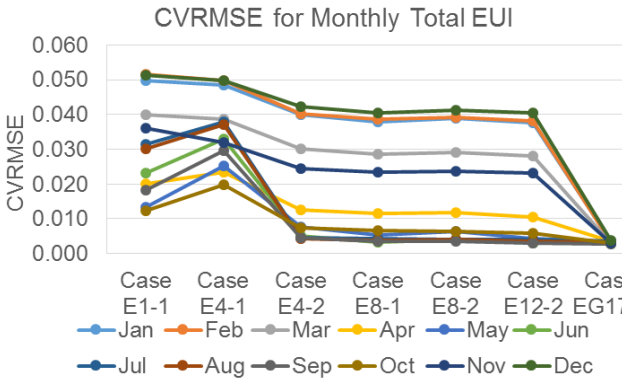


(b) CVRMSE for monthly total EUI

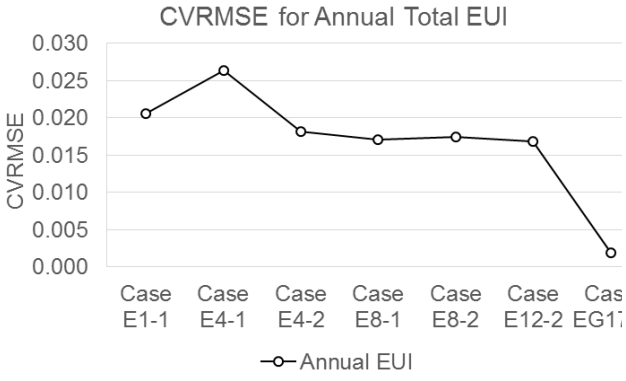


(c) CVRMSE for annual total EUI

Figure 4-22 CVRMSE for case E

#### 4.2.3.4.4 Case G

Figure 4-23 presents the CVRMSE results when the calibration uses only gas energy use data. It has a very large error in all cases. Since there were only five months of gas use data, the number of data was insufficient. Another possible explanation for large error is that the ratio of gas to the total building energy consumption is small. In terms of informative data, there was not much difference between informative and uninformative data when using three monthly gas energy data. It has been found that the accuracy is reduced when calibrating using only gas data in the target building.

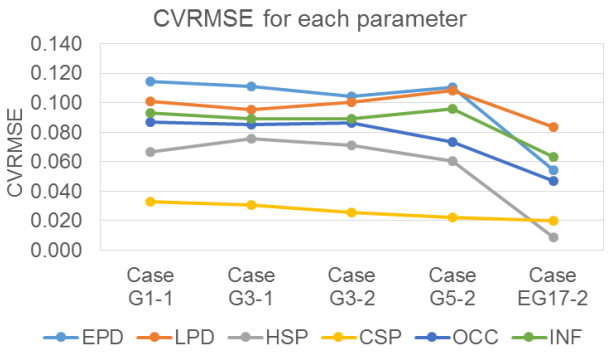


(a) CVRMSE for each parameter

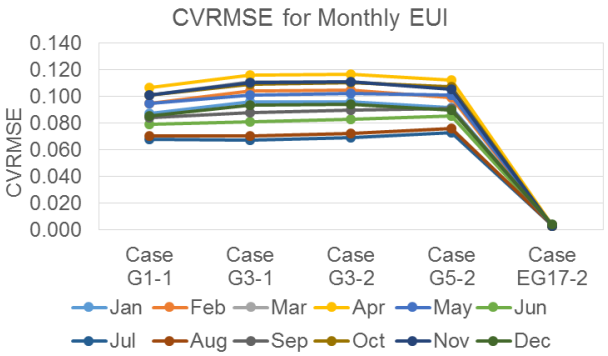


(b) CVRMSE for monthly total EUI

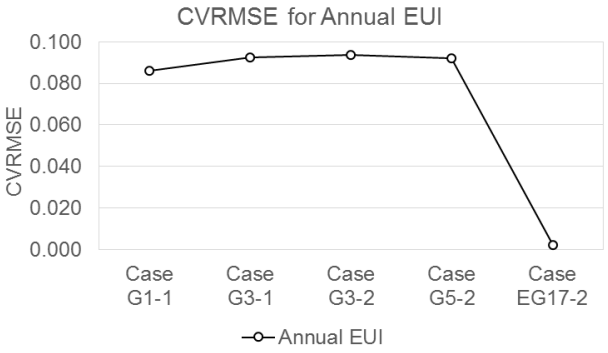


(c) CVRMSE for annual total EUI

Figure 4-23 CVRMSE for case G

In summary, this study compared the effect of informative and uninformative data on the Bayesian calibration. Generally, using more energy data showed more accurate calibration results. However, as more energy data is used, the number of meta-models increases, so it took longer to calibrate. Through the proposed method based on correlation and clustering analysis, the characteristics of energy data can be

comprehended and classified into several groups. The use of informative energy data pulled from different groups had more accurate calibration results. When there are different energy end-use types, using different types of energy data together showed better results than using one energy type data. In this case, if we only focus on calibrating the energy usage, it is recommended to use informative energy data with total energy data. If we are concerned about the estimation of the input parameters, using informative electricity and gas data can lead to accurate model calibration. By using this process, it can be judged whether sufficient accurate calibration can be acquired even if there is missing energy data.

### 4.2.4 Conclusion

The aim of the study is to determine informative energy data and to examine those effect on the Bayesian calibration of building energy models. In the given case study, the obtained energy use data was classified into three groups using correlation analysis and hierarchical clustering method. The energy data from the same group can be treated uninformative data. By contrast, the energy data from different groups are considered informative data because they present various energy usage patterns.

It was found that different combinations of energy data have a significant impact on the accuracy and computational time for Bayesian calibration. The informative energy data from different groups leads to reliable result with low computational cost.

Even though there is insufficient energy data in the Bayesian calibration, one can obtain reliable results if the informative data was selected using the proposed method. Furthermore, computational cost can be reduced by using only informative energy data for Bayesian calibration. The selection of informative energy data should be chosen considering the purpose of the calibration.

# CHAPTER 5: PREDICT BUILDING STOCK ENERGY USE WITH STOCHASTIC-DETERMINISTIC-COUPLED APPROACH

## 5.1 Introduction

In the previous chapter, the proposed stochastic methodology was applied and analyzed for a single building to understand the features of Bayesian calibration comprehensively. The effect of accuracy of meta-model and informative energy data were studied in the process of Bayesian calibration. As the meta-models are accurate and the building energy data is informative, the accurate Bayesian calibration can be achieved.

In this chapter, the proposed stochastic methodology is applied to a building stock. The method of expanding to building stock is examined. The issues to be considered in the process and the differences from the Bayesian calibration for an individual building are examined. A commercial virtual building stock is developed to determine whether the suggested stochastic-deterministic-coupled building stock energy model can estimate the input target distribution of building stock. Then, we examine whether the inferred posterior distribution of input parameters can be used for an energy conservation measure analysis.

The residential virtual building stock is also developed to figure out how to calculate the integrated EUI for different building stocks. Then, the daily energy use pattern from the two virtual building stocks are estimated to figure out the peak energy load. The stochastic building stock energy model is established through this process.

5.2 Process of stochastic building stock energy model

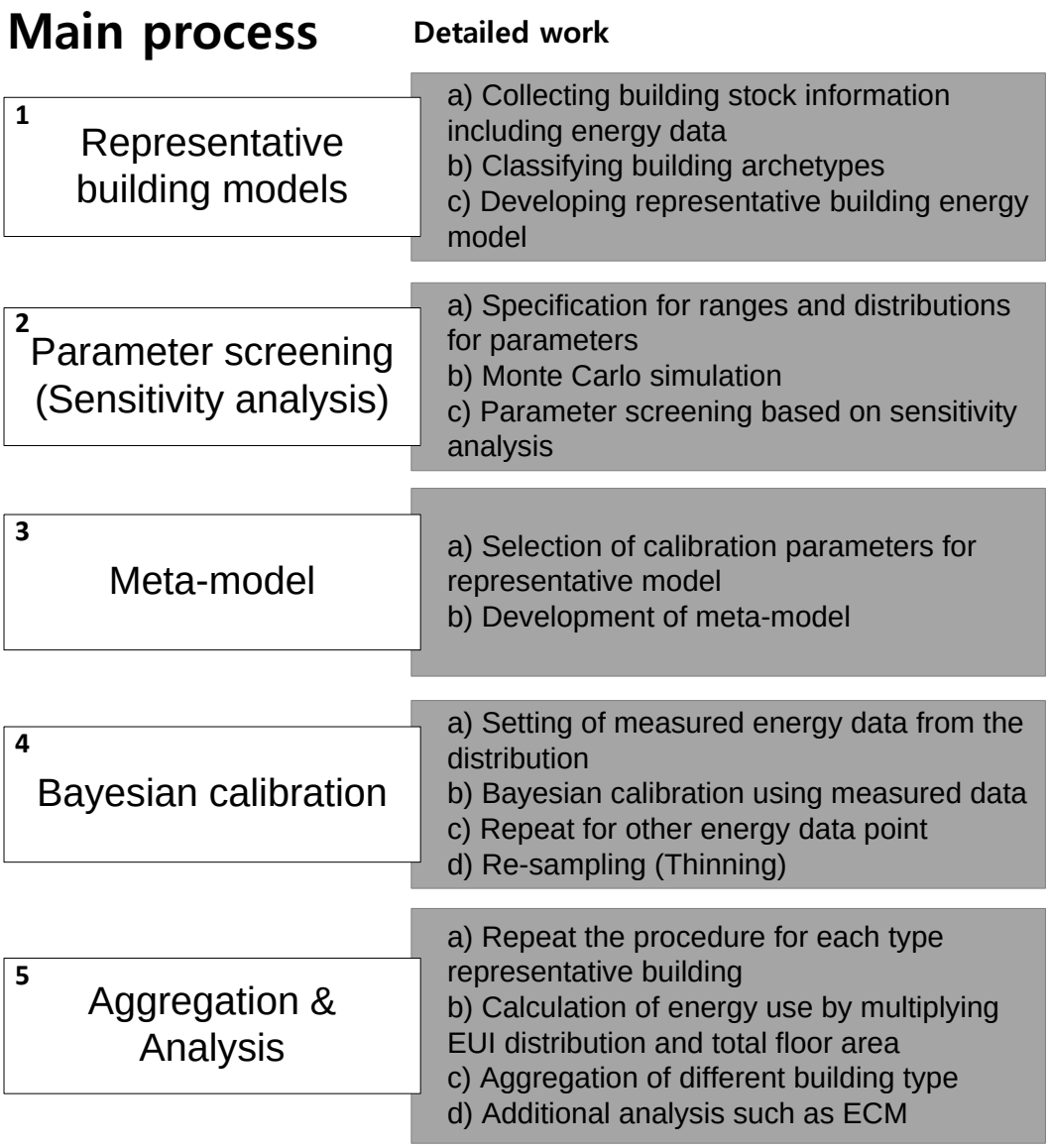


Figure 5-1 Main process of stochastic building stock energy model

Figure 5-1 presents the main process of stochastic-deterministic-coupled building stock energy model. The first step involves the development of representative building energy models using building energy simulation programs. Based on data analysis using collected building stock information, the buildings in the target district can be classified into several groups. The classification considers building features such as shape typology, building geometry such as building height and WWR, building function, age of construction, and material. For each group, representative building energy models are developed. A

degree of uncertainty is determined by selecting unknown parameters and those variations. The next step is uncertainty propagation. The combinations of inputs are constructed using a sampling method (Monte Carlo simulation). These combinations are fed into the building energy simulation program (e.g. EnergyPlus) to obtain input-output sets. This process is called "uncertainty propagation." A large number of the input-output sets are required to supply sufficient data for the next step. Then, a sensitivity analysis uses the input-output sets to select dominant parameters. This step identifies the dominant input parameters affecting the output (energy consumption). By selecting only important variables as calibration parameters, we can exclusively focus on the important parameters and reduce the simulation runs in the calibration process. The third step is to create meta-models using the input-output set from the step two. Bayesian calibration will use the meta-models rather than the dynamic energy simulation program to reduce the simulation time significantly. The fourth step is to estimate the unknown parameters using the Bayesian calibration.

From step 1 to step 3-(b) are similar to the process for individual building. The subsequent steps are for expanding the application of Bayesian calibration to the building stock. Another energy use data point (target building) is extracted from the energy use distribution, and the Bayesian calibration is performed on the energy data for new target building. Sufficient point should be sampled to represent the population, and the Bayesian calibration is repeated for each energy data. After the iteration of Bayesian calibration, the posterior distributions for each building are combined and then re-sampled to reduce sample size for simplicity of calculation (thinning). The next step is aggregation and analysis. Step 2 to step 4 are iterated for each representative building type. Then, total energy use for each building type is calculated by multiplying EUI distribution and total floor area. Finally, the distributions of total energy use for each building type are summed to obtain the energy consumption distribution for the overall building stock.

### 5.2.1 Differences in stochastic models for individual building and building stock

There are several differences in stochastic models for individual building and building stock:

#### 5.2.1.1 Development of representative building model

In the Bayesian calibration for an individual building, the purpose of building energy modeling is to construct the energy models as similar as possible to the actual target building. In the building stock, the buildings in the target district are classified into several sub-groups. The representative building model (archetype) for the sub-group should cover all buildings for the type of building. The most common characteristics such as an average value of building geometry and the most used type of HVAC systems can be used to model the representative building energy model.

#### 5.2.1.2 Uncertainty for input parameters

In the Bayesian calibration for the individual building, the prior distribution for an input parameter is treated as an uncertainty of the input parameter. In other words, such uncertainty is caused by insufficient building information, construction error, or human behaviors. On the other hand, in the building stock model, the uncertainty of the input variables can be considered as the distribution of each parameter in the building stock. For example, in the case of R-value of wall insulation, the uncertainty of the single building indicates the probability of R-value, while the uncertainty of the building stock can be treated as a spatial distribution of R-values.

#### 5.2.1.3 Iteration of Bayesian calibration

Bayesian calibration process for the individual building uses one set of energy data for the target building to calibrate. Therefore, if the building energy model is robust, the estimated posterior distribution for input parameter can be regarded as the actual target value. In the building stock, the Bayesian calibration is repeated for the several sets, which represent energy data points from the building energy distribution. Each distribution as a result of Bayesian calibration is combined. This is similar to the kernel density estimation procedure as shown in Figure 5-2 (Shawe-Taylor & Cristianini, 2004). Therefore, Bayesian calibration for building stock requires more computational time as the Bayesian calibration is iterated using each building energy data set of 30 buildings in the virtual building stock.

#### 5.2.1.4 Aggregation

Bayesian calibration for the building stock requires the aggregation process. There are two concepts of the term of aggregation. The first is the process from the representative building to the building stock. Each posterior distribution from the iterated Bayesian calibration are combined to represent one type building stock. Another aggregation is for the different building types. If there are several building classifications, each result for building types is combined to represent the all building stock.

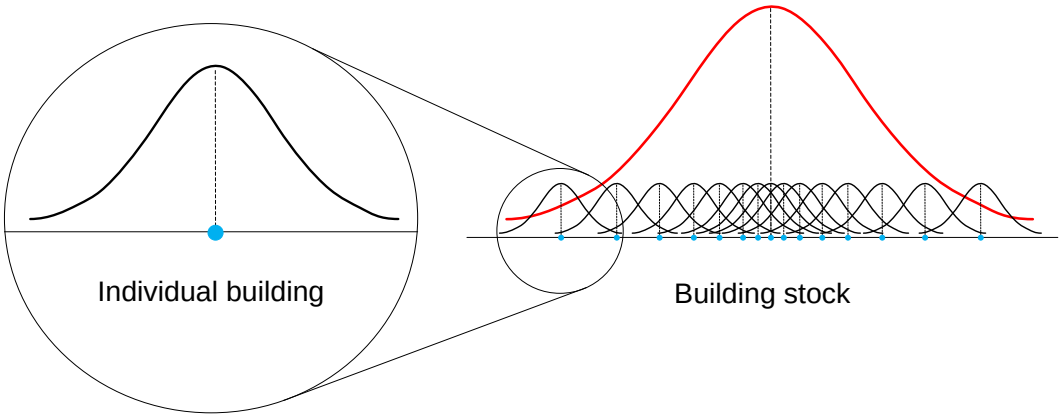


Figure 5-2 A conceptual illustration of an individual building and a building stock in Bayesian calibration.

## 5.3 Development of commercial Virtual Building Stock

In the actual building district, the building information such as thermal properties, specifications of HVAC systems for each building is rarely available for the level of detail required in the building energy modeling. Even if the detailed information could be acquired from drawings and specifications, the actual values of properties would be different due to construction and measurement errors. Therefore, the commercial virtual building stock (VBS) was developed in this chapter. By identifying the detailed input variables for each building in the building stock, the accuracy of the proposed stochastic-deterministic-coupled building stock energy model can be evaluated quantitatively.

The commercial VBS is based on the DOE commercial reference building - medium office. The office building has three stories, and the total floor area is 4,982 $m^2$. For the HVAC systems, it has a gas

furnace and electric reheat for heating and packaged air condition unit for cooling. The main features of the DOE reference medium office building are shown in Table 5-1.

Table 5-1 Main features of the DOE reference office building

| Component | Item | Parameters | Unit |
|---|---|---|---|
| Envelope | Floor area | 4982 | $m^2$ |
| | Floor levels | 3 | - |
| | Window-wall ratio | 0.33 | - |
| | Thermal Zoning | core zone with four perimeter zones on each floor | - |
| | Wall U-value | See Table 5-2 | $W/m^2K$ |
| | Roof U-value | See Table 5-2 | $W/m^2K$ |
| | Window U-value | See Table 5-2 | $W/m^2K$ |
| | SHGC (solar heat gain coefficient) | See Table 5-2 | - |
| | Infiltration rate (Air changes per hours) | See Table 5-2 | $W/m^2$ |
| Internal heat gains | Lighting power density | See Table 5-2 | $W/m^2$ |
| | Equipment power density | See Table 5-2 | $W/m^2$ |
| | Occupancy | See Table 5-2 | $m^2$/person |
| | Hourly schedules for set-point for heating and cooling, occupants, lights, and equipment | DOE Reference building | - |
| HVAC systems | System Type | MZ-VAV | - |
| | Heating Type | Gas furnace and electric reheat | - |
| | Heating efficiency | See Table 5-2 | - |
| | Heating set-point | See Table 5-2 | $^oC$ |
| | Cooling Type | PACU | - |
| | Cooling COP | See Table 5-2 | - |
| | Cooling set-point | See Table 5-2 | $^oC$ |

All buildings were assumed to have the same geometry and HVAC systems. The variation was applied only for 12 parameters: roof U-value, wall U-value, windows U-value, windows SHGC, equipment power density, lighting power density, heating set-point, cooling set-point, occupancy, infiltration, heating efficiency, the coefficient of performance for cooling. Table 5-2 lists the range of 12 input parameters. All distributions of parameters were assumed to be a triangular distribution. Using the quasi-random sampling (Sobol' sequence), 30 combinations of samples were generated and fed into the EnergyPlus to obtain energy use data. Therefore, 30 buildings were developed in the virtual building stock. Figure 5-4 presents the average monthly EUI of total, electricity, and gas energy for the commercial VBS. Figure 5-5 shows the distribution of annual EUI as a result of EnergyPlus. The developed commercial virtual building stock was utilized as a target for the calibration.

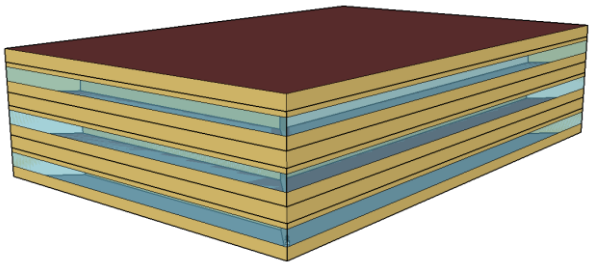

Figure 5-3 DOE reference medium office building

Table 5-2 Input parameters and distributions

| **Parameters [Unit]** | **Triangular distribution** | | |
|---|---|---|---|
| | min | mode | max |
| ROOF U-value [W/m$^2$K] | 0.4 | 0.5 | 0.6 |
| WALL U-value [W/m$^2$K] | 0.5 | 0.6 | 0.7 |
| Window U-value [W/m$^2$K] | 3.2 | 3.4 | 3.6 |
| Window SHGC [-] | 0.37 | 0.38 | 0.39 |
| EPD [W/m$^2$] | 11 | 13 | 15 |
| LPD [W/m$^2$] | 12.5 | 15 | 17.5 |
| HSP [$^o$C] | 19.5 | 21 | 22.5 |
| CSP [$^o$C] | 22.5 | 24 | 25.5 |

| | | | |
|---|---|---|---|
| OCC [m²/per] | 15 | 20 | 25 |
| INF [ACH] | 0.6 | 0.7 | 0.8 |
| HEATEFF [-] | 0.75 | 0.8 | 0.85 |
| COP [-] | 2.7 | 2.9 | 3.1 |

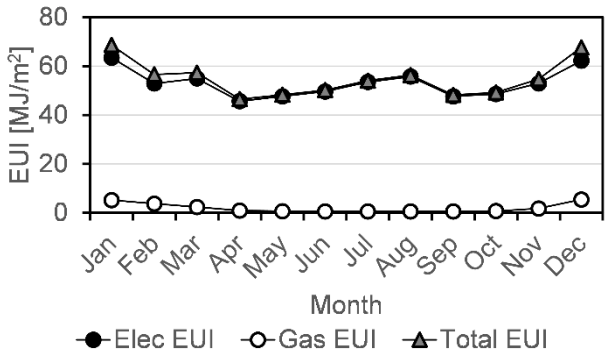


Figure 5-4 Average monthly EUI

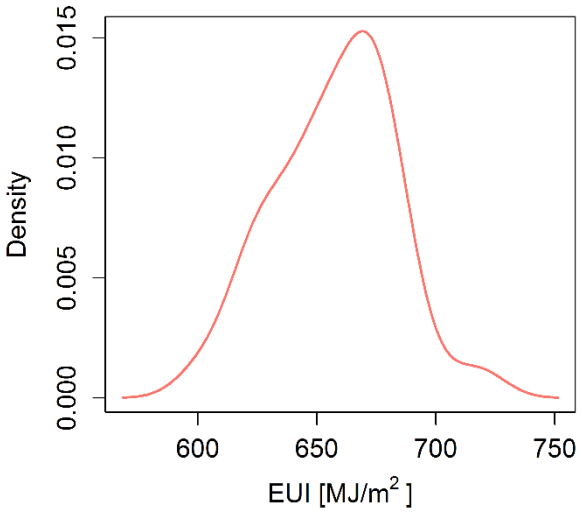


Figure 5-5 Annual EUI distribution

## 5.4 Identification of unknown parameters for building stock

### 5.4.1 Methodology

The stochastic-deterministic-coupled building stock energy model proposed in chapter 5.2 is applied in this section. For the first step, the same medium office building model (DOE reference office building - medium) was used for representative energy model. The error from the discrepancy of building geometry can be reduced by selecting the same building model. In the second step, a sensitivity analysis was conducted using the same range of each parameter in the VBS, but uniform distribution is assumed for the distribution of each parameter (Table 5-3). The sensitivity value index (SVI) proposed in Chapter 4 was adopted to screen dominant parameters on the annual electricity and gas energy use.

Table 5-3 Range for sensitivity analysis

| Parameters [Unit] | Uniform distribution | |
|---|---|---|
| | Min | Max |
| ROOF [W/m$^2$K] | 0.4 | 0.6 |
| WALL [W/m$^2$K] | 0.5 | 0.7 |
| WIN [W/m$^2$K] | 3.2 | 3.6 |
| SHGC [-] | 0.37 | 0.39 |
| EPD [W/m$^2$] | 11 | 15 |
| LPD [W/m$^2$] | 12.5 | 17.5 |
| HSP [$^o$C] | 19.5 | 22.5 |
| CSP [$^o$C] | 22.5 | 25.5 |
| OCC [m$^2$/per] | 15 | 25 |
| INF [ACH] | 0.6 | 0.8 |
| HEATEFF [-] | 0.75 | 0.85 |
| COP [-] | 2.7 | 3.1 |

Table 5-4 shows the ranking from sensitivity analysis using the SVI. Only six parameters were selected as calibration parameters: EPD, LPD, HSP, CSP, OCC, and INF. The uncertainty propagation was performed again only using dominant six parameters to remove the error from the non-dominant parameters. The newly generated input-output sets using six parameters were employed to build meta-models in the next step.

Table 5-4 Result of sensitivity analysis using the SVI

| Parameter | SVI | Rank |
|---|---|---|
| ROOF | 1.9% | 7 |
| WALL | 1.5% | 8 |
| WIN | 0.7% | 11 |
| SHGC | 0.5% | 12 |
| EPD | 23.6% | 2 |
| LPD | 12.6% | 5 |
| HSP | 14.1% | 4 |
| CSP | 24.0% | 1 |
| OCC | 16.8% | 3 |
| INF | 2.0% | 6 |
| HEATEFF | 1.0% | 10 |
| COP | 1.3% | 9 |

Three meta-models were utilized to compare the effect of meta-model's accuracy: Multiple linear regression models (MLR), Gaussian process emulator (GPE), perfect model (PM). The effect of meta-model's accuracy of Bayesian calibration for an individual building has been examined in chapter 4.1. This study investigated the effect of accuracy of meta-models on the building stock. The perfect model indicates an exact meta-model to predict the energy use output of EnergyPlus model. The artificial energy output data sets were generated using the MLR and the identical input variables. In the condition of the generated artificial input-output sets, the R-squared value of MLR is one without error. That is the reason it is designated the "perfect model." The perfect model can be regarded as calibration using an EnergyPlus without meta-models.

In the Bayesian calibration process, two types of prior distributions were considered: base and wide range. The base range case is based on the assumption that we know the range of input variable in the target building stock, but the distributions were assumed as a uniform distribution. The wide range case is expanded about 30 percent for each input range of base case. These two types of prior distribution were to examine the effect of prior range on the building stock calibration (Table 5-5). The cases considering the meta-models and the range of input variables are listed in Table 5-6. In the wide range case, the meta-models were developed using the input-output sets from the wide range of parameters. 12-month electricity and 5-month gas energy use data were used to calibrate the model.

The Bayesian calibration was iterated for each building energy data among 30 office buildings. After the iteration of Bayesian calibration, the posterior distributions for each building were combined and then re-sampled to reduce sample size for simplicity of calculation (thinning). Aggregation and additional analysis will be discussed in detail in Chapter 5.5 and 5.6.

Table 5-5 Dominant input parameters and ranges

| Parameters | Short names | Range | | Unit |
|---|---|---|---|---|
| | | Base | Wide | |
| Equipment Power Density | EPD | 11 - 15 | 7.7 - 19.5 | W/m$^2$ |
| Lighting Power Density | LPD | 12.5 - 17.5 | 8.75 - 22.75 | W/m$^2$ |
| Heating Set-point | HPS | 19.5 - 22.5 | 15.5 - 26.5 | $^o$C |
| Cooling Set-point | CSP | 22.5 - 25.5 | 18.5 - 29.5 | $^o$C |
| Occupancy | OCC | 15 - 25 | 10.5 - 32.5 | m$^2$/person |
| Infiltration | INF | 0.6 - 0.8 | 0.42 - 1.04 | ACH |

Table 5-6 Cases

| | MLR | GPE | Perfect model |
|---|---|---|---|
| **Base** | Case 1-1 | Case 2-1 | Case 3-1 |
| **Wide** | Case1-2 | Case 2-2 | Case 3-2 |

The purpose of this study is to verify whether the posterior distribution of the parameters obtained through the proposed stochastic-deterministic-coupled building stock energy model matches the target distribution. The results of Bayesian calibration were evaluated graphically and quantitatively. The probability density function distributions of each parameter were compared in the figure. In addition, the p-values from Kolmogorov-Smirnov test (K-S test) were used to evaluate the similarity of two distributions quantitatively (Massey Jr, 1951).

The Kolmogorov-Smirnov test verifies whether the two data samples come from the same distribution. The test hypothesizes that two samples are from the same distribution, denoted as $H_0$.

$H_0$: The distributions are the same

$H_1$: The distributions are not the same

Suppose we have two samples, $X_1 \cdots, X_m$ and $Y_1, \cdots, Y_n$ drawn from continuous distributions. The two samples can be depicccted by their cumulative distribution function (CDF). The Kolmogorov-Smirnov statistic, $D$ is

$$D = \max_{x} \left| \hat{F}_1(x) - \hat{F}_2(x) \right| \tag{5.1}$$

where $F_1(x)$ is the CDF for the distribution of the first population and $F_2(y)$ is the CDF for the second. $\hat{F}_1$ and $\hat{F}_2$ are the empirical distribution functions of the first and the second treatment.

If both X and Y are drawn from the same distribution and their value are such that D=d, a large D value would appear to be inconsistent with the null hypothesis that both samples are drawn from the same distribution. The p-value for the K-S test is identified as following:

$$p - \text{value} = \frac{number\ of\ (D \geq d)}{total\ number\ of\ permutations} \tag{5.2}$$

For typical analysis, using the 5% of significance level, the null hypothesis is rejected when $p < 0.05$ and not rejected when $p > 0.05$. Since the p-value is greater than our assumed significance level of 0.05, we fail to reject the null hypothesis and conclude that there is no evidence in the data to suggest that the two CDFs are different.

### 5.4.2 Results

#### 5.4.2.1 The influence of the meta-model accuracy

Figure 5-6 to Figure 5-8 present the prior, target (VBS), and posterior distributions for six parameters. Those include the Bayesian calibration results using the MLR, GPE, and PM with the base range of prior input distribution. The dotted red lines are target distributions of virtual building stock, the gray dotted lines are prior distributions, and the solid orange lines are posterior distribution as results of Bayesian calibration. The accuracy of calibration can be evaluated graphically by comparing the orange solid line of each case. When the MLR was used in Bayesian calibration, the posterior distributions for parameters showed a large difference with the target distributions. As confirmed in Bayesian calibration for individual building (Chapter 4), the difference comes from the inaccuracy of the meta-models. As shown in Figure 5-7, the posterior distributions of calibration using the GPE are much closer to the target distribution, because the GPE is more accurate than the MLR. However, there is still a few differences between the target and the posterior distributions. Moreover, computational time for the Bayesian

calibration has increased significantly. Assuming that only one CPU process is used for the Bayesian calibration, the processing time using the MLR was about 180 seconds, while the calibration using the GPE took 1931 hours.

If we use a perfect meta-model (As mentioned above, this is the case where there is no error in the meta-model, and it can be regarded as a case where EnergyPlus model is used for Bayesian calibration without meta-model), no significant difference between the target and the posterior distribution was evident.

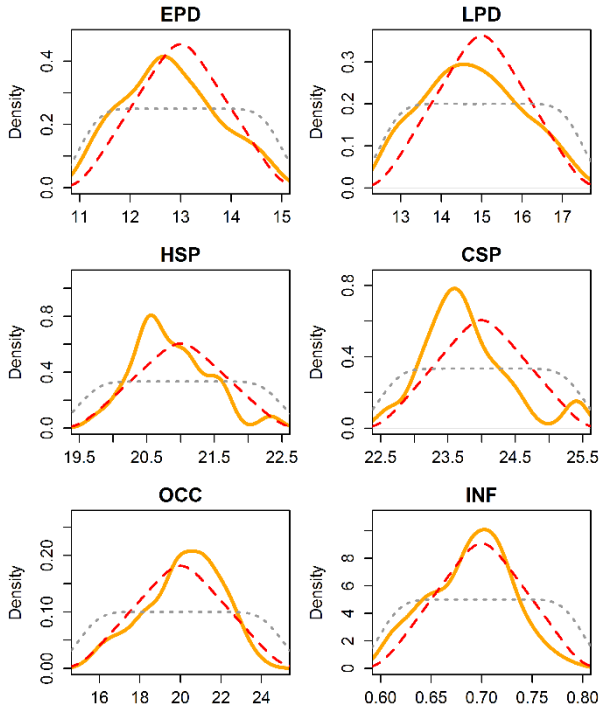


Figure 5-6 Distributions of parameters for case 1-1. Base MLR

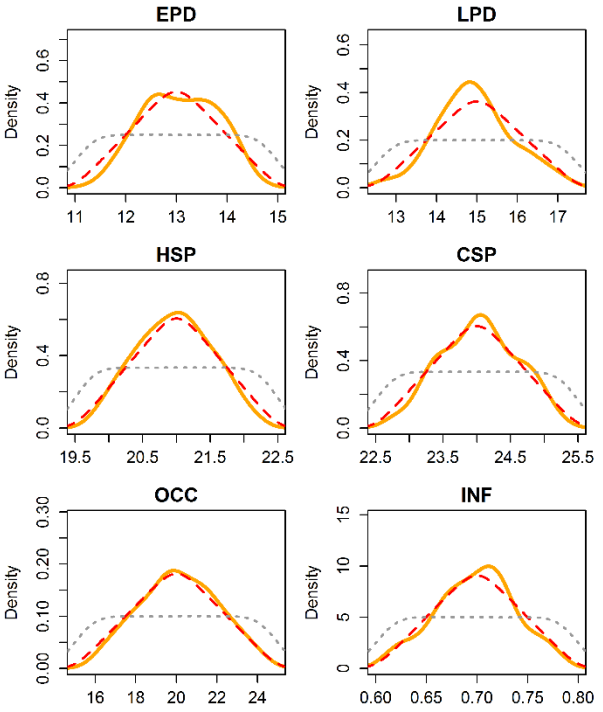


Figure 5-7 Distributions of parameters for case 2-1. Base GPE

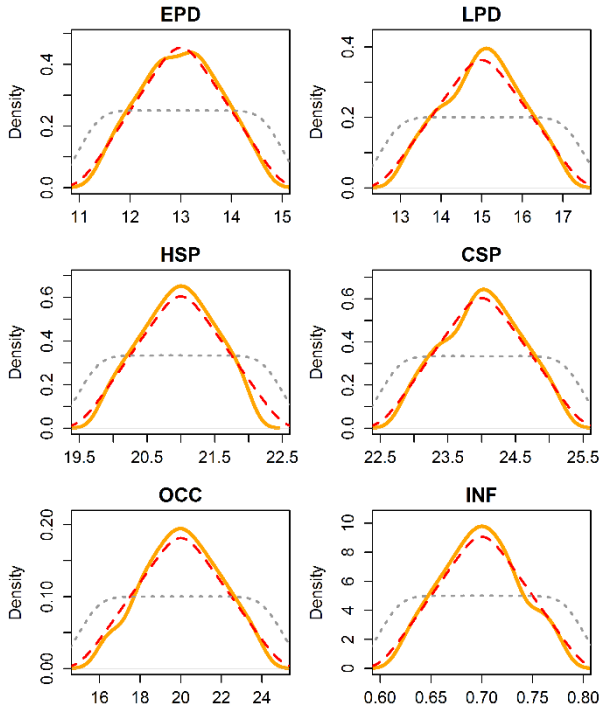


Figure 5-8 Distributions of parameters for case 3-1. Base PM

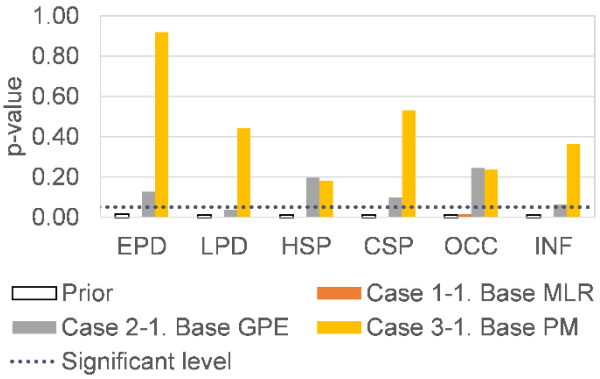


Figure 5-9 K-S test results for base cases

Table 5-7 K-S test results for base cases

| Cases | EPD | LPD | HSP | CSP | OCC | INF |
|---|---|---|---|---|---|---|
| Prior | 0.0162 | 0.0126 | 0.0126 | 0.0126 | 0.0126 | 0.0126 |
| Case 1-1. Base MLR | 0.0001 | 0.0005 | 0.0000 | 0.0000 | 0.0151 | 0.0015 |
| Case 2-1. Base GPE | 0.1273 | 0.0360 | 0.1964 | 0.0999 | 0.2444 | 0.0635 |
| Case 3-1. Base PM | 0.9185 | 0.4424 | 0.1805 | 0.5314 | 0.2361 | 0.3641 |

Figure 5-9 and Table 5-7 show the p-values as results of K-S test for quantitative comparison. In all the parameters, p-values of K-S test between prior and target distributions were 0.0126 which is lower than the significant level (p=0.05). Therefore, we can reject that two distributions come from the same distribution. In the results of calibration using MLR (case 1-1), p-values for all parameters were lower than significant level of 0.05. Therefore, we conclude that two distributions are significantly different in the case

of calibration using the MLR and base range. In the case 2-1, the p-values of all the parameters except LPD exceeded the significant level which means we cannot reject the hypothesis that two distributions come from the same distribution. This is because the accuracy of the GPE is higher than the MLR. In case 3-1 where there is no error in the meta-model, the p-values for all the parameters were over the significant level. It means that the target and posterior distributions are very similar.

#### 5.4.2.2 Influence of range of prior distribution

From Figure 5-10 to Figure 5-12 show the prior, target (VBS), and posterior distribution distributions for six parameters when the wide range is used for input parameters. Compared to the base case, it can be confirmed that the overall accuracy is lowered. In the results of case 1-2 (wide MLR), the posterior distributions (orange solid line) are significantly different to the target distributions (red dotted line). This result was due to the reduced accuracy of meta-model as the prior range increased. The same trend was found in case 2-2 (wide GPE). The posterior distributions of case 2-2 showed a different shape from the target distribution as compared to case 2-1 (base GPE). The broader the range of input parameters, the lower the accuracy of the meta-model. However, as in the base case, the calibration results using the GPE yielded better results than the calibration using the MLR. In case 3-2, the target and the posterior distributions are very similar, as in case 3-1. Since the perfect model has no error in predicting the building energy use, it was confirmed that the Bayesian calibration was correct even in a wide range case.

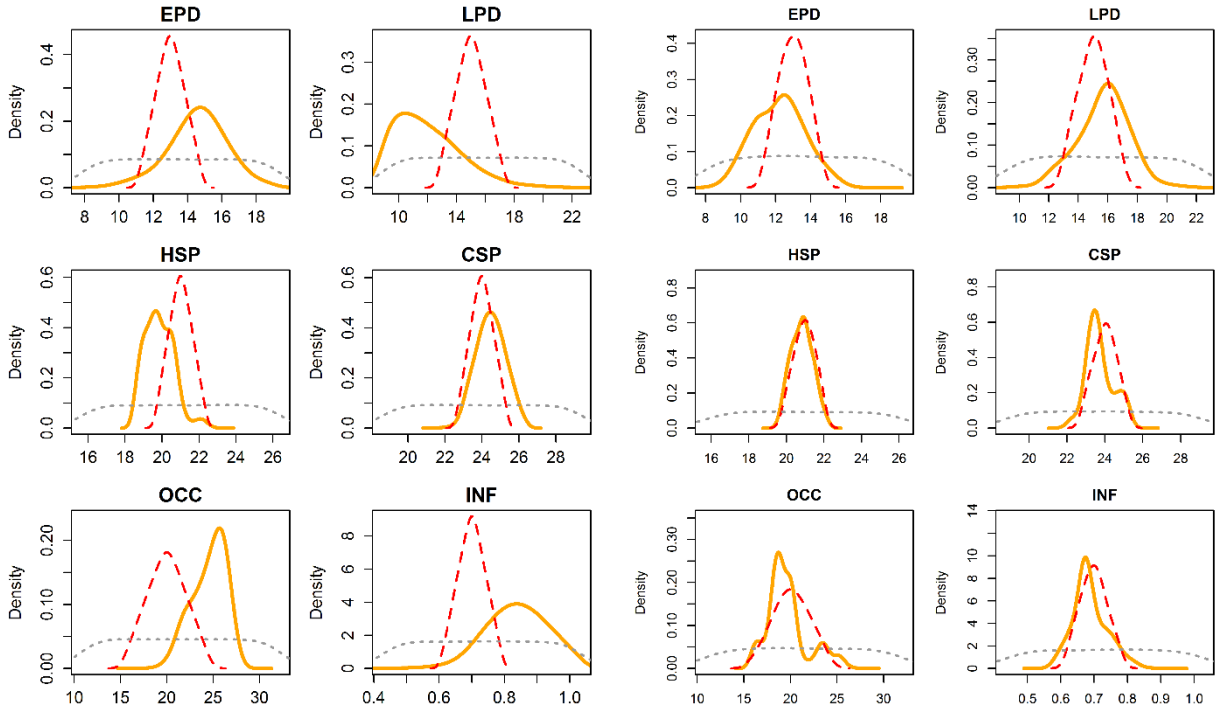


Figure 5-10 Distributions of parameters for case 1-2. Wide MLR




Figure 5-11 Distributions of parameters for case 2-2. Wide GPE

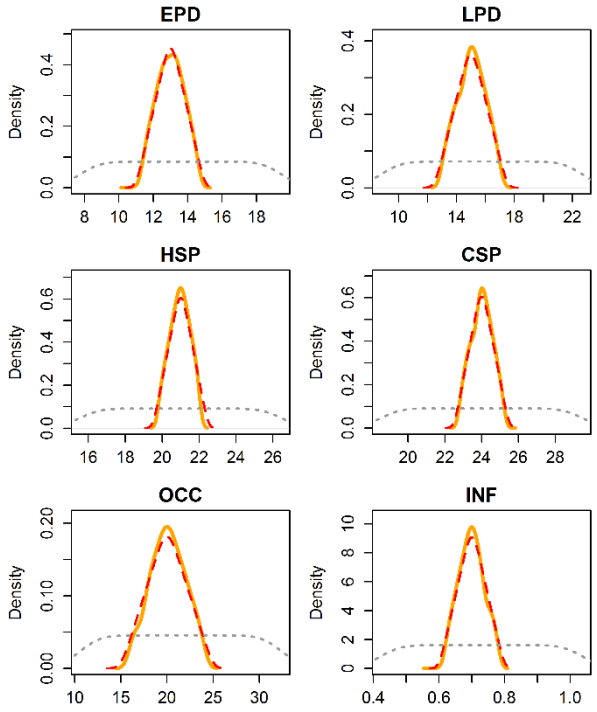


Figure 5-12 Distributions of parameters for case 3-2. Wide PM

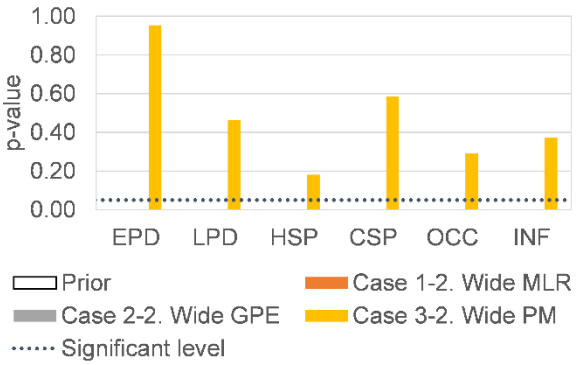


Figure 5-13 K-S test results for wide cases

Table 5-8 K-S test results for wide cases

| Cases | EPD | LPD | HSP | CSP | OCC | INF |
|---|---|---|---|---|---|---|
| **Prior** | 0.0000 | 0.0000 | 0.0000 | 0.0000 | 0.0000 | 0.0000 |
| **Case 1-2. Wide MLR** | 0.0000 | 0.0000 | 0.0000 | 0.0000 | 0.0000 | 0.0000 |
| **Case 2-2. Wide GPE** | 0.0000 | 0.0000 | 0.0000 | 0.0000 | 0.0000 | 0.0000 |
| **Case 3-2. Wide PM** | 0.9531 | 0.4639 | 0.1805 | 0.5859 | 0.2909 | 0.3714 |

Figure 5-13 and Table 5-8show the p-values of K-S test for wide range case. Only the p-values in case 3-2 (wide PM) exceeded the significant level. It can be concluded that only the posterior distributions of case 3-2 are similar to the target distributions, and the posterior distributions of the other cases are clearly different from the target distributions.

5.4.2.3 Annual and Monthly EUI distribution

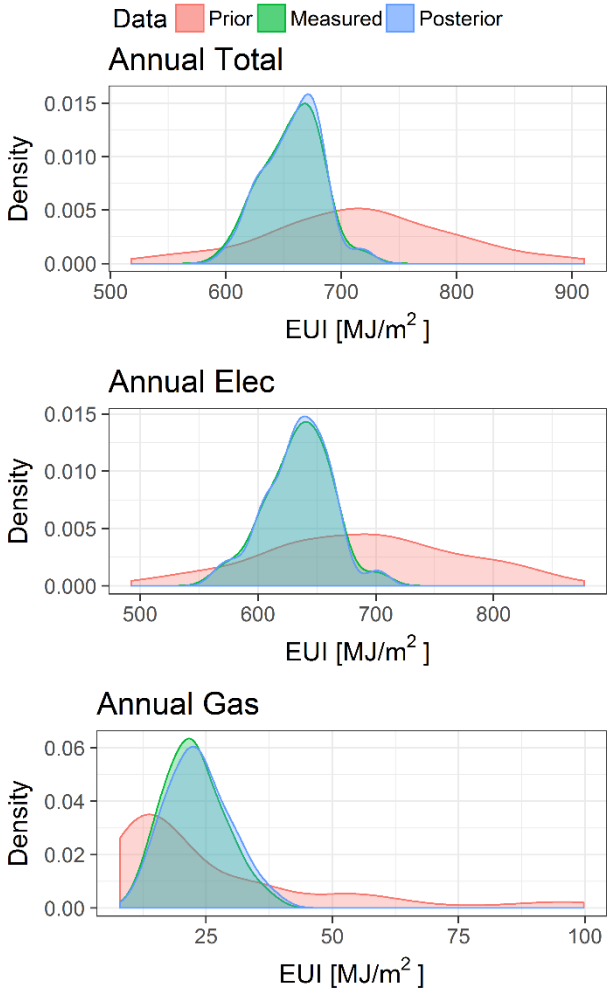


Figure 5-14 Annual EUI distributions for case 1-2. Wide MLR

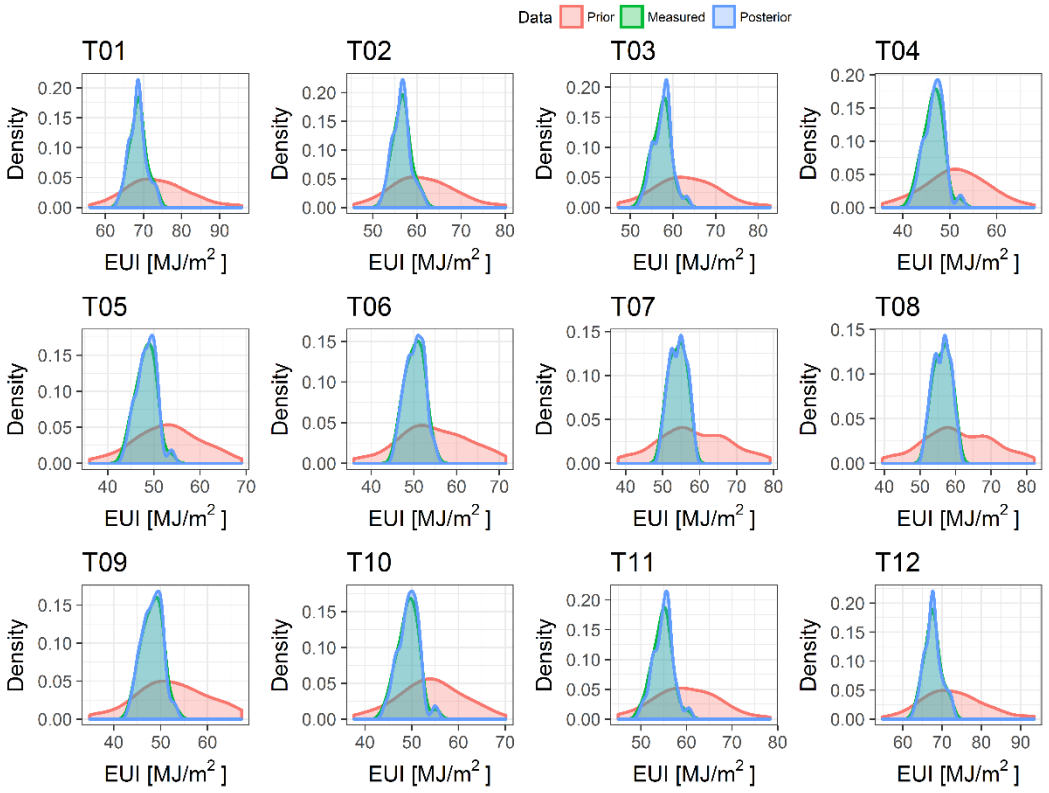


Figure 5-15 Monthly EUI distributions for case 1-2. Wide MLR

Figure 5-14 and Figure 5-15 show the Bayesian calibration results for annual and monthly EUI in the case 1-2 which is using the MLR and wide prior range. Figure 5-14 presents the EUI distributions for annual total, electricity, and gas. Figure 5-15 compares monthly total EUI distributions for prior, posterior, and measured data. It is confirmed that even if there are discrepancies in the parameter estimating (as shown in Figure 5-10), the estimation for annual usage per energy type was accurate. Moreover, the proposed stochastic-deterministic-coupled building stock energy model can calibrate monthly energy use as well as annual energy use.

### 5.4.3 Conclusion

The posterior distributions for the parameter were significantly different with the target distribution in both base and wide range cases when the Bayesian calibration utilized the MLR. When using the GPE as a meta-model, it gives more accurate posterior distribution than using the MLR in both base and wide

ranges. However, there is still a difference from the target distribution. Furthermore, Bayesian calibration using the GPE took considerable computational time than using the MLR.

In the case of using the PM, the posterior distribution for parameters showed good agreement with the target distributions since there is no error in the PM. Therefore, it can be concluded that the inaccuracy of meta-models is one of the factors that cause the discrepancy between the target distribution and the posterior distribution.

Using meta-models in the Bayesian process is indispensable to reduce the computational time. However, the errors of the meta-models cause the inaccurate posterior distribution to the target distribution. Moreover, there is another issue. The current virtual building stock has the same geometry design such as a number of floors, total floor area, window-wall-ratio, building orientation. If the building geometry of each building is different, it is hard to find the actual target distribution with the representative building model.

Although there are errors to estimate the target distribution of parameters, the MLR was selected as a meta-model in the Bayesian calibration process due to the computational time (calibration using GPE took 3.5 days using four computers). The results of this study raise a new question: Can we utilize the distorted posterior distributions of parameters to evaluate the ECMs (energy conservation measures)? In the following chapter, we will conduct ECM analysis to answer the question.

## 5.5 Applicability of the proposed method in ECM analysis

### 5.5.1 Methodology

As shown in Figure 5-6, when the Bayesian calibration uses the meta-model, the proposed method cannot estimate the target distributions for parameters due to the error of meta-models. The posterior distributions were distorted to match model results with the energy use data in the representative building energy model. Based on the discussion above, in this section, we determine whether the posterior distribution from the proposed methodology can be used to evaluate the energy conservation measures.

Figure 5-16 provides a conceptual diagram of a process in this section. The target parameter distribution (a in Figure 5-16) is the actual values for each parameter (red dotted line in Figure 5-6). The ECM applied target parameter distribution (b in Figure 5-16) indicates changed target distribution by applying the ECM. The posterior parameter distribution using MLR (c in Figure 5-16) is the estimated distribution for parameters from the Bayesian calibration using the MLR as a meta-model. Lastly, the ECM applied posterior parameter distribution using MLR (d in Figure 5-16) is the distribution of ECM applied to the estimated posterior distribution.

There are two objectives of the ECM analysis: the first is to confirm the applicability of the distorted posterior distribution in the ECM analysis by comparing the annual total EUI distributions from the ECM applied target parameter distribution (b in Figure 5-16) and ECM applied posterior parameter distribution using MLR. The second objective is to analyze the effect of applying ECM by comparing the annual total EUI distributions from the posterior parameter distribution using MLR (c in Figure 5-16) and the ECM applied posterior parameter distribution using MLR (d in Figure 5-16).

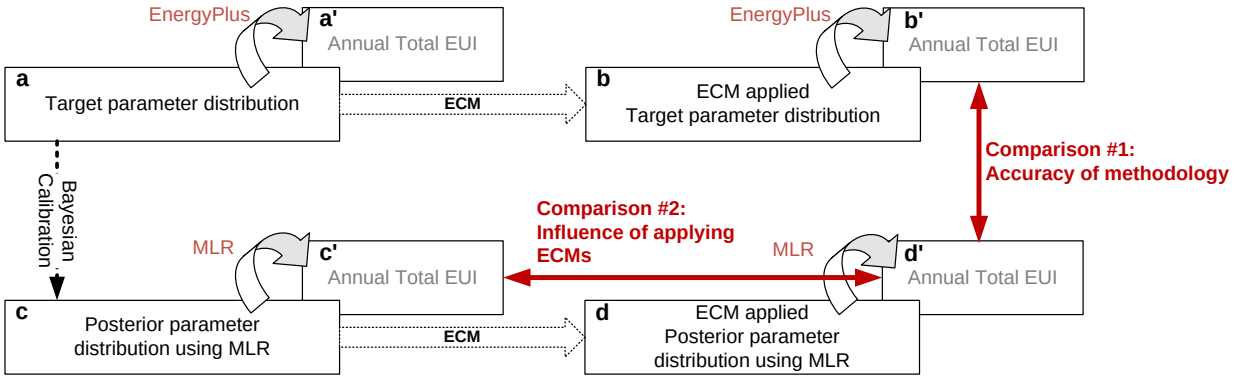


Figure 5-16 Conceptual diagram of ECM analysis process

The parameter distributions for ECM analysis are summarized in Table 5-9. The base case is the target distribution of VBS. The ECM applied the distribution of parameters is indicated in bold in Table 5-9. Case 1 is an energy conservation measure for the most dominant parameter, HSP (See Table 5-4). The distribution of heating set point is shifted to the lower side by 4% from the base case. Case 2 is the least dominant parameter, INF. The distribution of infiltration rate is shifted to the lower side by 10%. The third case is to check the combination of ECMs. In case 3, case 1 and case 2 were applied at the same time, and the distribution of EPD was further reduced by 10%. The changed input parameter distributions are fed into the EnergyPlus and the MLR. The outputs (annual total EUI) are obtained. The distributions of annual total EUI are compared graphically to analyze the effect of ECM. Moreover, the mean values of each distribution are compared for quantitative comparison.

Table 5-9 Summary of distribution for parameters

| | Base case | | | ECM Case 1. 4% decreased HSP | | | ECM Case 2. 10% decreased INF | | | ECM Case 3. 4% decreased HSP + 10% decreased INF + 10% decreased EPD | | |
|---|---|---|---|---|---|---|---|---|---|---|---|---|
| Triangular | Min | Mode | Max | Min | Mode | Max | Min | Mode | Max | Min | Mode | Max |
| EPD | 11 | 13 | 15 | 11 | 13 | 15 | 11 | 13 | 15 | **9.7** | **11.7** | **13.7** |
| LPD | 12.5 | 15 | 17.5 | 12.5 | 15 | 17.5 | 12.5 | 15 | 17.5 | 12.5 | 15 | 17.5 |
| HSP | 19.5 | 21 | 22.5 | **18.66** | **20.16** | **21.66** | 19.5 | 21 | 22.5 | **18.66** | **20.16** | **21.66** |
| CSP | 22.5 | 24 | 25.5 | 22.5 | 24 | 25.5 | 22.5 | 24 | 25.5 | 22.5 | 24 | 25.5 |
| OCC | 15 | 20 | 25 | 15 | 20 | 25 | 15 | 20 | 25 | 15 | 20 | 25 |
| INF | 0.6 | 0.7 | 0.8 | 0.6 | 0.7 | 0.8 | **0.53** | **0.63** | **0.73** | **0.53** | **0.63** | **0.73** |

### 5.5.2 Results of ECM analysis

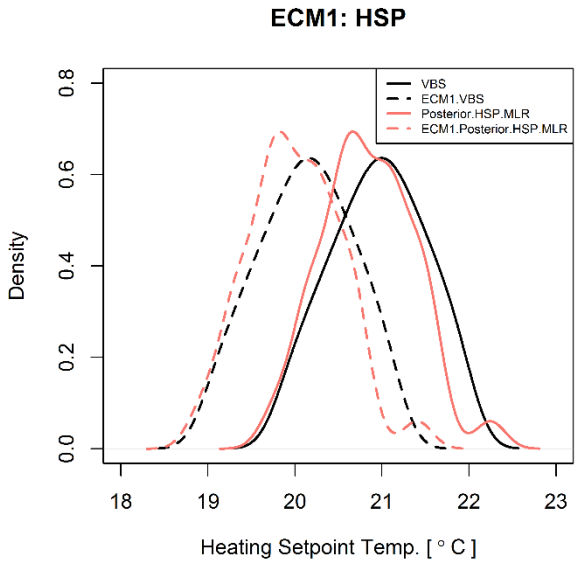


Figure 5-17 Distributions for HSP

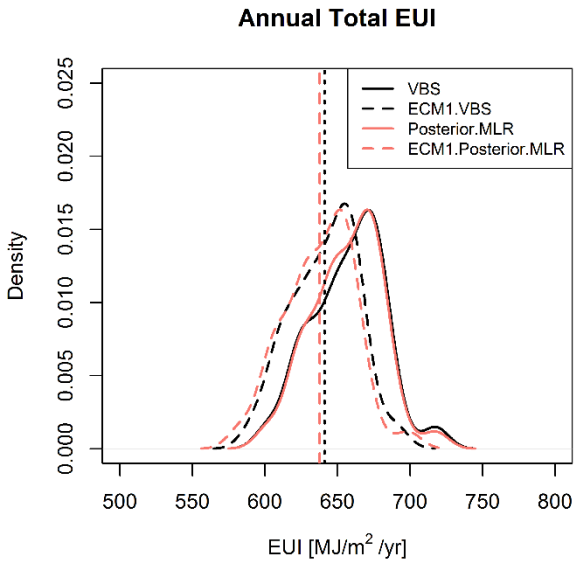


Figure 5-18 Distribution for annual total EUI (ECM case 1)

Figure 5-17 shows the variation of HSP distribution by applying the ECM case 1. The solid black line is HSP distribution for the base case (‘a’ in Figure 5-16). The dotted black line represents 4% decreased HSP distribution (‘b’ in Figure 5-16). The solid red distribution illustrates the posterior distribution as a result of Bayesian calibration using the MLR (‘c’ in Figure 5-16). The dotted red line indicates 4% decreased from the posterior distribution of Bayesian calibration (‘d’ in Figure 5-16).

Figure 5-18 compares the distributions of total EUI. The solid black line is total EUI distribution for the VBS, and this distribution is regarded as a measured energy data (‘a'’ in Figure 5-16). The solid red line shows total EUI distribution as a result of the Bayesian calibration using the MLR (‘c'’ in Figure 5-16). The dotted black line is total EUI distribution of the ECM 1 applied target (‘b'’ in Figure 5-16). Additional EnergyPlus simulations are necessary to obtain this distribution. The changed dataset by applying ECM 1 are put into EnergyPlus to calculate new annual total EUI distribution. The dotted red line is the ECM 1 applied annual EUI distribution calculated by the MLR (d' in Figure 5-16). The posterior distributions for parameters were modified to represent the ECM 1 and then put into the MLR. This process can be calculated faster than using EnergyPlus due to the simplicity of meta-model. The dotted black and red lines indicate the mean values of ECM applied total EUI distributions from the target distribution and calibrated distribution. As seen from Figure 5-18, the shapes of the posterior EUI distribution and the ECM applied EUI distribution are the same. This is because we utilized the multiple linear regression (MLR) models to predict the ECM case 1. Meanwhile, the shape of ECM applied target EUI distribution is different from the original target EUI distribution because EnergyPlus is a non-linear model. In case 1, ECM was applied to HSP, which is the most dominant factor. The EUI distribution of the ECM applied posterior was not significantly different from the ECM applied target EUI distribution. In the both distributions, the influence of applying the reduced HSP on the annual total EUI are verified.

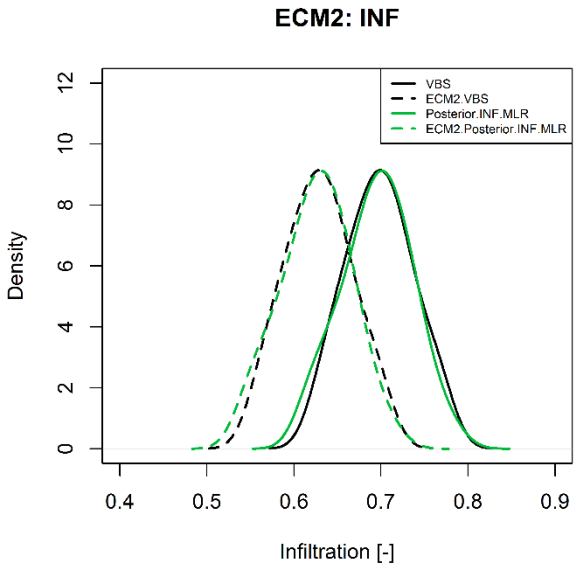


Figure 5-19 Distributions for INF

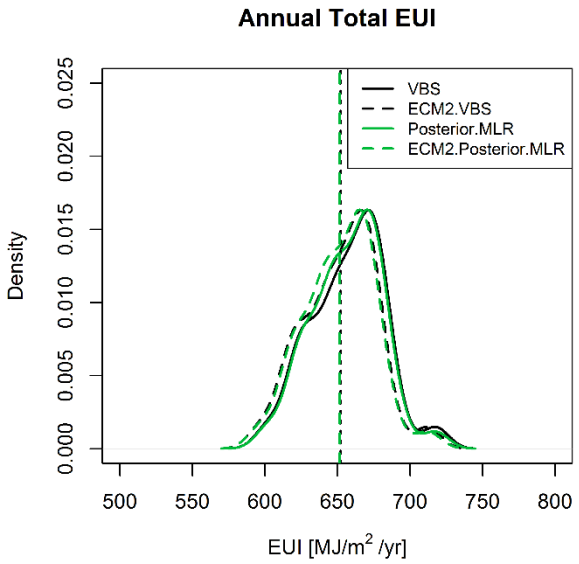


Figure 5-20 Distribution for annual total EUI (ECM case 2)

Figure 5-19 presents the distributions of infiltration rate, which is the least dominant factor. The black lines are the same as the above. The solid green lines indicate the posterior distribution as results of Bayesian calibration and the dotted green lines are ECM 2 applied distributions. In Figure 5-20, the ECM applied posterior EUI distribution has almost coincided with the ECM applied target distribution (comparison b' and d' in Figure 5-16). Slight difference is found between two vertical lines. For the least dominant parameter (INF), the posterior distribution obtained by the Bayesian calibration using the MLR can be utilized to analyze the ECM. To evaluate the effectiveness of the ECM, there is only a few changes made by reducing infiltration by 10% compared to ECM case 1. This may be explained by the fact that INF is a less important parameter.

The results of ECM case 3 are shown Figure 5-22. The case 3 is to check the case where ECMs are combined. ECM case 1 and ECM case 2 were applied together. Also, 10% reduced EPD was adopted. Figure 5-21 provides the distributions of EPD. The posterior distribution of EPD (solid blue line) shows a quite different shape compared to the target distribution (solid black line). The changed distributions for three parameters were put into the EnergyPlus and the MLR to calculate the annual total EUI. In Figure

5-22, when we compare between the ECM applied target EUI distribution and ECM applied posterior EUI distribution, although the difference is larger than other cases, they still have similar distributions and shapes. Even if the ECMs are combined, it is expected that the proposed method can simulate the actual effect of ECM similarly.

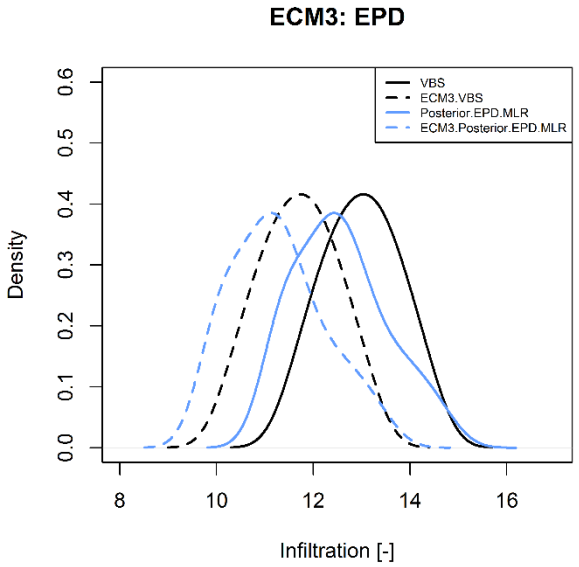


Figure 5-21 Distributions for EPD

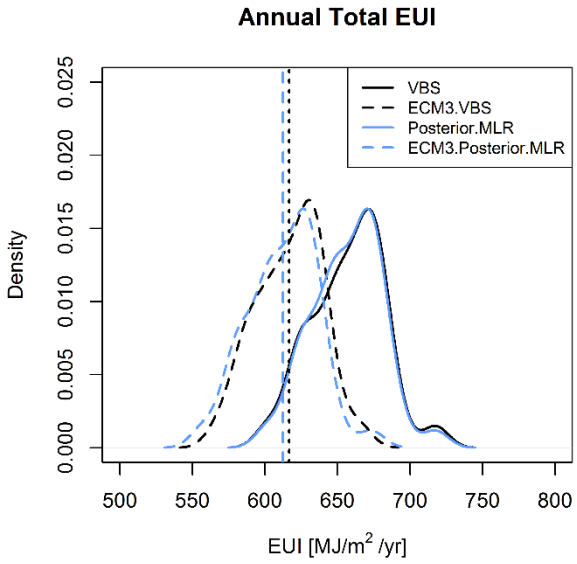


Figure 5-22 Distribution for annual total EUI (ECM case 3)

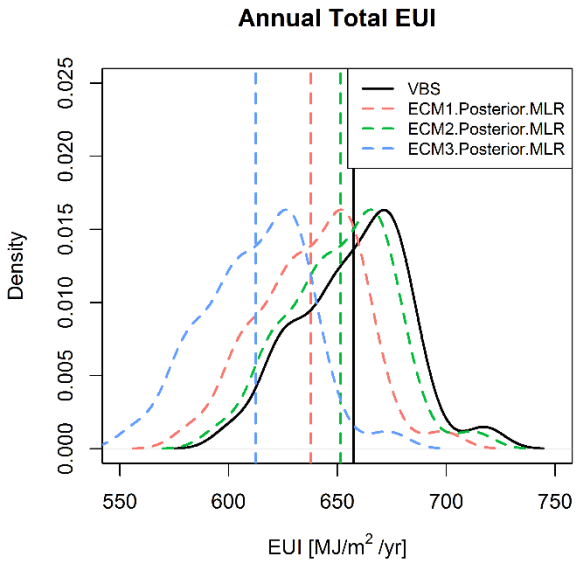


Figure 5-23 Comparison of annual total EUI

Table 5-10 Comparison of ECM cases

| Comparison | Description | Unit | ECM case 1 | ECM case 2 | ECM case 3 |
|---|---|---|---|---|---|
| Comparison 1. | Difference between ECM applied EUI distributions (b' vs. d') | MJ/m$^2$/yr | 3.37 | 0.81 | 4.36 |
| | Percentage error | % | 0.53 | 0.12 | 0.71 |
| Comparison 2. | Measured EUI reduction by ECM (mean) (a' vs. b') | MJ/m$^2$/yr | 16.26 | 5.20 | 40.61 |
| | Reduction percentage | % | 2.47 | 0.79 | 6.18 |
| | Estimated EUI reduction by ECM (mean) (c' vs d') | MJ/m$^2$/yr | 18.88 | 5.26 | 44.22 |
| | Reduction percentage | % | 2.88 | 0.80 | 6.73 |

The results of analysis are summarized and compared quantitatively in Table 5-10. The 'comparison 1' indicates that the difference of mean values from the ECM applied posterior EUI distribution and the ECM applied target EUI distribution (comparison b' and d' in Figure 5-16). The percentage errors of estimation using the distorted posteriors were 0.53%, 0.12%, and 0.71% for respective cases. These results suggest that even if the posterior distribution for parameters is distorted due to errors in the meta-model in the Bayesian calibration, we can analyze the ECMs using the distorted posterior distribution. The 'comparison 2' in Table 5-10 and Figure 5-23 show the effect of each ECMs in the virtual building stock. It comes as no surprise that the ECM for the dominant parameter is more effective than ECM for the less dominant parameter. Therefore, when considering ECMs or policies on building stocks, focusing on more dominant parameters will have a greater effect.

## 5.6 Aggregation of different building stock types

### 5.6.1 Development of Residence Virtual Building Stock

In this section, the aggregation of different building stock types is examined. A residential virtual building stock was developed to consider another building stock.

The process of development is similar to that of commercial virtual building stock stated in chapter 5.3. The residential virtual building stock is based on the Residential Prototype Building Models - single family house with crawlspace ("Residential Prototype Building Models," n.d.). The residential building has two stories, and the total floor area is 445 $m^2$. For the HVAC system, it has a natural gas furnace for heating and central electric air conditioning unit for cooling. The main features of the DOE prototype single family residential building are summarized in Table 5-11.

As with the commercial VBS, there are 30 buildings in the residential VBS, and we assumed that all buildings have the same geometry, HVAC system, and occupancy schedules. The variation was applied only for the 12 parameters: roof U-value, wall U-value, windows U-value, windows SHGC, equipment power density, lighting power density, heating set-point, cooling set-point, occupancy, infiltration, heating

efficiency, the coefficient of performance for cooling. Table 5-12 lists the range of 12 input parameters. All distribution of parameters is assumed as a triangular distribution. Using the quasi-random sampling (Sobol' sequence), 30 sample sets were generated and put into the EnergyPlus to calculate energy use. Therefore, 30 houses were developed in the residential virtual building stock. Figure 5-25 presents the average monthly EUI of total, electricity, and gas energy for the residential VBS. Figure 5-26 shows the distribution of annual energy use intensity as a result of EnergyPlus. The developed commercial and residential virtual building stocks will be further used in next chapter.

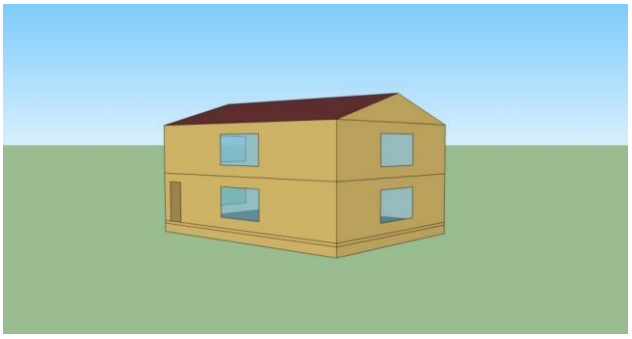

Figure 5-24 DOE prototype single family residential building

Table 5-11 main features of the DOE prototype single family residential building

| Component | Item | Parameters | Unit |
|---|---|---|---|
| Envelope | Floor area | 446.1399 | $m^2$ |
| | Conditioned Building Area | 220.7376 | $m^2$ |
| | Floor levels | 2 | - |
| | Window-wall ratio | 0.15 | - |
| | Wall U-value | See Table 5-12 | $W/m^2K$ |
| | Roof U-value | See Table 5-12 | $W/m^2K$ |
| | Window U-value | See Table 5-12 | $W/m^2K$ |
| | SHGC (solar heat gain coefficient) | See Table 5-12 | - |
| | Infiltration rate (Air changes per hours) | See Table 5-12 | $W/m^2$ |
| Internal heat gains | Lighting power density | See Table 5-12 | $W/m^2$ |

| | | | |
|---|---|---|---|
| | Equipment power density | See Table 5-12 | W/m$^2$ |
| | Hourly schedules for set-point for heating and cooling, occupants, lights, and equipment | Residential Prototype Building Models | - |
| HVAC | Heating Type | Natural gas furnace | - |
| | Cooling Type | Central electric air conditioning | - |

Table 5-12 Input parameters and distributions

| **Parameters [Unit]** | **Triangular distribution** | | |
|---|---|---|---|
| | **min** | **mode** | **max** |
| ROOF U-value [W/m2K] | 0.2 | 0.3 | 0.4 |
| WALL U-value [W/m2K] | 0.5 | 0.6 | 0.7 |
| Window U-value [W/m2K] | 2.5 | 3 | 3.5 |
| Window SHGC [-] | 0.37 | 0.38 | 0.39 |
| EPD [W/m2] | 5 | 7 | 9 |
| LPD [W/m2] | 3 | 4 | 5 |
| HSP [$^o$C] | 19.5 | 21 | 22.5 |
| CSP [$^o$C] | 22.5 | 24 | 25.5 |
| OCC [person] | 1 | 3 | 6 |
| INF [ACH] | 0.6 | 0.7 | 0.8 |
| HEATEFF [-] | 0.75 | 0.8 | 0.85 |
| COP [-] | 3.25 | 3.5 | 3.75 |

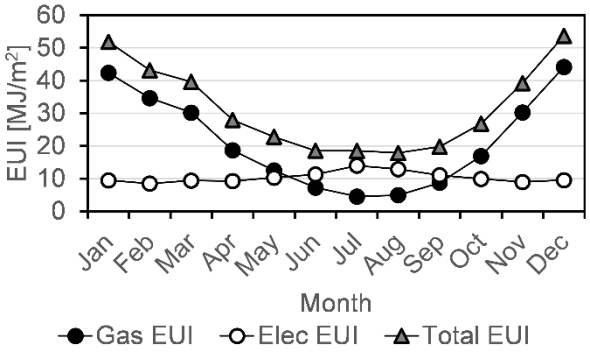


Figure 5-25 Average monthly EUI

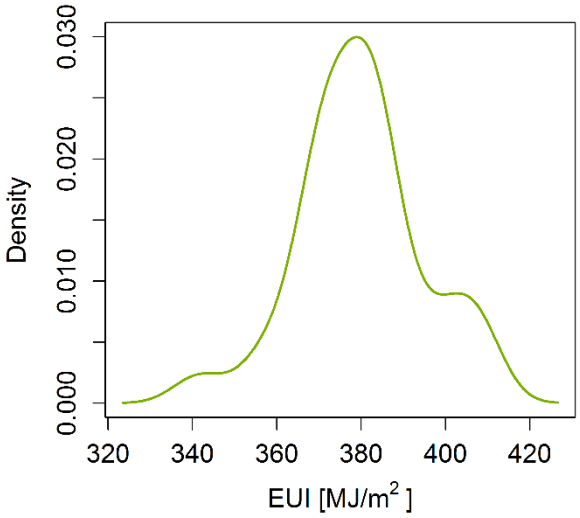


Figure 5-26 Distribution of annual total EUI

### 5.6.2 Sum of EUI distributions from different building stocks

This section examines how to aggregate different building stock. The first is how to sum two energy use distributions. If two distributions are independent normal distributions, then their sum is also normal distribution with its mean value being the sum of the two means, and its variance being the sum of the two variances as shown in equation (5.3) (Eisenberg & Sullivan, 2008). There is another study about the sums of parametric distributions (Petrov, 2012).

$$X \sim N(\mu_X, \sigma_X^2)$$

$$Y \sim N(\mu_Y, \sigma_Y^2) \tag{5.3}$$

$$\mathrm{Z} = \mathrm{X} + \mathrm{Y}$$

$$\text{Then, } \mathrm{Z} \sim \mathrm{N}(\mu_X + \mu_Y, \sigma_X^2 + \sigma_Y^2)$$

However, the posterior distribution, which is the result of Bayesian calibration, is mostly non-parametric distribution. In that case, it is not possible to use the equations for parametric distribution. To sum two non-parametric distributions, the most preferred method is finding all combinations of two distributions and then summing each combination.

In the R environment, if we have two distribution, A and B, a data frame of all combinations of A and B can be obtained using 'expand.grid' fuction, and function 'rowSums' will add them.

```
rowSums(expand.grid(A, B))
```

The second is how to aggregate EUI distributions from different building stocks. The EUI (energy use intensity) is the normalized value calculating energy consumption divided by total floor area. When we compute the overall EUI for the district which includes more than one building stock type, simply calculating the average of EUI distributions leads to error.

To aggregate the EUI distributions of different building stocks, the overall EUI distribution should be calculated by dividing the total energy usage by the total floor area as shown in equation (5.4). Figure 5-27 shows the comparison of two approaches. The dotted purple line is the average distribution of two VBS distributions which is the wrong approach. The dotted blue line indicates the floor area considered overall EUI distribution. The overall EUI distribution considering area is biased towards the commercial VBS EUI distribution. This is because that the total energy of commercial VBS is larger than that of residential VBS.

$$\text{Total EUI} = \frac{\sum_{i=1}^{n}(EUI_i \times Total\ Area_i)}{\sum_{i=1}^{n} Total\ Area_i} \tag{5.4}$$

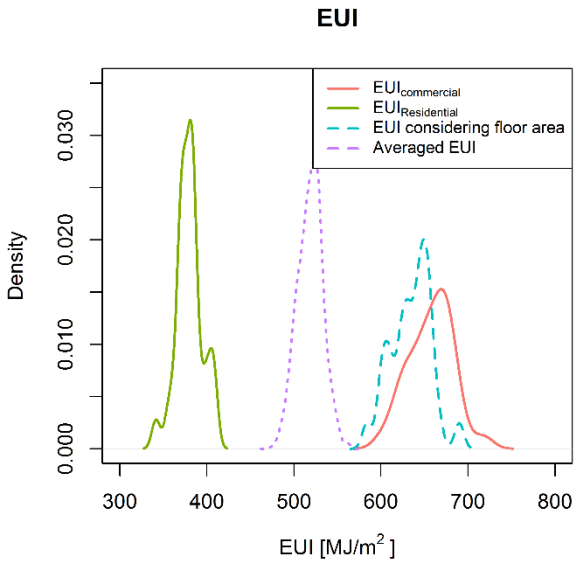


Figure 5-27 Aggregation of EUI distributions

### 5.6.3 Estimation of peak energy demand

Using the method above, energy demand patterns of different temporal scales can be obtained. In this section, the hourly energy demand pattern was analyzed for the VBS. The hourly energy use was calculated using the commercial and residential virtual building stock. Figure 5-28 and Figure 5-29 show hourly EUI distribution on July 21st which is cooling design day for commercial and residential VBS, respectively. Figure 5-30 presents the hourly aggregated EUI distribution for 60 buildings of overall VBS. In the proposed virtual building stocks, the energy use intensity of commercial building stock is dominant on the overall EUI. Using this analysis, the peak energy demand can be evaluated for the target district. Once the energy peak load and pattern were evaluated, it will help design the distributed generation such as district heating and cooling or co-generation. The hourly schedules and peak loads have a decisive impact on the energy use pattern. In this methodology, the hourly schedules are deterministic, while the peak loads are stochastic. More research is required to consider the probabilistic effect of hourly schedule for better analysis of hourly peaks and diversity.

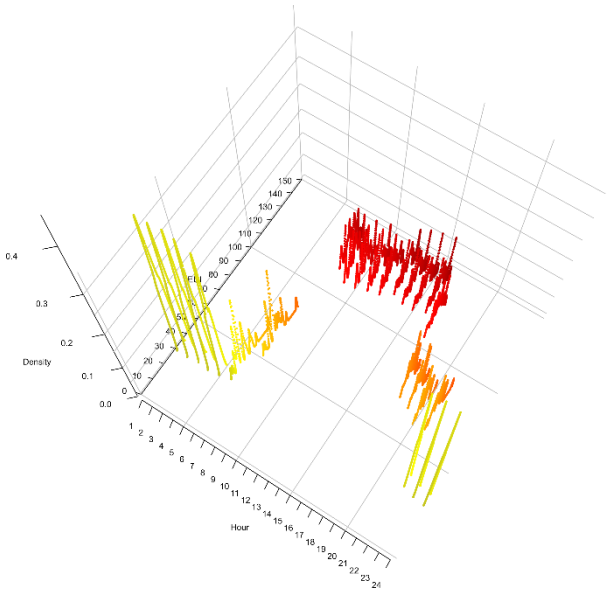


Figure 5-28 Hourly Total EUI for commercial VBS

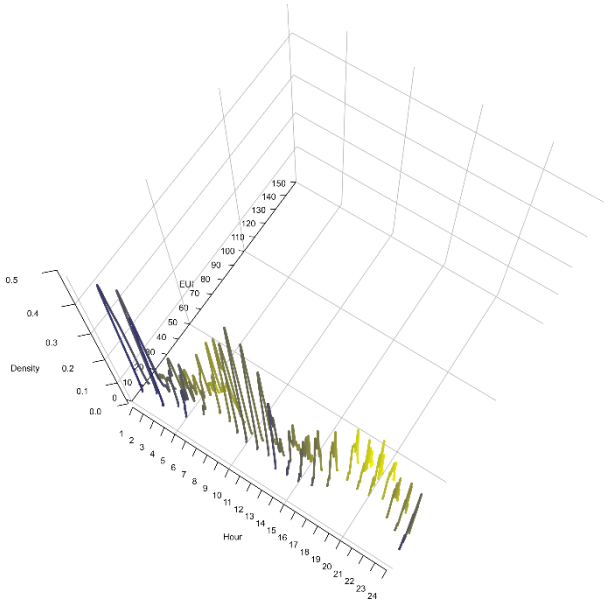


Figure 5-29 Hourly Total EUI for residential VBS

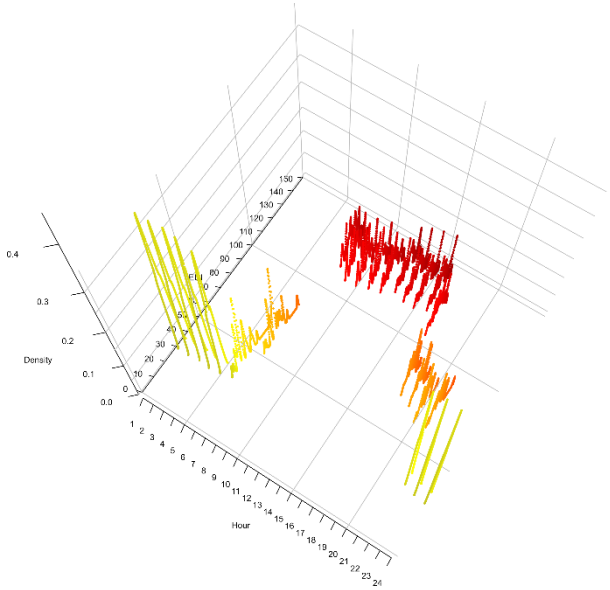


Figure 5-30 Hourly Total EUI for overall VBS

## 5.7 Conclusion

The purpose of this chapter was to examine the stochastic building energy model to expand for the building stock. The main research tasks and findings are as follows:

- The stochastic-deterministic-coupled building stock energy model was proposed to predict the building energy consumption in the large-scale. The difference between the stochastic individual building model and stochastic building stock model was examined by comparing both models.
- Commercial and residential virtual building stocks were developed for quantitative comparison of the proposed stochastic-deterministic-coupled building stock energy model.
- Six cases were analyzed to compare the effect of meta-models' accuracy and the range of prior distributions. The results indicate that the proposed method produces the distorted posterior distributions which differ from the target distribution for input parameters due to the error of meta-models. However, in all cases, the estimation of energy usage was accurate. The Bayesian calibration using the multiple linear regression models was recommended than using the Gaussian process emulator because of computational time.
- The energy conservation measure analysis was performed to determine whether the distorted posterior distribution for input parameters can be used to evaluate the applying the ECMs. As a result, in the case of the Bayesian calibration using the MLR and base range of prior distribution, the errors with the target values were within 0.71 %.
- To aggregate EUI distributions of different types of building stock, the total floor area of each type of building stock should be considered.
- Using the stochastic-deterministic-coupled building stock energy model and the proposed aggregation method, diverse temporal energy analysis is possible to identify the peak load of energy demand for the district. This can be a preliminary analysis for the design of the distributed generation such as district heating, co-generation.

# CHAPTER 6: INFLUENCE OF UNCERTAINTY IN BUILDING STOCK DATA ON ENERGY PREDICTION

## 6.1 Introduction

This chapter focuses on influences of building stock information. Sufficient quantity of stock information is necessary to have acceptable results for proposed stochastic-deterministic-coupled building stock energy model. The required building stock information is organized and classified based on the degree of detail. Combination cases of lacking information are considered to examine the influence of insufficient building stock information on the accuracy of the stochastic building stock energy model.

## 6.2 Definitions of required information for the proposed methodology

### 6.2.1 Detailed list of available data

The stochastic-deterministic-coupled building stock energy model was proposed and refined from Chapter 3 to 5. Through the previous analyses, the necessary information for the proposed methodology was determined. There are three data sets that are important for this study; energy use data, building features, and total floor area. The energy use data is required in the process of calibration. The building features include all geometric and non-geometric building factors. Buildings are grouped according to characteristics of the building. The information is used to develop the representative building. Total floor area for each building type is needed to aggregate from the representative building to building stock. The obtained EUI distribution from the proposed methodology is multiplied by the total floor area to calculate the energy consumption of the building stock.

The building features, energy usage data, and total floor area are rarely available for the building stock energy models. In this section, the essential information for the proposed stochastic-deterministic-coupled building stock energy model is categorized by level of detail of available data. Collecting detailed information will lead to accurate energy usage estimates for the target area. Even if there is no accurate information, the building stock model can be implemented through alternative information. The proposed

classification will provide guidelines for building stock information collection in the early stages of the building stock energy modeling.

#### 6.2.1.1 Energy use data

The energy use data refers a measured energy consumption in the building. In the proposed stochastic-deterministic-coupled building stock energy model, the unit of energy use is an energy use intensity (EUI). The detailed analysis was performed in Chapter 4.2 to examine the influence of energy use data in the Bayesian calibration. Bayesian calibration's accuracy increases with more informative energy use data. However, measured energy data often unavailable for modelers. The available energy use data sets are sorted by availability. Each available data is described how to use the available data in the building stock model. The building stock information is divided into two types when it is available and when it is not. The degree was further divided according to the details of the information.

- Available
    - Detailed energy use data
        - It is a case that can access energy usage by monthly and energy type in detail. In the informative energy use analysis (Chapter 4.2), 12 monthly electricity and gas energy use data are classified as level 1. If there are many monthly energy use data, more accurate calibration is possible. However, since the number of meta-models increases, the computational cost also increases.
    - Partial monthly energy data
        - For example, there is missing data in the monthly utility data, and there is only energy use data for several months. As shown in Chapter 4.2, even if only partial monthly energy data is available, accurate calibration can be achieved if the energy use data is informative.

- Annual energy data
    - This case indicates only the annual total energy usage data is accessible. In this case, the accuracy of predicting each monthly energy consumption is low while the prediction of annual energy use is accurate.

- Unavailable
    - Inaccessible energy data
        - Energy usage data for calibration is still needed when energy data is unknown. In this case, the energy use data can be extracted from literature data such as national surveys and report. Howard et al. (Howard et al., 2012) obtained annual electricity and natural gas, steam, or fuel oil consumption data from municipal office. Zhou et al. (Zhou et al., 2012) calibrated results from an eQUEST simulation using the residential energy consumption survey (RECS) and commercial building energy consumption Survey (CBECS). Zhao (Fei Zhao et al., 2016) obtained EUI distribution for 765 office buildings for the target area from the CBECS using a data filtering.

#### 6.2.1.2 Building features

In this study, the term "building features" refers to all properties that can characterize buildings in the stock. The building features includes building geometry factors such as floor numbers, floor area, shape typology, window-wall ratio and non-geometry factors such as building use type (e.g. residential, office, etc.), thermal properties (e.g. envelope construction, infiltration), HVAC systems, occupant factors (e.g. occupancy schedule, internal loads, set-points). Based on these building features, buildings in the target district are classified into several sub-groups. The archetypes to represent each group are developed according to building information.

- Available
    - Detailed information
        - This is a case that is accessible to all detailed information mentioned above. That information can be obtained floor plan drawing, HVAC specification, survey data, and energy audit data. For the representative building energy model, the average value and common features can be used for a building geometry. Moreover, all values of non-geometry factors in buildings can be regarded as a distribution.
- Unavailable
    - Inferring using building type and age
        - If the detailed building information is not accessible, that information can be inferred from the type and age of the building. Table 6-1 shows main parameters in the representative building model. ROOF, WALL, WIN, SHGC, INF, HEATEFF, and COP are related to the building age. EPD, LPD, HSP, CSP, OCC, GAS, and WATERUSE can be inferred from the building type. The distribution of parameters can be extracted from literature data such as building code and standards, survey, report, and expert's knowledge. Since there is no information about building geometries, the DOE reference building energy model can be used to build the representative building model.

Table 6-1 Inference of main parameters

| Building Age | Building Type |
|---|---|
| ROOF | EPD |
| WALL | LPD |

| | |
|---|---|
| WIN | HSP |
| SHGC | CSP |
| INF | OCC |
| HEATEFF | GAS |
| COP | WATERUSE |

- No building information
    - When building information is unavailable, the DOE reference buildings can be used for the representative building model. The literature data can be utilized for the non-geometry parameters. However, the range of parameters is wider than level 2, and uncertainty will increase.

#### 6.2.1.3 Total floor area

The proposed stochastic-deterministic-coupled building stock energy model obtains EUI distributions for each representative building type. It calculates the energy usage by multiplying the total floor area of the type. The estimation of the floor area is essential for accurate prediction of building energy consumption.

- Available
    - Total floor area for each building type
        - If the accurate total floor area for each building type is accessible, total energy use can be calculated by multiplying an EUI distribution and a total floor area. The floor area is available as part of GIS data or tax lot assessment database.

$$\text{Total EUI} = \frac{\sum_{i=1}^{n}(EUI_i \times Total\ Area_i)}{\sum_{i=1}^{n} Total\ Area_i} \quad (1)$$

- Unavailable
    - Inferring using map
        - In a case of the inaccessible area by building type, the building area can be estimated using the map. The ground floor area of the building is inferred through the building footprint on the map. The building footprint can be extracted from high-resolution satellite imagery (Alobeid et al., 2009; Shackelford et al., 2004) and LIDAR data (Haithcoat et al., 2001; K. Zhang et al., 2006).
        - Once the ground floor area is extracted, gross floor area can be computed by multiplying the ground floor area by the number of stories. The number of stories is obtained by dividing the building height by typical floor-to-floor height.
        - The building height can be estimated using building shadow on a high-resolution satellite imagery (Qi et al., 2016; Shao et al., 2011), SAR images (Brunner et al., 2010; Guillaso et al., 2005; Wegner et al., 2010), and LIDAR (Rottensteiner & Briese, 2002).
        - However, when calculating the total floor area of a building through a map image, it is not possible to consider buildings having different floor types for each floor. Also, estimation of the number of floors through the building height also has a large uncertainty because it cannot consider buildings having various floor-to-floor height.

## 6.3 Influence of insufficient building stock information

This section discusses the impact of insufficient building stock information on the accuracy of the building stock energy model. The information summarized in the previous chapter is difficult to compare directly with each other due to the differences in each data set. Therefore, specific cases are considered to compare the uncertainties in building stock information.

### 6.3.1 Methodology

The commercial and residential virtual building stock (VBS) developed in Chapter 5 were used for a case study. The procedure is the same with previous Chapters. The cases contain comparisons of three main building stock information: building energy use data, building features, and total floor area. The building features include building type and main parameters. The cases are set according to the degree of detail for each information. The suggested case study is summarized in Table 6-2.

The base case assumes that the most detailed information is available. 12 monthly electricity and gas energy use data is used for the energy use data. The building function type can be accessible for 60 buildings in the VBS for the building type. Two representative building energy models are developed to represent the commercial and residential building. The range of 12 main input parameters is available for the prior distribution for the main parameters. The prior distribution is assumed as a uniform distribution while actual distribution was a triangular distribution.

Case 1 is for the comparison of uncertainties in energy use data. Based on the base case, only the detail of the energy use data is changed. There are three sub-cases depending on the detail level. In Case 1-1, three monthly informative electricity and gas usage data are available: January, April, and July. According to the analysis performed in Chapter 4.2, these three monthly energy data are informative. Case 1-2 uses three monthly uninformative electricity and gas usage data: June, July, and August. Case 1-3 is a case that only annual total energy is available.

Case 2 is for the building features. Case 2-1 is based on the base case. The 20% expanded ranges for 12 target parameters are used as a prior distribution in both commercial and residential representative

buildings. This assumes that the parameter distribution for the VBS was not known and acquired from the literature.

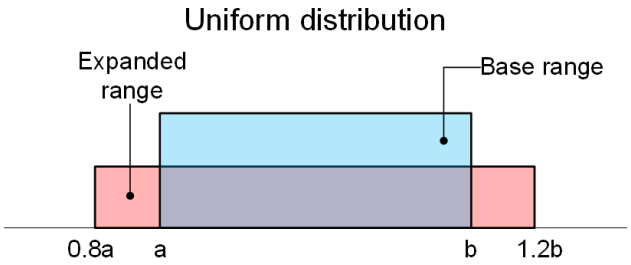


Figure 6-1 Concept of expanded range

In Case 2-2, type of buildings assumed unavailable. 60 buildings in the VBS are classified into one archetype, and the Bayesian calibration is carried out. The representative building energy model is developed based on the DOE office reference building model. In this case, the prior distribution for parameters should include both ranges for commercial and residential representative building (See Figure 6-2)

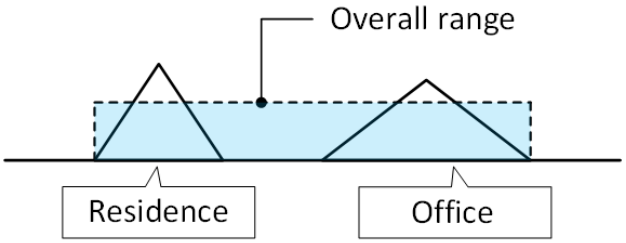


Figure 6-2 Concept of overall range

In case 3, inaccurate information for total floor area is examined. Case 3-1 assumes that the entire area is obtained through a map. To express the uncertainty of the total floor area, we assume a normal distribution with the mean of the actual total floor area. The standard deviation values are set so that 95% of the distribution is within the range plus and minus 10% of actual total floor area. (See Figure 6-3)

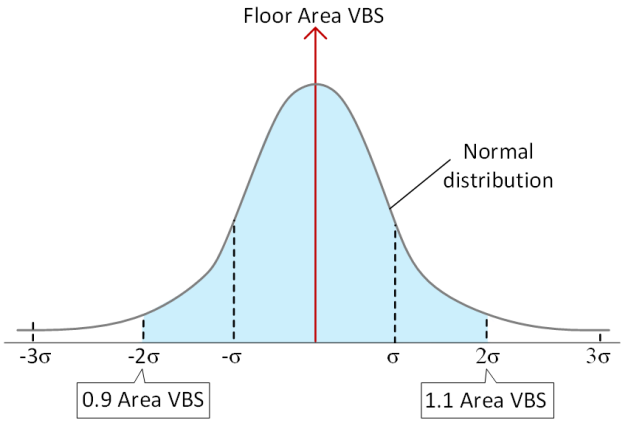


Figure 6-3 Concept of uncertain total floor area

Case 4 is combinations of diverse levels of each information. Case 4-1 is the worst case which is a combination of case 1-3, case 2-1, case 2-2, and case 3-1. The annual total energy use data is used for building energy data. 20% expanded prior distribution is used, and building type is not available. The proposed normal distribution is used for the total floor area. Case 4-2 is the case where the building type is known in case 4-1. Commercial and residential representative buildings are developed to represent each 30 buildings. Case 4-3 is the case where energy use data is changed in case 4-2. It uses three monthly electricity and gas energy use data.

The criteria for the comparison of results are CVRMSE for monthly and annual total energy use. The accuracy of Bayesian calibration results is evaluated by the CVRMSE to the observed data of the target virtual building stock.

Table 6-2 Summary of cases

| Objective | Case | Energy data | Building features | | Building total floor area |
|---|---|---|---|---|---|
| | | | Main parameters | Building type | |
| Base case | Base | 24 monthly (12 Elec & 12 Gas) | Available 12 input parameters | Available (C, R) | Available |
| Energy data | Case 1-1 | 6 monthly (3 Elec & 3 Gas) - informative | Available 12 input parameters | Available (C, R) | Available |

| | | | | | |
|---|---|---|---|---|---|
| | Case 1-2 | 6 monthly (3 Elec & 3 Gas) -uninformative | Available 12 input parameters | Available (C, R) | Available |
| | Case 1-3 | 1 annual (1 Total) | Available 12 input parameters | Available (C, R) | Available |
| Building features | Case 2-1 | 24 monthly (12 Elec & 12 Gas) | Obtained from codes (20% expanded 12 input parameters) | Available (C, R) | Available |
| | Case 2-2 | 24 monthly (12 Elec & 12 Gas) | Obtained from codes (combine range for office and residence parameters) | Unavailable (using only commercial archetype) | Available |
| Total floor area | Case 3-1 | 24 monthly (12 Elec & 12 Gas) | Available 12 input parameters | Available (C, R) | Obtained from map (applied 10% uncertainty) |
| Combinations | Case 4-1 | 1 annual (1 Total) | obtained from codes (20% expanded 12 input parameters) | Unavailable (using only commercial archetype) | Obtained from map (applied 10% uncertainty) |
| | Case 4-2 | 1 annual (1 Total) | obtained from codes (20% expanded 12 input parameters) | Available (C, R) | Obtained from map (applied 10% uncertainty) |
| | Case 4-3 | 6 monthly (3 Elec & 3 Gas) | obtained from codes (20% expanded 12 input parameters) | Available (C, R) | Obtained from map (applied 10% uncertainty) |

### 6.3.2 Results

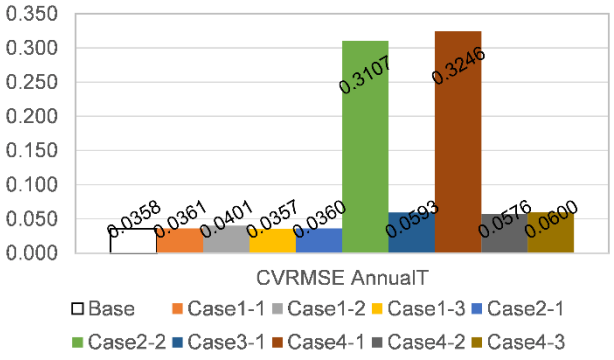


Figure 6-4 CVRMSE for annual total energy use

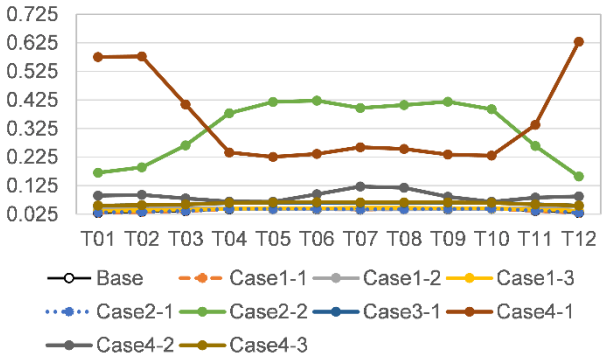


Figure 6-5 CVRMSE for monthly total energy use

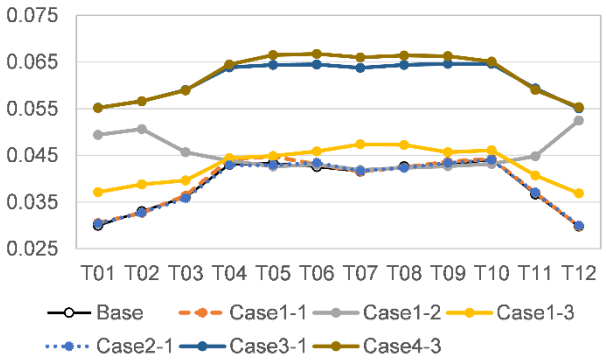


Figure 6-6 Enlarged view of lower part of Figure 6-5

The CVRMSE results are shown in Figure 6-4 and Figure 6-5 for annual and monthly total energy use. Figure 6-6 is an enlarged view of the lower part of Figure 6-5. The CVRMSE value for annual total energy use of base case is 0.0358 in Figure 6-4. Case 1-1, case 1-3 and case 2-1 have similar CVRMSE

values to the base case. In case 1-1, it can be seen that even using only the electricity and gas energy use data for three months (Jan., Apr., and Jul.), it is sufficiently informative for calibration. In case 1-3, the accuracy of annual total energy use is high because it is calibrated only with annual total energy data. However, the accuracy of monthly energy usage is lower than case 1-1.

The results in case 2-1 show that 20% expanded prior distribution does not have a significant effect on the prediction of annual energy. In a comparison of monthly energy accuracies for these cases (Figure 6-6), case 2-1 does not show much difference from the base case. Case1-1 has slightly larger CVRMSE values that the base case. Case 1-2 has larger CVRMSE values than the base case. Since case 1-2 was calibrated only with annual total energy usage data, errors on monthly energy use were large. The CVRMSE of annual total energy use for Case 1-2 is 0.0401 which is slightly larger than case 1-1, case 1-3, and case 2-1. This is because case 1-2 utilized uninformative monthly energy data for the calibration (electricity and gas energy data for Jun., Jul., and Aug.). In the monthly CVRMSE figure, the CVRMSE values for winter shows the larger difference with the base case while there are no significant differences with the base case in summer.

The case with the worst accuracy is case 4-1. The second worst case is case 2-2. In a given case study, if there is no information about building type, a large error occurs because two different energy use distributions are calibrated with one representative building. Comparing the two cases, it can be concluded that large portion of errors in case 4-1 is caused by the lack of information on the building type. In addition, comparing cases 4-1 and 4-2, it can be seen that having information on the type of building can improve the prediction accuracy of annual and monthly energy consumption.

Comparing the case 3-1 to the base case, the effect of the total floor area information on the accuracy of the building stock model is confirmed. Both accuracies for annual and monthly energy usage were significantly reduced compared to cases 1-1, case 1-2, case 1-3 and case 2-1. This result suggests that the total floor area information in a given case study is more influential than the information on the main parameters or energy use data.

### 6.3.3 Concluding Remarks

A case study was conducted assuming various conditions considering three main information: building energy use data, building features, and total floor area since it is difficult to compare information on building stock with a single standard. Each case was compared using the proposed stochastic-deterministic-coupled building stock energy model and the virtual building stock the accuracy of monthly and annual energy use forecasts. As results, for the energy use data, if the energy use data is informative, even with a small amount of data, we can obtain results similar to a calibration with detailed energy information. Calibrating with only the annual energy use data reduced the prediction accuracy of the monthly energy, but the prediction of the annual energy was accurate. For the information for building features, in a given case study, it is important to have information on the building type to improve the accuracy of the building stock model. The influence on the prior distribution of the parameters in the energy prediction was not significant. The information on the total floor area of each type of building also has a significant effect on accuracy. Based on the results of the case study, the type and floor area of the building have a great influence on the accuracy of the energy prediction of building stock.

## 6.4 Summary and Conclusion

This chapter presents a comprehensive study of building stock information. First, the building stock information required for the proposed stochastic-deterministic-coupled building stock energy model is summarized. The model requires three main information: building energy use data, building features, and total floor area. For each main information, methods were classified according to the degree of detail. A case study was conducted to compare the impacts of insufficient building stock information. As a result, it was confirmed that the influence of information on building type was greatest.

# CHAPTER 7: APPLICATION OF STOCHASTIC-DETERMINISTIC-COUPLED APPROACH FOR CAMPUS BUILDING ENERGY PREDICTION

## 7.1 Introduction

The stochastic-deterministic-coupled building stock energy model was proposed and refined to estimate the distribution of building energy consumption at the large scale in Chapter 3. Then, several analyses were performed to understand the Bayesian calibration for the individual building in chapter 4. In Chapter 5, Bayesian calibration was applied to the virtual building stock, and we examined the availability of the estimated posterior distribution to estimate the energy conservation measure. In Chapter 6, we classified the level of required information for the stochastic-deterministic-coupled building stock energy model and compared the uncertainties when we have insufficient information.

In this section, the proposed methodology was applied to actual building stock, and the prediction of the total building energy use was verified with the measured data. This chapter is organized as following. The method is applied to estimate building energy consumption at a campus scale. The advantage, disadvantage, and precautions using this methodology are discussed in each process in detail. The estimated energy consumption for each building type is aggregated and compared to the observed data. Then, the energy conservation measures are considered to reduce energy use in the campus.

## 7.2 Methodology

Figure 7-1 depicts the process of the proposed stochastic-deterministic-coupled building stock energy model. The first step involves developing representative building energy models of the campus. Diverse building information is collected to identify the representative buildings in the target area. The building information includes building function, age, floors number, total floor area, and HVAC system type. Furthermore, the measured energy consumption data is necessary to calibrate the model. Based on the collected information, the buildings are classified as several representative buildings according to criteria such as building function, age, and building height. The building energy models are developed using the

EnergyPlus. These representative building energy models should reflect the building geometry, construction, HVAC system type and schedule of the building stock. The second step is parameter screening based on the sensitivity analysis. The sensitivity value index (SVI) suggested in chapter 4 will be used to identify the dominant input parameters on the simulation output.

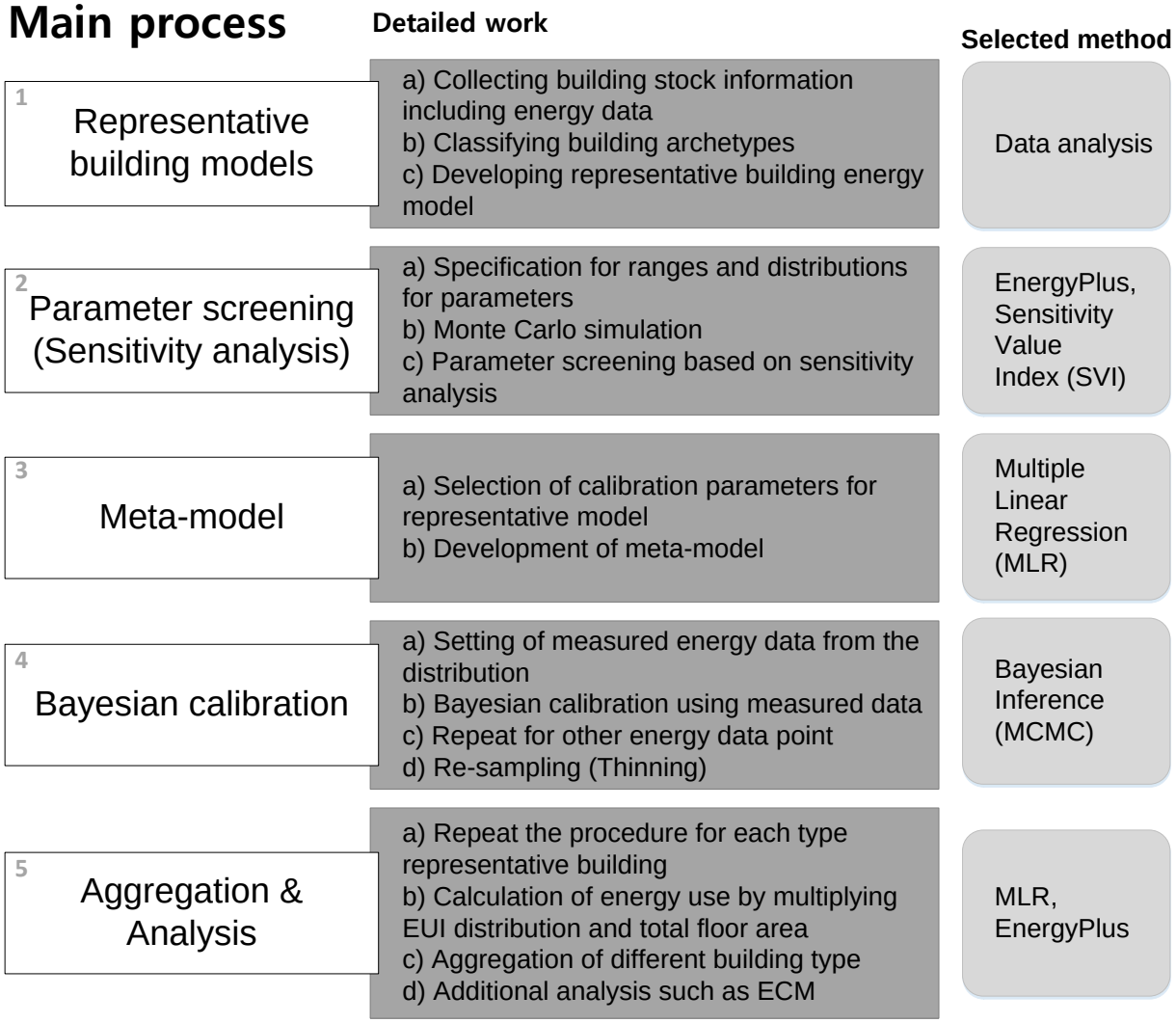


Figure 7-1 Main process of proposed method

The third step is developing the meta-model using the multiple linear regression model (MLR). The computational run time can be significantly reduced by using the statistical meta-model compared to the original EnergyPlus model. Then, Bayesian calibration is conducted using MLR based on Bayes' theorem to match the output of the model to the observed energy use data. Subsequently, the calibration allows for

the calculations of the posterior distributions for each unknown input parameters and energy use intensity (EUI) distribution for each building type in the campus. Finally, total building energy consumption for each building stock and the entire campus can be estimated by multiplying the obtained EUI distributions and the total floor area for representative building type. Various energy conservation measures can be evaluated using the calibrated posterior distributions of parameters.

## 7.3 Case study

### 7.3.1 Modeling of representative building

#### 7.3.1.1 Introduction of CU

The proposed stochastic-deterministic-coupled building stock energy modeling method was applied to the campus scale. We chose a campus of the University of Colorado Boulder (from now on CU) located in Boulder, Colorado. Boulder has a moderate dry climate. Under the ASHRAE Climate Zone (ASHRAE 169-2006 standard), Boulder is 5B zone. There are 163 buildings within the CU campus (Oct. 1, 2016), with a variety of building types, which can be thought of as a small city. Moreover, the buildings in the CU campus are monitored for energy usage and detailed building information such as building plans and specification can be obtained. Among all buildings in the campus, only 80 buildings that have detailed building information were selected for the case study. The building information includes building type, total floor area, the number of floors, built year, renovation year and energy consumption data. That information can be obtained from (Facilities Management, n.d.-a, n.d.-b, n.d.-c; University of Colorado Boulder, n.d.).

#### 7.3.1.2 Data analysis

The collected building information data was analyzed to classify into several representative building types. Current and historical energy usage data were obtained from the utility and energy services department of CU who is responsible for the design, operation, maintenance, and repair of the campus's energy generation and distribution infrastructure for steam, chilled water, and electricity (Facilities Management, n.d.-d). Specifically, the EnergyCAP provides the energy consumption of electricity, steam,

natural gas, and chilled water (Facilities Management, n.d.-b). Each building uses different energy source. For the convenience of analysis, the electricity use and the chilled water use were combined and considered as electricity.

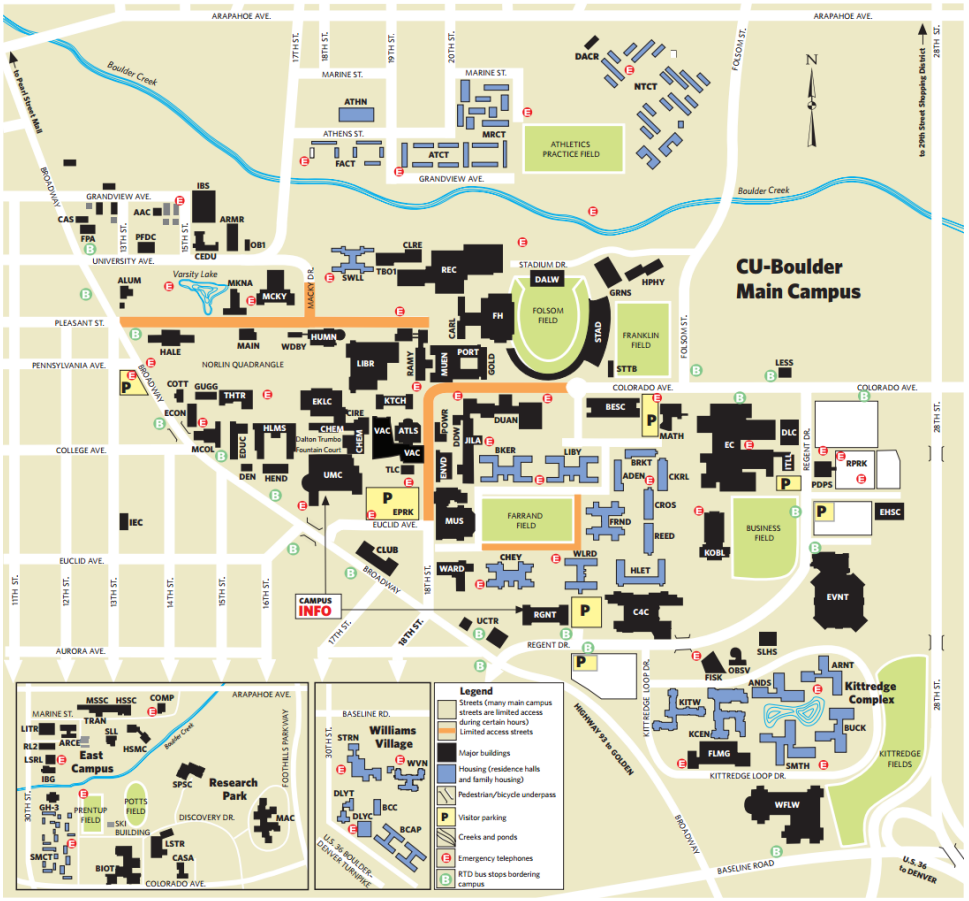


Figure 7-2 Campus map of the University of Colorado Boulder

The steam use and natural gas use were combined and considered as natural gas. The EUI normalizes the energy consumption by the total floor area of the building. The built year indicates the year a building construction was completed. If there is a significant renovation such as the replacement of HVAC systems, additional insulation, and replacement of window in the building, the latest renovation year was regarded as the built year. (See Appendix B)

Figure 7-3 is a scatter plot that shows the energy use intensity (EUI) of 80 buildings as a function of the built year. The buildings were classified as three building ages: Pre-1980, Post-1980, and New buildings after 2004. The high EUI buildings are concentrated in the post-1980 age. The old buildings have

relatively small EUI than the newer ones. On a closer inspection between average EUI and built age on CU (See Figure 7-4), there were no strong correlations between the EUI and the building age. Instead, the ranges of EUI were significantly different regarding the building functions as shown in Figure 7-5. The EUI of laboratories was higher than that of others because there is much equipment in the laboratories.

According to the analysis of the energy use and building features at the CU campus, it was concluded that the EUI was affected by building type rather than the building age Therefore, 80 CU buildings were classified into four types of representative buildings based on the building function and the energy use intensity as shown in Table 7-1.

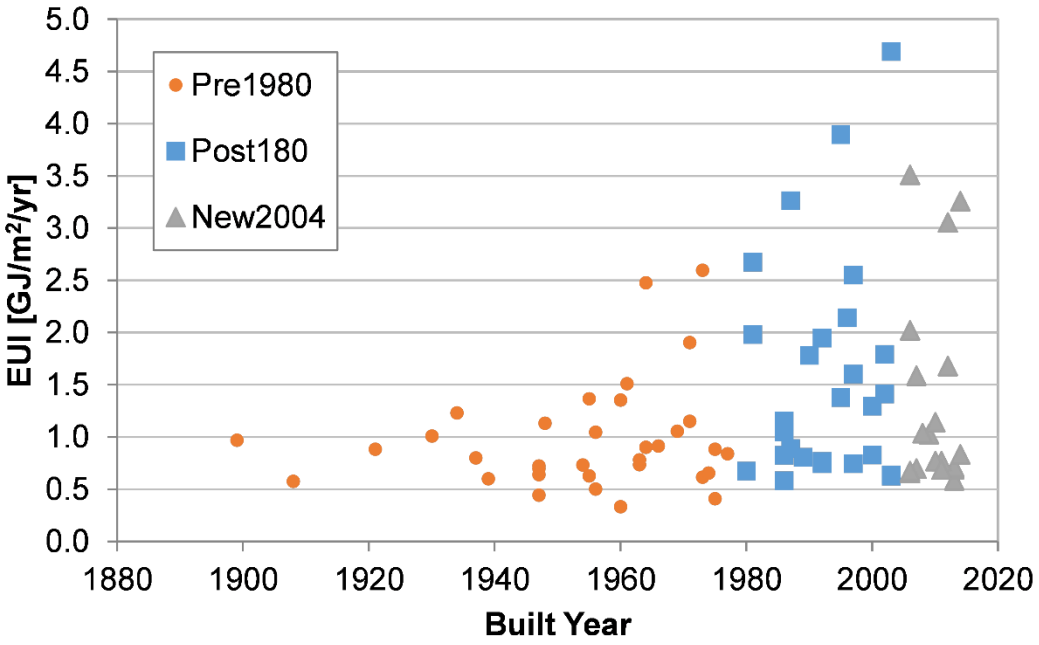


Figure 7-3 EUI as a function of the built year

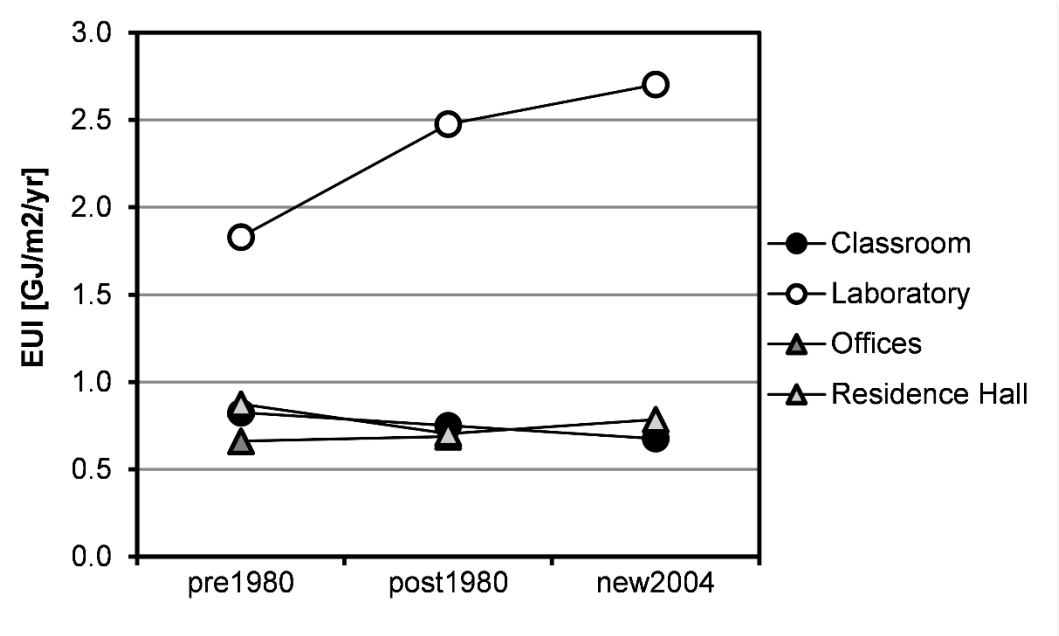


Figure 7-4 EUI as a function of building type and age

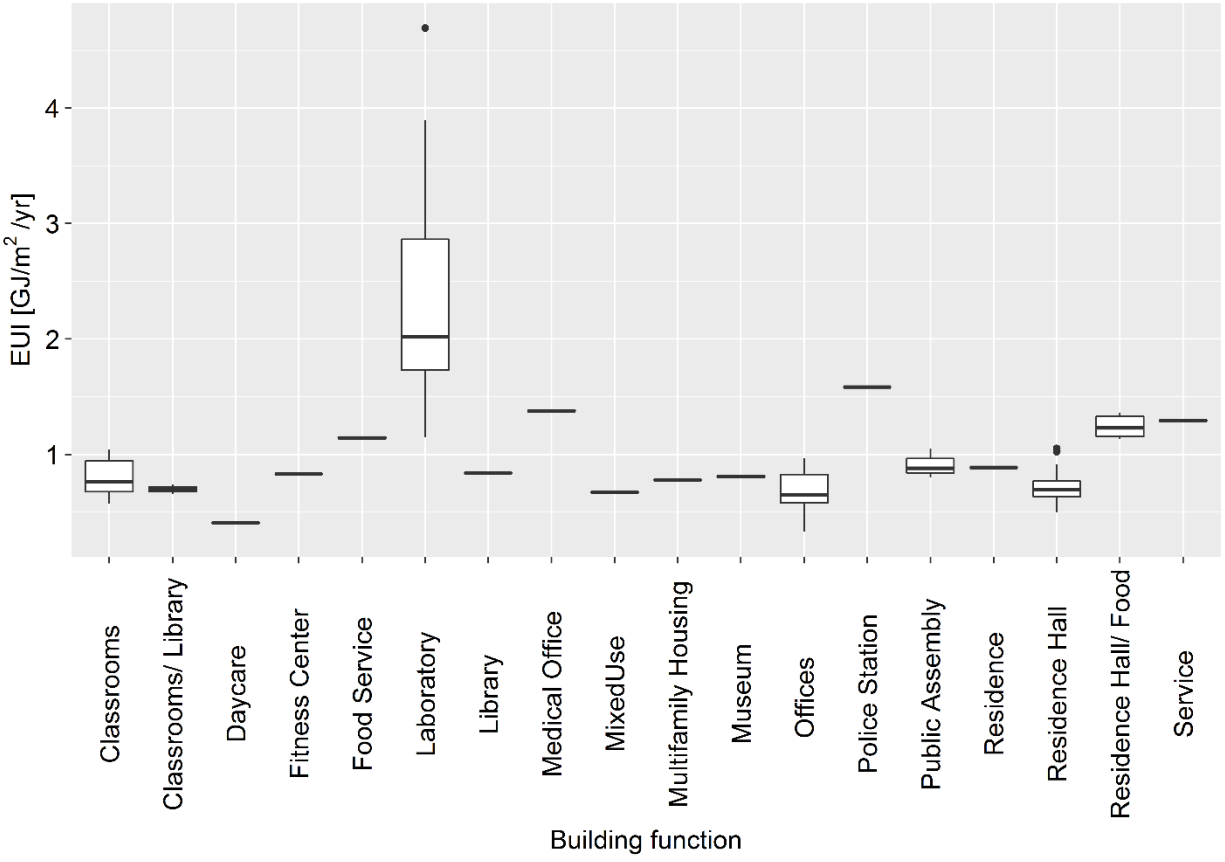


Figure 7-5 EUI as a function of building type

Table 7-1 Classification of representative buildings

| CU Primary Use | # of building | Classified Function | # of building | Average Floors | Average Total area [$m^2$] |
|---|---|---|---|---|---|
| Classroom | 7 | Education | 22 | 3 (plus basement) | 7491.43 |
| Classrooms/ Library | 3 | | | | |
| Daycare | 1 | | | | |
| Library | 1 | | | | |
| Offices | 9 | | | | |
| Public Assembly | 1 | | | | |
| Laboratory | 23 | Laboratory | 23 | 4 (plus basement) | 9,364 |
| Multifamily Housing | 1 | Residence | 24 | 4 | 10,000 |
| Residence | 1 | | | | |
| Residence Hall | 19 | | | | |
| Residence Hall/ Food | 3 | | | | |
| Service | 1 | Service | 11 | 3 (plus basement) | 9,583 |
| Fitness Center | 1 | | | | |
| Food Service | 2 | | | | |
| Medical Office | 1 | | | | |
| Mixed Use | 1 | | | | |
| Museum | 2 | | | | |
| Police Station | 1 | | | | |
| Public Assembly | 2 | | | | |
| Total | 80 | | 80 | | |

7.3.1.3 Modeling of Representative buildings

According to the data analysis of building information in CU, we developed four representative buildings: education type, laboratory type, residence type, and service type. Figure 7-6 exhibits the isometric views of EnergyPlus models for each type of representative building.

Each representative building energy model was created based on the DOE commercial reference buildings (Deru et al., 2011). The building geometries were conditioned by average number of floors and average total floor area of building type. The TMY3 weather file of Boulder, CO was used in EnergyPlus simulation. Table 7-2 summarized the main features of each representative building.

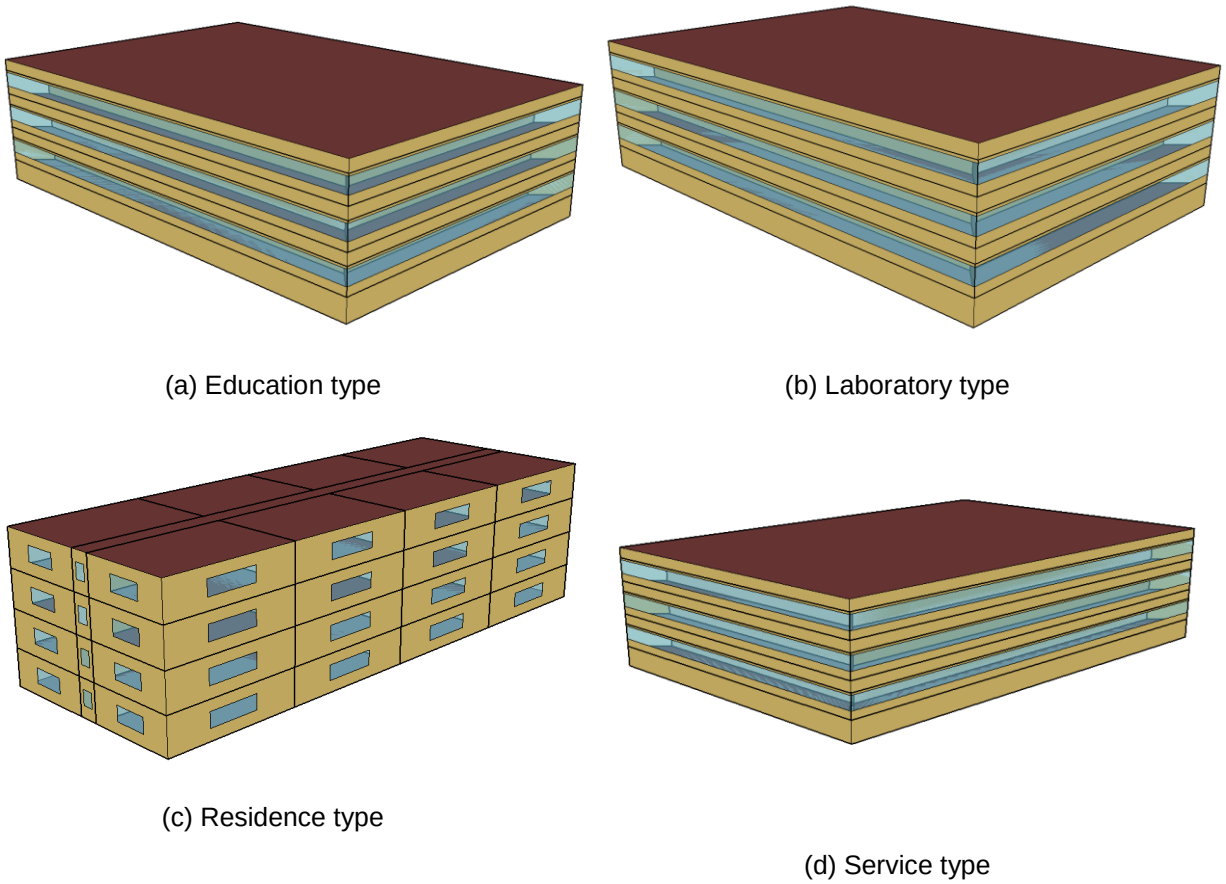

(a) Education type

(b) Laboratory type

(c) Residence type

(d) Service type

Figure 7-6 Representative building models for CU campus

Table 7-2 Main features of representative buildings

| Component | Item | Representative buildings | | | |
|---|---|---|---|---|---|
| | | Education | Laboratory | Residence | Service |
| **Base building model** | | Reference Building Large Office New 90.1-2004 | Reference Building Large Office New 90.1-2004 | Midrise Apartment Reference Building new construction 90.1-2004 | Reference Building Large Office New 90.1-2004 |
| **Envelope** | Floor area | 7491.43 | 9364.29 | 3134.59 | 9583.33 |
| | Number of Floors | 3 (plus basement) | 4 (plus basement) | 4 | 3 (plus basement) |
| | Window-wall ratio | 0.38 | 0.38 | 0.15 | 0.38 |
| | Thermal Zoning | core zone with four perimeter zones on each floor | core zone with four perimeter zones on each floor | 8 apartments with central corridor on each floor, office on the first floor | core zone with four perimeter zones on each floor |
| | Wall construction type | Mass wall | Mass wall | Steel frame | Mass wall |
| | Wall U-value | See Table | See Table | See Table | See Table |
| | Roof construction type | IEAD | IEAD | IEAD | IEAD |
| | Roof U-value | See Table | See Table | See Table | See Table |
| | Window U-value | See Table | See Table | See Table | See Table |
| | SHGC (solar heat gain coefficient) | See Table | See Table | See Table | See Table |
| | Infiltration rate (Air | See Table | See Table | See Table | See Table |

| | | | | | |
|---|---|---|---|---|---|
| | changes per hours) | | | | |
| **Internal heat gains** | Lighting power density | See Table | See Table | See Table | See Table |
| | Equipment power density | See Table | See Table | See Table | See Table |
| | Hourly schedules for set-point for heating and cooling, occupants, lights, and equipment | DOE Reference building | DOE Reference building | DOE Reference building | DOE Reference building |
| **HVAC** | System Type | MZ-VAV | MZ-VAV | - | MZ-VAV |
| | Heating Type | Gas boiler | Gas boiler | Gas furnace | Gas boiler |
| | Cooling Type | 2 water cooled chillers | 2 water cooled chillers | Split system DX | 2 water cooled chillers |
| | SWH Type | gas water heater | gas water heater | gas water heater | gas water heater |

### 7.3.2 Parameter screening

We selected 14 parameters that have significant impacts on the building energy user based on the existing literature (Booth et al., 2012; Tian & Choudhary, 2012; Fei Zhao, 2012). Table 7-3 lists the values of input parameters and the ranges of these parameters. The ranges of the parameters could be obtained from a survey report, expert's knowledge, building codes, and standards to define the possible values for the unknown parameters (ASHRAE, 2004; Bonnema et al., 2013; Deru et al., 2011; Eisenhower, 2011; Gowri et al., 2007; Griffith et al., 2008; Shem Heiple & Sailor, 2008; Y. Heo, 2011; Huang & Franconi, 1999; Mathew et al., 2004; Pacific Gas and Electric Company, 2011; Pless et al., 2007; Schnackenberg et al., 2009; Thornton et al., 2011; Tian & Choudhary, 2012; Yu & Chan, 2004; J. Zhang et al., 2010; F Zhao et al., 2011). The prior distribution for each parameter was assumed a uniform distribution. 14 parameters includes roof U-value [W/m$^2$K], wall U-value [W/m$^2$K], window U-value [W/m$^2$K], window solar heat gain coefficient (SHGC) [-], equipment power density [W/m$^2$], lighting power density [W/m$^2$], heating set-point [$^o$C], cooling set-point [$^o$C], occupancy [m$^2$/person], infiltration [ACH], heating efficiency [-], cooling COP [-], gas equipment [W/m$^2$], and water use per floor [m$^3$/s].

Table 7-3 Input parameters and prior range

| Parameter | Short name | Unit | EDU | | LAB | | Residence | | Service | |
|---|---|---|---|---|---|---|---|---|---|---|
| | | | min | max | min | max | min | max | min | max |
| **Roof U-value** | ROOF | W/m$^2$K | 0.2 | 1.5 | 0.2 | 1.5 | 0.2 | 1.9 | 0.2 | 1.5 |
| **Wall U-value** | WALL | W/m$^2$K | 0.2 | 2 | 0.2 | 2 | 0.2 | 1.9 | 0.2 | 2 |
| **Windows U-value** | WIN | W/m$^2$K | 1.5 | 6 | 1.5 | 6 | 1.5 | 6 | 1.5 | 6 |
| **Solar Heat Gain Coefficient** | SHGC | - | 0.2 | 0.6 | 0.2 | 0.6 | 0.2 | 0.6 | 0.2 | 0.6 |
| **Equipment power density** | EPD | W/m$^2$ | 1 | 35 | 10 | 215 | 2.5 | 15 | 1 | 40 |
| **Lighting power density** | LPD | W/m$^2$ | 1 | 25 | 10 | 35 | 2.5 | 15 | 1 | 30 |

| | | | | | | | | | | |
|---|---|---|---|---|---|---|---|---|---|---|
| **Heating set-point** | HSP | $^{o}$C | 17 | 24 | 17 | 24 | 17 | 24 | 17 | 24 |
| **Cooling set-point** | CSP | $^{o}$C | 21 | 28 | 21 | 28 | 21 | 28 | 21 | 28 |
| **Occupancy** | OCC | $m^2$/person | 3.14 | 46.66 | 9 | 30 | 20 | 90 | 1 | 56.7 |
| **Infiltration** | INF | ACH | 0.1 | 1.25 | 0.1 | 1.25 | 0.1 | 1 | 0.1 | 1.25 |
| **Heating efficiency** | HEATEFF | - | 0.5 | 0.95 | 0.5 | 0.95 | 0.5 | 0.95 | 0.5 | 0.95 |
| **Cooling COP** | COP | - | 5 | 6.3 | 5 | 6.3 | 2 | 4 | 5 | 6.3 |
| **Water use per floor** | WATER | [$m^3$/s] | 2.22 E-05 | 2.50 E-04 | 2.22 E-05 | 2.50 E-04 | 2.78 E-07 | 5.56 E-05 | 1.11 E-05 | 2.78 E-04 |
| **Gas equipment power density** | GAS | | 0 | 0 | 0 | 150 | 0 | 60 | 0 | 60 |

The uncertainty propagation was performed using a Monte Carlo (MC) simulation. The MC simulation picks a random value from the given range of the input parameters. 100 of training input data was sampled using a Latin Hypercube Sampling (LHS) (McKay et al., 1979), and 100 of testing input data was sampled using the Sobol's sequence (Sobol, 1998). Then, the sampled input parameter sets were plugged into the energy simulation (EnergyPlus) to calculate their corresponding energy use as an output. The obtained input-output sets can be employed in a sensitivity analysis and the development of the meta-models later.

Figure 7-7 shows the box plot of EUI comparison between the prior estimation and the measured data on CU campus. Considerable distinctions between the two ranges indicate that the prediction of the actual energy consumption with the developed representative models is not feasible the given input ranges, thus requiring the calibration process.

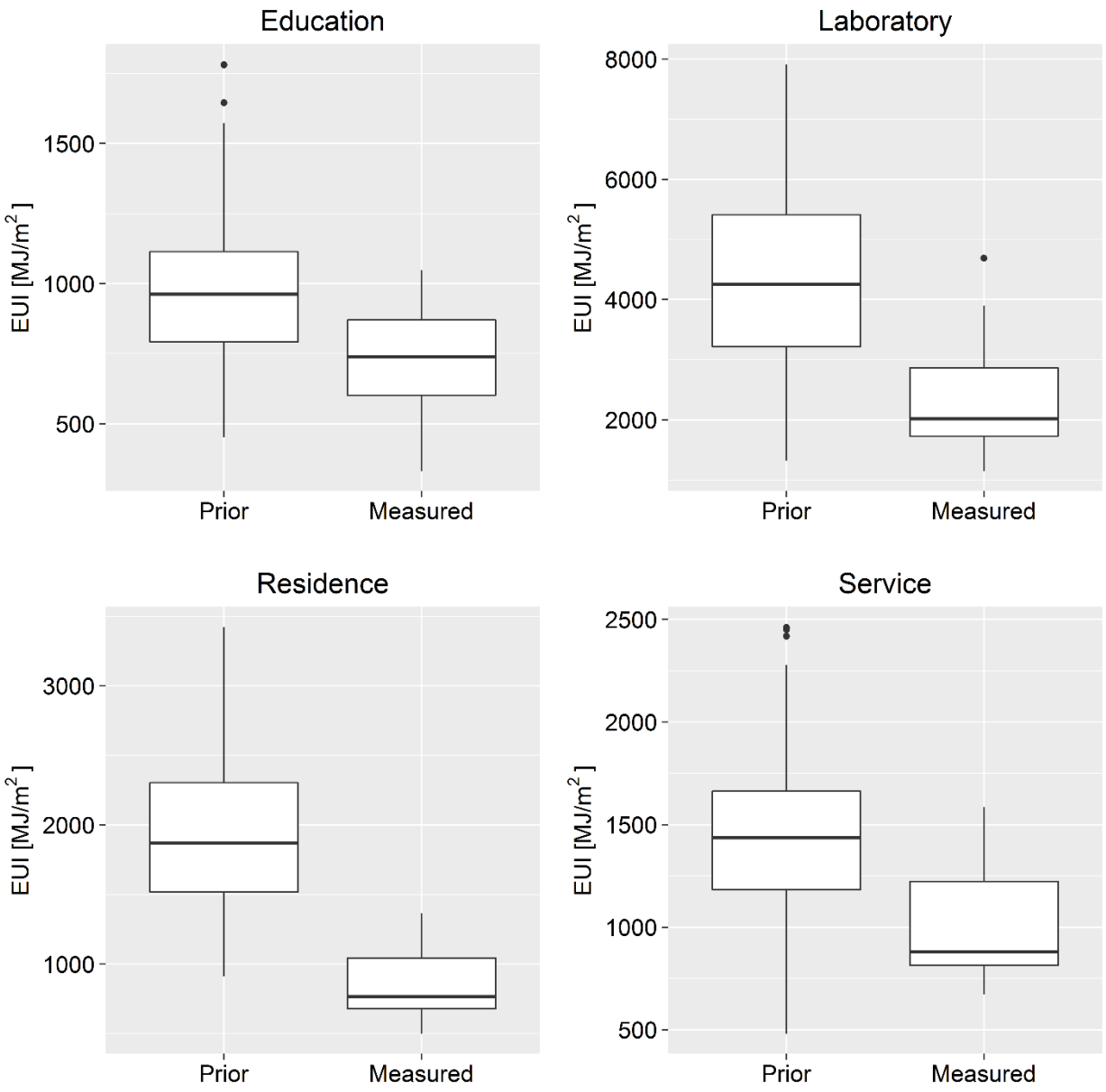


Figure 7-7 Boxplot - EUI comparison between prior and measured

### 7.3.3 Sensitivity analysis

Before executing the Bayesian calibration, it is important to select a proper number of parameters for calibration due to the accuracy and the effectiveness of Bayesian inference. To figure out the dominant parameters for each representative model, a sensitivity analysis was conducted.

In this study, we utilized three different approaches to offer robust analysis result: SRC (standardized regression coefficient), random forest variable importance and T-value. For detailed

information, please refer to (Tian, 2013). The sensitivity analysis was conducted using the annual electricity and the annual gas use data. To consider different values from the three sensitivity analyses (SRC, Random forest variable importance, and T-value) and two target outputs (annual electricity and gas use), the sensitivity value index (SVI) was suggested as shown in the equation 1. The values from the sensitivity analysis were normalized and then aggregated so that the importance of parameters can be compared considering the difference of sensitivity methods and target output.

$$\sum_{l=1}^{m} \frac{\frac{\sum_{j=1}^{k}\left(\frac{V_{i,j}}{\sum_{i=1}^{n}|V_{i,j}|}\right)}{k}}{m \cdot k} \times 100 = Sensitivity\ Value\ Index\ (SVI)(\%) \tag{7.1}$$

Where $i$ is the parameter, $n$ is the number of parameters ($n = 6$), $j$ is the sensitivity method, $k$ is the number of sensitivity methods ($k = 3$, (SRC, Random forest variable importance, and T-value)), $l$ is the target output, $m$ is the number of target output ($m = 2$ (annual electricity and gas)).

Table 7-4 SVI results

| Parameter | Edu | Lab | Res | Svc |
|---|---|---|---|---|
| **ROOF** | 2.0% | 1.0% | 2.8% | 1.1% |
| **WALL** | 1.5% | 1.1% | 3.3% | 1.5% |
| **WIN** | 5.0% | 2.2% | 1.4% | 3.1% |
| **SHGC** | 1.9% | 1.5% | 2.1% | 2.1% |
| **EPD** | 32.6% | 40.3% | 24.6% | 29.7% |
| **LPD** | 13.9% | 3.3% | 10.7% | 15.3% |
| **HSP** | 15.3% | 5.2% | 2.8% | 7.4% |
| **CSP** | 7.6% | 4.6% | 4.5% | 4.3% |
| **OCC** | 5.6% | 1.0% | 1.3% | 4.9% |
| **INF** | 2.0% | 0.8% | 3.0% | 1.4% |
| **HEATEFF** | 7.9% | 3.0% | 8.4% | 4.0% |
| **COP** | 1.6% | 0.9% | 2.5% | 0.8% |
| **WATER** | 2.9% | 1.4% | 20.8% | 2.1% |
| **GAS** | 0.0% | 33.5% | 11.7% | 22.3% |
| **Total** | 100.0% | 100.0% | 100.0% | 100.0% |

Using the SVI, the 14 parameters were ranked by the SVI in order of importance in the each representative building type. To screen the dominant parameter, the changes in R-squared value were identified when adding the parameter in an important sequence. After these processes, the first eight parameters were chosen for the education, residence, and service building type. The laboratory building type appears to have the first six parameters. Input parameters of each representative building model are dependent of the building function.

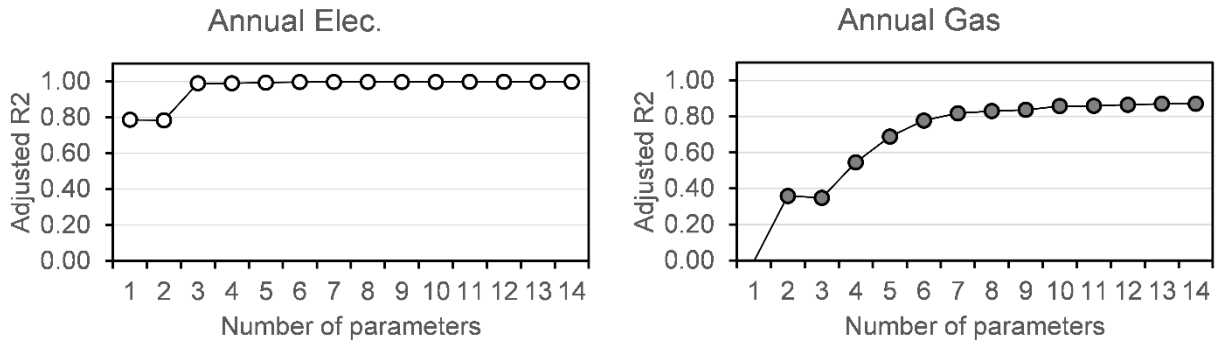


Figure 7-8 R2 for electricity and gas annual use (Education type)

Table 7-5 Parameter selection

| Ranking | Edu | Lab | Res | Svc |
|---|---|---|---|---|
| 1 | EPD | EPD | EPD | EPD |
| 2 | HSP | GAS | WATER | GAS |
| 3 | LPD | HSP | GAS | LPD |
| 4 | HEATEFF | CSP | LPD | HSP |
| 5 | CSP | LPD | HEATEFF | OCC |
| 6 | OCC | HEATEFF | CSP | CSP |
| 7 | WIN | | WALL | HEATEFF |
| 8 | WATER | | INF | WIN |

### 7.3.4 Meta-models

The Bayesian calibration requires massive simulation runs. The meta-models can replace the whole building transient simulation model with a significant reduction of simulation run time.

In chapter 4, we already confirmed that the calibration using the multiple linear regression (MLR) models yields enough reasonable calibration result in the prediction of energy use. Since the purpose of this study is to calibrate the building energy consumption rather than to estimate the actual input parameter value. Further, the computational time for the Bayesian calibration can be decreased by using the MLR.

Figure 7-9 shows R-squared and RMSE values of the MLR for each monthly energy use in the education building type. R-squared values for 12 monthly electricity were close to one. It means that the monthly electricity MLR models can represent the original EnergyPlus building energy model well. Although R-squared values for summer gas were lower than others, it does not reduce the accuracy of the overall model because RMSE of gas is also small in the summer. The developed MLR will be further used in the Bayesian inference to calibrate the input parameter with the measured energy consumption data.

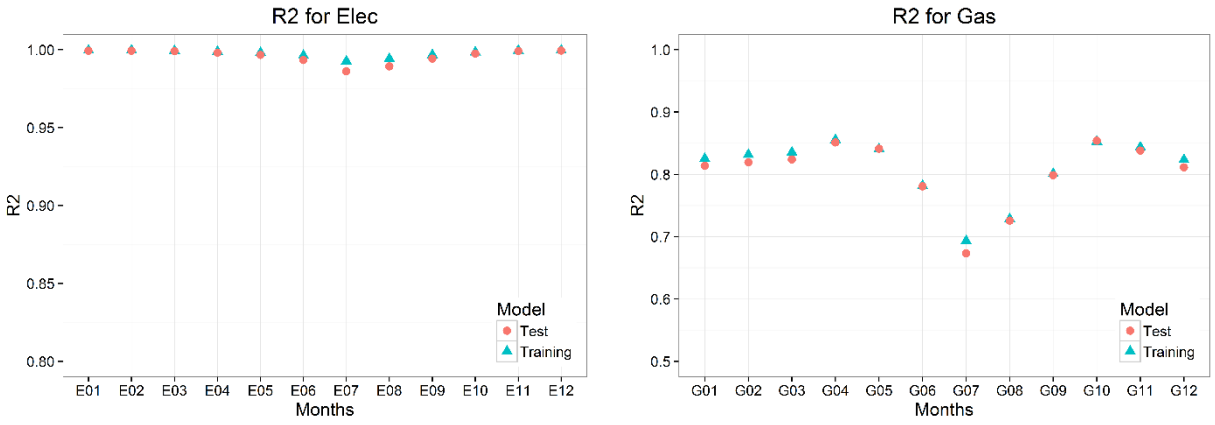

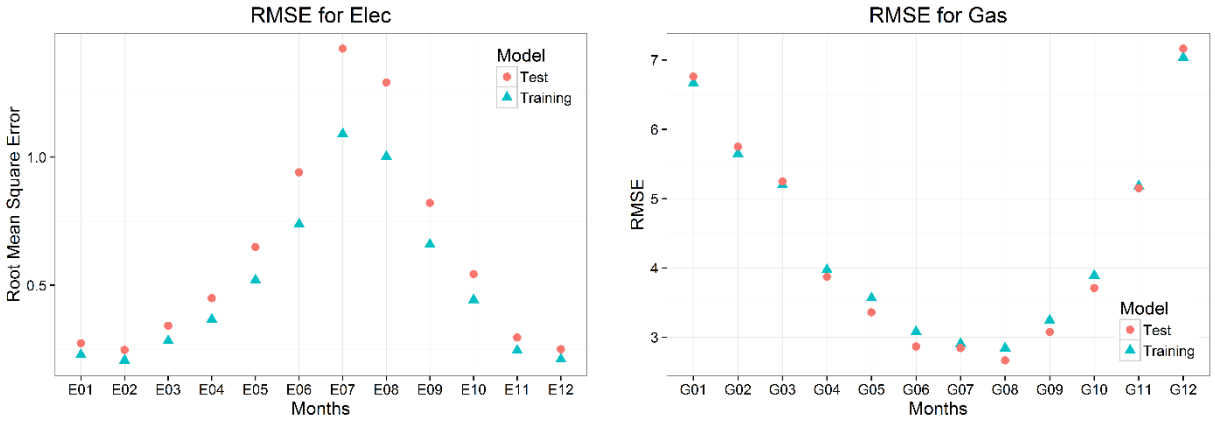


Figure 7-9 R-square and RMSE of MLR (Education type)

### 7.3.5 Bayesian calibration

Bayesian analysis is a statistical method that utilized Bayes' theorem in Equation (2) to obtain a posterior distribution for unknown parameters ($\theta$) given the observed data ($y$). All the uncertainties in building energy models are expressed in probabilities. The input parameters are considered to be uncertain and have a probabilistic distribution based on their plausible values. The uncertain parameters of the building energy model are revised to match the model prediction and the observed data. As a result, Bayesian calibration provides the posterior distribution $p(\theta|y)$ in a form of plausible distribution of calibration parameters.

$$p(\theta|y) = \frac{p(y|\theta) \cdot p(\theta)}{p(y)} \propto p(y|\theta) \cdot p(\theta) \tag{7.2}$$

Where $p(\theta)$ is prior distributions assigned for uncertain parameters; $p(y|\theta)$ is a likelihood function that measures how closely model predictions match the observed data.

A Markov Chain Monte Carlo (MCMC) method is commonly referred to draw the posterior distribution. The MCMC method generates a random walk through the parameter space such that the set of sample points can approximate theoretical posterior density functions. The method draws a proposed point based on the current position in an iterative process and accepts the proposed point when it satisfies an acceptance criterion (Yeonsook Heo et al., 2011). The Metropolis-Hastings algorithm defines the criterion by the ratio of a posterior density at the proposed point to that at the current point (Gelman et al., 2014).

In an MCMC process, a sufficient number of iterations are required to explore the entire feasible range. 100,000 of iteration number was used in this study. A preliminary study using the Gelman and Rubin diagnostic (Gelman et al., 2014) showed that the potential scale reduction factor (PSRF) for each parameter was lower than 1.1, indicating that the Markov Chain has converged when the iteration number is larger than 100,000. The burn-in length was 10,000 to avoid the effect of the initial value for each parameter.

#### 7.3.5.1 Regressed measured data

When setting up the target distribution in the Bayesian calibration, a problem that did not exist in the previous chapter emerged. In chapter 5, when the virtual building stock was developed, we applied sets of sampled input parameters to the one representative building model. In other words, the buildings in the virtual building stock have the same geometry, HVAC systems, and schedule while the input parameter such as roof U-value, and equipment power density were different. Figure 7-10 shows the monthly total energy use pattern from the virtual building stock. The magnitude of the energy use is all different, while the patterns of each building are similar.

On the other hand, in this CU case study, the calibration was conducted with the actual energy use data. As shown in Figure 7-11, although the buildings are the same building type which is the education type, the monthly patterns of actual energy use were substantially different. When the Bayesian calibration employs one representative building model to calibrate to the diverse energy use patterns, it will cause a significant error. To prevent large error, we suggest a method that samples a regressed energy use pattern from the actual energy use data.

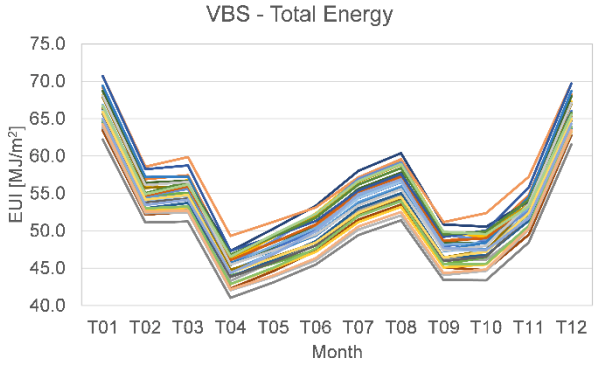


Figure 7-10 Monthly energy use patterns of VBS

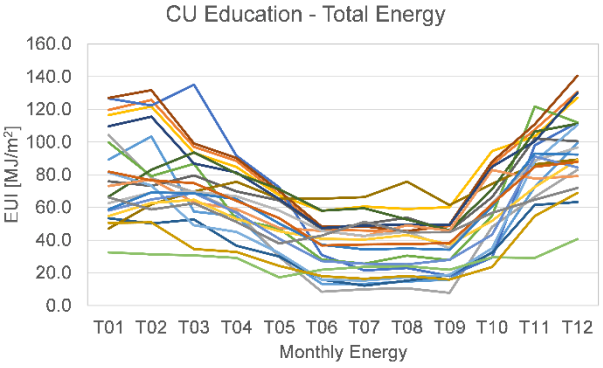


Figure 7-11 Monthly energy use patterns of CU education type

The first step involves fitting a distribution. To find the best-fitted distribution, graphical methods can be used as shown in Figure 7-12. For the quantitative comparison, the best-fitted distributions were found from the actual monthly energy use distribution using 'fitdist' function of 'fitdistrplus' package in R. The 'fitdist' function gives an AIC (Akaike information criterion) as a result. The distribution with the lowest AIC value is the best-fitted distribution. The AIC is a method of the relative quality of statistical models for a given set of data (Akaike, 2011). The best-fitted distribution was found among the normal, Weibull, gamma, and log-normal distribution. Table 7-6 shows the comparison of the AIC and the selected distribution among the alternatives we chose to explore. The second step is drawing new samples using the Sobol sequences from the best-fitted distribution. Figure 7-13 and Figure 7-14 present the comparison between the measured energy use distribution and the sampled one. Although there was a slight disagreement, it appeared to be entirely consistent. The third step is selecting a combination from the sampled monthly electricity and gas energy use. The samples were sorted and selected by energy use in each sampled monthly energy use. Figure 7-15 compares the patterns of the measured energy use and the sampled energy use. Through the process, the patterns of the energy use became similar. Finally, by comparing the measured total energy use distribution and the sampled one, the validity of the sampled data can be checked (Figure 7-16).

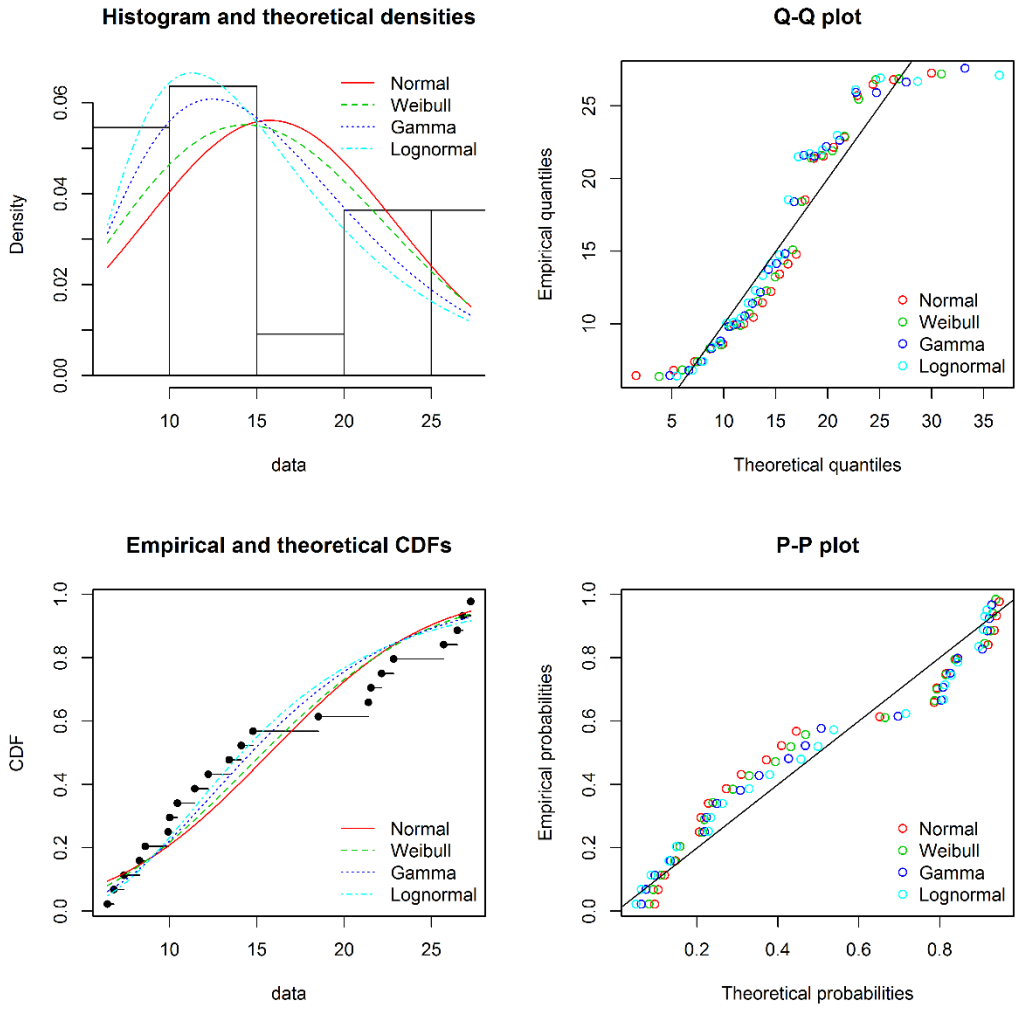


Figure 7-12 fitting a distribution using graphical methods

Table 7-6 AIC values and the best-fitted distribution

| Monthly Energy | Normal | Weibull | Gamma | Log-normal | Best fitted |
|---|---|---|---|---|---|
| **E01** | 152.7 | 150.6 | 150.2 | 150.2 | Gamma |
| **E02** | 162.0 | 159.8 | 159.5 | 159.7 | Gamma |
| **E03** | 168.6 | 166.0 | 165.7 | 165.8 | Gamma |
| **E04** | 168.9 | 166.5 | 166.6 | 166.9 | Weibull |
| **E05** | 163.4 | 160.8 | 160.5 | 160.6 | Gamma |
| **E06** | 178.9 | 175.0 | 174.4 | 174.3 | Log-normal |
| **E07** | 181.6 | 177.8 | 177.0 | 176.9 | Log-normal |
| **E08** | 180.9 | 177.2 | 176.2 | 176.0 | Log-normal |

| | | | | | |
|---|---|---|---|---|---|
| **E09** | 175.5 | 172.5 | 172.3 | 172.8 | Gamma |
| **E10** | 176.6 | 174.2 | 174.2 | 174.8 | Weibull |
| **E11** | 172.6 | 170.1 | 169.7 | 169.7 | Log-normal |
| **E12** | 169.9 | 166.8 | 166.3 | 166.1 | Log-normal |
| **G01** | 217.6 | 215.1 | 214.9 | 215.5 | Gamma |
| **G02** | 217.7 | 214.6 | 213.9 | 214.5 | Gamma |
| **G03** | 207.2 | 204.7 | 203.5 | 204.6 | Gamma |
| **G04** | 197.0 | 195.0 | 194.7 | 196.5 | Gamma |
| **G05** | 188.5 | 198.6 | 198.1 | 235.1 | Normal |
| **G06** | 171.7 | 151.8 | 145.7 | 175.1 | Gamma |
| **G07** | 172.1 | 139.0 | 133.6 | 159.7 | Gamma |
| **G08** | 169.7 | 146.1 | 140.2 | 168.7 | Gamma |
| **G09** | 175.1 | 146.9 | 141.1 | 168.8 | Gamma |
| **G10** | 197.2 | 191.2 | 189.3 | 188.1 | Log-normal |
| **G11** | 203.4 | 204.0 | 207.9 | 213.4 | Normal |
| **G12** | 212.9 | 212.4 | 213.5 | 215.9 | Weibull |

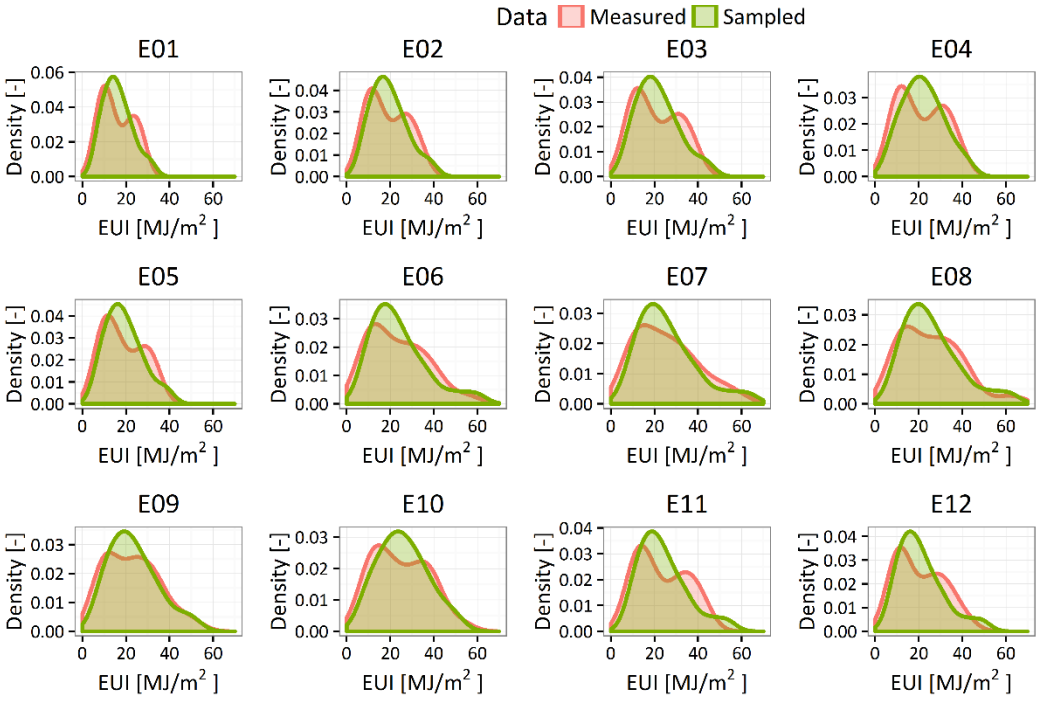


Figure 7-13 Comparison between measured data and parametric data (Electricity)

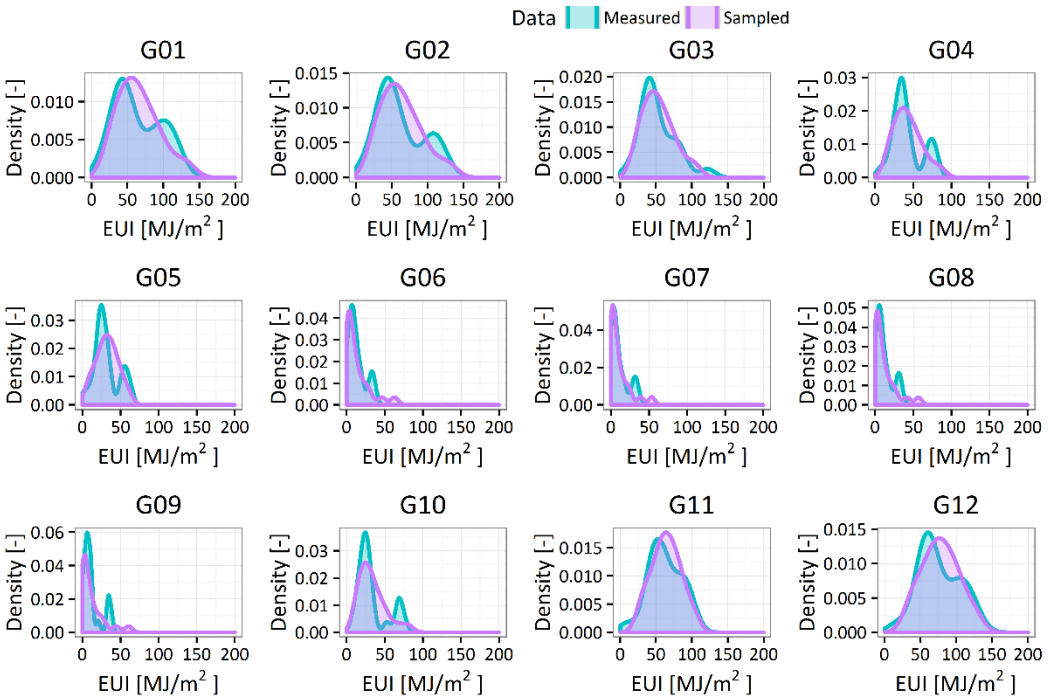


Figure 7-14 Comparison between measured data and parametric data (Gas)

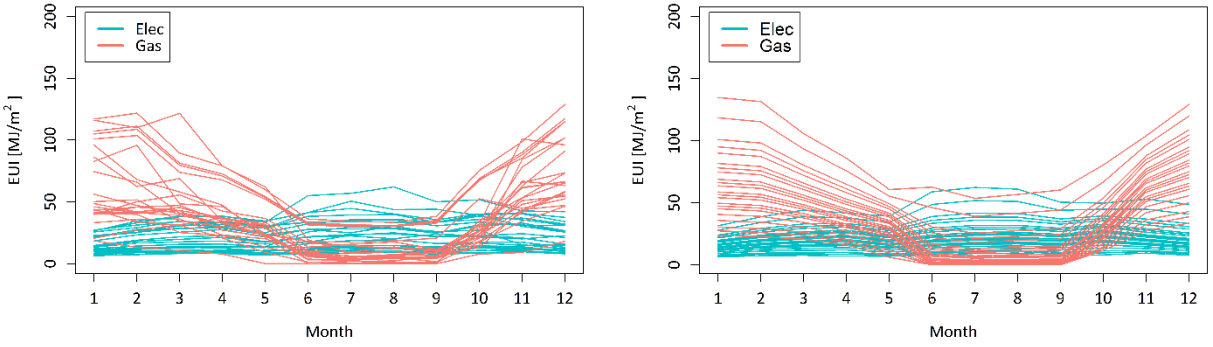


(a) Measured monthly energy data patterns

(b) Sampled monthly energy data patterns

Figure 7-15 Comparison of the patterns of the monthly energy use

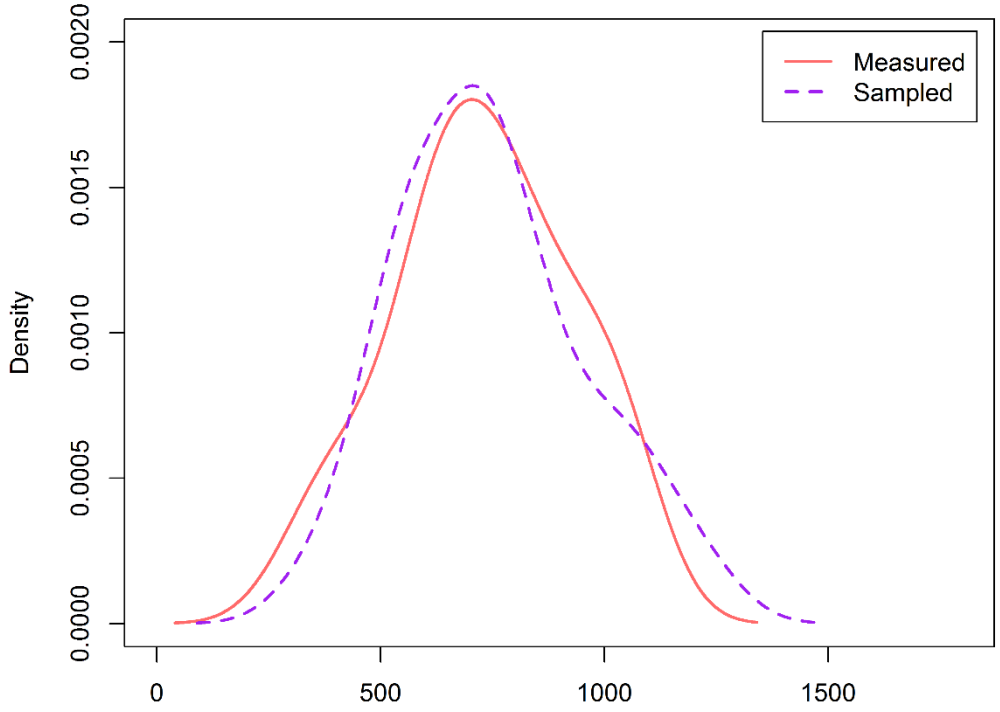


Figure 7-16 Comparison of the distributions

#### 7.3.5.2 Calibration Results

##### 7.3.5.2.1 Input parameters and EUI distributions

Figure 7-17 shows the prior and posterior distribution for the parameters from the Bayesian calibration. The gray dotted line represents the prior distribution, and the solid orange line indicates the posterior distribution. Since the actual distributions of each parameter are not available, the actual target distribution does not exist. The posterior distributions of parameters were changed to fit the measured energy consumption in the education building type. The estimated posterior distribution for building parameter should not be considered as the actual distribution of building parameter in the education buildings in CU campus. Since one representative building covers different sizes and shapes of the education buildings, the estimated posterior distribution should be regarded as "best guess" that

approximates energy consumptions of the actual building stock. Figure 7-18 and Figure 7-19 present the prior, measured, and posterior distributions of annual and monthly energy use. Although we used the regressed data from the actual energy use data for calibration, the comparison of energy use distributions was conducted using the measures data. After the calibration, the posterior distribution became closer to the measured distribution. The results of other building types were shown from Figure 7-20 to Figure 7-28.

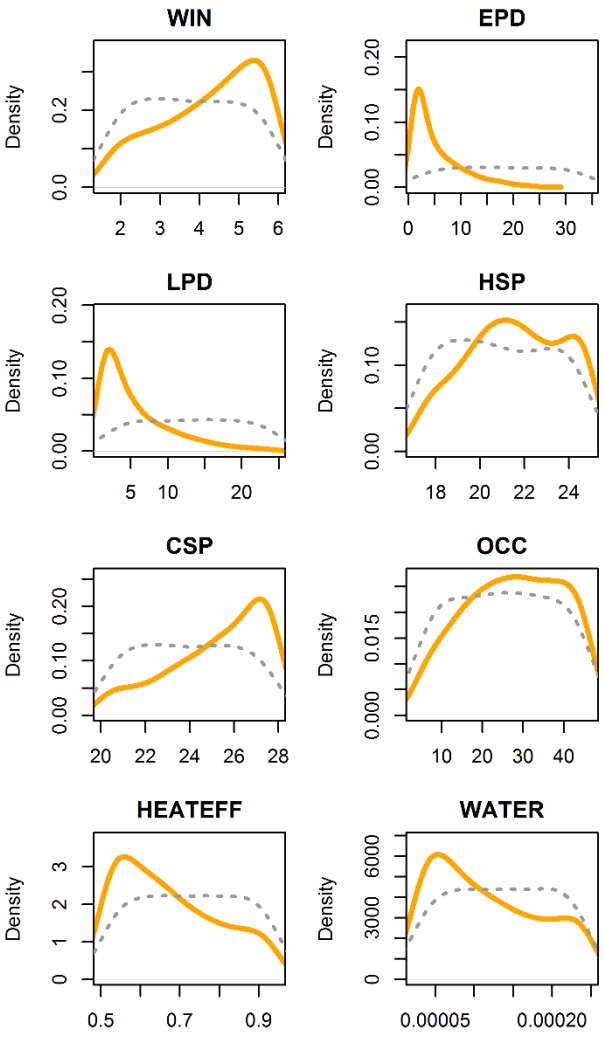


Figure 7-17 Parameter distributions (Education)

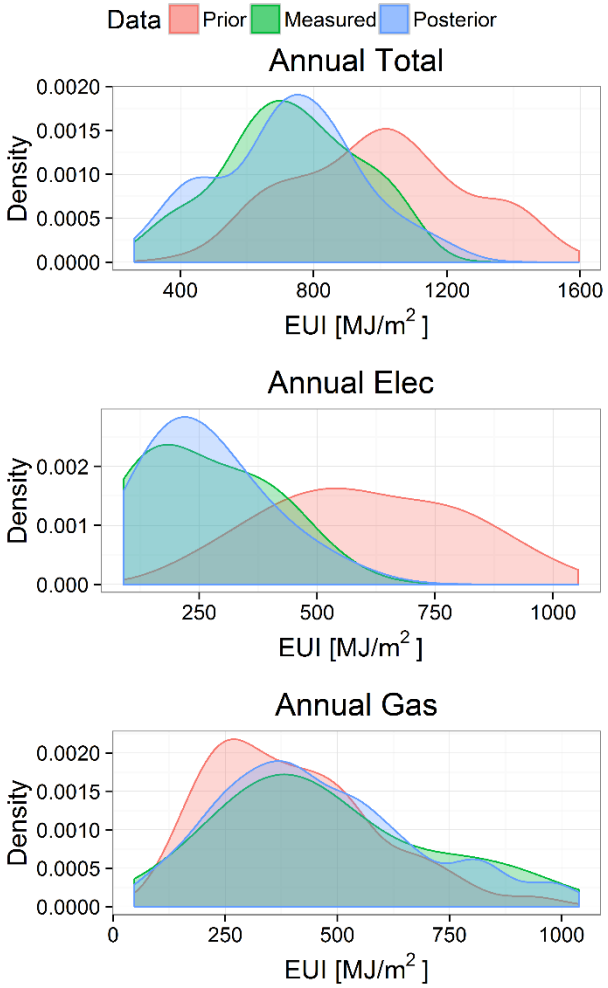


Figure 7-18 Annual energy use distributions (Education)

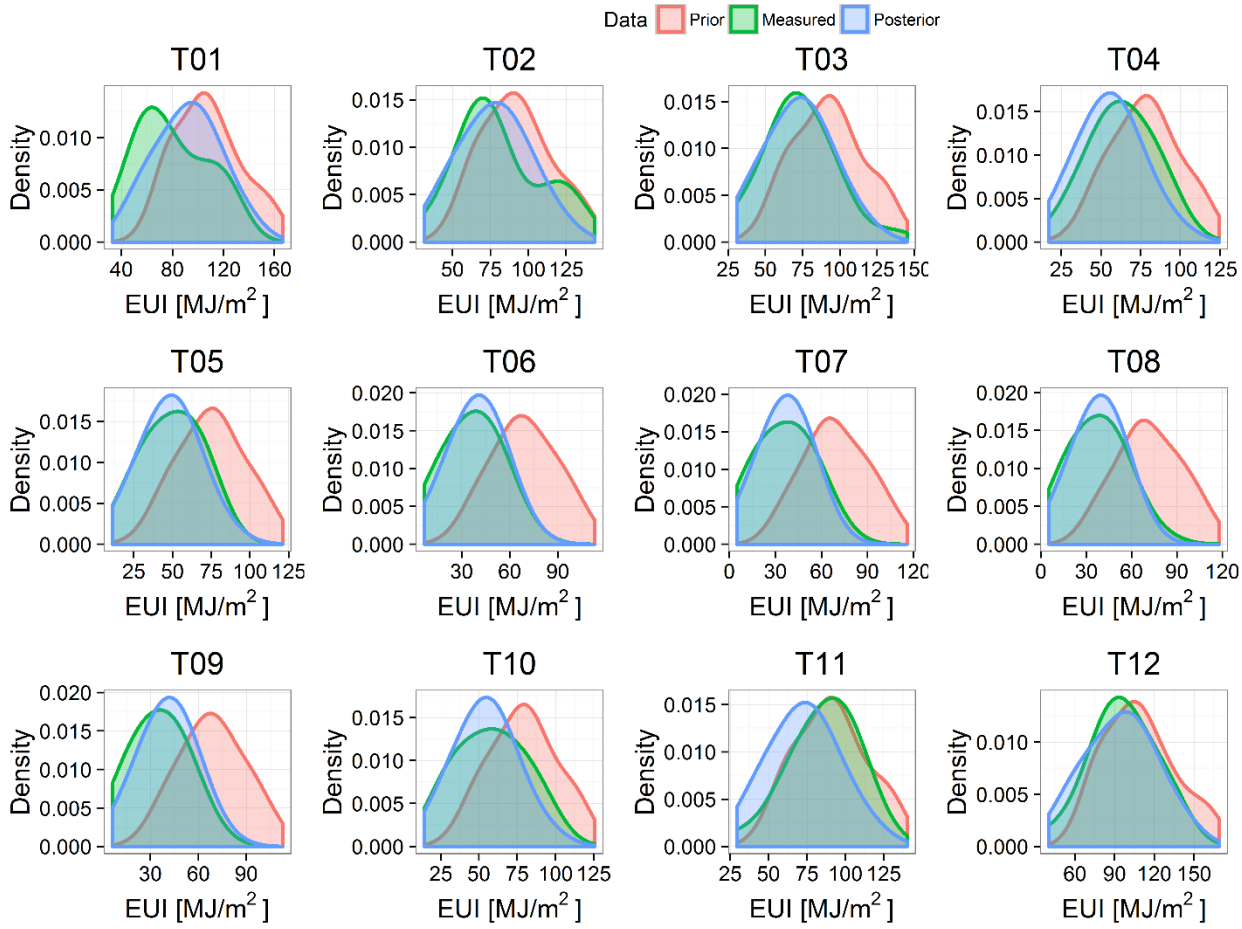


Figure 7-19 Monthly total energy use distributions (Education)

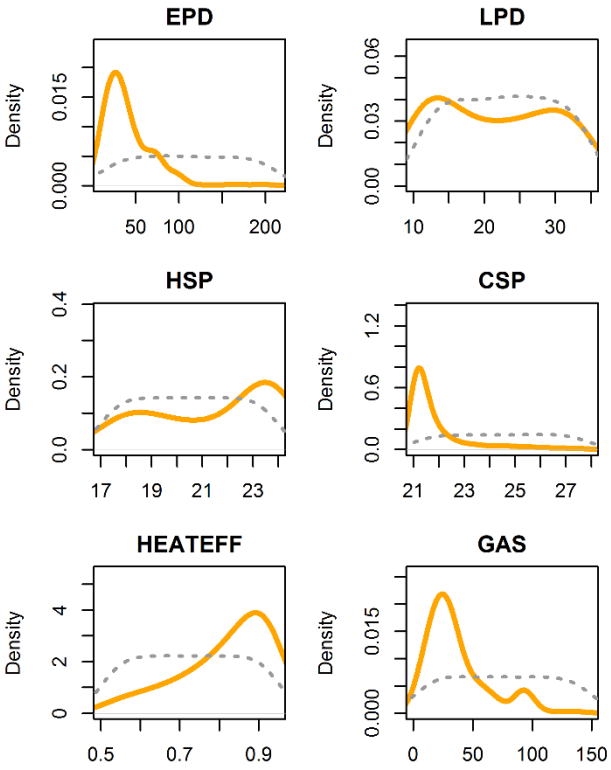


Figure 7-20 Parameter distributions (Laboratory)

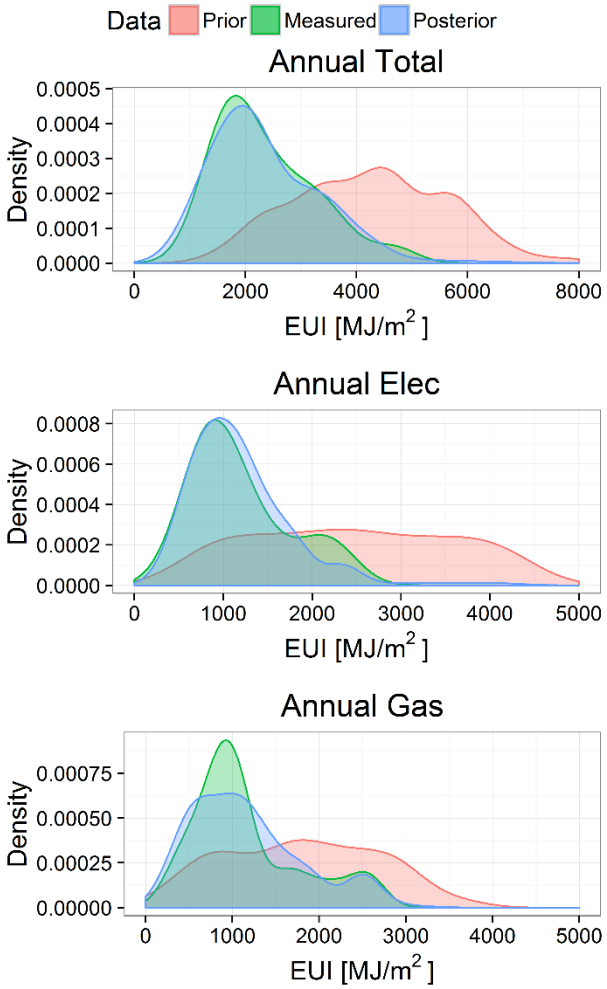


Figure 7-21 Annual energy use distributions (Laboratory)

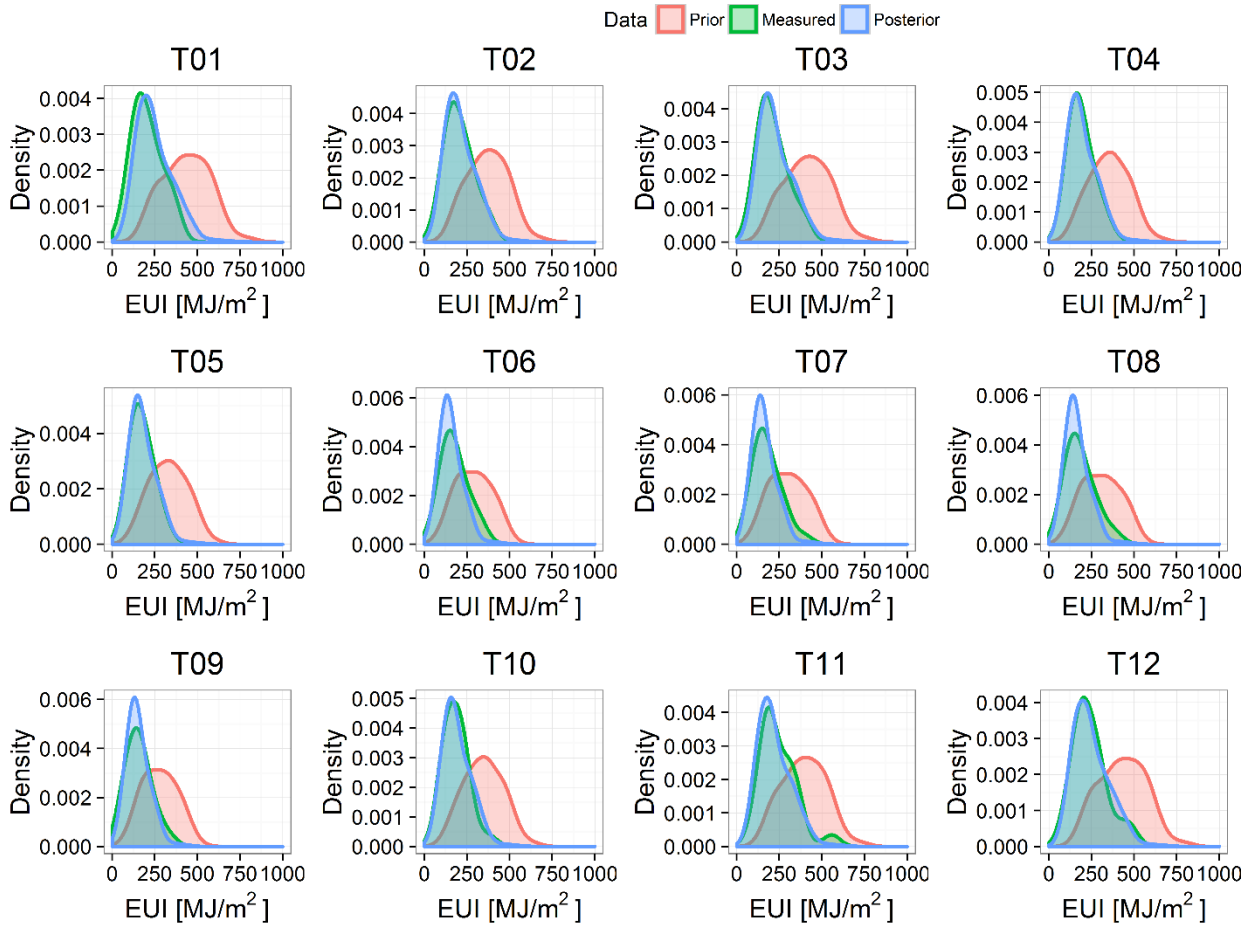


Figure 7-22 Monthly total energy use distributions (Laboratory)

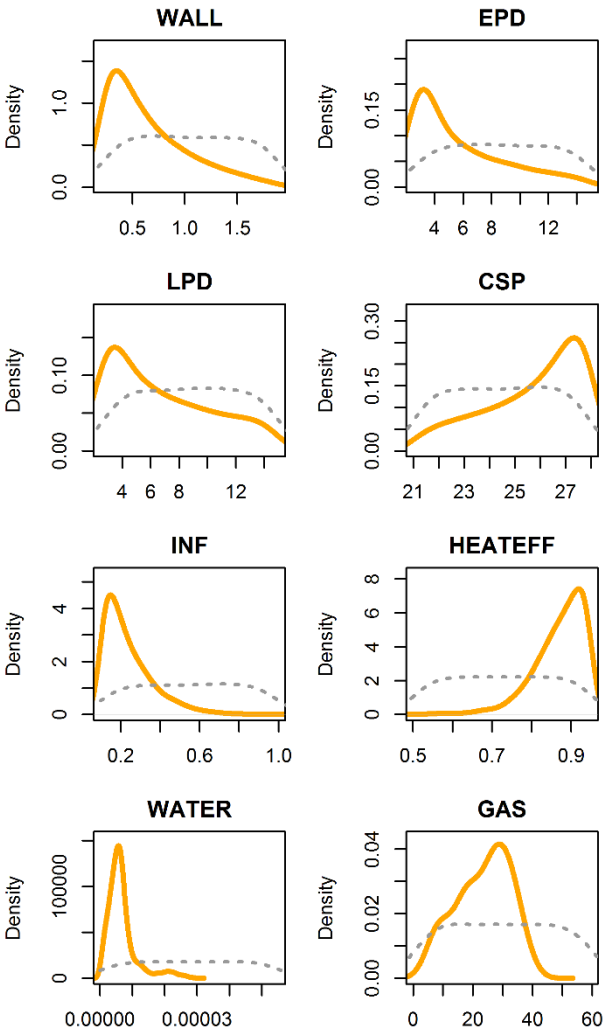


Figure 7-23 Parameter distributions (Residence)

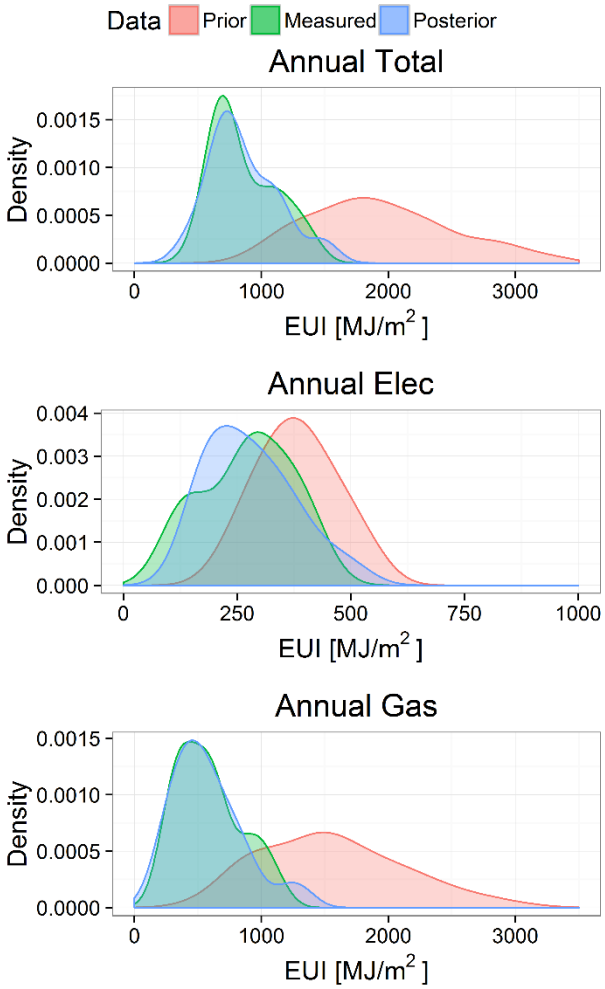


Figure 7-24 Annual energy use distributions (Residence)

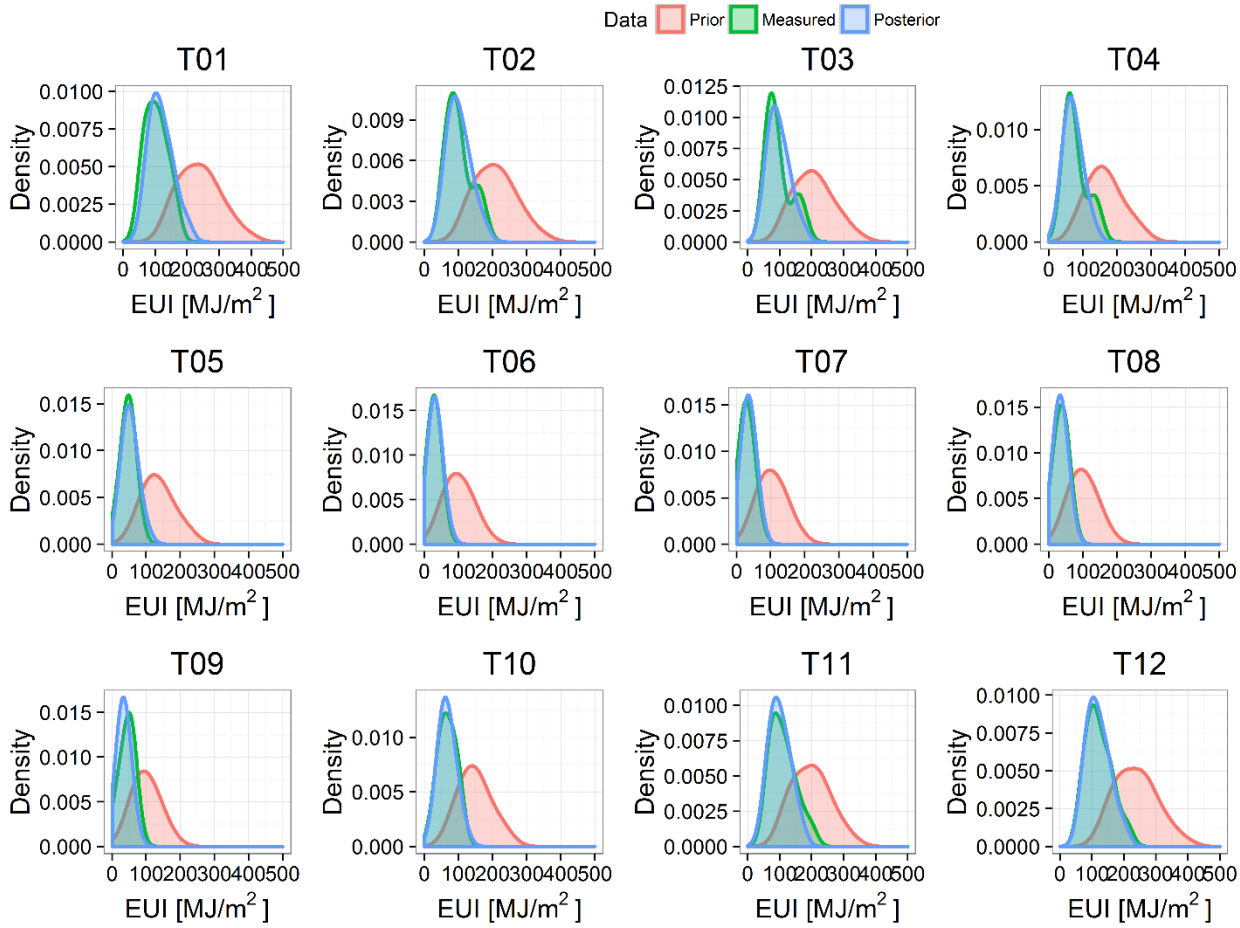


Figure 7-25 Monthly total energy use distributions (Residence)

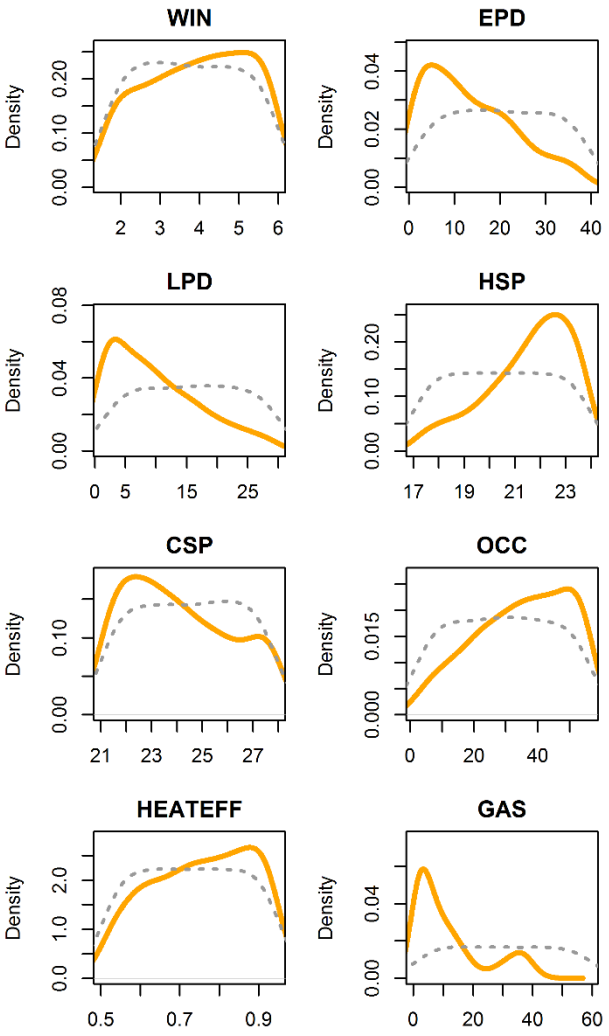


Figure 7-26 Parameter distributions (Service)

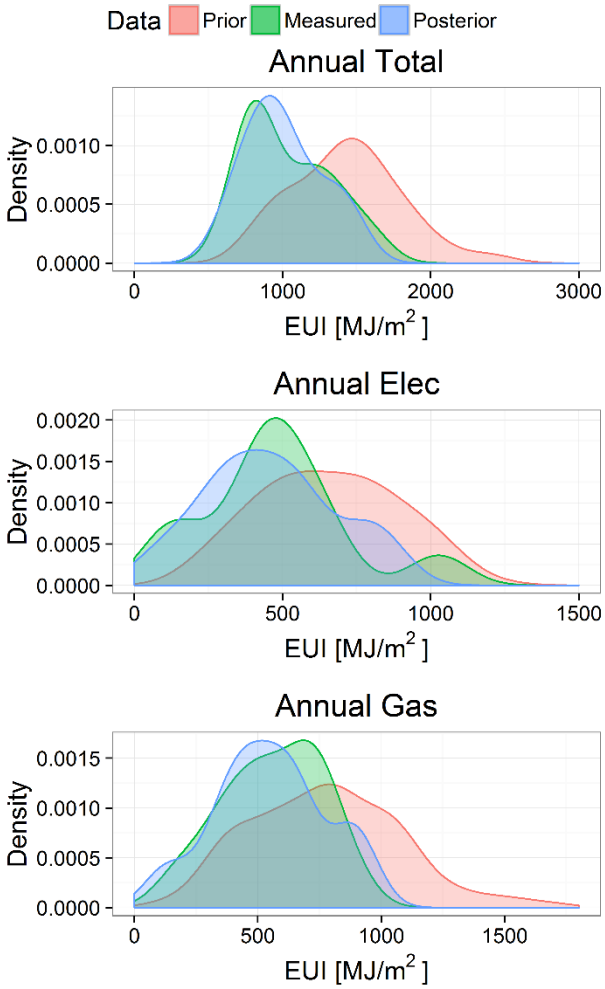


Figure 7-27 Annual energy use distributions (Service)

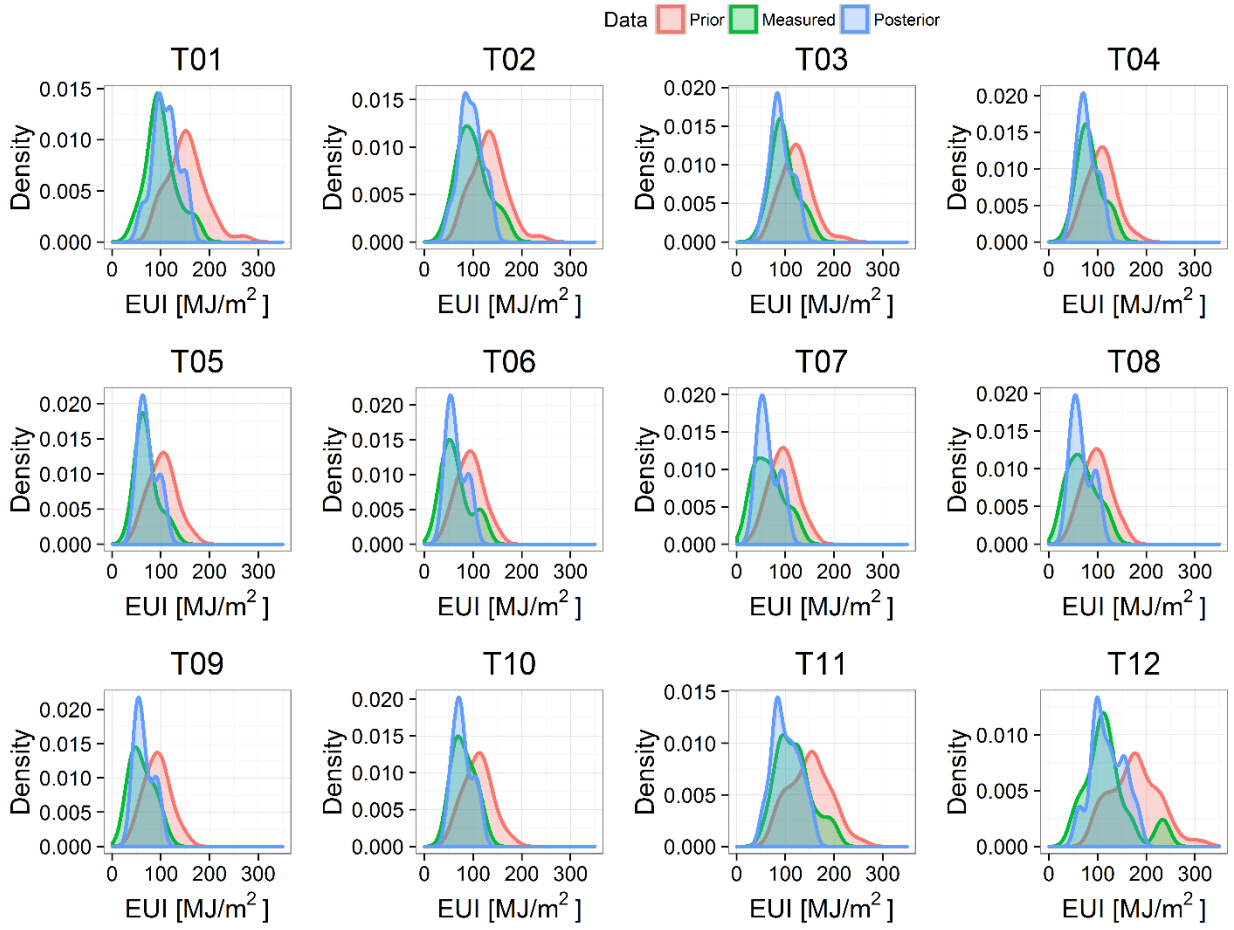


Figure 7-28 Monthly total energy use distributions (Service)

7.3.5.2.2 KS Test

Figure 7-29 shows the results of two-sample Kolmogorov–Smirnov test (KS test) for each building type. If the p-value is lower than 0.05, we can reject the null hypothesis that assumed two distributions are induced from the same distribution. The p-values from the comparison between the prior distribution and the target distribution were lower than 0.05, which means we can reject that the prior distribution and the target distribution came from the same distribution. However, after the calibration, the p-values were increased when comparing the posterior distribution and target distribution in almost all cases. Through the suggested stochastic-deterministic-coupled building stock energy model, we could calibrate not only the annual energy use but also the monthly energy use while taking into account different energy types.

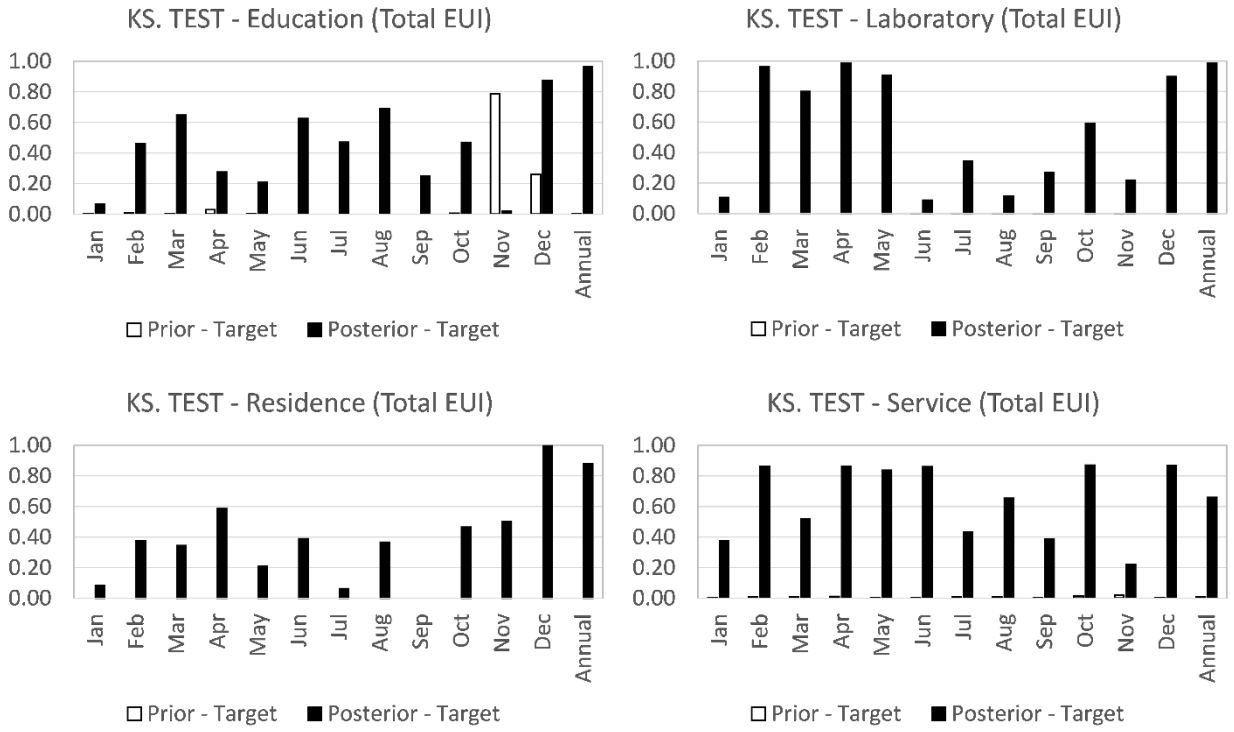


Figure 7-29 KS test results

### 7.3.6 Aggregation

An aggregation of building energy consumption is one of the challenges in the building stock model. The aggregation at the national level typically employs weighting factors to scale up the energy use of individual prototypical buildings. It is hard to develop reasonable weighting factor at the national level and almost impossible at the state or local levels (Deru et al., 2011). Recent development of Geographic Information System (GIS) enabled the aggregation at the state or city level by scaling up energy use by the actual building floor area.

Figure 7-30 presents EUI distributions for each building type and the whole CU campus. As seen in Chapter 5, the total floor area for each building type should be considered to calculate the EUI for the whole campus.

$$\text{Total EUI} = \frac{\sum_{i=1}^{n}(EUI_i \times Total\ Area_i)}{\sum_{i=1}^{n} Total\ Area_i} \tag{7.3}$$

The mean value of EUI for the CU campus is 1295.82 MJ/m$^2$. The maximum value is 2580.19 MJ/m$^2$ and the minimum value is 652.05 MJ/m$^2$.

The energy consumption of an entire campus can be roughly estimated by equation (7.4).

$$\text{E} = \sum_{j=1}^{M}\left\{\sum_{i=1}^{N}\left(EUI_{i,j} \cdot A_{i,j}\right)\right\} + \varepsilon \tag{7.4}$$

Where $N$ is the total number of buildings in a particular building type $j$; $M$ is the number of building types; $EUI_{i,j}$ is the energy use intensity of a building $i$ in a particular building type $j$ in $TJ/m^2/yr$; $A_{i,j}$ is the building floor area of a building $i$ in a particular building type $j$ in $m^2$. The term $\varepsilon$ is the measurement error term.

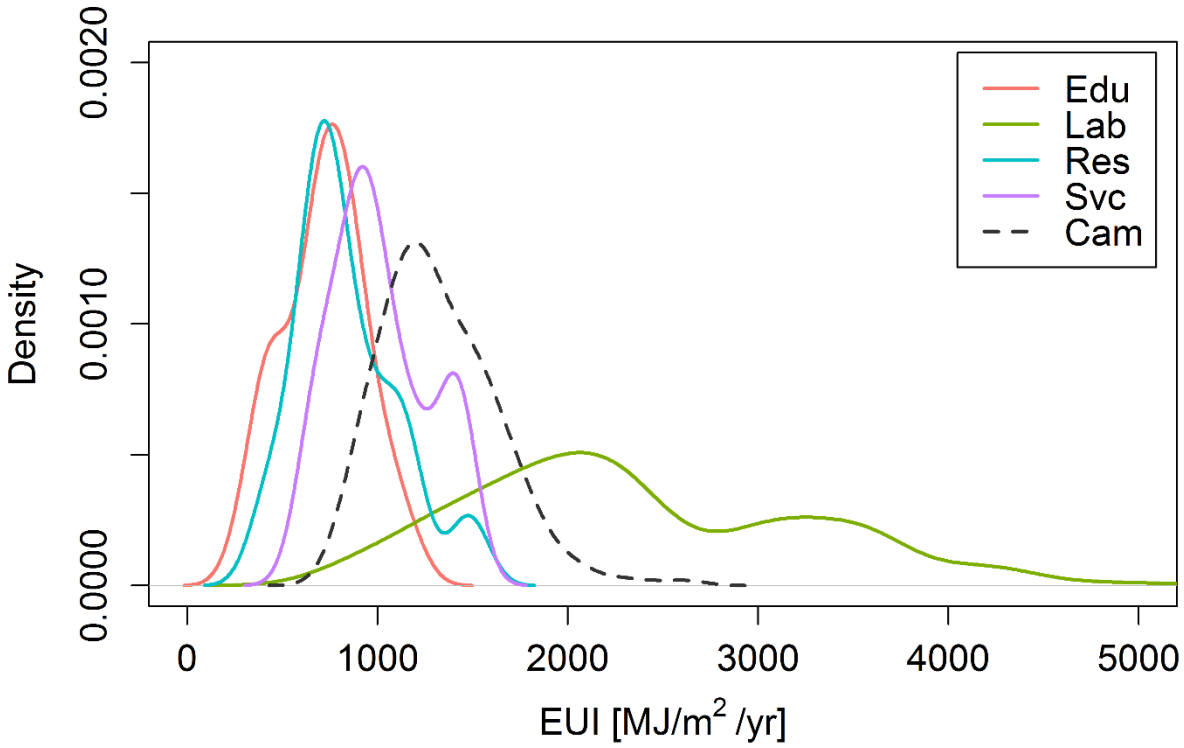


Figure 7-30 EUI distributions for each building type

Figure 7-31 show the prior and posterior distributions of energy consumptions for each building type. The prior and posterior EUI distributions were multiplied by the total floor area for each building type to estimate the energy consumption of each building stock. The vertical dotted lines indicate the measured energy consumption for each building stock. In all cases, the posterior distribution moved closer to the actual energy use value, and the ranges of distribution became narrower than the proir distribution.

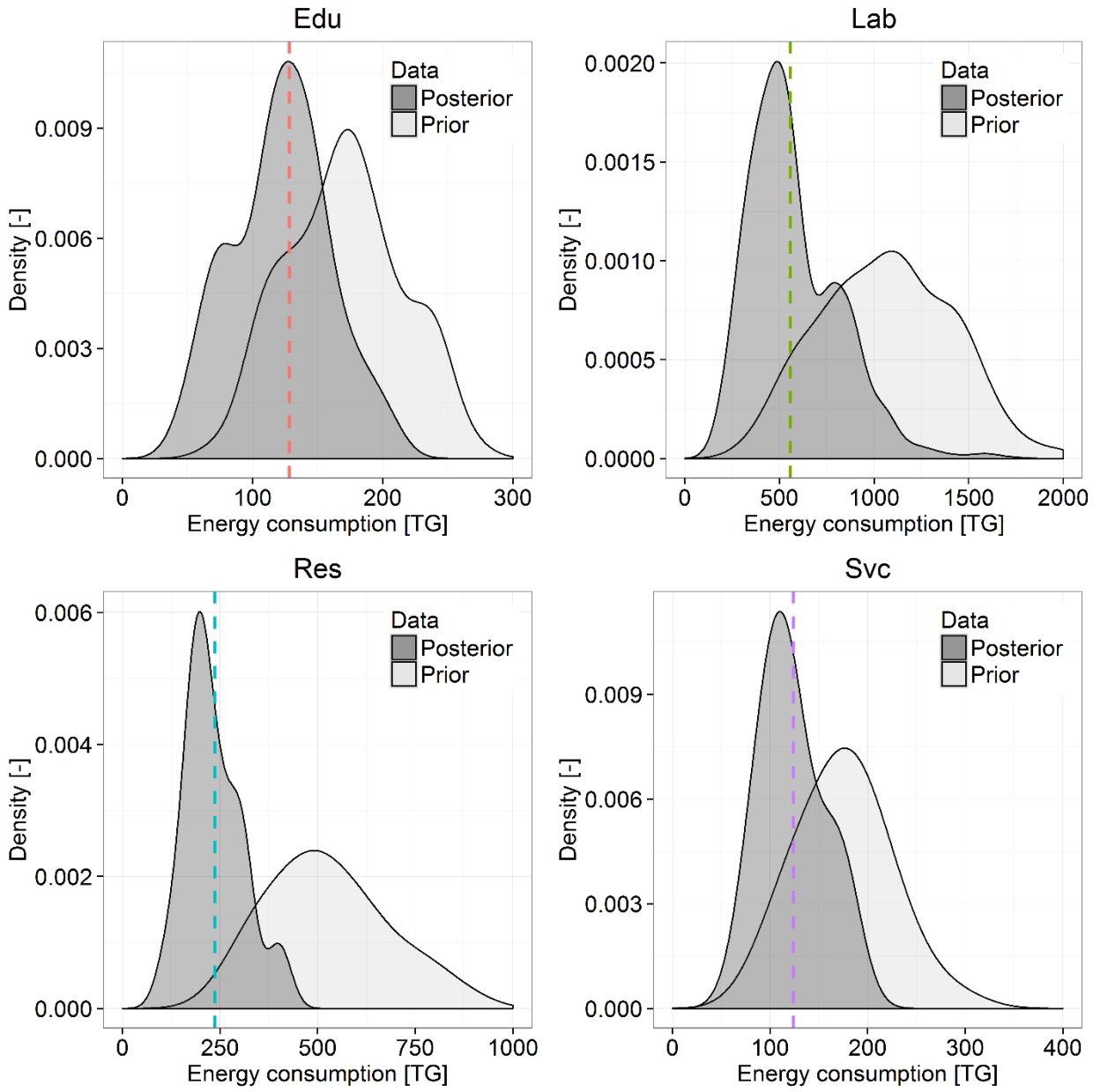


Figure 7-31 Total energy use distribution for each building type

Figure 7-32 shows the energy use distributions of each building type and the entire CU campus. To sum the two energy use distributions, all combinations from each distribution were considered using 'expand.grid' function in R. In this process, each building type has 10,000 samples and such a large number of samples may cause a computational burden. To save computing time and computer memory, we sampled 1,000 samples and carried out the calculations. Average values of energy consumption for prior and posterior distribution were compared to the observed data in Table 7-7. After Bayesian calibration, the

mean value of the posterior distribution matched well with the measured data in each type of building stock. The proposed stochastic-deterministic-coupled building stock energy methodology enables the estimation of the building energy consumption at campus-scale for both entire buildings and each type of building stock.

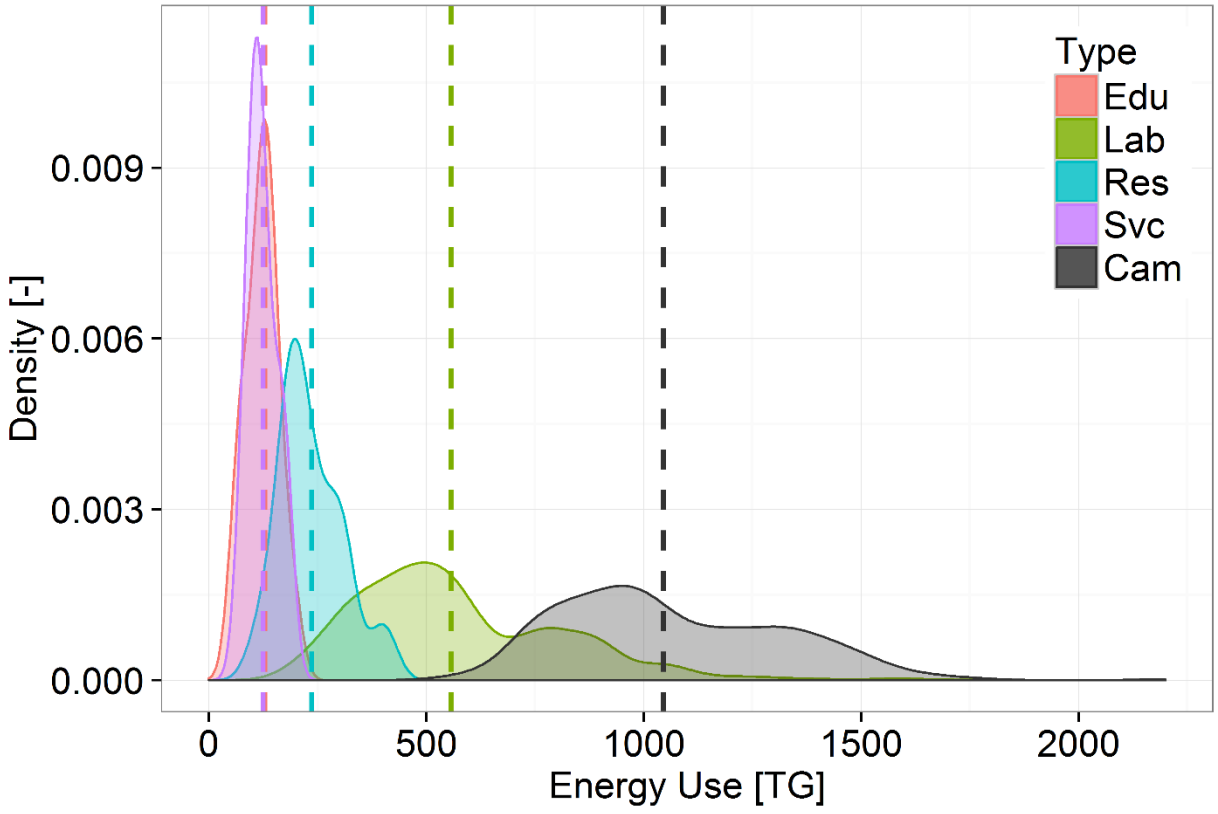


Figure 7-32 Total energy use distribution of CU campus

Table 7-7 Average value of total energy consumption distribution (values in parenthesis indicate the percentage to the measured data)

| | Edu | Lab | Res | Svc | Campus |
|---|---|---|---|---|---|
| **Measured [TJ]** | 128.2 | 556.3 | 236.7 | 124.0 | 1045.2 |
| **Aver. Prior [TJ]** | 170.8 (+33.3%) | 1065.8 (+91.6%) | 526.4 (+122.4%) | 175.2 (+41.2%) | 1922.9 (+84.0%) |
| **Aver. Posterior [TJ]** | 122.2 (-4.6%) | 597.9 (-7.5%) | 226.5 (-4.3%) | 123.9 (-0.1%) | 1076.6 (+3.0%) |

### 7.3.7 The analysis of energy conservation measures

Three cases of energy conservation measures (ECM) analyses are considered for quantifying their benefits for the CU campus: Case 1 is applying ECM to the most dominant parameter for each building type. Case 2 is a comparison between two ECMs. ECM for the non-dominant parameters is applied in Case 3.

#### 7.3.7.1 ECM Case 1. Applying ECM to the most dominant parameter

The first case aimed to examine the effect of ECM for the most dominant parameter. Table 7-8 shows the ranking of the parameter from the sensitivity analysis using the prior distribution. The ranking was changed when the sensitivity analysis used the posterior distribution as shown in Table 7-9. However, the most dominant parameters were not changed in all building types. In all building types, the equipment power density (EPD) was determined as the most dominant parameter. Therefore, we decided to apply the ECM to the EPD. 10% reduction is applied to the posterior EPD distribution for all building types as shown in Figure 7-33.

Table 7-8 Ranking of dominant parameters using the prior distribution

| Rank | Edu | Lab | Res | Svc |
|---|---|---|---|---|
| 1 | EPD | EPD | EPD | EPD |
| 2 | HSP | GAS | WATER | GAS |
| 3 | LPD | HSP | GAS | LPD |
| 4 | HEATEFF | CSP | LPD | HSP |
| 5 | CSP | LPD | HEATEFF | OCC |
| 6 | OCC | HEATEFF | CSP | CSP |
| 7 | WIN | | WALL | HEATEFF |
| 8 | WATER | | INF | WIN |

Table 7-9 Ranking of dominant parameters using the posterior distribution

| Rank | Edu | Lab | Res | Svc |
|---|---|---|---|---|
| 1 | EPD | EPD | EPD | EPD |
| 2 | LPD | GAS | LPD | GAS |
| 3 | HSP | HSP | GAS | LPD |
| 4 | CSP | LPD | WATER | HSP |

| | | | | |
|---|---|---|---|---|
| 5 | HEATEFF | CSP | HEATEFF | OCC |
| 6 | OCC | HEATEFF | CSP | LPD |
| 7 | WIN | | WALL | HEATEFF |
| 8 | WATER | | INF | WIN |

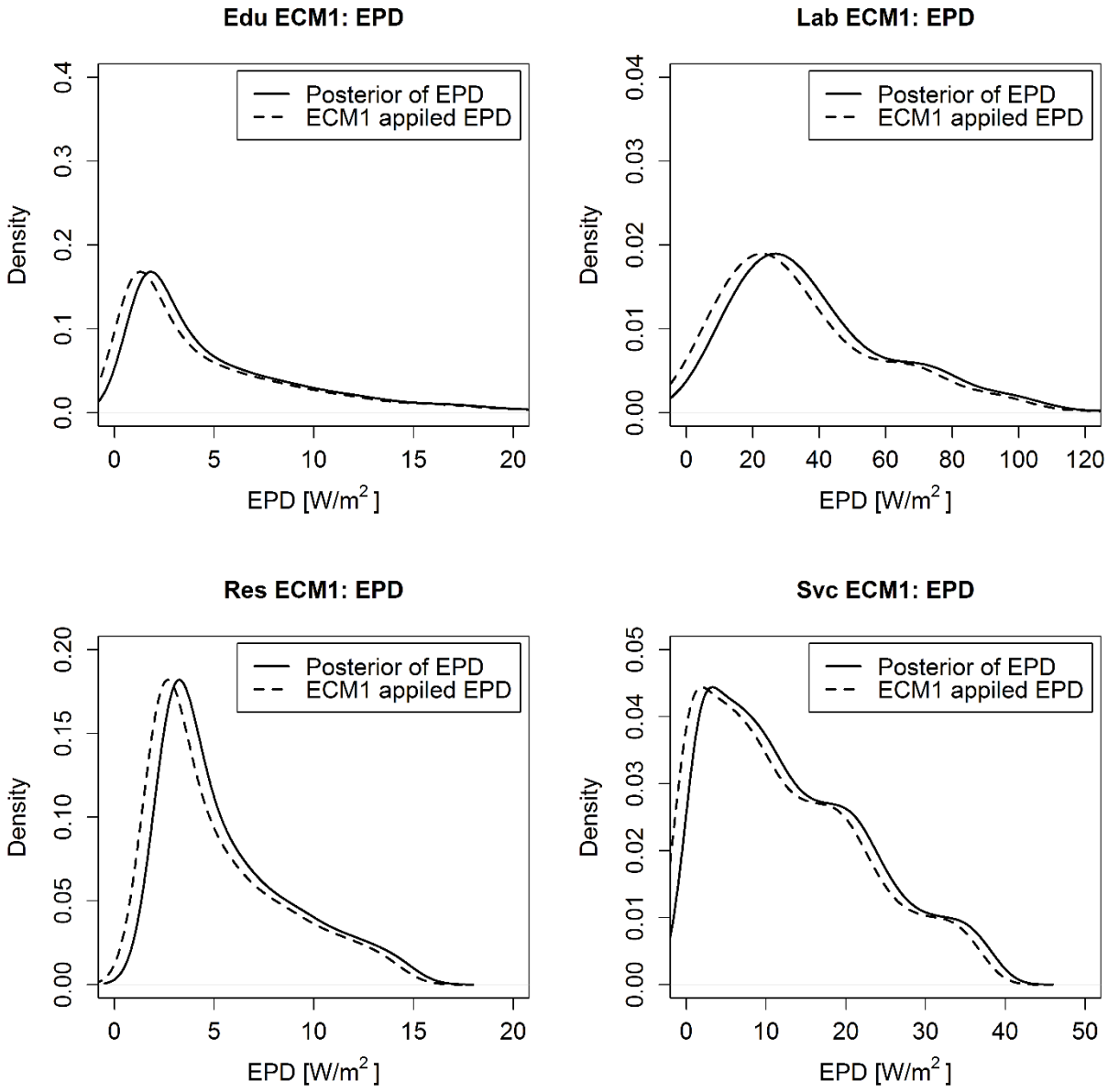


Figure 7-33 ECM 1 applied parameter distribution

The meta-model (MLR) was utilized to calculate the effect of ECMs. The availability of the meta-model to evaluate ECM has already been identified in Chapter 5. The use of meta-model for the evaluation of the ECM is one of the advantages of the proposed stochastic-deterministic-coupled building stock energy model since it reduces computing time without running the dynamic building simulation (EnergyPlus).

The ECM applied energy use distributions were just shifted along with the same shape because the meta-model was the multiple linear regression model as seen in Figure 7-34.

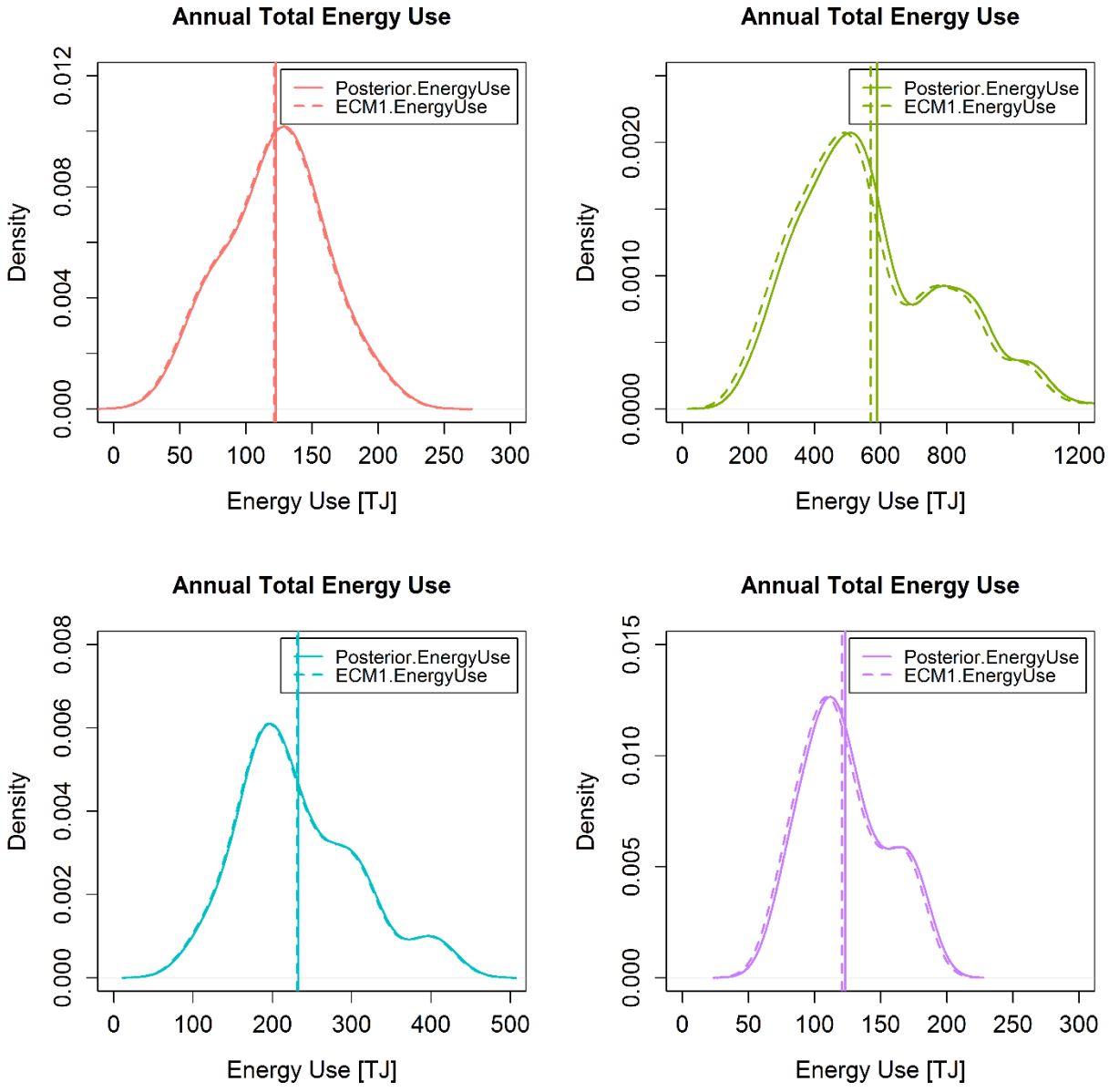

Figure 7-34 Annual total energy use distribution for ECM1

Table 7-10 Results of ECM 1

| Building type | Parameter | EUI | | Energy Use | |
|---|---|---|---|---|---|
| | | EUI reduction [MJ/m$^2$] | Reduction % | Energy Use reduction [TJ] | Reduction % |
| Edu | EPD | 7.56 | 1.05 | 1.29 | 1.05 |
| Lab | EPD | 76.16 | 3.23 | 19.03 | 3.23 |
| Res | EPD | 6.06 | 0.71 | 1.64 | 0.71 |
| Svc | EPD | 20.54 | 2.04 | 2.51 | 2.04 |
| Campus | - | - | - | 24.47 | 2.29 |

Table 7-10 presents the reduction of EUI and energy consumption for each building type and overall CU campus as a result of ECM1. The EPD range of the laboratory building stock was larger than others so that the reduction of energy also use larger than other building types. As a result, the ECM 1 (decreasing 10% of EPD for all buildings) can reduce 24.47 TJ of energy use, and it is equivalent to 2.29% of reduction in energy use.

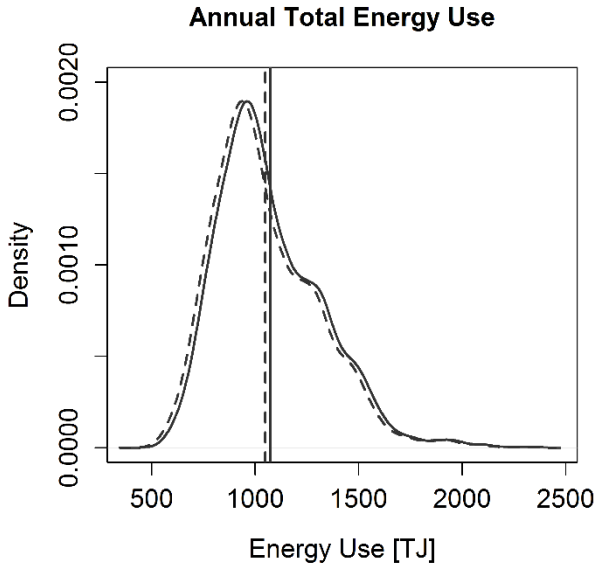


Figure 7-35 Comparison campus total energy use by ECM1

7.3.7.2 ECM Case 2. Comparison two ECMs

The second case is examined to compare ECMs. When we have limited resources, we can compare the efficiencies of ECM in the building stock. Table 7-11 shows the measured energy use data and total floor area for each building stock. In the CU campus, the laboratory building stock and the residence building stock have similar total floor area. The energy use of the laboratory building type is about three times greater than the one of the residence building type. In the ranking of parameters (Table 7-9), lighting power density (LPD) is the fourth dominant parameter in the laboratory type and second dominant parameter in the residence building type. In such context, we can compare the efficiencies between the reduction of 10% in LPD in the laboratory building stock and that of 10% in LPD in the residence building stock.

As shown in Figure 7-36, the posterior distributions of LPD were shifted to the left and fed into the meta-model (MLR). Figure 7-37 and Table 7-12 compare the reduction of energy use by reducing 10% of LPD.

Table 7-11 CU energy use and total floor area data

| | Edu | Lab | Res | Svc | Campus |
|---|---|---|---|---|---|
| **Energy Use [GJ]** | 128,151 | 556,324 | 193,145 | 124,009 | 1,001,629 |
| **Energy Use Ratio [%]** | 13% | 56% | 19% | 12% | 100% |
| **Total floor area [$m^2$]** | 170,374 | 249,889 | 235,668 | 122,164 | 778,095 |
| **Total floor area Ratio [%]** | 22% | 32% | 30% | 16% | 100% |

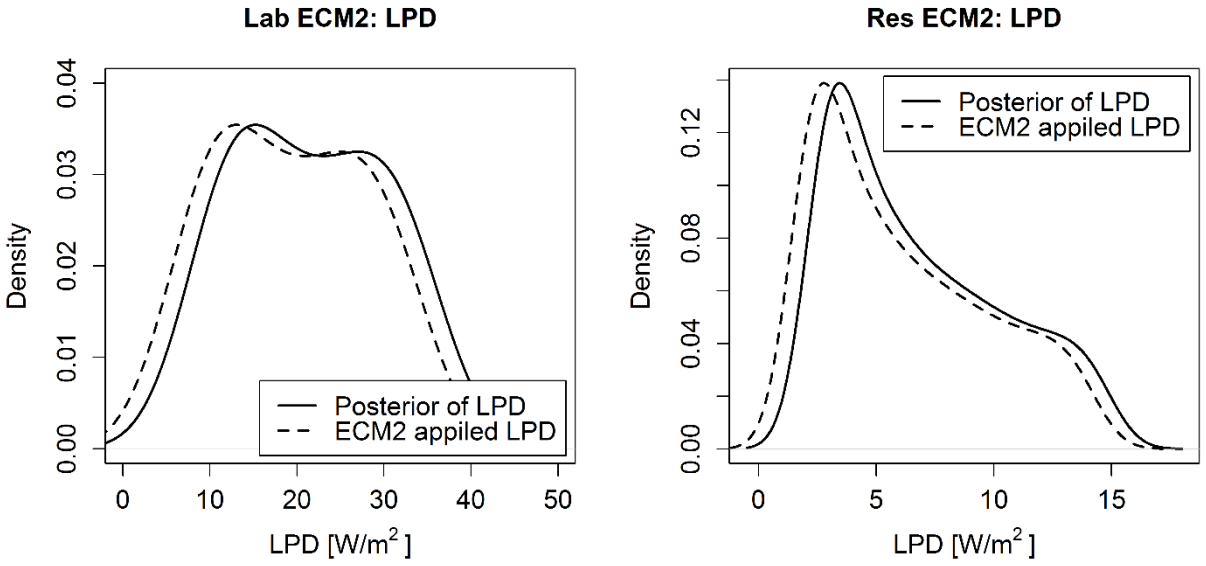


(a) Case 2-1. LPD distribution of Laboratory (b) Case 2-2. LPD distribution of Residence

Figure 7-36 ECM 2 applied parameter distribution

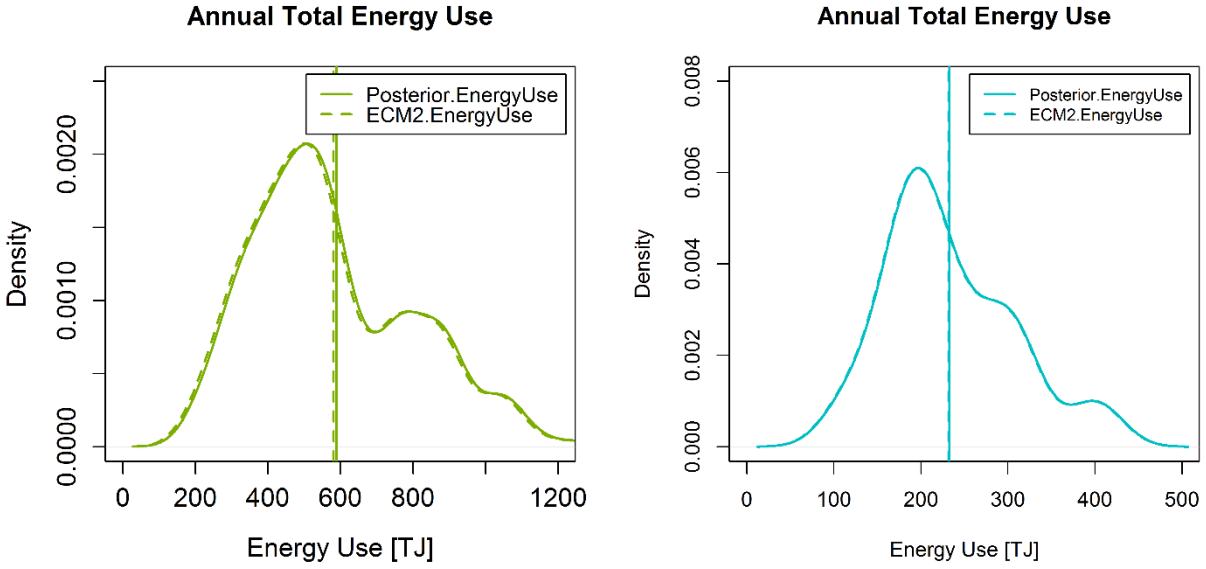


(a) Case 2-1. Laboratory (b) Case 2-2. Residence

Figure 7-37 Annual total energy use distribution for ECM 2

Table 7-12 Results of ECM 2

| Building type | Parameter | EUI | | Energy Use | |
|---|---|---|---|---|---|
| | | EUI reduction [MJ/m$^2$] | Reduction % | Energy Use reduction [TJ] | Reduction % |
| **Case 2-1. Lab** | LPD | 31.04 | 1.32 | 7.76 | 1.32 |
| **Case 2-2. Res** | LPD | 2.88 | 0.34 | 0.78 | 0.34 |

As a result, reducing 10% of LPD in the laboratory building stock was more effective than 10% reducing of LPD in the residence building. Using this method, we can determine the effectiveness of each ECM in the CU campus.

#### 7.3.7.3 ECM Case 3. How to apply ECM for non-dominant parameter

The third case applied the ECM to the non-dominant parameters. The meta-model (MLR) can be used to evaluate the ECM for the dominant parameters. However, a question remains in the evaluation of the ECM for the non-dominant parameters or new technologies that are not related to the dominant parameters. In this case, we decided to replace the poor glazing window (over 2.8 $W/m^2K$) with the double glazing window (2.8 $W/m^2K$) in the residence building stock. This ECM can be considered as a code enforced retrofit.

The process is as follows. The first step is extracting samples from the posterior distribution. After the Bayesian calibration, there are 10,000 samples for each parameter. The developed meta-model cannot express the non-dominant parameters or new technology; the ECM applied samples should be fed into the EnergyPlus. However, 10,000 of samples are too large to run the EnergyPlus. Therefore, only 200 samples were extracted from the posterior distribution. The second step involves the creation of ECM applied input parameter. In the prior distribution, the distribution of window U-value was uniform, ranging from 1.5 to 6.0 $W/m^2K$. The 200 samples from the prior distribution of window U-value were the baseline for the ECM application. we applied the ECM to the 200 samples that were extracted from the uniform distribution. If the window U-value exceeds 2.8 $W/m^2K$, the U-value was changed to 2.8 $W/m^2K$. Figure 7-38 compares the baseline and ECM applied window U-value distributions. The maximum value of ECM applied window U-value was 2.8 $W/m^2K$. The third step is feeding the baseline and ECM applied samples into the EnergyPlus.

Figure 7-39 shows the change in the annual total energy use in the residence building stock as a result of ECM 3. Unlike previous results, the shape of distribution has been modified after the application of ECM since the shape of distribution for ECM applied window U-value was changed from the original uniform distribution. The vertical line presents the average value of each distribution and the energy reduction caused by ECM 3 is presented in Table 7-13. As a result of ECM 3, when the windows greater than 2.8 $W/m^2K$ of U-value were replaced with the double glazing window, approximately 3.28 TJ can be saved in the residence building.

Indeed, the ECM case 3 shows the advantage of the stochastic method. While existing deterministic methods only consider applying the ECM to the whole building stock, the proposed building stock energy model can reflect the effect of implementing the ECM to the partial building stock.

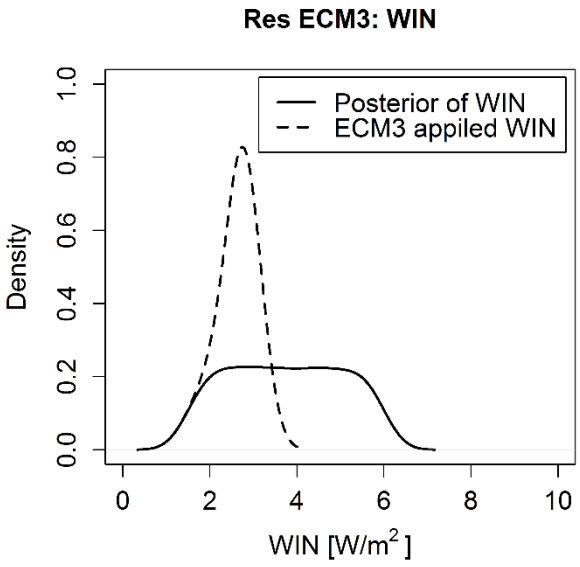


Figure 7-38 ECM 3 applied parameter distribution

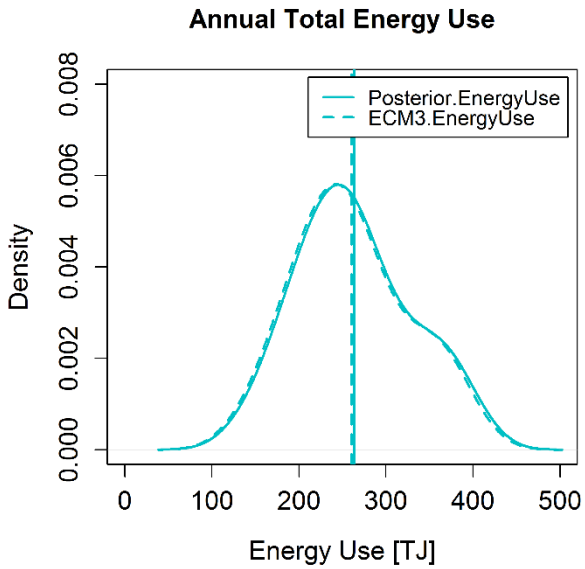


Figure 7-39 Annual total energy use distribution for Residence

Table 7-13 Results of ECM 3

| Building type | Parameter | EUI | | Energy Use | |
|---|---|---|---|---|---|
| | | EUI reduction [MJ/m$^2$] | Reduction % | Energy Use reduction [TJ] | Reduction % |
| **Case 3. Res** | WIN | 12.08 | 1.24 | 3.28 | 1.24 |

## 7.4 Discussion and Conclusion

The purpose of this chapter was to estimate the building energy consumption at the campus-scale using the proposed stochastic-deterministic-coupled building stock energy model. The measured energy

use data and various building information such as building function, floor numbers, building age and total floor area were analyzed to classify the representative building type. As a result of the data analysis, we concluded that the building energy consumption depends on the building function rather than the building age on the CU campus, and then we classified 80 buildings into four types of representative buildings.

The sensitivity analysis was performed to determine dominant variables for each representative building. The results of the sensitivity analysis showed that each representative building had different dominant parameters. These findings suggest that we need different strategies to reduce the building energy consumption for each type of building stock.

The multiple linear regression meta-model and Bayesian inference were used for the calibration of developed building stock model. We obtained calibrated distributions of dominant parameters. These calibrated distributions of parameters should be considered as the best guess to match the actual energy use rather than an actual distribution of the parameter. After the calibration, the estimated building energy consumption at the CU campus was matched successfully for both entire campus and each type of building stock. Using the proposed method, the annual energy use as well as monthly energy use has been calibrated by energy type.

Then, the estimated posterior distributions for parameters were employed to estimate the energy conservation measures. The probabilistic methodology can produce a more advanced analysis compare to deterministic methods. In this ECM analysis using the probabilistic method, for example, we compared two ECMs to assess which measure is more effective on the whole CU campus with limited resources given. It is also possible to evaluate the effect applying the energy conservation measures to only a part of building stock. In this chapter, the proposed stochastic-deterministic-coupled building stock energy model was validated at the campus-scale. The method can be further improved by employing other techniques such as more accurate regression model, classification using the machine learning, detailed representative building model, and data gathering using geographic information system (GIS) data.

# CHAPTER 8: CONCLUSIONS AND FUTURE WORK

## 8.1 Summary and conclusions

Many building stock models have been developed due to the increased interest in estimation of building energy consumption in existing building stock. The building stock models can be broadly divided into two methods: top-down and bottom-up. The bottom-up models can be further classified into two types of approaches: statistical and engineering models. Top-down models have limitations to consider at an individual building level. The bottom-up statistical models require numerous empirical data and have a limited capability to assess the impact of new technologies. The bottom-up deterministic engineering models cannot consider an uncertainty problems. To overcome the uncertainty issue, stochastic methods such as Monte Carlo, Bayesian calibration were applied to the engineering models. However, there have been few stochastic building stock models and existing stochastic models also have some limitations in terms of computational cost, insufficient building stock information, and calibration process.

The purpose of this dissertation is the development of improved stochastic building stock energy model for predicting the urban scale building energy use. In order to overcome the limitations of current models, this dissertation proposed a stochastic-deterministic-coupled model was proposed based on the Bayesian calibration and meta-models. Detailed analyses were conducted for each step of the proposed methodology. The main findings and conclusions drawn are:

- Bayesian calibration and inverse models were compared to choose a stochastic method. Bayesian calibration was selected to take advantage of existing knowledge and various meta-models. It has been quantitatively confirmed that using meta-models instead of the original dynamic building energy model can save computational time.

- In order to reduce the computation time in the Bayesian calibration process, the dominant parameters were selected through the sensitivity analysis and the calibration was performed for the dominant parameters. The sensitivity value index (SVI) was presented that can synthesize the difference by various sensitivity analysis methods and various target outputs.

- A meta-model is used to reduce the time to process the MCMC in Bayesian calibration. Analysis of the effect of meta-models' accuracy on the results of Bayesian calibration was carried out. The accuracy of the five meta-models (MLR, NN, SVM, MARS, and GPE) was compared, and the Bayesian calibration results using the meta-models were compared. This study has confirmed that the computing time and the accuracy of calibration varied according to the type of meta-model. Using the GPE showed the best accuracy while it took a long time than others. The calibration using MLR is less accurate than others in predicting parameter values due to model errors. However, estimation of energy use showed good agreement (In the base range case, the CVRMSE were less than 1.2% for monthly EUI and 0.3% for annual EUI). Focusing only on simulation time and energy usage prediction, the availability of Bayesian calibration using MLR has been confirmed.

- Energy usage data is essential for the calibration. A methodology using a correlation analysis and a hierarchical clustering was proposed to determine informative energy data for the Bayesian calibration. The influence of the quantity and quality of energy data on the accuracy of the Bayesian calibration was analyzed in an individual building. Even though there is insufficient energy data, one can obtain reliable results if the informative data was selected using the proposed method. Furthermore, computational cost can be reduced by using only informative energy data for Bayesian calibration. The selection of informative energy data should be chosen considering the purpose of the calibration and computational cost.

- The proposed stochastic-deterministic-coupled building stock energy model was analyzed using commercial and residential virtual building stocks. The differences between the stochastic individual building model and stochastic building stock model were examined by comparing both models. The proposed method produces distorted posterior distributions which differ from the target distribution for input parameters due to meta-model error. It is confirmed that the distorted posterior distribution can be used to evaluate the effect of ECM. An aggregation method of the EUI distributions for different building type stocks was examined, and it can be applied to other temporal scales to find peak energy demand for the target district.

- There are three kinds of building stock information needed to implement the proposed stochastic-deterministic-coupled building stock energy model: building energy use data, building features, and total floor area. The necessary information was summarized according to the degree of detail, and the alternative information to replace the insufficient information was examined. Then, influence of uncertainty in building stock data on energy prediction was analyzed. In a given case, the influence of the building type information was the greatest.

- The proposed stochastic-deterministic-coupled building stock energy model was applied at campus scale. 80 buildings in the target campus are classified into four building types. A regression method was proposed to reduce calibration errors due to different energy usage patterns in the same building type. After the calibration, the estimated building energy consumption at the campus was matched successfully for both entire campus (within 3%) and each type of building stock (within 7.5%). Using the proposed method, the annual energy use as well as monthly energy use has been calibrated by energy type. Moreover, the estimated posterior distributions for parameters were employed to estimate the energy conservation measures. The probabilistic methodology can produce a more advanced analysis compare to deterministic methods.

- The proposed method allows modeling current energy use and evaluating potential energy conservation measures at various spatial and temporal resolution. The methodology can be used by policy-makers and urban planners to evaluate effects of retrofits and to provide energy demand for energy supply alternatives such as distributed generation and district heating and cooling. By enabling stochastic results of building stocks, the proposed method can help local governments and utilities decide on energy-related policies and incentives.

## 8.2 Future work

The work undertaken in this thesis has highlighted interesting research questions and future investigations. In this context, some of the recommendations for future work have been identified:

- Expansion of the proposed model into urban-scale
    - The proposed stochastic building stock energy model was demonstrated at campus scale. The proposed model needs to be validated on a larger scale. New problems that did not occur on the campus scale are expected. The most challenge is to access building stock information. Collaboration with local government and utility companies is needed.
    - Once the building stock data is collected, buildings should be grouped according to building properties. In the influence study on building stock information (Chapter 6), information about the type of building was found to be important. Therefore, more research on how to organize and classify the information of many buildings will be needed. In the current model, the building data analysis and classification of buildings were performed manually. This work may be subjective of the modeler. Clustering and classification techniques such as machine learning can be introduced to define archetypes.

- Improving the accuracy of meta-model
    - The proposed model uses the multiple linear regression models (MLR) as a meta-model because of computational time. In chapter 4, it was found that accurate meta-model leads to accurate calibration results. There is a need for a way to increase the accuracy of MLR without significantly increasing computational time. A various transformation such as interaction and second-order terms can be included to increase the predictive performance.

- Including statistical parameters
    - The proposed model is based on engineering building model. It is expected that the accuracy of the model can be improved by combining statistical parameters in the current model. For example, even in the same type of housing, there will be a difference in energy use depending on the annual income or age of people. The combination of these

statistical parameters will reduce the uncertainty that the engineering model does not cover.

- Uncertainty of occupancy schedule
    - The parameters related human behavior in building energy modeling remain the greatest uncertainty yet. Moreover, these are the most characteristic parameters that classify the building type and function. Building schedules have traditionally been simplified by using deterministic hourly schedules and peak loads. The proposed stochastic-deterministic-coupled building stock energy model also uses deterministic building schedules. Further study on schedule model considering uncertainty due to human behavior is required.

- Development of interactive map
    - By developing the proposed model, an interactive map can be developed that is linked with GIS data. GIS will make it easier to obtain building stock information. The floor area data from the GIS will facilitate the aggregation process. An understanding of building stock energy will be enhanced through the interactive map of various temporal and spatial analyses, including energy retrofit analysis.

## REFERENCE


Akaike, H. (2011). Akaike's Information Criterion. In *International Encyclopedia of Statistical Science* (p. 25). Springer.

Alfons, A. (2012). cvTools: Cross-validation tools for regression models.

Alobeid, A., Jacobsen, K., & Heipke, C. (2009). Building height estimation in urban areas from very high resolution satellite stereo images. In *ISPRS Hannover Workshop* (pp. 2–5).

Anderson, B. R., Clark, A. J., Baldwin, R., & Milbank, N. O. (1985). *BREDEM: The BRE Domestic Energy Model*. Building Research Establishment.

Angelikopoulos, P., Papadimitriou, C., & Koumoutsakos, P. (2012). Bayesian uncertainty quantification and propagation in molecular dynamics simulations: a high performance computing framework. *The Journal of Chemical Physics*, *137*(14), 144103. https://doi.org/10.1063/1.4757266

ASHRAE, A. S. (2004). Standard 90.1-2004, Energy standard for buildings except low rise residential buildings. *American Society of Heating, Refrigerating and Air-Conditioning Engineers, Inc*.

Aydinalp, M., Ugursal, V. I., & Fung, A. S. (2004). Modeling of the space and domestic hot-water heating energy-consumption in the residential sector using neural networks. *Applied Energy*, *79*(2), 159–178. https://doi.org/10.1016/j.apenergy.2003.12.006

Ballarini, I., Corgnati, S. P., & Corrado, V. (2014). Use of reference buildings to assess the energy saving potentials of the residential building stock: The experience of TABULA project. *Energy Policy*, *68*, 273–284. https://doi.org/10.1016/j.enpol.2014.01.027

Berger, J., Orlande, H. R. B., Mendes, N., & Guernouti, S. (2016). Bayesian inference for estimating thermal properties of a historic building wall. *Building and Environment*, *106*, 327–339. https://doi.org/10.1016/j.buildenv.2016.06.037

Birol, F. (2008). World energy outlook. *Paris: International Energy Agency*, *23*(4), 329. https://doi.org/10.1049/ep.1977.0180

Blangiardo, M., & Richardson, S. (2008). A Bayesian calibration model for combining different pre-processing methods in Affymetrix chips. *BMC Bioinformatics*, *9*, 512. https://doi.org/10.1186/1471-2105-9-512

Boardman, B. (2007). Examining the carbon agenda via the 40% House scenario. *Building Research & Information*, *35*(4), 363–378. https://doi.org/10.1080/09613210701238276

Boardman, B., Darby, S., Killip, G., Hinnells, M., Jardine, C. N., Palmer, J., … Peacock, A. (2005). *40% House*. Oxford: Environmental Change Institute, University of Oxford.

Bolstad, W. M. (2011). *Understanding computational Bayesian statistics* (Vol. 644). John Wiley & Sons.

Bonnema, E., Leach, M., Pless, S., & Torcellini, P. (2013). *Development of the Advanced Energy Design Guide for K-12 Schools–50% Energy Savings*. *Contract*.

Booth, A. T., & Choudhary, R. (2013). Decision making under uncertainty in the retrofit analysis of the UK housing stock: Implications for the Green Deal. *Energy and Buildings*, *64*, 292–308. https://doi.org/10.1016/j.enbuild.2013.05.014

Booth, A. T., Choudhary, R., & Spiegelhalter, D. J. (2012). Handling uncertainty in housing stock models. *Building and Environment*, *48*(1), 35–47. https://doi.org/10.1016/j.buildenv.2011.08.016

Booth, A. T., Choudhary, R., & Spiegelhalter, D. J. (2013). A hierarchical Bayesian framework for calibrating micro-level models with macro-level data. *Journal of Building Performance Simulation*, *6*(4), 293–318. https://doi.org/10.1080/19401493.2012.723750

Breiman, L. (2001). Random forests. *Machine Learning*, *45*(1), 5–32.

Brooks, S., & Gelman, A. (1998). General methods for monitoring convergence of iterative simulations. *Journal of Computational and Graphical Statistics*, *7*(4), 434–455.

Brunner, D., Lemoine, G., Bruzzone, L., & Greidanus, H. (2010). Building height retrieval from VHR SAR imagery based on an iterative simulation and matching technique. *IEEE Transactions on Geoscience and Remote Sensing*, *48*(3 PART2), 1487–1504. https://doi.org/10.1109/TGRS.2009.2031910

Burhenne, S., Jacob, D., & Henze, G. P. (2011). Sampling based on Sobol'sequences for Monte Carlo techniques applied to building simulations. In *Proceedings of Building Simulation 2011*.

C.~Cortes, C.~Cortes, V.~Vapnik, & V.~Vapnik. (1995). Support Vector Networks. *Machine Learning*, *20*(3), 273~-~297. https://doi.org/10.1007/BF00994018

Caputo, P., Costa, G., & Ferrari, S. (2013). A supporting method for defining energy strategies in the building sector at urban scale. *Energy Policy*, *55*, 261–270. https://doi.org/10.1016/j.enpol.2012.12.006

Chen, Z., Xu, J., & Soh, Y. C. (2015). Modeling regular occupancy in commercial buildings using stochastic models. *Energy and Buildings*, *103*, 216–223. https://doi.org/10.1016/j.enbuild.2015.06.009

Cheng, M.-Y., & Cao, M. (2014). Accurately predicting building energy performance using evolutionary multivariate adaptive regression splines. *Applied Soft Computing*, *22*, 178–188. https://doi.org/10.1016/j.asoc.2014.05.015

Choudhary, R. (2012). Energy analysis of the non-domestic building stock of Greater London. *Building and Environment*, *51*, 243–254. https://doi.org/10.1016/j.buildenv.2011.10.006

Choudhary, R., & Tian, W. (2013). Influence of district features on energy consumption in non-domestic

buildings. *Building Research & Information*, *42*(1), 32–46. https://doi.org/10.1080/09613218.2014.832559

Clarke, J., Strachan, P. A., & Pernot, C. (1993). An approach to the calibration of building energy simulation models. *Transitions-American Society of Heating Refrigerating and Air Conditioning Engineers*, (Judkoff 1983), 917–930.

Clevenger, C. M., Haymaker, J. R., & Jalili, M. (2014). Demonstrating the Impact of the Occupant on Building Performance. *Journal of Computing in Civil Engineering*, *28*(1), 99–102. https://doi.org/10.1061/(ASCE)CP.1943-5487.0000323

Coakley, D., Raftery, P., & Keane, M. (2014). A review of methods to match building energy simulation models to measured data. *Renewable and Sustainable Energy Reviews*, *37*, 123–141. https://doi.org/10.1016/j.rser.2014.05.007

Comodi, G., Cioccolanti, L., & Gargiulo, M. (2012). Municipal scale scenario: Analysis of an Italian seaside town with MarkAL-TIMES. *Energy Policy*, *41*, 303–315. https://doi.org/10.1016/j.enpol.2011.10.049

Corrado, V., & Mechri, H. E. (2009). Uncertainty and Sensitivity Analysis for Building Energy Rating. *Journal of Building Physics*, *33*(2), 125–156. https://doi.org/10.1177/1744259109104884

Crawley, D. B., Lawrie, L. K., Winkelmann, F. C., Buhl, W. F., Huang, Y. J., Pedersen, C. O., … Glazer, J. (2001). EnergyPlus: Creating a new-generation building energy simulation program. *Energy and Buildings*, *33*(4), 319–331. https://doi.org/10.1016/S0378-7788(00)00114-6

Dancik, G. M. (2013). mlegp: Maximum Likelihood Estimates of Gaussian Processes.

Davila, C. C., Reinhart, C., & Bemis, J. (2016). Modeling Boston: A workflow for the generation of complete urban building energy demand models from existing urban geospatial datasets. *Energy*, *117*, 237–250. https://doi.org/10.1016/j.energy.2016.10.057

de Wilde, P., & Tian, W. (2010). Predicting the performance of an office under climate change: A study of metrics, sensitivity and zonal resolution. *Energy and Buildings*, *42*(10), 1674–1684. https://doi.org/10.1016/j.enbuild.2010.04.011

Department of Economic and Social Affairs. (2012). *World Urbanization Prospects The 2011 Revision*. *Population*.

Deru, M., Field, K., Studer, D., & Benne, K. (2011). *US Department of Energy commercial reference building models of the national building stock*. https://doi.org/NREL Report No. TP-5500-46861

Diaz-Uriarte, R., & Alvarez de Andres, S. (2005). Variable selection from random forests : application to gene expression data, 1–11.

Diraco, G., Leone, A., & Siciliano, P. (2015). People occupancy detection and profiling with 3D depth

sensors for building energy management. *Energy and Buildings*, *92*, 246–266. https://doi.org/10.1016/j.enbuild.2015.01.043

Dorer, V., Allegrini, J., Orehounig, K., Moonen, P., Upadhyay, G., Kämpf, J., & Carmeliet, J. (2013). Modelling the urban microclimate and its impact on the energy demand of buildings and building clusters. *Proceedings of BS 2013: 13th Conference of the International Building Performance Simulation Association*, 3483–3489.

Duarte, C., Van Den Wymelenberg, K., & Rieger, C. (2013). Revealing occupancy patterns in an office building through the use of occupancy sensor data. *Energy and Buildings*, *67*, 587–595. https://doi.org/10.1016/j.enbuild.2013.08.062

Dunham, M. H. (2006). *Data mining: Introductory and advanced topics*. Pearson Education India.

Ebden, M. (2008). Gaussian processes for regression: A quick introduction. *The Website of Robotics Research Group in Department on Engineering Science, University of Oxford*, (August).

Edmonds, J. E., Wise, M. A., & MacCracken, C. N. (1994). *Advanced energy technologies and climate change: An analysis using the global change assessment model (GCAM)*. Fondazione ENI Enrico Mattei.

EIA. (2016). *Annual Energy Outlook 2016*. *U.S. Energy Information Administration*. https://doi.org/EIA-0383(2016)

Eisenberg, B., & Sullivan, R. (2008). Why Is the Sum of Independent Normal Random Variables Normal? *Mathematics Magazine*, *81*(5), 362–366. https://doi.org/10.2307/27643141

Eisenhower, B. (2011). Uncertainty and Sensitivity Analysis in Building Energy Models.

Eisenhower, B., O'Neill, Z., Fonoberov, V. A., & Mezić, I. (2012). Uncertainty and sensitivity decomposition of building energy models. *Journal of Building Performance Simulation*, *5*(3), 171–184. https://doi.org/10.1080/19401493.2010.549964

Eisenhower, B., O'Neill, Z., Narayanan, S., Fonoberov, V. a., & Mezić, I. (2012). A methodology for meta-model based optimization in building energy models. *Energy and Buildings*, *47*, 292–301. https://doi.org/10.1016/j.enbuild.2011.12.001

Ekici, B. B., & Aksoy, U. T. (2009). Prediction of building energy consumption by using artificial neural networks. *Advances in Engineering Software*, *40*(5), 356–362. https://doi.org/10.1016/j.advengsoft.2008.05.003

Energy Information Administration. (2003). Commercial Building Energy Consumption Survey. U.S. Department of Energy.

Energy Information Administration. (2005). Residential Energy Consumption Survey. U.S. Department of

Energy.

Energy Information Administration. (2009). *The National Energy Modeling System:An Overview 2009*.

Energy Management Michigan. (n.d.). Retrieved from http://energymanagement.umich.edu/

Evins, R., Orehounig, K., & Dorer, V. (2015). Variability between domestic buildings: the impact on energy use. *Journal of Building Performance Simulation*, *1493*(July), 1–14. https://doi.org/10.1080/19401493.2015.1006526

Fabrizio, E., & Monetti, V. (2015). Methodologies and advancements in the calibration of building energy models. *Energies*, *8*(4), 2548–2574. https://doi.org/10.3390/en8042548

Facilities Management. (n.d.-a). Alphabetical List of Major Buildings and Facilities. Retrieved from http://www.colorado.edu/fm/planning/alphabetical-list-major-buildings-and-facilities

Facilities Management. (n.d.-b). Energy Data (EnergyCAP). Retrieved from http://www.colorado.edu/fm/utility-services/energy-data

Facilities Management. (n.d.-c). Planning. Retrieved from http://www.colorado.edu/fm/planning-design-construction/planning

Facilities Management. (n.d.-d). Utility and Energy Services. Retrieved from http://www.colorado.edu/fm/departments/utility-services

Farahbakhsh, H., Ugursal, V. I., & Fung, a. S. (1998). A residential end-use energy consumption model for Canada. *International Journal of Energy Research*, *22*(13), 1133–1143. https://doi.org/10.1002/(SICI)1099-114X(19981025)22:13<1133::AID-ER434>3.0.CO;2-E

Faraway, J. J. (2014). *Linear models with R*. CRC Press.

Fels, M. F. (1986). PRISM: An introduction. *Energy and Buildings*, *9*(1–2), 5–18. https://doi.org/10.1016/0378-7788(86)90003-4

Firth, S. K., Lomas, K. J., & Wright, a. J. (2010). Targeting household energy-efficiency measures using sensitivity analysis. *Building Research & Information*, *38*(1), 25–41. https://doi.org/10.1080/09613210903236706

Fishbone, L. G., & Abilock, H. (1981). Markal, a linear-programming model for energy systems analysis: Technical description of the bnl version. *International Journal of Energy Research*, *5*(4), 353–375.

Fonseca, J. A., & Schlueter, A. (2015). Integrated model for characterization of spatiotemporal building energy consumption patterns in neighborhoods and city districts. *Applied Energy*, *142*, 247–265. https://doi.org/10.1016/j.apenergy.2014.12.068

Foucquier, A., Robert, S., Suard, F., Stéphan, L., & Jay, A. (2013). State of the art in building modelling

and energy performances prediction: A review. *Renewable and Sustainable Energy Reviews*, *23*, 272–288. https://doi.org/10.1016/j.rser.2013.03.004

Friedman, J. H. (1991). Multivariate adaptive regression splines. *The Annals of Statistics*, 1–67.

Friedman, J., Hastie, T., & Tibshirani, R. (2001). *The elements of statistical learning* (Vol. 1). Springer series in statistics Springer, Berlin.

Fritsch, S., & Guenther, F. (2016). neuralnet: Training of Neural Networks. https://doi.org/10.1109/SP.2010.25

Fumo, N. (2014). A review on the basics of building energy estimation. *Renewable and Sustainable Energy Reviews*, *31*, 53–60. https://doi.org/10.1016/j.rser.2013.11.040

Gelman, A., Carlin, J. B., Stern, H. S., & Rubin, D. B. (2014). *Bayesian data analysis* (Vol. 2). Taylor & Francis.

Gelman, A., & Rubin, D. B. (1992). Inference from iterative simulation using multiple sequences. *Statistical Science*, 457–472.

Gilks, W. R. (2005). *Markov chain monte carlo*. Wiley Online Library.

Girardin, L., Marechal, F., Dubuis, M., Calame-Darbellay, N., & Favrat, D. (2010). EnerGis: A geographical information based system for the evaluation of integrated energy conversion systems in urban areas. *Energy*, *35*(2), 830–840. https://doi.org/10.1016/j.energy.2009.08.018

Gowri, K., Halverson, M., & Richman, E. (2007). *Analysis of Energy Saving Impacts of ASHRAE 90.1-2004 for the State of New York. Richland, WA: Pacific Northwest …*.

Griffith, B., Long, N., Torcellini, P., & Judkoff, R. (2008). *Methodology for modeling building energy performance across the commercial sector*.

Guillas, S., Rougier, J., Maute, a., Richmond, a. D., & Linkletter, C. D. (2009). Bayesian calibration of the Thermosphere-Ionosphere Electrodynamics General Circulation Model (TIE-GCM). *Geoscientific Model Development Discussions*, *2*(1), 485–506. https://doi.org/10.5194/gmdd-2-485-2009

Guillaso, S., Ferro-Famil, L., Reigber, A., & Pottier, E. (2005). Building characterization using L-band polarimetric interferometric SAR data. *IEEE Geoscience and Remote Sensing Letters*, *2*(3), 347–351. https://doi.org/10.1109/LGRS.2005.851543

Haithcoat, T. L., Song, W., & Hipple, J. D. (2001). Building footprint extraction and 3-D reconstruction from LIDAR data. In *IEEE/ISPRS Joint Workshop on Remote Sensing and Data Fusion over Urban Areas, DFUA 2001* (pp. 74–78). IEEE. https://doi.org/10.1109/DFUA.2001.985730

Haldi, F., & Robinson, D. (2011). The impact of occupants' behaviour on building energy demand. *Journal*

*of Building Performance Simulation*, *4*(4), 323–338. https://doi.org/10.1080/19401493.2011.558213

Hashimoto, S., Yamaguchi, Y., Shimoda, O., & Mizuno, M. (2007). Simulation model for multi-purpose evaluation of urban energy system. In *Proceedings: Building Simulation 2007* (pp. 554–561).

HASTINGS, W. K. (1970). Monte Carlo sampling methods using Markov chains and their applications. *Biometrika* , *57*(1), 97–109. https://doi.org/10.1093/biomet/57.1.97

He, M., Lee, T., Taylor, S., Firth, S. K., & Lomas, K. J. (2015). Coupling a stochastic occupancy model to EnergyPlus to predict hourly thermal demand of a neighbourhood, 2101–2108.

Heiple, S. (2007). *Using building energy simulation and geospatial modeling techniques to determine high resolution building sector energy consumption profiles*. Portland State University.

Heiple, S., & Sailor, D. J. (2008). Using building energy simulation and geospatial modeling techniques to determine high resolution building sector energy consumption profiles. *Energy and Buildings*, *40*(8), 1426–1436. https://doi.org/10.1016/j.enbuild.2008.01.005

Henze, G. P., Pavlak, G. S., Florita, A. R., Dodier, R. H., Hirsch, A. I., Henze, G. P., … Hirsch, A. I. (2014). An Energy Signal Tool for Decision Support in Building Energy Systems An Energy Signal Tool for Decision Support in Building Energy Systems, (December), 1–53.

Heo, Y. (2011). *Bayesian calibration of building energy models for energy retrofit decision-making under uncertainty*. Georgia Institute of Technology.

Heo, Y., Augenbroe, G., & Choudhary, R. (2011). Risk analysis of energy-efficiency projects based on Bayesian calibration of building energy models. In *Building simulation* (Vol. 2002, pp. 2579–2586).

Heo, Y., Augenbroe, G., & Choudhary, R. (2013). Quantitative risk management for energy retrofit projects. *Journal of Building Performance Simulation*, *6*(4), 257–268. https://doi.org/10.1080/19401493.2012.706388

Heo, Y., Augenbroe, G., Graziano, D., Muehleisen, R. T., & Guzowski, L. (2015). Scalable methodology for large scale building energy improvement: Relevance of calibration in model-based retrofit analysis. *Building and Environment*, *87*, 342–350. https://doi.org/10.1016/j.buildenv.2014.12.016

Heo, Y., Choudhary, R., & Augenbroe, G. A. (2012). Calibration of building energy models for retrofit analysis under uncertainty. *Energy and Buildings*, *47*, 550–560. https://doi.org/10.1016/j.enbuild.2011.12.029

Heo, Y., Graziano, D. J., Guzowski, L., & Muehleisen, R. T. (2015). Evaluation of calibration efficacy under different levels of uncertainty. *Journal of Building Performance Simulation*, *8*(3), 135–144. https://doi.org/10.1080/19401493.2014.896947

Hirsch, J. J. (2006). eQuest, the QUick Energy Simulation Tool. *DOE2. Com*.

Hong, T., & Lin, H.-W. (2013). Occupant Behavior: Impact on Energy Use of Private Offices. *ASim 2012 - 1st Asia Conference of International Building Performance Simulation Association.*, 12.

Hopfe, C. (2009). *Uncertainty and sensitivity analysis in building performance simulation for decision support and design optimization*. *Technische Universiteit Eindhoven*. Technische Universiteit Eindhoven.

Hopfe, C. J., & Hensen, J. L. M. (2011). Uncertainty analysis in building performance simulation for design support. *Energy and Buildings*, *43*(10), 2798–2805. https://doi.org/10.1016/j.enbuild.2011.06.034

Howard, B., Parshall, L., Thompson, J., Hammer, S., Dickinson, J., & Modi, V. (2012). Spatial distribution of urban building energy consumption by end use. *Energy and Buildings*, *45*, 141–151. https://doi.org/10.1016/j.enbuild.2011.10.061

Huang, Y., & Franconi, E. (1999). *Commercial heating and cooling loads component analysis*. *Energy Analysis Program*. Berkeley, CA.

ISO, E. N. (2004). 13790-Thermal performance of buildings-Calculation of energy use for space heating. *International Organization for Standardization*.

Jacob, D., Burhenne, S., Florita, A., & Henze, G. (2010). Optimizing building energy simulation models in the face of uncertainty. In *Fourth National Conference of IBPSA-USA* (pp. 11–13). New York City, New York.

Johnston, D. (2003). *A physically-based energy and carbon dioxide emission model of the UK housing stock*. Leeds Metropolitan University.

Jones, P., Patterson, J., & Lannon, S. (2007). Modelling the built environment at an urban scale—Energy and health impacts in relation to housing. *Landscape and Urban Planning*, *83*(1), 39–49. https://doi.org/10.1016/j.landurbplan.2007.05.015

Jones, P., Williams, J., & Lannon, S. (2000). Planning for a sustainable city: an energy and environmental prediction model. *Journal of Environmental Planning and Management*, *43*(6), 855–872.

Kainuma, M., Matsuoka, Y., & Morita, T. (1998). *Analysis of post-Kyoto scenarios: The AIM model*. *Economic Modeling of Climate Change: OECD Workshop Report*.

Kalogirou, S. (2000). Artificial neural networks for the prediction of the energy consumption of a passive solar building. *Energy*, *25*(5), 479–491. https://doi.org/10.1016/S0360-5442(99)00086-9

Kämpf, J. J. H. (2009). *On the modelling and optimisation of urban energy fluxes*. ÉCOLE POLYTECHNIQUE FÉDÉRALE DE LAUSANNE. https://doi.org/10.5075/epfl-thesis-4548

Kämpf, J., & Robinson, D. (2009). Optimisation of urban Energy Demand using an evolutionary Algorithm. *Eleventh International IBPSA Conference, …*, 668–673.

Kang, Y., & Krarti, M. (2016). Bayesian-Emulator based parameter identification for calibrating energy models for existing buildings. *Building Simulation*, 411–428. https://doi.org/10.1007/s12273-016-0291-6

Karatzoglou, A., Smola, A., Hornik, K., & Zeileis, A. (2004). kernlab – An S4 Package for Kernel Methods in R. *Journal of Statistical Software*, *11*(9), 1–20. https://doi.org/10.1016/j.csda.2009.09.023

Kavgic, M., Mavrogianni, A., Mumovic, D., Summerfield, A., Stevanovic, Z., & Djurovic-Petrovic, M. (2010). A review of bottom-up building stock models for energy consumption in the residential sector. *Building and Environment*, *45*(7), 1683–1697. https://doi.org/10.1016/j.buildenv.2010.01.021

Kennedy, M. C., & O'Hagan, A. (2001). Bayesian calibration of computer models. *Journal of the Royal Statistical Society: Series B (Statistical Methodology)*, *63*(3), 425–464. https://doi.org/10.1111/1467-9868.00294

Kim, J.-H., Augenbroe, G., Suh, H.-S., & Wang, Q. (2015). DOMESTIC BUILDING ENERGY PREDICTION IN DESIGN STAGE UTILIZING LARGE-SCALE CONSUMPTION DATA FROM REALIZED PROJECTS. In *Proceedings of BS2015: 14th Conference of International Building Performance Simulation Association*. Hyderabad, India.

Kim, Y.-J., Ahn, K.-U., Park, C.-S., & Kim, I.-H. (2013). Gaussian emulator for stochastic optimal design of a double glazing system. In *Proceedings of the 13th IBPSA Conference (International Building Performance Simulation Association)* (pp. 2217–2224). Chambery, France.

Kim, Y.-J., Yoon, S.-H., & Park, C.-S. (2013). Stochastic comparison between simplified energy calculation and dynamic simulation. *Energy and Buildings*, *64*, 332–342. https://doi.org/10.1016/j.enbuild.2013.05.026

Kim, Y. J. (2016). Comparative study of surrogate models for uncertainty quantification of building energy model: Gaussian Process Emulator vs. Polynomial Chaos Expansion. *Energy and Buildings*, *133*, 46–58. https://doi.org/10.1016/j.enbuild.2016.09.032

Kolter, J., & Ferreira, J. (2011). A Large-Scale Study on Predicting and Contextualizing Building Energy Usage. *AAAI*, 1349–1356.

Korolija, I., Marjanovic-Halburd, L., Zhang, Y., & Hanby, V. I. (2013). UK office buildings archetypal model as methodological approach in development of regression models for predicting building energy consumption from heating and cooling demands. *Energy and Buildings*, *60*, 152–162. https://doi.org/10.1016/j.enbuild.2012.12.032

Kucherenko, S., Albrecht, D., & Saltelli, A. (2011). Comparison of Latin Hypercube and Quasi Monte Carlo Sampling Techniques. *The 8th IMACS Seminar on Monte Carlo Methods*, 1–32.

Kyle, P., Clarke, L., Rong, F., & Smith, S. J. (2010). Climate Policy and the Long-Term Evolution of the

U.S. Buildings Sector. *The Energy Journal*, *31*(2), 301–314. https://doi.org/10.5547/ISSN0195-6574-EJ-Vol31-No2-6

Lee, S., Zhao, F., & Augenbroe, G. (2011). The use of normative energy calculation beyond building performance rating systems. In *Proceedings of the 12th International Building Performance Simulation Association Conference*. Sydney, Australia.

Li, Q., Augenbroe, G., & Brown, J. (2016). Assessment of linear emulators in lightweight Bayesian calibration of dynamic building energy models for parameter estimation and performance prediction. *Energy and Buildings*, *124*, 194–202. https://doi.org/10.1016/j.enbuild.2016.04.025

Li, Q., Gu, L., Augenbroe, G., & Brown, J. (2015). Calibration of Dynamic Building Energy Models with Multiple Responses Using Bayesian Inference and Linear Regression Models. *6th International Building Physics Conference, IBPC 2015*, (JUNE), 13–19. https://doi.org/10.1016/j.egypro.2015.11.037

Li, Q., Meng, Q., Cai, J., Yoshino, H., & Mochida, A. (2009). Applying support vector machine to predict hourly cooling load in the building. *Applied Energy*, *86*(10), 2249–2256. https://doi.org/10.1016/j.apenergy.2008.11.035

Liu, Y., Yang, P., Hu, C., & Guo, H. (2008). Water quality modeling for load reduction under uncertainty: a Bayesian approach. *Water Research*, *42*(13), 3305–14. https://doi.org/10.1016/j.watres.2008.04.007

Lomas, K. J., & Eppel, H. (1992). Sensitivity analysis techniques for building thermal simulation programs. *Energy and Buildings*, *19*(1), 21–44. https://doi.org/10.1016/0378-7788(92)90033-D

Loulou, R., Remme, U., Kanudia, A., Lehtila, A., & Goldstein, G. (2005). Documentation for the TIMES Model. Energy Technology Systems Analysis Programme (ETSAP).

MacDonald, B., Ranjan, P., & Chipman, H. (2015). GPfit: An R Package for Fitting a Gaussian Process Model to Deterministic Simulator Outputs. *Journal of Statistical Software*, *64*(12), ??-?? https://doi.org/http://dx.doi.org/10.18637/jss.v064.i12

Macdonald, I. (2002). *Quantifying the effects of uncertainty in building simulation*. University of Strathclyde.

Manfren, M., Aste, N., & Moshksar, R. (2013). Calibration and uncertainty analysis for computer models – A meta-model based approach for integrated building energy simulation. *Applied Energy*, *103*, 627–641. https://doi.org/10.1016/j.apenergy.2012.10.031

Massey Jr, F. J. (1951). The Kolmogorov-Smirnov test for goodness of fit. *Journal of the American Statistical Association*, *46*(253), 68–78.

Mathew, P., Sartor, D., van Geet, O., & Reily, S. (2004). Rating Energy Efficiency and Sustainability in

Laboratories : Results and Lessons from the Labs21 Program Energy Benchmarking. *ACEEE Summer Study of Energy Efficiency in Buildings*.

Matsuoka, Y., Kainuma, M., & Morita, T. (1995). Scenario analysis of global warming using the Asian Pacific Integrated Model (AIM). *Energy Policy*, *23*(4), 357–371.

McCulloch, W. S., & Pitts, W. (1943). A logical calculus of the ideas immanent in nervous activity. *The Bulletin of Mathematical Biophysics*, *5*(4), 115–133.

McKay, M., Beckman, R., & Conover, W. (1979). A Comparison of three methods for selecting values of input variables in the analysis of output from a computer code. *Technometrics*, *21*(2), 239–245. https://doi.org/10.1080/00401706.1979.10489755

Mckay, M. D., Beckman, R. J., & Conover, W. J. (2000). A Comparison of Three Methods for Selecting Values of Input Variables in the Analysis of Output From a Computer Code. *Technometrics*, *42*(1), 55–61. https://doi.org/10.1080/00401706.2000.10485979

Menberg, K., Heo, Y., & Choudhary, R. (2016). Sensitivity analysis methods for building energy models: Comparing computational costs and extractable information. *Energy and Buildings*, *133*, 433–445. https://doi.org/10.1016/j.enbuild.2016.10.005

Metropolis, N., Rosenbluth, A. W., Rosenbluth, M. N., Teller, A. H., & Teller, E. (1953). Equation of State Calculations by Fast Computing Machines. *The Journal of Chemical Physics*, *21*(6), 1087. https://doi.org/10.1063/1.1699114

Milborrow, S. (2017). earth: Multivariate Adaptive Regression Spline Models. Derived from mda: mars by Trevor Hastie and Rob Tibshirani. Uses Alan Miller's Fortran Utilities with Thomas Lumley's Leaps Wrapper. R Package Version 4.4.9.

Natarajan, S., & Levermore, G. J. (2007a). Domestic futures—Which way to a low-carbon housing stock? *Energy Policy*, *35*(11), 5728–5736. https://doi.org/10.1016/j.enpol.2007.05.033

Natarajan, S., & Levermore, G. J. (2007b). Predicting future UK housing stock and carbon emissions. *Energy Policy*, *35*(11), 5719–5727. https://doi.org/10.1016/j.enpol.2007.05.034

Nishio, K., & Asano, H. (2006). A residential end-use demand model for analyzing the energy conservation potential of new energy efficient technologies. In *Proceedings of energy efficiency in domestic appliances and lighting*. London, England.

O'Neill, Z., & Niu, F. (2017). Uncertainty and sensitivity analysis of spatio-temporal occupant behaviors on residential building energy usage utilizing Karhunen-Loève expansion. *Building and Environment*, *115*, 157–172. https://doi.org/10.1016/j.buildenv.2017.01.025

Oijen, M. Van, Rougier, J., & Smith, R. (2005). Bayesian calibration of process-based forest models:

bridging the gap between models and data. *Tree Physiology*, *25*(7), 915–927. https://doi.org/10.1093/treephys/25.7.915

Oladokun, M. G., & Odesola, I. A. (2015). Household energy consumption and carbon emissions for sustainable cities – A critical review of modelling approaches. *International Journal of Sustainable Built Environment*, *4*(2), 231–247. https://doi.org/10.1016/j.ijsbe.2015.07.005

Österbring, M., Mata, É., Thuvander, L., Mangold, M., Johnsson, F., & Wallbaum, H. (2016). A differentiated description of building-stocks for a georeferenced urban bottom-up building-stock model. *Energy and Buildings*, *120*, 78–84. https://doi.org/10.1016/j.enbuild.2016.03.060

Pacific Gas and Electric Company. (2011). *High Performance Laboratories*.

Page, J., Robinson, D., & Scartezzini, J. (2007). Stochastic simulation of occupant presence and behaviour in buildings. *… Int. IBPSA Conf: Building Simulation*, (April), 757–764. https://doi.org/10.5075/epfl-thesis-3900

Pavlak, G. S., Florita, A. R., Henze, G. P., & Rajagopalan, B. (2013). Comparison of Traditional and Bayesian Calibration Techniques for Gray-Box Modeling. *Journal of Architectural …*. https://doi.org/10.1061/(ASCE)AE.1943-5568.0000145.

Perez, D., Vautey, C., & Kämpf, J. (2012). Urban Energy Flow Microsimulation in a Heating Dominated Continental Climate. *SIMUL 2012, The Fourth International …*, (c), 18–23.

Petrov, V. (2012). *Sums of independent random variables* (Vol. 82). Springer Science & Business Media.

Pianosi, F., Beven, K., Freer, J., Hall, J. W., Rougier, J., Stephenson, D. B., & Wagener, T. (2016). Sensitivity analysis of environmental models: A systematic review with practical workflow. *Environmental Modelling and Software*, *79*, 214–232. https://doi.org/10.1016/j.envsoft.2016.02.008

Pless, S., Torcellini, P., & Long, N. (2007). *Technical Support Document: Development of the Advanced Energy Design Guide for K-12 Schools--30% Energy Savings*.

Qi, F., Zhai, J. Z., & Dang, G. (2016). Building height estimation using Google Earth. *Energy and Buildings*, *118*, 123–132. https://doi.org/10.1016/j.enbuild.2016.02.044

Qian, S. S., Reckhow, K. H., Zhai, J., & McMahon, G. (2005). Nonlinear regression modeling of nutrient loads in streams: A Bayesian approach. *Water Resources Research*, *41*(7), 1–10. https://doi.org/10.1029/2005WR003986

Quadrianto, N., Kersting, K., & Xu, Z. (2010). Gaussian Process. In C. Sammut & G. I. Webb (Eds.), *Encyclopedia of Machine Learning* (pp. 428–439). Boston, MA: Springer US. https://doi.org/10.1007/978-0-387-30164-8_324

R Core Team. (2016). R: A Language and Environment for Statistical Computing. Vienna, Austria: R

Foundation for Statistical Computing.

Rahn, K.-H., Butterbach-Bahl, K., & Werner, C. (2011). Selection of likelihood parameters for complex models determines the effectiveness of Bayesian calibration. *Ecological Informatics*, *6*(6), 333–340.

Ranjan, P., Haynes, R., & Karsten, R. (2011). A Computationally Stable Approach to Gaussian Process Interpolation of Deterministic Computer Simulation Data. *Technometrics*, *53*(4), 366–378. https://doi.org/10.1198/TECH.2011.09141

Rasmussen, C. C. E. (2006). *Gaussian processes for machine learning*. MIT Press.

Reddy, T. A. (2006). Literature Review on Calibration of Building Energy Simulation Programs. *ASHRAE Transactions*, *112*(1), 226–240. https://doi.org/Article

Reddy, T. A. (2011). *Applied data analysis and modeling for energy engineers and scientists*. Springer Science & Business Media.

Reddy, T., Maor, I., & Panjapornpon, C. (2007). Calibrating detailed building energy simulation programs with measured data—part II: application to three case study office buildings (RP-1051). *HVAC&R Research*, (January 2014), 37–41.

Reinhart, C. F., & Cerezo Davila, C. (2016). Urban building energy modeling - A review of a nascent field. *Building and Environment*. https://doi.org/10.1016/j.buildenv.2015.12.001

Residential Prototype Building Models. (n.d.). Retrieved from https://www.energycodes.gov/development/residential/iecc_models

Riddle, M., & Muehleisen, R. T. (2014). A guide to Bayesian calibration of building energy models. In *ASHRAE/IBPSA-USA Building Simulation Conference* (pp. 276–283). https://doi.org/10.13140/2.1.1674.9127

Roberts, G. O. (1996). Markov chain concepts related to sampling algorithms. In *Markov chain Monte Carlo in practice* (pp. 45–57). Springer.

Robinson, D., Campbell, N., Gaiser, W., Kabel, K., Le-Mouel, A., Morel, N., … Stone, A. (2007). SUNtool - A new modelling paradigm for simulating and optimising urban sustainability. *Solar Energy*, *81*(9), 1196–1211. https://doi.org/10.1016/j.solener.2007.06.002

Robinson, D., Haldi, F., Kämpf, J., & Leroux, P. (2009). CitySim: Comprehensive micro-simulation of resource flows for sustainable urban planning. In *Proceedings of Building Simulation 2009: 11th Conference of International Building Performance Simulation Association* (pp. 1083–1090). Glasgow, Scotland: International Building Performance Simulation Association.

Robinson, D., Wilke, U., & Haldi, F. (2011). MULTI AGENT SIMULATION OF OCCUPANTS'PRESENCE AND BEHAVIOUR. *Proceedings of Building Simulation*, 14–16.

Rottensteiner, F., & Briese, C. (2002). A new method for building extraction in urban areas from high-resolution LIDAR data. *International Archives of Photogrammetry Remote Sensing and Spatial Information Sciences*, *34*(3/A), 295–301. https://doi.org/10.3390/s120506347

Ruch, D., & Claridge, D. E. (1992). A four-parameter change-point model for predicting energy consumption in commercial buildings. *Journal of Solar Energy Engineering*, *114*(2), 77–83. https://doi.org/10.1115/1.2929993

Sailor, D. J., & Lu, L. (2004). A top–down methodology for developing diurnal and seasonal anthropogenic heating profiles for urban areas. *Atmospheric Environment*, *38*(17), 2737–2748. https://doi.org/10.1016/j.atmosenv.2004.01.034

Saltelli, A., Chan, K., & Scott, E. M. (2000). *Sensitivity analysis* (Vol. 1). Wiley New York.

Sandberg, N. H., Bergsdal, H., & Brattebø, H. (2011). Historical energy analysis of the Norwegian dwelling stock. *Building Research & Information*, *39*(1), 1–15. https://doi.org/10.1080/09613218.2010.528186

Sandberg, N. H., & Brattebø, H. (2012). Analysis of energy and carbon flows in the future Norwegian dwelling stock. *Building Research & Information*, *40*(March 2015), 123–139. https://doi.org/10.1080/09613218.2012.655071

Santner, T. J., Williams, B. J., & Notz, W. (2003). *The Design and Analysis of Computer Experiments*. Springer Science & Business Media.

Sartori, I., Wachenfeldt, B. J., & Hestnes, A. G. (2009). Energy demand in the Norwegian building stock: Scenarios on potential reduction. *Energy Policy*, *37*(5), 1614–1627. https://doi.org/10.1016/j.enpol.2008.12.031

Schnackenberg, M., Hamilton, D., & Richard, C. B. (2009). POST-OCCUPANCY EVALUATION : Oregon Health & Science University Center for Health and Healing. *October*, (October), 1–70.

Schwarz, G. (1978). Estimating the dimension of a model. *The Annals of Statistics*, *6*(2), 461–464. https://doi.org/10.1214/aos/1176344136

Shackelford, a. K., Davis, C. H., & Wang, X. W. X. (2004). Automated 2-D building footprint extraction from high-resolution satellite multispectral imagery. *IGARSS 2004. 2004 IEEE International Geoscience and Remote Sensing Symposium*, *3*(c), 1996–1999. https://doi.org/10.1109/IGARSS.2004.1370739

Shao, Y., Taff, G. N., & Walsh, S. J. (2011). Shadow detection and building-height estimation using IKONOS data. *International Journal of Remote Sensing*, *32*(22), 6929–6944. https://doi.org/10.1080/01431161.2010.517226

Shawe-Taylor, J., & Cristianini, N. (2004). *Kernel Methods for Pattern Analysis*. Cambridge University

Press.

Shimoda, Y., Asahi, T., Taniguchi, A., & Mizuno, M. (2007). Evaluation of city-scale impact of residential energy conservation measures using the detailed end-use simulation model. *Energy*, *32*(9), 1617–1633. https://doi.org/10.1016/j.energy.2007.01.007

Shimoda, Y., Fujii, T., Morikawa, T., & Mizuno, M. (2003). Development of residential energy end-use simulation model at city scale. In *Eighth International IBPSA Conference* (pp. 1201–1208). Eindhoven, Netherlands.

Shimoda, Y., Fujii, T., Morikawa, T., & Mizuno, M. (2004). Residential end-use energy simulation at city scale. *Building and Environment*, *39*(8), 959–967. https://doi.org/10.1016/j.buildenv.2004.01.020

Shimoda, Y., Okamura, T., Yamaguchi, Y., Yamaguchi, Y., Taniguchi, A., & Morikawa, T. (2010). City-level energy and CO2 reduction effect by introducing new residential water heaters. *Energy*, *35*(12), 4880–4891. https://doi.org/10.1016/j.energy.2010.08.043

Shimoda, Y., Yamaguchi, Y. Y., Okamura, T., Taniguchi, A., & Yamaguchi, Y. (2010). Prediction of greenhouse gas reduction potential in Japanese residential sector by residential energy end-use model. *Applied Energy*, *87*(6), 1944–1952. https://doi.org/10.1016/j.apenergy.2009.10.021

Shorrock, L., & Dunster, J. (1997). The physically-based model BREHOMES and its use in deriving scenarios for the energy use and carbon dioxide emissions of the UK housing stock. *Energy Policy*, *25*(12), 1027–1037.

Silva, A. S., & Ghisi, E. (2014). Uncertainty analysis of user behaviour and physical parameters in residential building performance simulation. *Energy and Buildings*, *76*, 381–391. https://doi.org/10.1016/j.enbuild.2014.03.001

Smith, S. T. (2009). *Modelling thermal loads for a non-domestic building stock: associating a priori probability with building form and construction - using building control laws and regulations. Knowledge Creation Diffusion Utilization*. University of Nottingham.

Smola, a J., & Schölkopf, B. (2004). A tutorial on support vector regression. *Statistics and Computing*, *14*, 199–222. https://doi.org/10.1023/B:STCO.0000035301.49549.88

Sobol, I. M. (1998). On quasi-Monte Carlo integrations. *Mathematics and Computers in Simulation*, *47*(2–5), 103–112. https://doi.org/10.1016/S0378-4754(98)00096-2

Sokol, J., Cerezo Davila, C., & Reinhart, C. F. (2017). Validation of a Bayesian-based method for defining residential archetypes in urban building energy models. *Energy and Buildings*, *134*, 11–24. https://doi.org/10.1016/j.enbuild.2016.10.050

Summerfield, a. J., Lowe, R. J., & Oreszczyn, T. (2010). Two models for benchmarking UK domestic

delivered energy. *Building Research & Information*, *38*(1), 12–24. https://doi.org/10.1080/09613210903399025

Swan, L. (2010). Residential Sector Energy and GHG Emissions Model for the Assessment of New Technologies. *Analysis*, (August).

Swan, L. G., & Ugursal, V. I. (2009). Modeling of end-use energy consumption in the residential sector: A review of modeling techniques. *Renewable and Sustainable Energy Reviews*, *13*(8), 1819–1835. https://doi.org/10.1016/j.rser.2008.09.033

Thomas Lumley based on Fortran code by Alan Miller. (2017). leaps: Regression Subset Selection.

Thornton, B., Wang, W., Xie, Y., Cho, H., Liu, B., & Zhang, J. (2011). *Achieving the 30% Goal: Energy and Cost Savings Analysis of ASHRAE Standard 90.1-2010*.

Tian, W. (2013). A review of sensitivity analysis methods in building energy analysis. *Renewable and Sustainable Energy Reviews*, *20*, 411–419. https://doi.org/10.1016/j.rser.2012.12.014

Tian, W., & Choudhary, R. (2012). A probabilistic energy model for non-domestic building sectors applied to analysis of school buildings in greater London. *Energy and Buildings*, *54*, 1–11. https://doi.org/10.1016/j.enbuild.2012.06.031

Tian, W., Choudhary, R., Augenbroe, G., & Lee, S. H. (2015). Importance analysis and meta-model construction with correlated variables in evaluation of thermal performance of campus buildings. *Building and Environment*, *92*, 61–74. https://doi.org/10.1016/j.buildenv.2015.04.021

Tian, W., & de Wilde, P. (2011). Uncertainty and sensitivity analysis of building performance using probabilistic climate projections: A UK case study. *Automation in Construction*, *20*(8), 1096–1109. https://doi.org/10.1016/j.autcon.2011.04.011

Tian, W., Song, J., Li, Z., & de Wilde, P. (2014). Bootstrap techniques for sensitivity analysis and model selection in building thermal performance analysis. *Applied Energy*, *135*, 320–328. https://doi.org/10.1016/j.apenergy.2014.08.110

Tian, W., Wang, Q., Song, J., & Wei, S. (2014). Calibrating Dynamic Building Energy Models using Regression Model and Bayesian Analysis in Building Retrofit Projects. *eSim 2014*, (Ashrae).

Tian, W., Yang, S., Li, Z., Wei, S., Pan, W., & Liu, Y. (2016). Identifying informative energy data in Bayesian calibration of building energy models. *Energy and Buildings*, *119*, 363–376. https://doi.org/10.1016/j.enbuild.2016.03.042

Tierney, J. E., & Tingley, M. P. (2014). A Bayesian, spatially-varying calibration model for the TEX 86 proxy. *Geochimica et Cosmochimica Acta*, *127*, 83–106.

Turiel, I., Craig, P., Levine, M., McMahon, J., McCollister, G., Hesterberg, B., & Robinson, M. (1987).

Estimation of energy intensity by end-use for commercial buildings. *Energy*, *12*(6), 435–446. https://doi.org/10.1016/0360-5442(87)90003-X

U.S. Department of Energy. (n.d.). EnergyPlus Example File Generator. Retrieved from http://apps1.eere.energy.gov/buildings/energyplus/cfm/inputs/index.cfm

University of Colorado Boulder. (n.d.). Places. Retrieved from http://places.colorado.edu/index

University of Michigan. (n.d.). Campus Information. Retrieved from http://campusinfo.umich.edu/building-search

Van den Meersche, K., Soetaert, K., & Oevelen, D. Van. (2009). xsample (): an R function for sampling linear inverse problems. *Journal of Statistical Software*, *30*(April), 1–15.

Vanhatalo, J., & Riihimäki, J. (2012). Bayesian modeling with Gaussian processes using the GPstuff toolbox. *arXiv Preprint arXiv: …*.

Vásquez, F., Løvik, A. N., Sandberg, N. H., & Müller, D. B. (2016). Dynamic type-cohort-time approach for the analysis of energy reductions strategies in the building stock. *Energy and Buildings*, *111*, 37–55. https://doi.org/10.1016/j.enbuild.2015.11.018

Vermeulen, T., Kämpf, J. H., & Beckers, B. (2013). Urban Form Optimization for the Energy Performance of Buildings Using CitySim. *CISBAT 2013 Proceedings Vol.II*, 915–920.

Wang, Q., Augenbroe, G., Kim, J. H., & Gu, L. (2016). Meta-modeling of occupancy variables and analysis of their impact on energy outcomes of office buildings. *Applied Energy*, *174*, 166–180. https://doi.org/10.1016/j.apenergy.2016.04.062

Weather Data | EnergyPlus. (n.d.). Retrieved from https://energyplus.net/weather

Wegner, J. D., Ziehn, J. R., & Soergel, U. (2010). Building detection and height estimation from high-resolution InSAR and optical data. In *International Geoscience and Remote Sensing Symposium (IGARSS)* (pp. 1928–1931). IEEE. https://doi.org/10.1109/IGARSS.2010.5653386

Wei, L., Tian, W., Silva, E. A., Choudhary, R., Meng, Q., & Yang, S. (2015). Comparative Study on Machine Learning for Urban Building Energy Analysis. *Procedia Engineering*, *121*, 285–292. https://doi.org/10.1016/j.proeng.2015.08.1070

WHO, & UN Habitat. (2016). *Global report on urban health: equitable, healthier cities for sustainable development. World Health Organization*. World Health Organization. https://doi.org/10.1017/CBO9781107415324.004

Wit, S. De, & Augenbroe, G. (2002). Analysis of uncertainty in building design evaluations and its implications. *Energy and Buildings*, *34*, 951–958.

Yamaguchi, Y., Choudhary, R., Booth, A., Suzuki, Y., & Shimoda, Y. (2013). Urban-scale energy

modelling of food supermarket considering uncertainty. In *The proceedings of BS*. Chambery, France.

Yamaguchi, Y., Hensen, J., & Shimoda, Y. (2005). District level energy management using a bottom-up modeling approach. *Proceedings of the 9th International IBPSA Conference*.

Yamaguchi, Y., & Shimoda, Y. (2010). District-scale simulation for multi-purpose evaluation of urban energy systems. *Journal of Building Performance Simulation*, *3*(4), 289–305. https://doi.org/10.1080/19401491003746621

Yamaguchi, Y., Shimoda, Y., & Mizuno, M. (2003). Development of district energy system simulation model based on detailed energy demand model. *Proceeding of Eighth International IBPSA Conference*, 1443–1450.

Yamaguchi, Y., Shimoda, Y., & Mizuno, M. (2007a). Proposal of a modeling approach considering urban form for evaluation of city level energy management. *Energy and Buildings*, *39*(5), 580–592. https://doi.org/10.1016/j.enbuild.2006.09.011

Yamaguchi, Y., Shimoda, Y., & Mizuno, M. (2007b). Transition to a sustainable urban energy system from a long-term perspective: Case study in a Japanese business district. *Energy and Buildings*, *39*(1), 1–12. https://doi.org/10.1016/j.enbuild.2006.03.031

Yamaguchi, Y., Shimoda, Y., & Taniguchi, A. (2008). EVALUATION OF ENERGY SAVING MEASURES IN LONG TERM SCENARIO IN JAPANESE RESIDENTIAL SECTOR. *Proceedings of the World Conference SB08*, 2521–2528.

Yamaguchi, Y., Suzuki, Y., Choudhary, R., Booth, A., & Shimoda, Y. (2013). Urban-scale energy modeling of food supermarket considering uncertainty. In *Proceedings of BS2013: 13th Conference of International Building Performance Simulation Association*. Chambery, France.

Yang, J., Rivard, H., & Zmeureanu, R. (2005). Building Energy Prediction with Adaptive Artificial Neural Networks. In *Ninth International IBPSA Conference* (pp. 1401–1408).

Yoon, S., & Yu, Y. (2017). Extended virtual in-situ calibration method in building systems using Bayesian inference. *Automation in Construction*, *73*, 20–30. https://doi.org/10.1016/j.autcon.2016.10.008

Yu, F., & Chan, K. (2004). Improved energy efficiency standards for vapour compression chillers serving buildings.

Zhang, J., Schrock, D., & Fisher, D. (2010). *Technical support document: 50% energy savings for quick-service restaurants*.

Zhang, K., Yan, J., & Chen, S. C. (2006). Automatic construction of building footprints from airborne LIDAR data. *IEEE Transactions on Geoscience and Remote Sensing*, *44*(9), 2523–2533. https://doi.org/10.1109/TGRS.2006.874137

Zhang, W., & Arhonditsis, G. B. (2008). Predicting the frequency of water quality standard violations using Bayesian calibration of eutrophication models. *Journal of Great Lakes Research*, *34*(4), 698–720.

Zhang, Y. (2009). "Parallel" EnergyPlus and the development of a parametric analysis tool. *IBPSA Conference*, 1382–1388.

Zhang, Y., & Korolija, I. (2010). Performing complex parametric simulations with jEPlus. *SET2010-9th International Conference on Sustainable …*.

Zhao, F. (2012). *Agent-based modeling of commercial building stocks for energy policy and demand response analysis*. *Georgia Institute of Technology*. Georgia Institute of Technology.

Zhao, F., Lee, S. H., & Augenbroe, G. (2016). Reconstructing building stock to replicate energy consumption data. *Energy and Buildings*, *117*, 301–312. https://doi.org/10.1016/j.enbuild.2015.10.001

Zhao, F., Martinez-Moyano, I., & Augenbroe, G. (2011). Agent-based modeling of commercial building stocks for policy support. In *Proceedings of Building Simulation 2011: 12th Conference of International Building Performance Simulation Association* (pp. 2385–2392). Sydney.

Zhao, J., Lasternas, B., Lam, K. P., Yun, R., & Loftness, V. (2014). Occupant behavior and schedule modeling for building energy simulation through office appliance power consumption data mining. *Energy and Buildings*, *82*, 341–355. https://doi.org/10.1016/j.enbuild.2014.07.033

Zhou, Y., Weng, Q., Gurney, K. R., Shuai, Y., & Hu, X. (2012). Estimation of the relationship between remotely sensed anthropogenic heat discharge and building energy use. *ISPRS Journal of Photogrammetry and Remote Sensing*, *67*, 65–72. https://doi.org/10.1016/j.isprsjprs.2011.10.007

# APPENDIX

## Appendix A. Results of Chapter 4.2 (Determination of informative energy data)

*Case EG*

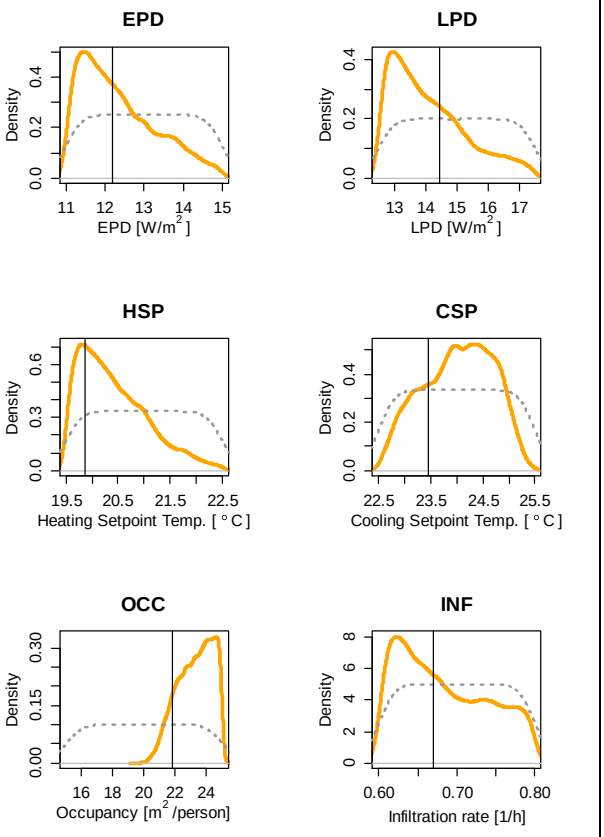


Parameter distribution for Case EG2-1

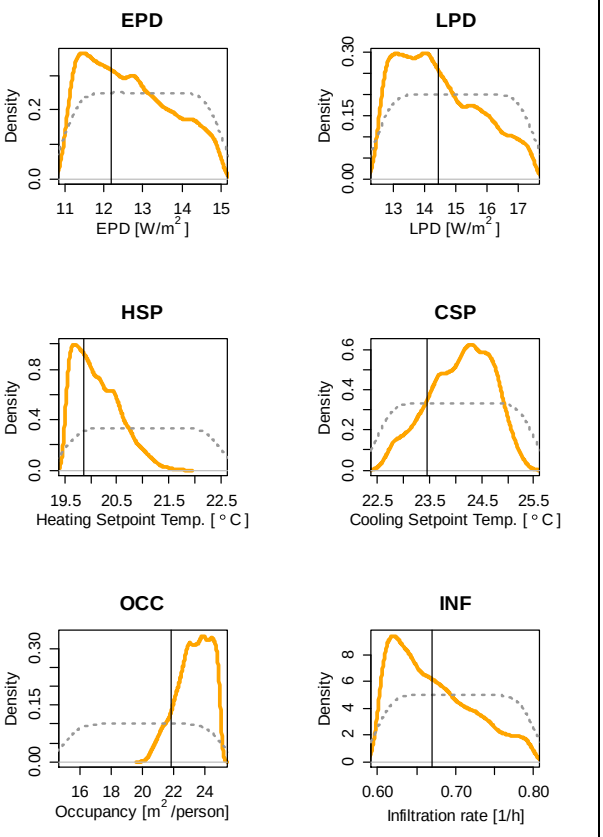


Parameter distribution for Case EG4-1

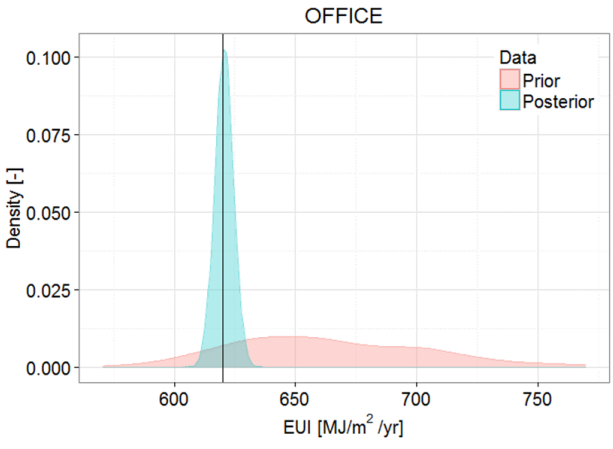


EUI distribution for Case EG2-1

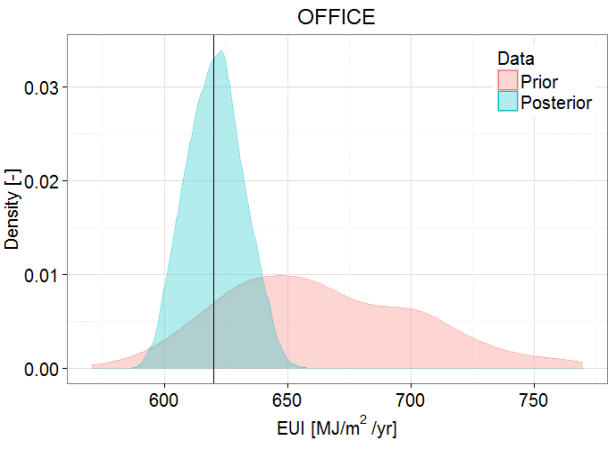


EUI distribution for Case EG4-1

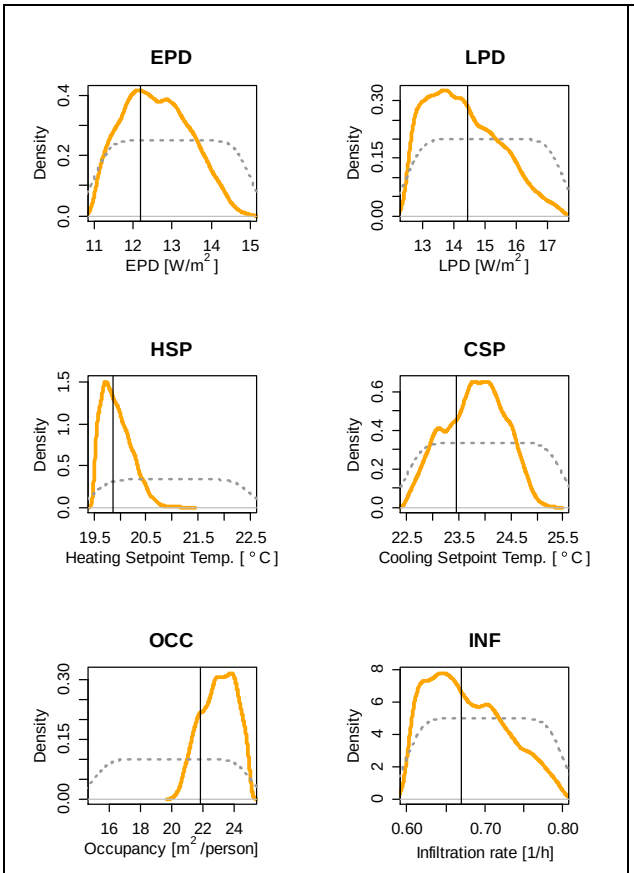


Parameter distribution for Case EG4-2

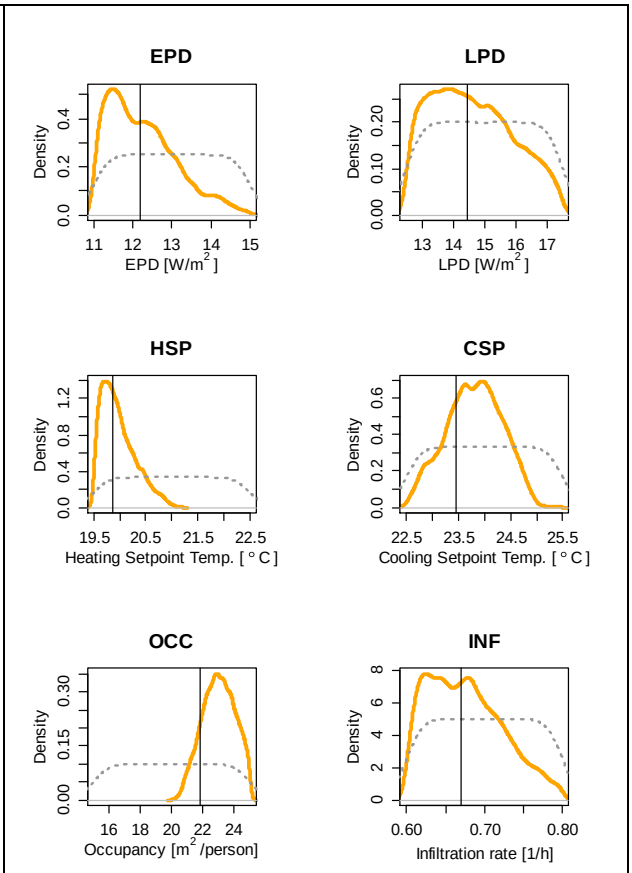


Parameter distribution for Case EG8-1

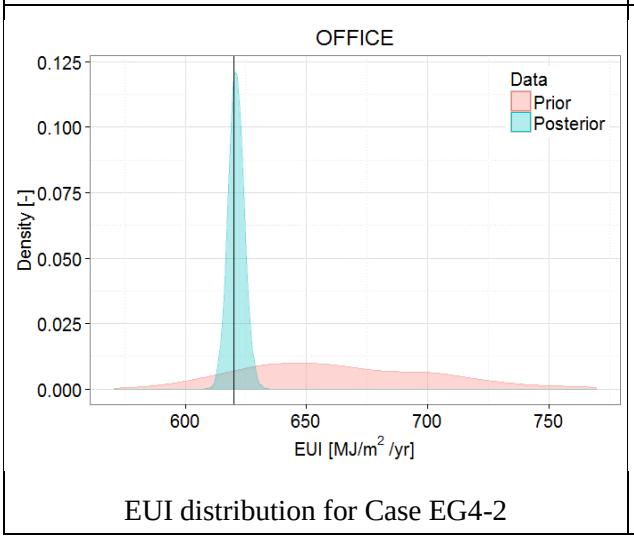


EUI distribution for Case EG4-2

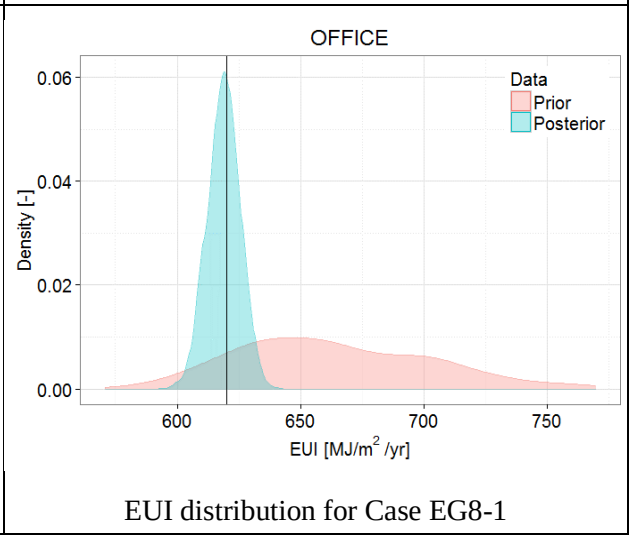


EUI distribution for Case EG8-1

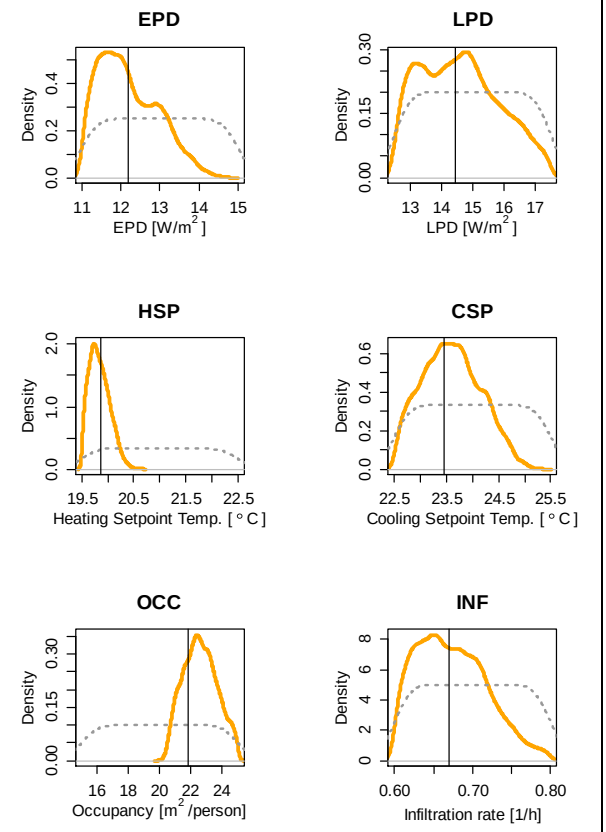


Parameter distribution for Case EG8-2

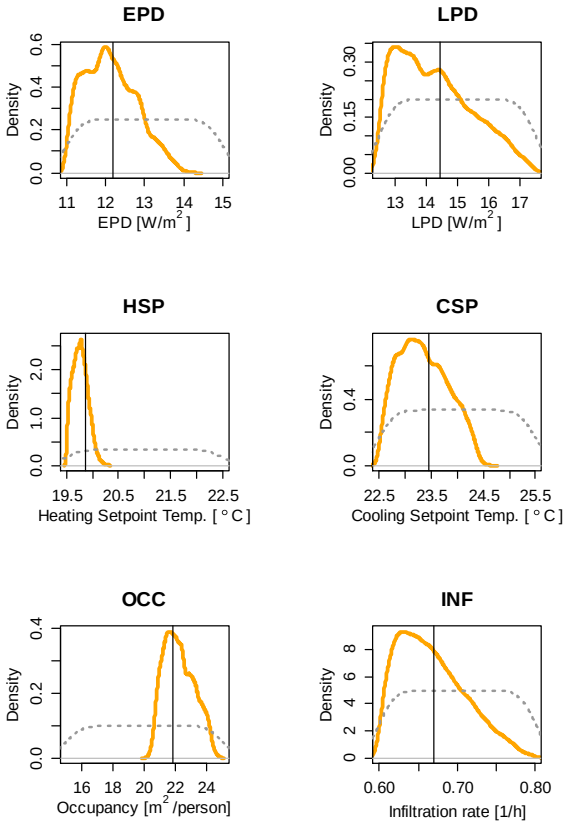


Parameter distribution for Case EG17-2

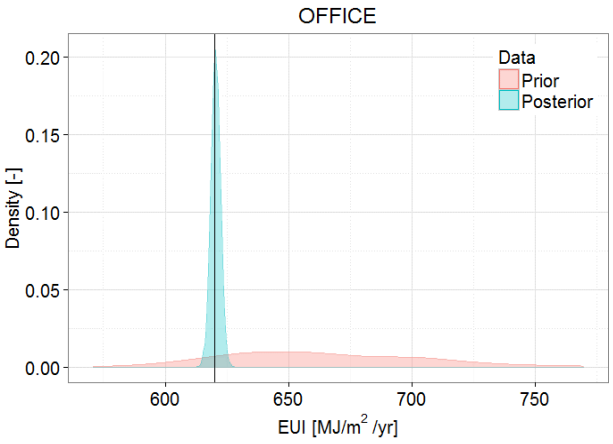


EUI distribution for Case EG8-2

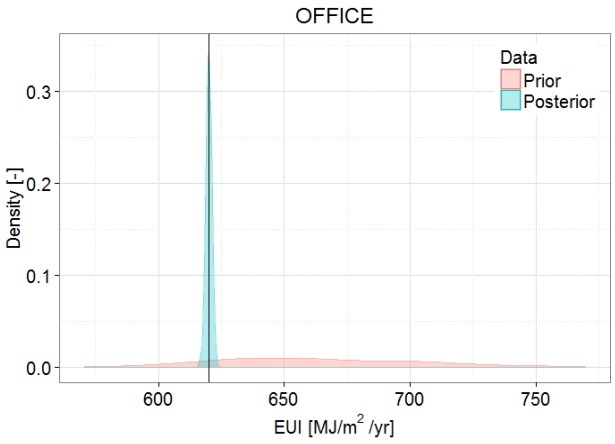


EUI distribution for Case EG17-2

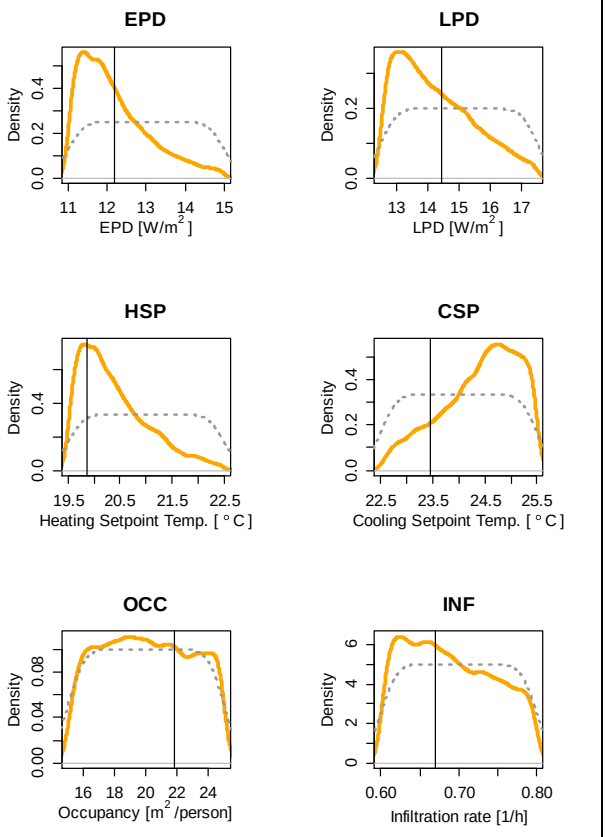


Parameter distribution for Case T1-1

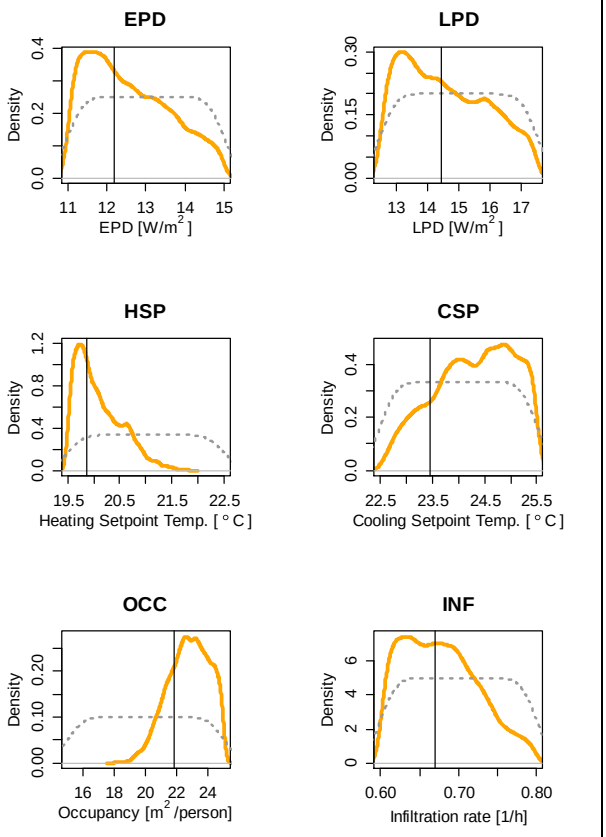


Parameter distribution for Case T4-1

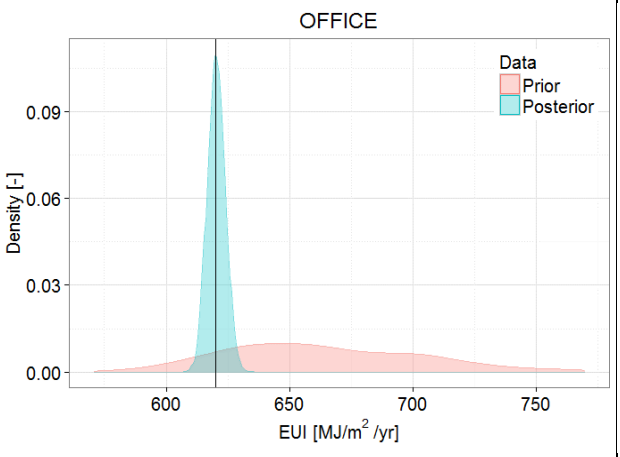


EUI distribution for Case T1-1

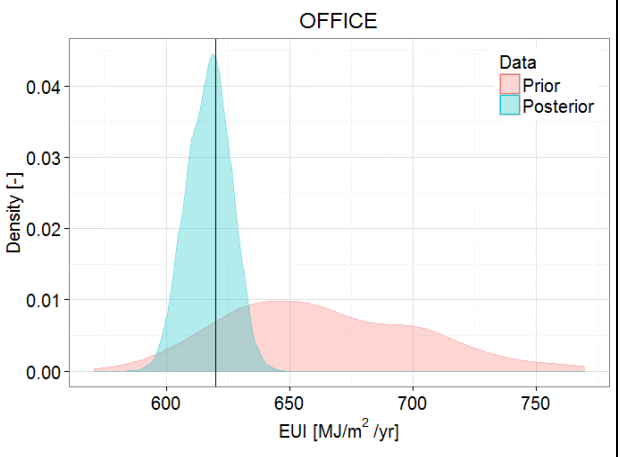


EUI distribution for Case T4-1

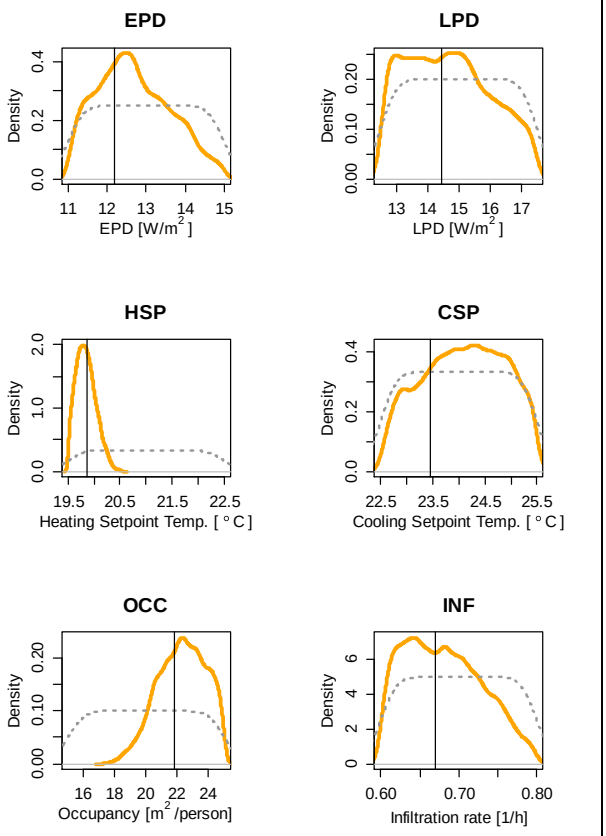


Parameter distribution for Case T4-2

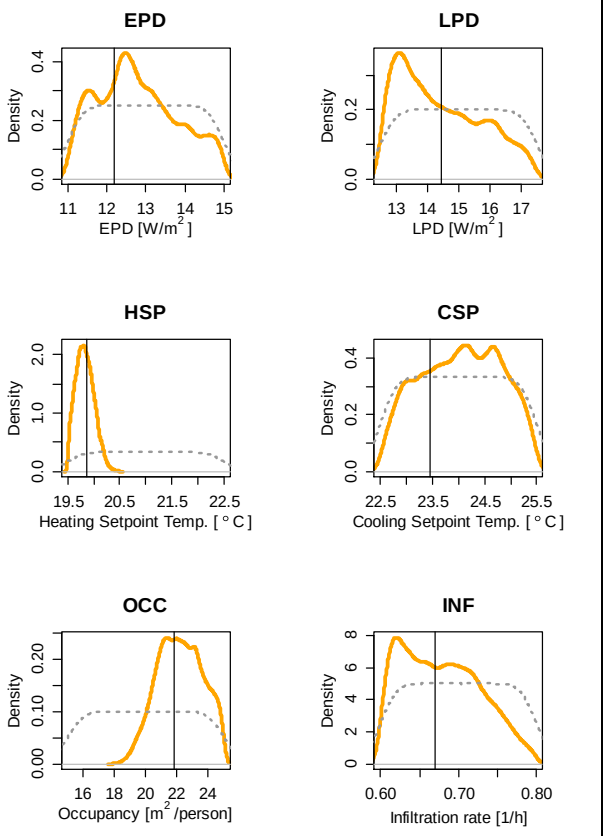


Parameter distribution for Case T8-1

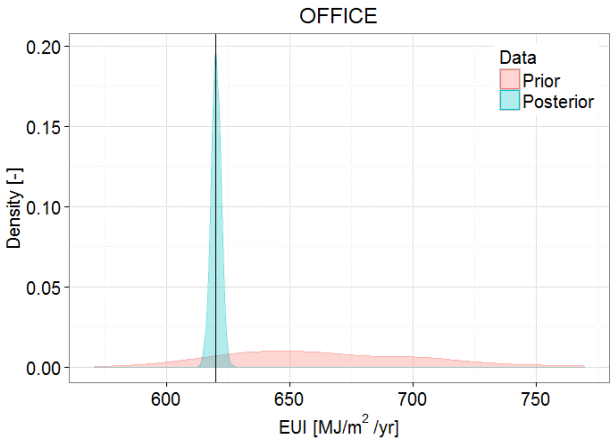


EUI distribution for Case T4-2

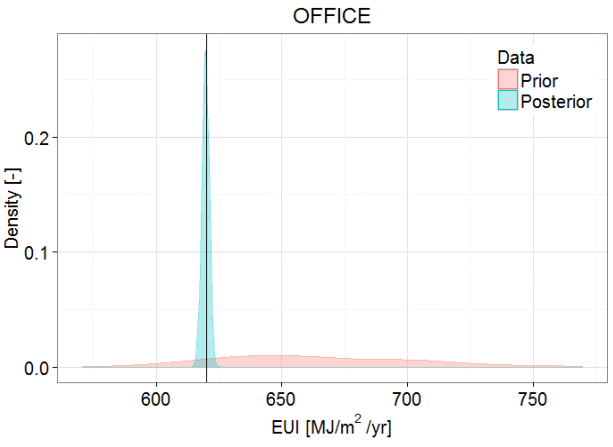


EUI distribution for Case T8-1

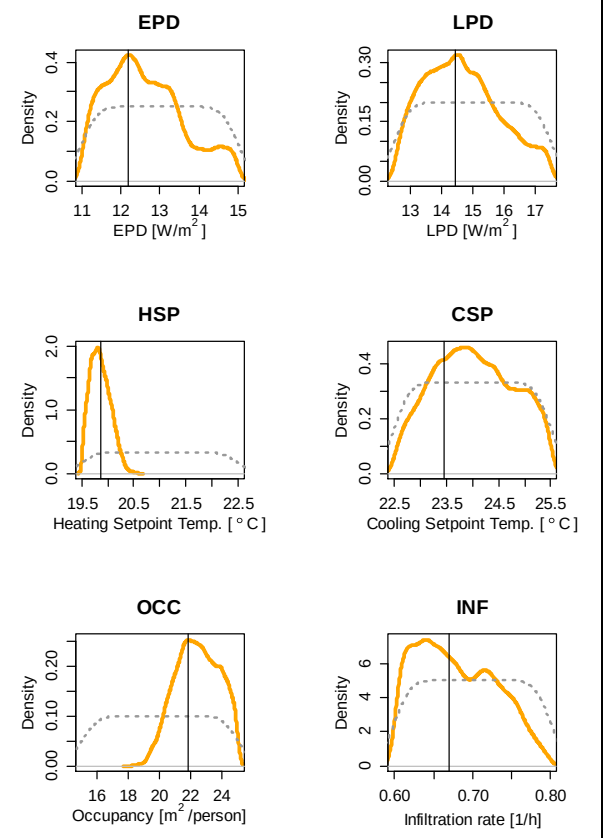


Parameter distribution for Case T8-2

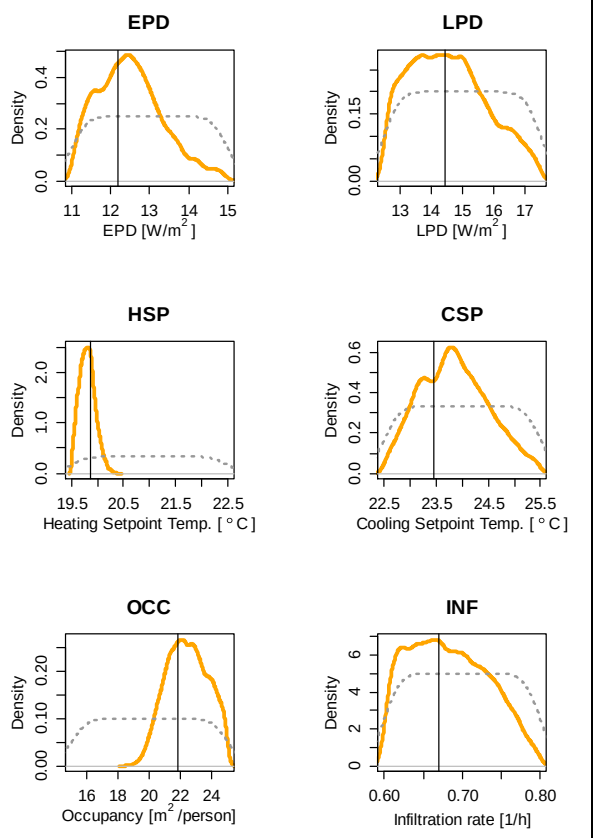


Parameter distribution for Case T12-2

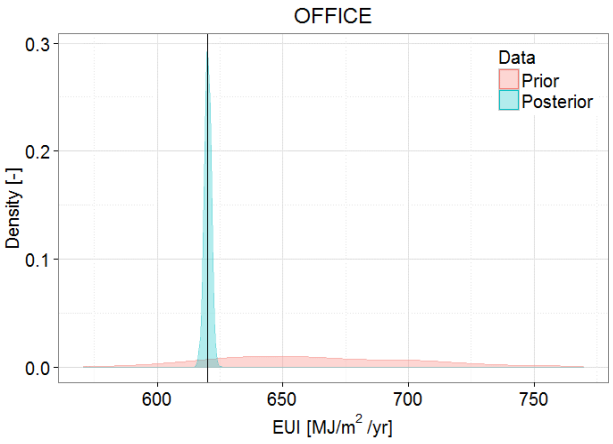


EUI distribution for Case T8-2

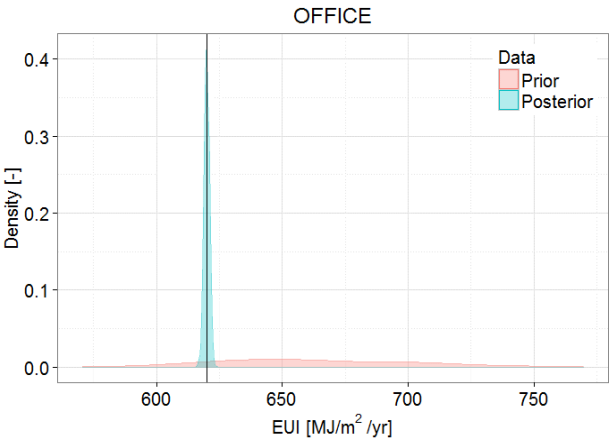


EUI distribution for Case T12-2

*Case E*

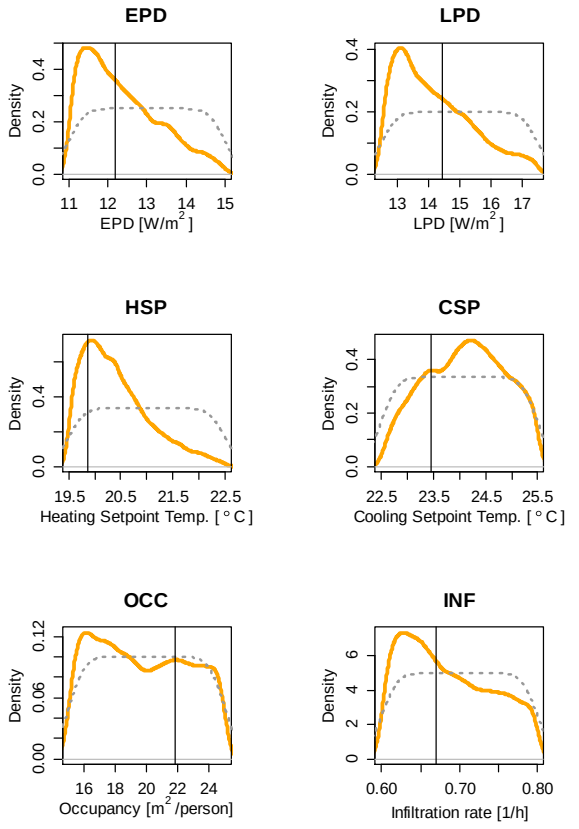


Parameter distribution for Case E1-1

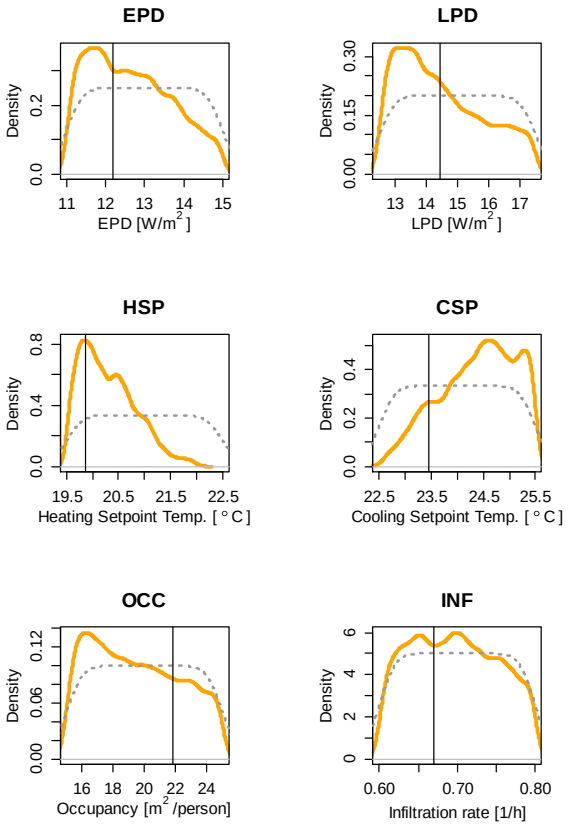


Parameter distribution for Case E4-1

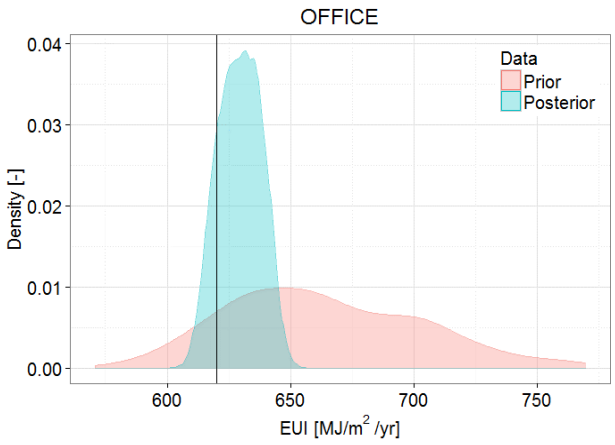


EUI distribution for Case E1-1

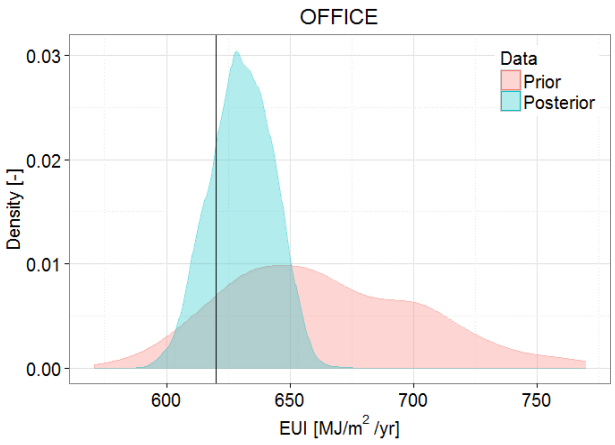


EUI distribution for Case E4-1

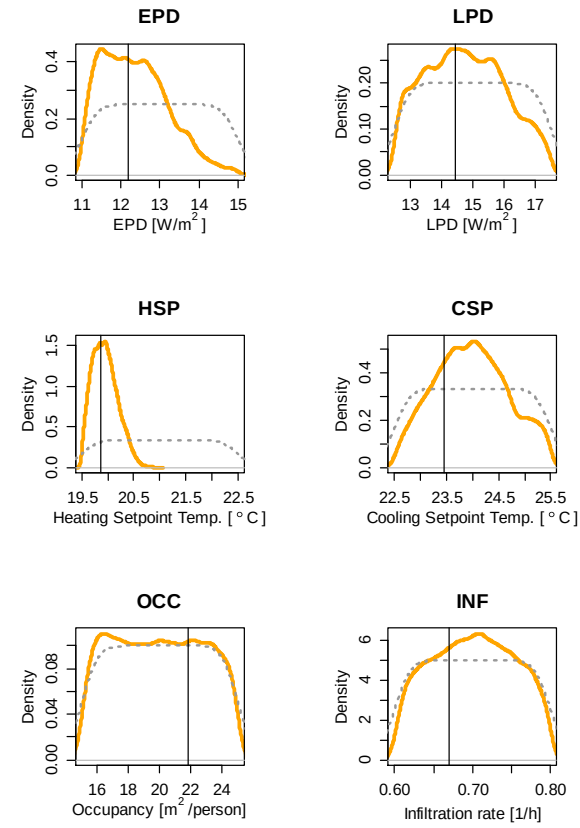


Parameter distribution for Case E4-2

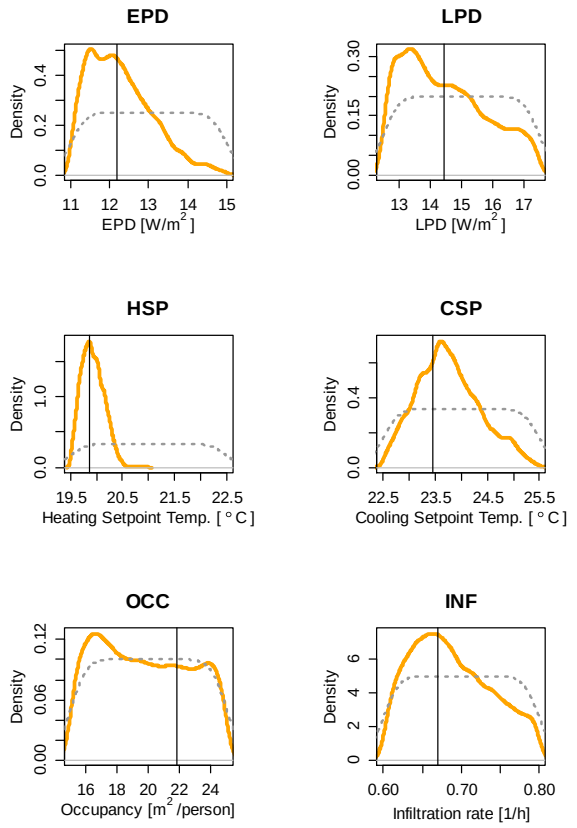


Parameter distribution for Case E8-1

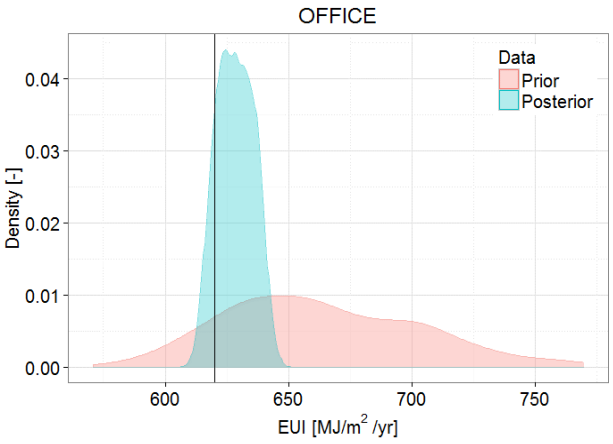


EUI distribution for Case E4-2

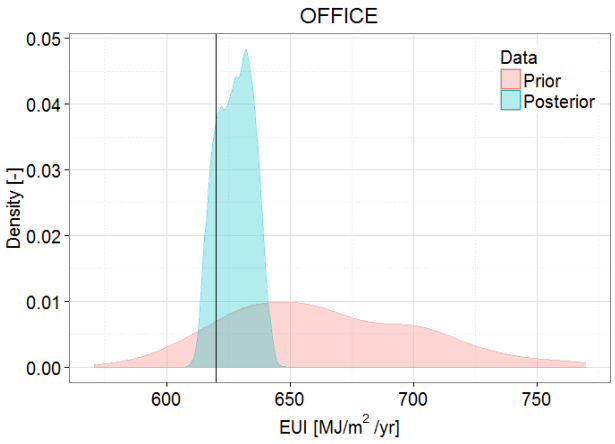


EUI distribution for Case E8-1

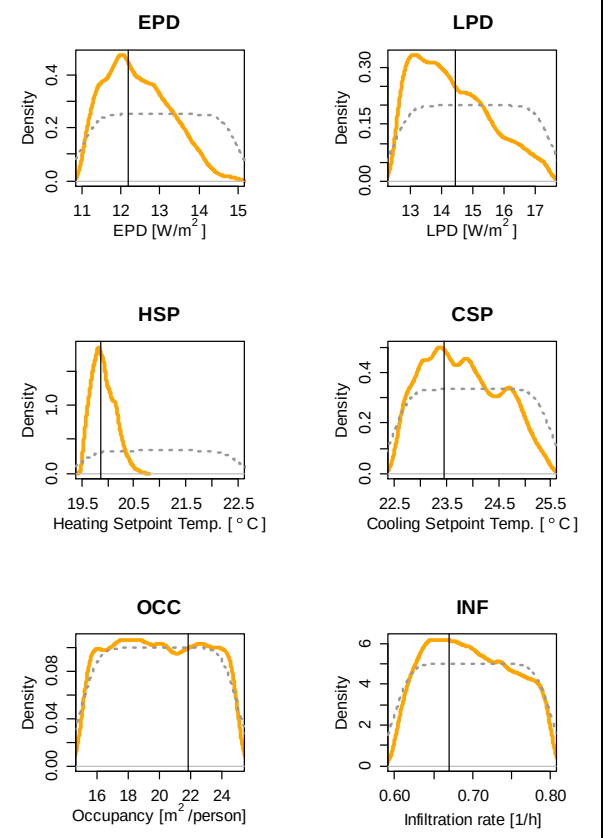


Parameter distribution for Case E8-2

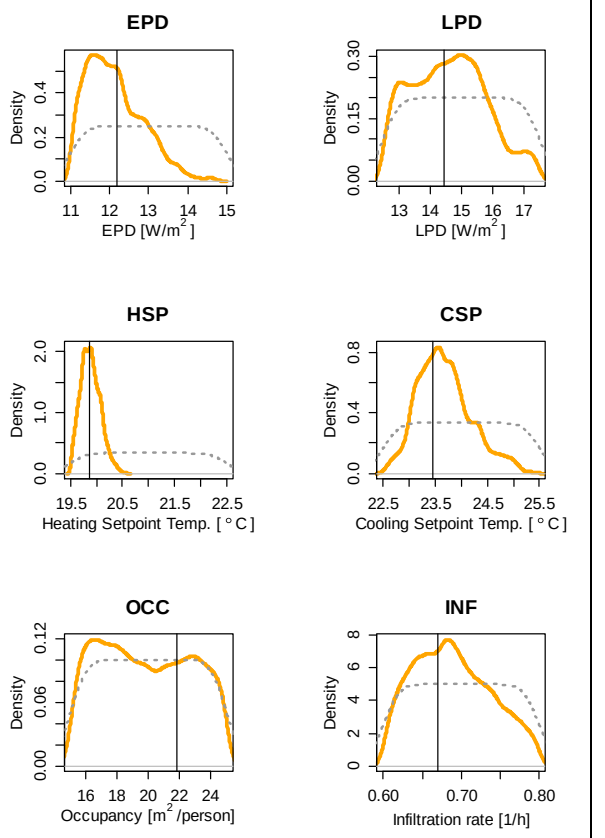


Parameter distribution for Case E12-2

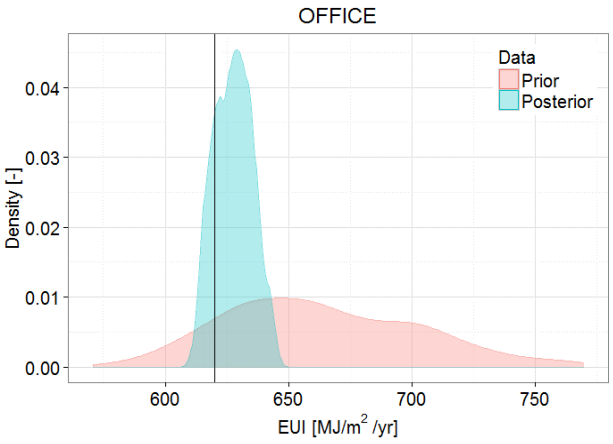


EUI distribution for Case E8-2

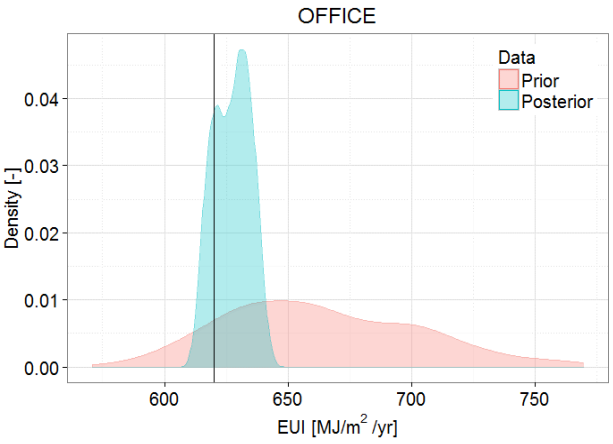


EUI distribution for Case E12-2

*Case G*

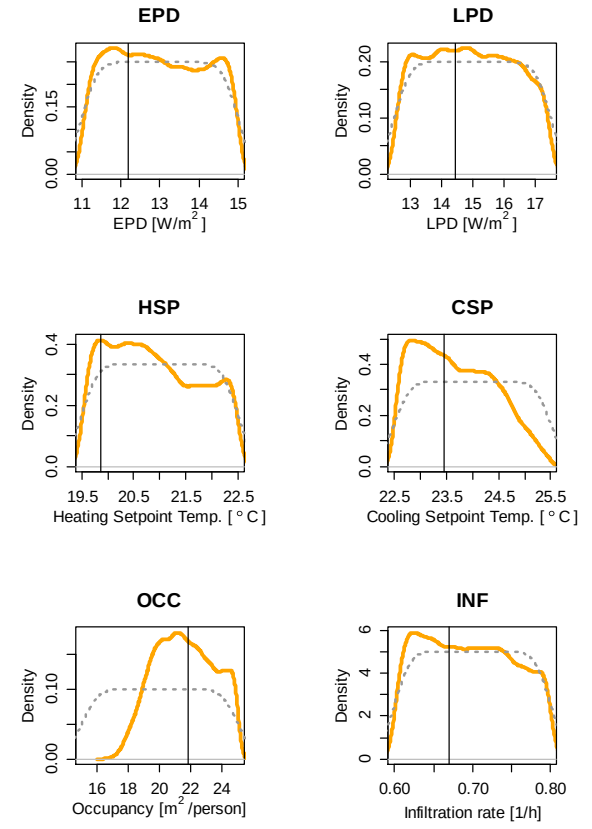


Parameter distribution for Case G1-1

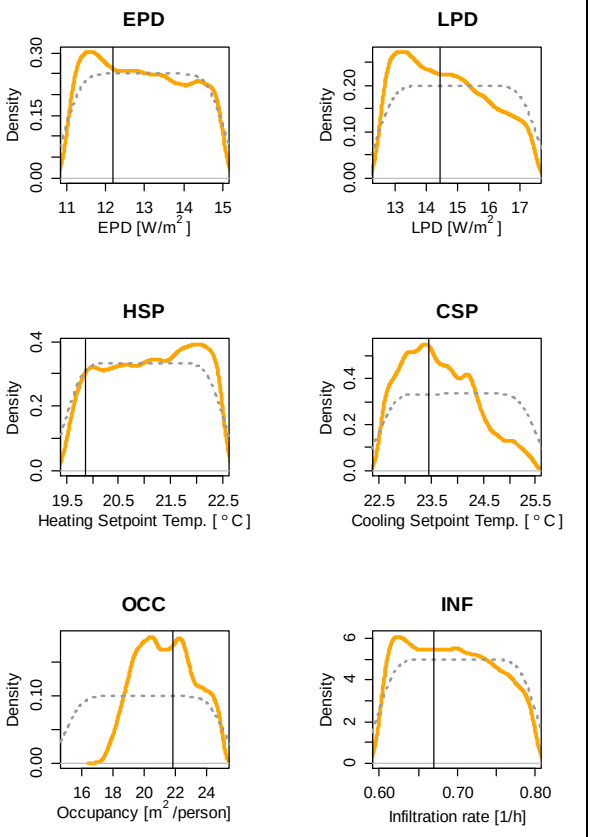


Parameter distribution for Case G3-1

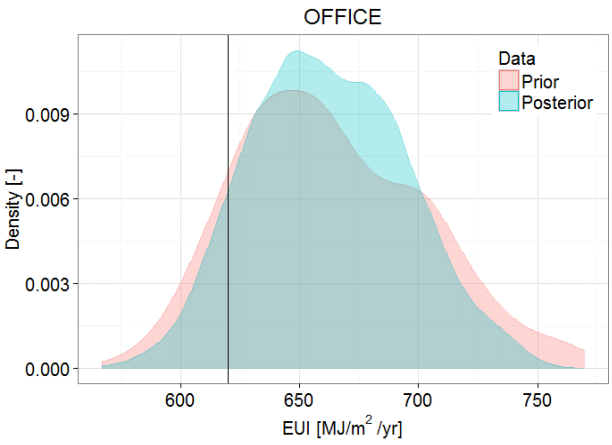


EUI distribution for Case G1-1

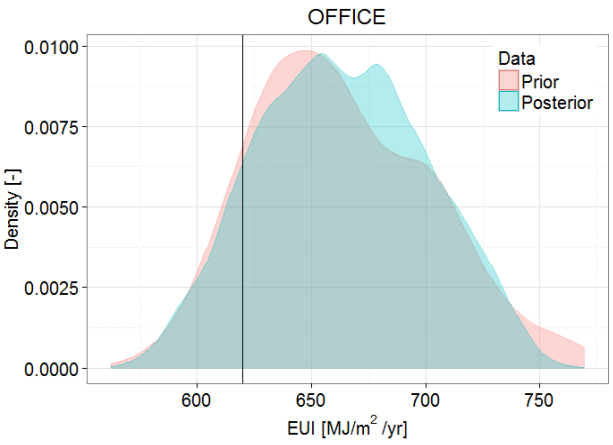


EUI distribution for Case G3-1

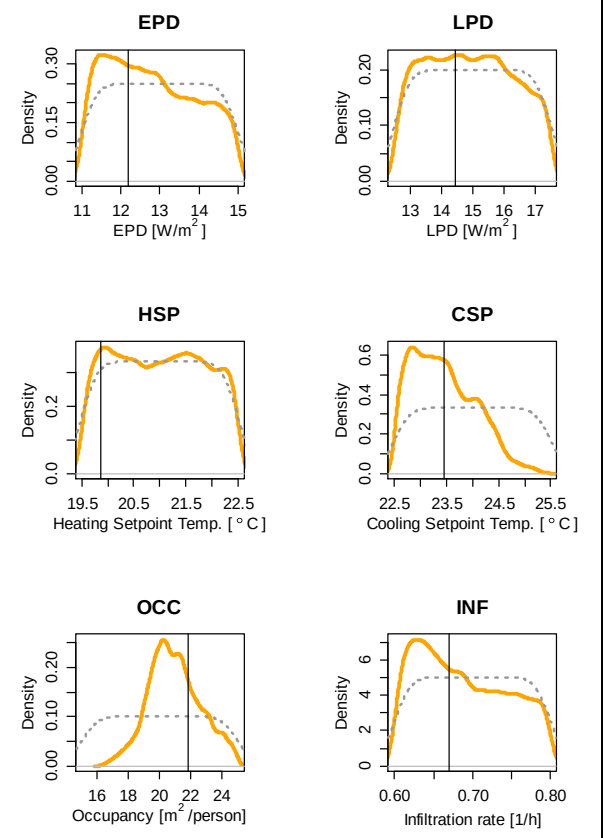


Parameter distribution for Case G3-2

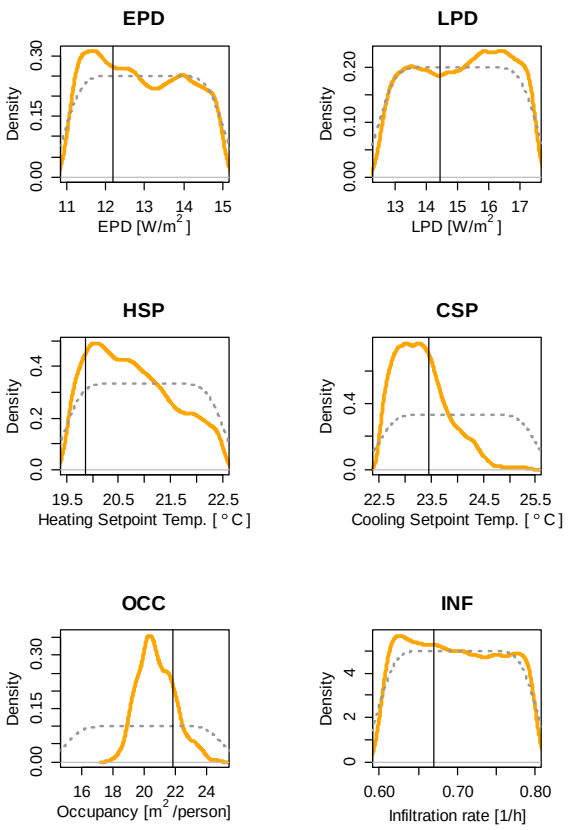


Parameter distribution for Case G5-2

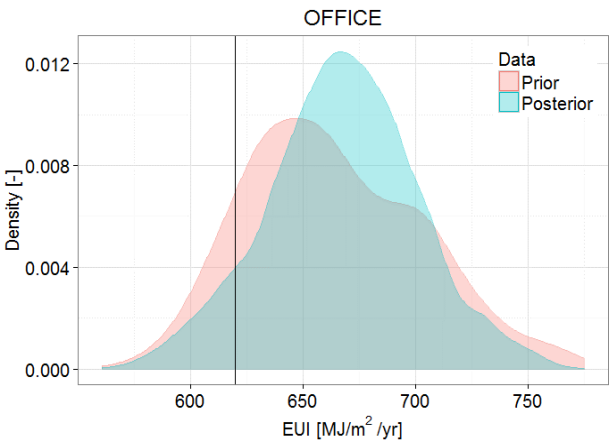


EUI distribution for Case G3-2

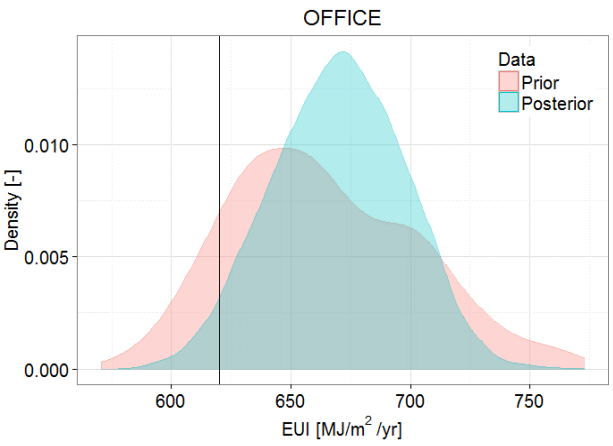


EUI distribution for Case G5-2

**Appendix B. CU Building list**

| No. | Name | Build Year | Renovation Year | Total Floor Area [$m^2$] | Floors | Original Primary Use | Function | EUI [$GJ/m^2$] |
|---|---|---|---|---|---|---|---|---|
| 1 | University Club | 1939 | 1939 | 2737.2 | 3 | Administrative Offices | Education | 0.598 |
| 2 | University Memorial Center | 1953 | 1986 | 24986.4 | 5 | Food Service | Service | 1.151 |
| 3 | Museum of Natural History | 1937 | 1937 | 3009.1 | 2 | Museum | Service | 0.797 |
| 4 | Bruce Curtis Building (Museum Collections) | 1911 | 2002 | 4201.5 | 4 | Research | Laboratory | 1.790 |
| 5 | Economics | 1930 | 1930 | 3175.1 | 3 | Classrooms | Education | 1.009 |
| 6 | Guggenheim Geography | 1908 | 1908 | 2474.0 | 3 | Classrooms | Education | 0.573 |
| 7 | Education | 1956 | 1956 | 4645.3 | 3 | Classrooms | Education | 1.046 |
| 8 | University Theatre | 1902 | 1989 | 6594.7 | 2 | Other - Entertainment/Public Assembly | Service | 0.804 |
| 9 | Hellems Arts and Sciences | 1921 | 1921 | 10797.7 | 3 | Classrooms | Education | 0.881 |
| 10 | Cristol Chemistry and Biochemistry | 1958 | 1997 | 13732.0 | 4 | Laboratory | Laboratory | 2.548 |
| 11 | Cooperative Institute for Research in Environmental Sciences | 1987 | 1987 | 2791.1 | 3 | Laboratory | Laboratory | 3.263 |
| 12 | Ekeley Sciences | 1925 | 2014 | 12703.6 | 3 | Laboratory | Laboratory | 3.257 |
| 13 | Roser ATLAS Center | 2006 | 2006 | 6946.3 | 4 | Museum | Service | 0.673 |
| 14 | Hale Science | 1899 | 1992 | 4290.8 | 4 | Classrooms | Education | 0.766 |

| | | | | | | | | |
|---|---|---|---|---|---|---|---|---|
| 15 | McKenna Languages | 1937 | 1947 | 2133.5 | 2 | General Office | Education | 0.442 |
| 16 | Old Main | 1899 | 1986 | 2349.8 | 4 | Other - Entertainment/Public Assembly | Education | 1.049 |
| 17 | Woodbury Arts and Sciences | 1890 | 2000 | 7302.1 | 3 | Administrative Offices | Education | 0.827 |
| 18 | Macky Auditorium | 1922 | 1986 | 8105.9 | 3 | Other - Entertainment/Public Assembly | Service | 0.824 |
| 19 | Norlin Library | 1939 | 1977 | 31130.0 | 4 | Library | Education | 0.839 |
| 20 | Koenig Alumni Center | 1899 | 1899 | 810.0 | 2 | Administrative Offices | Education | 0.969 |
| 21 | Center for Community | 2010 | 2010 | 29476.8 | 4 | Food Service | Service | 1.141 |
| 22 | Regent Administrative Center | 1964 | 1964 | 8872.9 | 3 | Administrative Offices | Education | 0.900 |
| 23 | University Administrative Center | 1930 | 1986 | 1409.7 | 3 | Administrative Offices | Education | 0.581 |
| 24 | Wardenburg Student Health Center | 1959 | 1995 | 6109.3 | 3 | Medical Office | Service | 1.378 |
| 25 | Cheyenne Arapaho Hall | 1954 | 1954 | 10452.1 | 4 | Residence Hall | Residence | 0.730 |
| 26 | Willard Hall | 1955 | 1955 | 9949.7 | 4 | Residence Hall | Residence | 0.626 |
| 27 | Hallett Hall | 1956 | 1956 | 8661.0 | 4 | Residence Hall | Residence | 0.501 |
| 28 | Reed Hall | 1947 | 1947 | 2389.0 | 3 | Residence Hall | Residence | 0.723 |
| 29 | Imig Music | 1955 | 1997 | 9927.6 | 2 | Classrooms | Education | 0.742 |
| 30 | Farrand Hall | 1948 | 1948 | 15239.2 | 5 | Residence Hall/ Food | Residence | 1.132 |
| 31 | Crosman Hall | 1947 | 1947 | 2553.0 | 3 | Residence Hall | Reside | 0.640 |

| | | | | | | | | |
|---|---|---|---|---|---|---|---|---|
| | | | | | | | nce | |
| 32 | Aden Hall | 1947 | 1947 | 2500.4 | 3 | Residence Hall | Residence | 0.697 |
| 33 | Baker Hall | 1937 | 2013 | 10558.3 | 5 | Residence Hall | Residence | 0.584 |
| 34 | Libby Hall | 1955 | 1955 | 10876.0 | 4 | Residence Hall/ Food | Residence | 1.364 |
| 35 | Joint Institute for Lab Astrophysics | 1965 | 2012 | 14880.4 | 10 | Laboratory | Laboratory | 3.053 |
| 36 | Duane Physics and Astrophysics | 1971 | 1971 | 18070.8 | 11 | Laboratory | Laboratory | 1.149 |
| 37 | Benson Earth Sciences | 1997 | 1997 | 8904.2 | 4 | Laboratory | Laboratory | 1.603 |
| 38 | Mathematics Building | 1992 | 1992 | 5699.2 | 4 | Classrooms/ Library | Education | 0.743 |
| 39 | Ramaley Biology | 1952 | 1981 | 10363.0 | 4 | Research | Laboratory | 2.672 |
| 40 | Gold Biosciences Building | 1995 | 1995 | 12746.0 | 5 | Research | Laboratory | 3.894 |
| 41 | Porter Biosciences | 1971 | 2003 | 10125.1 | 5 | Research | Laboratory | 4.692 |
| 42 | Muenzinger Psychology | 1971 | 1971 | 14272.7 | 5 | Research | Laboratory | 1.902 |
| 43 | Sewall Hall | 1934 | 1934 | 9289.7 | 5 | Residence Hall/ Food | Residence | 1.230 |
| 44 | Student Recreation Center | 1973 | 2014 | 29776.3 | 3 | Fitness Center | Service | 0.831 |
| 45 | Wolf Law | 2006 | 2006 | 17057.8 | 5 | Classrooms/ Library | Education | 0.655 |
| 46 | Fleming Law Building | 1958 | 1973 | 11899.6 | 3 | Classrooms | Education | 0.614 |
| 47 | Kittredge West Hall | 1981 | 2013 | 6902.3 | 3 | Residence Hall | Residence | 0.691 |
| 48 | Kittredge Central | 2013 | 2013 | 9302.8 | 3 | Residence Hall | Residence | 0.713 |

| | | | | | | | | |
|---|---|---|---|---|---|---|---|---|
| 49 | Smith Hall | 1963 | 2011 | 8847.8 | 3 | Residence Hall | Residence | 0.769 |
| 50 | Andrews Hall | 1963 | 2009 | 5823.6 | 3 | Residence Hall | Residence | 1.026 |
| 51 | Buckingham Hall | 1963 | 2010 | 6345.4 | 2 | Residence Hall | Residence | 0.769 |
| 52 | Arnett Hall | 1964 | 2008 | 5893.2 | 2 | Residence Hall | Residence | 1.034 |
| 53 | Fiske Planetarium and Science Center | 1975 | 1975 | 1897.5 | 1 | Other - Entertainment/Public Assembly | Service | 0.881 |
| 54 | Speech, Language, and Hearing Sciences | 1960 | 1960 | 2095.7 | 3 | General Office | Education | 0.332 |
| 55 | Koelbel Building | 1969 | 2007 | 16417.6 | 4 | Classrooms/ Library | Education | 0.698 |
| 56 | Engineering Center | 1965 | 1990 | 54590.8 | 3 | Laboratory | Laboratory | 1.781 |
| 57 | Integrated Teaching and Learning Laboratory | 1996 | 1996 | 3374.4 | 3 | Laboratory | Laboratory | 2.140 |
| 58 | Discovery Learning Center | 2002 | 2002 | 4740.8 | 4 | Laboratory | Laboratory | 1.412 |
| 59 | Environmental Health and Safety Center | 1980 | 2000 | 2110.1 | 2 | Service | Service | 1.295 |
| 60 | Police and Parking Services | 1991 | 2007 | 3151.5 | 2 | Police Station | Service | 1.585 |
| 61 | Smiley Court | 1963 | 1963 | 21355.0 | 4 | Multifamily Housing | Residence | 0.781 |
| 62 | Institute for Behavioral Genetics | 1966 | 2006 | 2385.5 | 2 | Research | Laboratory | 3.508 |
| 63 | Research Laboratory No. 4, Life Science | 1964 | 1964 | 1113.2 | 1 | Laboratory | Laboratory | 2.475 |
| 64 | Research Laboratory No. 2, RL2 | 1963 | 1963 | 7140.1 | 3 | General Office | Education | 0.735 |
| 65 | Research Laboratory No. 1, Litman | 1961 | 1961 | 5099.9 | 2 | Laboratory | Laboratory | 1.508 |

| | | | | | | | | |
|---|---|---|---|---|---|---|---|---|
| 66 | Administrative and Research Center | 1969 | 1974 | 17341.5 | 7 | General Office | Education | 0.653 |
| 67 | Research Laboratory No. 6, Marine Street Science Center | 1980 | 1992 | 4511.7 | 1 | General Office | Laboratory | 1.947 |
| 68 | Science Learning Laboratory | 1960 | 1960 | 2919.0 | 2 | Laboratory | Laboratory | 1.351 |
| 69 | Computing Center | 1973 | 1973 | 2680.1 | 2 | General Office | Laboratory | 2.594 |
| 70 | Jennie Smoly Caruthers Biotec Building | 2012 | 2012 | 31867.0 | 5 | Laboratory | Laboratory | 1.678 |
| 71 | Center for Astrophysics and Space Astronomy | 1981 | 1981 | 2896.8 | 1 | Laboratory | Laboratory | 1.979 |
| 72 | LASP Space Technology Research Center | 1991 | 2006 | 10919.8 | 3 | General Office | Laboratory | 2.019 |
| 73 | Family Housing Children's Center - Newton Court | 1975 | 1975 | 666.4 | 1 | Pre-school/Daycare | Education | 0.409 |
| 74 | Athens North Court | 1980 | 1980 | 4820.3 | 3 | Residence Hall | Residence | 0.671 |
| 75 | Darley Towers | 1969 | 1969 | 11263.1 | 15 | Residence Hall | Residence | 1.054 |
| 76 | Stearns Towers | 1966 | 1966 | 23281.8 | 15 | Residence Hall | Residence | 0.912 |
| 77 | Williams Village North Hall | 2011 | 2011 | 13256.6 | 6 | Residence Hall | Residence | 0.689 |
| 78 | Bear Creek Apartments at Williams Village - Building 1A | 2003 | 2003 | 17732.1 | 6 | Residence Hall | Residence | 0.635 |
| 79 | Bear Creek Apartments at Williams Village - Building 1B | 2003 | 2003 | 17733.9 | 6 | Residence Hall | Residence | 0.622 |
| 80 | University Residence | 1987 | 1987 | 641.6 | 2 | Residence | Residence | 0.888 |